T.R.
GEBZE TECHNICAL UNIVERSITY
GRADUATE SCHOOL OF NATURAL AND APPLIED SCIENCES

PERFORMANCE OF RELAYED DIVERSITY COMMUNICATION TECHNIQUES

EFENDİ FİDAN
A THESIS SUBMITTED FOR THE DEGREE OF
DOCTOR OF PHILOSOPHY
DEPARTMENT OF ELECTRONICS ENGINEERING

GEBZE
2020

T.R.

GEBZE TECHNICAL UNIVERSITY

GRADUATE SCHOOL OF NATURAL AND APPLIED SCIENCES

PERFORMANCE OF RELAYED DIVERSITY COMMUNICATION TECHNIQUES

EFENDİ FİDAN

A THESIS SUBMITTED FOR THE DEGREE OF

DOCTOR OF PHILOSOPHY

DEPARTMENT OF ELECTRONICS ENGINEERING

THESIS SUPERVISOR

PROF. DR. OĞUZ KUCUR

GEBZE

2020

T.C.
GEBZE TEKNİK ÜNİVERSİTESİ
FEN BİLİMLERİ ENSTİTÜSÜ

RÖLELİ VE ÇEŞİTLEMELİ HABERLEŞME TEKNİKLERİNİN PERFORMANSI

EFENDİ FİDAN

DOKTORA TEZİ
ELEKTRONİK MÜHENDİSLİĞİ ANABİLİM DALI

DANIŞMANI
PROF. DR. OĞUZ KUCUR

GEBZE
2020

GEBZE TEKNİK ÜNİVERSİTESİ	**DOKTORA JÜRİ ONAY FORMU**

GTÜ Fen Bilimleri Enstitüsü Yönetim Kurulu'nun 03/07/2020 tarih ve 2020/32 sayılı kararıyla oluşturulan jüri tarafından 07/07/2020 tarihinde tez savunma sınavı yapılan Efendi FİDAN'ın tez çalışması Elektronik Mühendisliği Anabilim Dalında DOKTORA tezi olarak kabul edilmiştir.

JÜRİ

ÜYE (TEZ DANIŞMANI)	: Prof. Dr. Oğuz KUCUR
ÜYE	: Prof. Dr. İbrahim ALTUNBAŞ
ÜYE	: Dr. Öğretim Üyesi A. Köksal HOCAOĞLU
ÜYE	: Prof. Dr. Güneş KARABULUT KURT
ÜYE	: Dr. Öğretim Üyesi Ferkan YILMAZ

ONAY

Gebze Teknik Üniversitesi Fen Bilimleri Enstitüsü Yönetim Kurulu'nun

……/……./..…… tarih ve …..…/…..... sayılı kararı.

SUMMARY

In this thesis, relayed diversity communication networks are investigated over Rayleigh, Nakagami-m, and generalized-K wireless media for half/full-duplex (HD/FD) transmission schemes, amplify/decode-and-forward (AF/DF) relay protocols, and (non-)orthogonal multiple access (OMA/NOMA) techniques. Improvement of coverage area, reduction of power consumption, effective utilization of bandwidth, services with high data rates, and massive connectivity are provided by the systems under consideration. Moreover, to mitigate degradation effects of fading, space diversity technique is considered with generalized antenna selection (AS) to reduce hardware complexity but keeps offered performance gain of multi-input multi-output systems. Additionally, cooperative communication is also investigated with relay selection (RS) to provide benefits of spatial diversity. Firstly, generalized AS for both transmission and reception over slow Rayleigh fading channels is elaborated in a two-way system with multi-antenna sources and an AF HD relay equipped with a single antenna. Secondly, the two-way system is investigated with multi-antenna sources and a multi-antenna relay where a single antenna is selected at the relay in addition to generalized AS at the sources. Thirdly, single AS for FD transmission and non-reciprocity of forward and backward paths between the sources and DF relay is considered for the two-way system with multi-antenna sources and a single antenna relay, where a novel transceiver antenna selection method selecting a pair of antennas for transmission and reception at terminal sources is proposed and analyzed. In the remaining three works, RS is investigated for unidirectional relayed networks. In the first work, generalized RS is investigated for an FD AF multi-relay cooperative (diversity) system with(out) a direct path between the source and destination is studied over slow Rayleigh fading channels. The last two works implementing RS out of multi HD/FD DF relays in two stages to maximize the data rate of the second user with providing priority to the first user are based on NOMA technique, where the first one is over Nakagami-m fades with two sources and the second one is over generalized-K fades with a single source. Imperfect successive interference cancellation is also considered for both systems. Finally, DF multi-hop system over Nakagami-m fades is revised with(out) a direct link between the source and destination.

Key Words: Antenna/Relay Selection (Space Diversity), NOMA, Half/Full-Duplex Relay, One/Two-Way System, Cooperative Diversity.

ÖZET

Bu tezde röleli ve çeşitlemeli haberleşme ağları, yarı (tam) çift yönlü iletim teknikleri (HD/FD), çöz (kuvvetlendir)-ve-aktar (DF/AF) röle iletim protokolleri ve dik(-olmayan) çoklu erişim (OMA/NOMA) teknikleri için Rayleigh, Nakagami-m ve genelleştirilmiş-K sönümlemeli/gölgelemeli ortamlarda incelenmiştir. Söz konusu sistemler haberleşmede kapsama alanını genişletmekte, güç tüketimini azaltmakta, spektrum verimliliğini arttırmakta, yüksek veri hızını gerektiren hizmetleri sunmakta ve kitlesel bağlantıyı gerçekleştirmektedir. Sönümlemenin bozucu etkisini azaltan uzaysal çeşitleme tekniği bu sistemlerde irdelenmiştir. Çok-girişli çok-çıkışlı sistemlerin sağladığı performans kazancını korumak fakat donanım karmaşıklığını azaltmak için de genelleştirilmiş anten seçimi (AS) yapılmıştır. Uzaysal çeşitlemenin yararlarını sağlamak için yardımlaşmalı haberleşmede röle seçimi (RS) de incelenmiştir. İlk olarak çok antenli iki kaynaktan ve tek antenli bir HD AF röleden oluşan iki yönlü bir sistemde yavaş sönümlemeli Rayleigh kanallar için genelleştirilmiş AS çalışılmıştır. Sonraki adımda, bütün birimlerin çok antenli olduğu iki yönlü sistem, rölede alıcı/verici AS ve kaynaklarda genelleştirilmiş AS için incelenmiştir. Son olarak da FD DF tek antenli röle ve çok antenli FD iki kaynaktan oluşan iki yönlü sistem Rayleigh sönümleme için çalışılmıştır. Bu sistemde önceki sistemlerin aksine röle ve kaynaklar arasındaki yolların aynı olmadığı varsayılmış ve kaynaklarda iletim ve alım için bir çift anten seçen yeni bir alıcı-verici anten seçim yöntemi önerilmiş ve analiz edilmiştir. İncelenen diğer üç sistemde RS tek yönlü iletimin yapıldığı ağlarda incelenmiştir. Birinci çalışmada kaynak ve hedef arasında direk görüş hattının olup olmamasını da içerecek şekilde genelleştirilmiş RS ele alınmıştır. Bu sistemde FD iletim AF rölelerle Rayleigh kanallarda gerçekleştirilmiştir. Diğer iki sistemde ise NOMA tabanlı iletim için iki aşamalı RS yapılmıştır; birinci kullanıcının veri hızını sağlayan DF rölelerin alt kümesi belirlendikten sonra ikinci kullanıcının veri hızını maksimize eden röle seçilerek FD/HD iletim gerçekleştirilmiştir. İlki iki kaynaklı olup Nakagami-m sönümlemeli ortamlar için incelenirken ikincisi ise tek kaynaklı olup genelleştirilmiş-K dağılımlı ortamlar (gölgelemeli sönümleme) için çalışılmıştır. Her iki sistemde hatalı ardışık karışım iptali de ele alınmıştır. Son olarak, DF çok atlamalı sistem direk görüş hattının olup olmaması durumunda Nakagami-m kanal için revize edilmiştir.

Anahtar Kelimeler: Anten/Röle Seçimi (Uzay Çeşitlemesi), Dik-Olmayan Çoklu Erişim, Yarı/Tam Çift Yönlü Röle, Tek/Çift Yönlü Sistem, Yardımlaşmalı Çeşitleme.

ACKNOWLEDGEMENT

I would like to express my very deepest appreciation to my advisor Prof. Dr. Oğuz Kucur for his forever support, patience, motivation, and immense knowledge. Besides my advisor, I would like to extend my sincere thanks to the rest of my thesis steering committee members, Prof. İbrahim Altunbaş and Assist. Prof. Köksal Hocaoğlu.

I would also like to thank Assist. Prof. Ahmet Yılmaz, meanwhile an invaluable friend, for sharing his templates, advice, and assistance in reporting methodology.

Further, I would also like to thank to Turkish Scientific and Technological Research Council (TUBITAK) for supporting Chapter 7 and 8 of this dissertation with the project number 118E274. Meanwhile, I'm extremely grateful to my workplace, National Metrology Institute of Turkey (TUBITAK UME), for permission to get Ph.D.

Last but not the least, I would like to thank my wife Remziye and my children-Beyza Nur, Hümeyra Ayşe, Mihriban Betül, and Ali Etka–for their support and patience throughout this work.

TABLE OF CONTENTS

ABBREVIATIONS

Abbreviations and Acronyms		Explanations
5G	:	Fifth Generation
AF	:	Amplify–and–Forward
AS	:	Antenna Selection
BPSK	:	Binary Phase Shift Keying
CA	:	Channel–Assisted
CDF	:	Cumulative Distribution Function
CDMA	:	Code Division Multiple Access
CINB	:	Channel–Self–Interference–Noise–Based
CNA	:	Channel–Noise–Assisted
CRN	:	Cooperative Relaying Networks
CSI	:	Channel State Information
DF	:	Decode-and-Forward
DO	:	Diversity Order
EGC	:	Equal Gain Combining
FDMA	:	Frequency Division Multiple Access
GKD	:	Generalized– K distribution
GRAS	:	Generalized Receive Antenna Selection
GRS	:	Generalized Relay Selection
GSC	:	Generalized Selection Combining
GST	:	Generalized Selection Transmission
GSTDP	:	Generalized Selection Transmission with Direct-Path
GTAS	:	Generalized Transmit Antenna Selection
HD	:	Half–Duplex
INR	:	Interference–to–Noise Ratio
i.i.d.	:	Independent Identically Distributed
i.n.i.d.	:	Independent Non–Identically Distributed
INR	:	Self–Interference-Plus-Noise Ratio
ipSIC	:	Imperfect Successive Interference Cancellation
JTRAS	:	Joint Transmit and Receive Antenna Selection

LOS	:	Line-Of-Sight
MAT	:	Multiple Access Technique
MGF	:	Moment Generating Function
MIMO	:	Multi-Input Multi-Output
mmWave	:	Millimeter–Wave
M-AM	:	M–Ary Amplitude Modulation
M-PSK	:	M–Ary Phase Shift Keying
M-QAM	:	M–Ary Quadrature Amplitude Modulation
MRC	:	Maximal Ratio Combining
MRT	:	Maximal Ratio Transmission
MWHM	:	Max–Weighted–Harmonic–Mean
NOMA	:	Non–Orthogonal Multiple Access
OFDM	:	Orthogonal Frequency Division Multiplexing
OFDMA	:	Orthogonal Frequency Division Multiple Access
OMA	:	Orthogonal Multiple Access
OOP	:	Overall Outage Probability
OP	:	Outage Probability
PA	:	Power Allocation
PDF	:	Probability Density Function
PHY	:	Physical
PRS	:	Partial Relay Selection
pSIC	:	Perfect Successive Interference Cancellation
QoS	:	Quality of Service
RAS	:	Receive Antenna Selection
RF	:	Radio Frequency
RV	:	Random Variable
SAF	:	Selection Attenuation (Amplification) Factor
SC	:	Selection Combining
SDMA	:	Spatial Division Multiple Access
SER	:	Symbol Error Rate
SI	:	Self–Interference
SIC	:	Successive Interference Cancellation
SINR	:	Signal–to–Interference-Plus-Noise Ratio

SNR	:	Signal–to–Noise Ratio
SOP	:	Sum Outage Probability
SSC	:	Switch and Stay Combining
SSER	:	Sum Symbol Error Rate
SSRS	:	Single-Stage Relay Selection
TAS	:	Transmit Antenna Selection
TDMA	:	Time Division Multiple Access
TRAS	:	Transceiver Antenna Selection
TSRS	:	Two Stage Relay Selection
TWRN	:	Two Way Relaying Network
WDMA	:	Wavelength Division Multiple Access
WMM	:	Weighted–Max–Min

LIST OF FIGURES

LIST OF TABLES

1. INTRODUCTION

Improvement of coverage area, reduction of power consumption, effective utilization of bandwidth (spectral efficiency), services with high data rates, and massive connectivity are the main factors to be satisfied in the next-generation wireless communication systems. Relaying transmission, which has recently been accepted by several standards such as IEEE 802.11s, IEEE 802.16j, and long term evolution-advanced (LTE-advanced), is offered to broaden the coverage area, consume less power and overcome channel impairments due to fading in a wireless communications system [1]. On the other hand, to overcome exponentially growing mobile data volume, simultaneous transmission of different data types is the key factor in the fifth-generation (5G) communication systems and beyond [2]. The volume of worldwide mobile data has been predicted to be about 136 exabytes or 5 zettabytes per month [3,4]. This enormously growing demand means more spectrum should be used. But more spectrum is only possible in millimeter-wave (mmWave) bands, however, transmission in mmWave bands comes with many challenges in addition to small-scale fading such as high path losses, blockages, and poor signal diffraction properties [5].

Diversity is an effective way to combat fading, which is the main impairment that deteriorates system performance since diversity makes several replicas of the same information-bearing signal available for the receiver in order to utilize to increase signal-to-noise ratio (SNR). For this reason, multi-relay and multi-antenna diversity schemes, later one is named as multi-input multi-output (MIMO) transmission technique, are used in wireless communication systems. MIMO transmission technique enhances error performance and capacity [6, 7], likely, orthogonal frequency division multiplexing. Additionally, cooperative communication is another method of providing benefits of spatial diversity.

Half-duplex (HD) one way relaying systems improve coverage area, reduce power consumption, and provide spectral efficiency, but they cause some reduction of spectral efficiency since two-time slots are required per single transmission. Two-way relaying network (TWRN) was proposed to overcome this reduction of spectral efficiency [8], which can be recovered by simultaneously exchanging information between two sources via a relay in two-time slots. Moreover, when the two-way transmission is carried out at the region of high spectral efficiency, it also provides higher energy efficiency than direct transmission and one-way relay transmission [9]. Hence, new systems that improve

spectral efficiency further and compensate for the shortcomings of HD systems should be adapted. For this reason, full-duplex (FD) systems are offered to improve achievable spectral efficiency by always transmitting and receiving in the entire bandwidth [10]. Theoretically, this means doubling capacity as compared to HD systems. However, as a drawback, this gain is limited by self-interference (SI) due to the large power difference between the power imposed by own transmissions and the low-power received signals arriving from remote transmit antennas. This SI may result in lower capacity than that of HD systems. Therefore, SI cancellation is a critical issue, which is usually classified into passive such as antenna separation, and active suppression such as analog and digital cancellation [11]. Generally, applying single SI cancellation is not adequate, therefore, two or more techniques are used together for improving system performance. Another, issue that cannot be addressed by the stated techniques is the sharing of block sources like time slots and frequency bands. Wasting of such sources disturbs researchers and, to cope with this un-solicited status, eventually, non-orthogonal multiple access (NOMA) technique has been offered for high spectral efficiency, low-latency, reliable, and fairness wireless connectivity [12–15]. Application of NOMA can be implemented in different domains such as code and power domains or mixed of them [16], where superposed signals can be simultaneously received (up-link NOMA) or transmitted (down-link NOMA). In the code domain, a unique spreading code is assigned to each user, similarly, a portion of the total power is assigned to each user in the power domain. Successive interference cancellation (SIC) is used to separate the superposed signals. However, due to the limited processing power at the end-users, power domain NOMA seems to be the dominant choice and gain more attention in the literature: Two different power allocation (PA) strategies, namely, assigning more power to the users having poor channel conditions or allocating power in accordance with quality of service (QoS) requirements, where PA factors may be independent of channel state information (CSI) or not.

To increase the communication quality MIMO transmission is used in mobile networks, namely, point-to-point, one way and two-way relay networks. The performance of TWRN with multi-antenna sources has been investigated in several works [17–21]. Similarly, beamforming, where the signal from multiple antennas are weighted according to the instantaneous channel coefficients, is applied at end sources to benefit from advantages of MIMO communications to enhance performance and reliability of communication between end sources [22–24]. However, beamforming needs a radio frequency (RF) chain for each antenna and complex signal processing techniques which mean high cost and complexity. To decrease complexity and cost by reducing the number

of RF chains, and use advantages of multiple antennas, antenna selection (AS) strategy was also proposed [25]. AS reduces the complexity and power requirements of the MIMO transmitter [26]. Several studies have focused on a single AS in sources or relay selection (RS) [26–34]. In almost all analyses of TWRNs, forward and backward paths between the sources and relay are assumed to be reciprocal which makes analyses to be asymptotic but in practice, they are never the same.

Similar to AS, RS is also an attractive and effective technique to enhance the performance of multi-relay communication systems in terms of lower power consumption and better symbol error rate (SER). It has been shown that RS significantly improves system performance since the number of relays increases diversity order and selection introduces lower hardware complexity [35]. Additionally, relayed communication is an attractive method for secure communication and different RS schemes are offered to analyze security-reliability trade-off, where it is proven that offered RS strategies outperform opportunistic RS in terms of security-reliability trade-off analysis [36–40]. The notion of selecting a relay in two-stages for security-reliability trade-off analyses has been adapted to NOMA based relayed communication systems [41–49].

In brief, firstly, to maintain the aforementioned advantages gained by the implementation of TWRNs, i.e, coverage extension, power reduction, capacity enhancement, and spectral efficiency improvement, generalized AS at both multi-antenna sources and AF relay is considered for TWRNs with HD transmission protocol [50–53]. Although AS reduces complexity and power requirements of the MIMO transmitter/receiver with respect to beamforming, AS results in a performance loss, which is generally the main target to be accomplished in proposed communication systems. As a solution, generalized AS, a compromise between beamforming and single AS, has been offered and analyzed in this thesis for HD AF TWRNs over independent identically distributed (i.i.d.) slow Rayleigh fading channels. Secondly, to improve spectral efficiency further while preserving achievements got by AS, single AS is offered and investigated in FD TWRNs over i.i.d. Rayleigh fades [54, 55]. Additionally, reciprocity assumption which is not the case in practical implementation is released to not asymptotically but exactly analyze the system under consideration. Thirdly, generalized RS implementing amplify-and-forward (AF) protocol is aimed and presented in one way relayed networks over independent non-identically distributed (i.n.i.d.) Rayleigh fades with also the inclusion of direct path (DP) which cannot be ignored even if it has too weak signal [56]. Since, in practice, i.i.d. fading channels are rare owing to the insufficient physical separations among relays and analysis of

decode-and-forward (DF) relaying is mathematically tractable, however, the reality of power-limited and/or complexity-limited nodes may hinder the practical implementation of DF relaying. Moreover, AF relaying has no decoding/re-encoding module to detect received signals, which means a much simpler amplifying and forwarding process can be achieved by AF relaying. Therefore, generalized RS with AF protocol and i.n.i.d. case is introduced, where DP is also taken into consideration. Fourthly, RS in one way multi-relay networks using NOMA is almost considered over Rayleigh fades, however, in practice, such fades are rarely happening. Hence, a more comprehensive model such as i.n.i.d. Nakagami-m fade as done in this thesis should be assumed together with the fact that perfect successive interference cancellation (SIC) is impossible, therefore, imperfect SIC situation also needs to be considered [57, 58]. Fifthly, the use of mmWave bands in 5G communication systems and beyond is unavoidable. However, transmission in mmWave bands gives rise to high path loss, blockages, and poor diffraction properties, where attenuation in the range 28 dB–40 dB takes place. Therefore, modeling the wireless medium even as Nakagami-m fade remains inadequate, in sequence, analyses depending on such distribution models avoid a comprehensive understanding of transmission techniques. Thereby, systems under consideration should be investigated for both small-scale and large-scale faded transmission medium. To model such environments, composite distributions such as Rayleigh/Log-normal, Rician/Log-normal, and Nakagami/Log-normal are proposed, however, it is mathematically intractable to analyze systems for such composite distributions. As an approximation, generalized-K distribution (GKD) is offered and RS with NOMA technique is presented for HD and FD transmission protocols with both perfect and imperfect SIC [59, 60]. Finally, the performance of multi-hop networks over i.n.i.d. Nakagami-m environment for DF protocol is revised to obtain simpler expressions for outage probability (OP), moment generating function (MGF), symbol error rate (SER), and ergodic capacity (achievable rate) [61].

The organization of this dissertation is as follows: The concepts and techniques used through this work are briefly mentioned in Chapter 2, the performance of two-way relay networks with generalized transmit and receive antenna selection (GST (MRT) and GSC) is investigated in Chapter 3, the performance of two-way AF MIMO relay networks with single and multiple antenna selection schemes (TAS/GSC and GST (MRT)/RAS) is provided in Chapter 4, the performance of transceiver antenna selection (TAS and RAS) in two way FD relay networks is presented in Chapter 5, the generalized relay selection (GST (MRT)) in unidirectional FD relay networks is demonstrated in Chapter 6, two-stage

HD/FD relay selection with imperfect SIC for NOMA based cooperative networks, where two sources transmit data to two end users via multiple relays, over Nakagami-m fading channels is illustrated in Chapter 7, two-stage HD/FD relay selection with imperfect SIC for NOMA based cooperative networks over shadowed fading channels, namely, generalized-K fade channels is analyzed in Chapter 8, where single source transmits data to two end users via multiple relays, DF multi-hop systems with/out DP between the source and destination are revised in Chapter 9, and the deductions of studied issues are given in Chapter 10.

2. CONCEPTS AND TECHNIQUES USED THROUGH THE THESIS

The basic concepts and techniques considered through this thesis, namely type of fading channels and their statistical descriptions, duplexing techniques, forwarding protocols, multiple access schemes, diversity strategies, combining methods, and performance measures such as ergodic capacity, outage probability, and symbol error rate are briefly introduced in this chapter.

2.1. Fading (Short-Term Fading) and Shadowing (Long-Term Fading)

In wireless communications, due to the obstacles such as buildings, trees, and other structures between the transmitter and the receiver, the signals reach the receiver after undergoing scattering, diffraction, reflection which means the transmitted signal is attenuated and absorbed. The multi-path attenuated incoming signals are reached to the receiver. The amplitude and phase of each multi-path are treated as a random variable, thereby, the instantaneous fluctuated received power is also a random variable. If the period of power fluctuations is very short, it is identified as short-term fading. This is where multiple scattering does not take place. However, signals may reach the receiver after multiple scattering which is the case the signal in the path encounters more than one object in its path. This phenomenon causes fluctuations in power to be longer than that of short-term fading and identified as long-term fading or shadowing. In short, short-term fading results in random fluctuations in instantaneous power, long-term fading leads to randomness in the average power. Signal degradation arises from fading and shadowing individually as well as the simultaneous existence of fading and shadowing. Several models are available in the literature for the description of the random variations in signal power. Therefore, it is important to accurately model the communication system under consideration. The models assumed through this dissertation are considered as slow, hence, fading does not alter the frequency characteristics or bandwidth capability of the channel. In other words, channels are considered as flat, where the relative speed of the transmitter/receiver is negligible, unlike the fast channels [62].

2.1.1. Statistical Models for Fading Channels

Several statistical models have been offered to describe the fading mobile media such as Rayleigh, Rician, Nakagami, Gamma, Generalized Gamma, and Weibull. In this thesis, Rayleigh and Nakagami-m models are used for short-term fading channels. Thereby, only the PDFs for the considered channels are provided.

For Rayleigh fade environments, the PDF of the received signal envelope, herein after through this chapter X represents the received signal envelope, is [63]

$$f_R(x) = \frac{x}{\sigma^2} e^{-\frac{x^2}{2\sigma^2}}, \tag{2.1}$$

where $x \geq 0$ and σ^2 is the scale parameter of the distribution and subscript R means Rayleigh distribution. Since the amplitude of the received signal is Rayleigh distributed, its square has exponential distribution, where the notation $Y = X^2$ is preferred to represent it, and the related PDF is

$$f_E(y) = \frac{1}{2\sigma^2} e^{-\frac{y}{2\sigma^2}}, \tag{2.2}$$

subscript E stands for exponential distribution and its variance is $2\sigma^2$. Moreover, the cumulative distribution function (CDF) of Y is

$$F_E(y) = 1 - e^{-\frac{y}{2\sigma^2}}. \tag{2.3}$$

Another critical model which includes many distributions as special cases in it is Nakagami-m distribution [64]. Its PDF is in the following format:

$$f_N(x) = \frac{2m^m x^{2m-1}}{\Omega^m \Gamma(m)} e^{-\frac{m}{\Omega}x^2}, \tag{2.4}$$

where N stands for the Nakagami-m distribution, $x \geq 0$, $m \geq 1/2$ and Ω are shaping and scaling factors, respectively, and the gamma function is $\Gamma(m) = \int_0^\infty t^{m-1} e^{-t} dt$ [65, eq. (8310.1)]. Square of a Nakagami-m RV is a Gamma RV whose PDF becomes

$$f_G(y) = \frac{m^m y^{m-1}}{\Omega^m \Gamma(m)} e^{-\frac{m}{\Omega}y}, \tag{2.5}$$

the subscript G represents the Gamma distribution and its CDF is

$$F_G(y) = \frac{\gamma\left(m, \frac{m}{\Omega}y\right)}{\Gamma(m)}, \tag{2.6}$$

where $\gamma(m, y) = \int_0^y t^{m-1}e^{-t}dt$ is the lower incomplete gamma function [65, eq. (8.350.1)].

2.1.2. Statistical Models for Shadowed Fading Channels

Variation of local power from point-to-point within a region is a result of shadowing which takes place because of terrain, buildings, structures, and so on. Briefly, deterministic mean power is lost because of shadowing. Thereby, it should be modeled as a RV. Shadowing is modelled as Lognormal distribution. However, it is not logical to individually treat a channel as only faded or shadowed. Consequently, simultaneous effect of fading and shadowing should be taken into account. For this reason, composite channels models are offered such as Nakagami-Lognormal, Nakagami-inverse-Gaussian, generalized Gamma, generalized-K (Nakagami-Gamma), and so on. Since other models are not mathematically tractable, in this dissertation, generalized-K is considered. Its PDF is [66]

$$f_{GK}(x) = \frac{4}{\Gamma(m_f)\Gamma(m_s)} b^{m_f+m_s} x^{m_f+m_s-1} K_{m_s-m_f}(2bx), \tag{2.7}$$

where GK stands for generalized-K distribution, $x \geq 0$, $b = \sqrt{\frac{m_f m_s}{\Omega_f \Omega_s}}$, and $m_f \geq 1/2$ and $m_s > 0$ are respectively fading and shadowing shape factors. Similarly, Ω_f and Ω_s are fading and shadowing scaling factors, respectively. $K_\nu(x)$ is the ν^{th} order modified Bessel function of the second kind [65, eq. (8.432.6)]. Hence, PDF related to its square turns to

$$f_{GK}(y) = \frac{2}{\Gamma(m_f)\Gamma(m_s)} b^{m_f+m_s} y^{\frac{m_f+m_s}{2}-1} K_{m_s-m_f}(2b\sqrt{y}). \tag{2.8}$$

Using the identity [67, eq. 1.12.1.2], the CDF for square of a generalized-K RV is derived as follows:

$$\begin{aligned} F_{GK}(y) =& \frac{\Gamma(m_s-m_f)(b^2y)^{m_f}}{\Gamma(m_s)\Gamma(m_f+1)} {}_1F_2(m_f; m_f-m_s+1, m_f+1; b^2y) + \\ & \frac{\Gamma(m_f-m_s)(b^2y)^{m_s}}{\Gamma(m_f)\Gamma(m_s+1)} {}_1F_2(m_s; m_s-m_f+1, m_s+1; b^2y), \end{aligned} \tag{2.9}$$

where ${}_1F_2(m;\nu,n;x)$ is the generalized hypergeometric function [65, eq. (9.14.1)].

2.2. Duplexing Techniques

In wireless communication, the sharing of different directions of communication is named as duplexing. Systems that can only be used in one direction are called simplex. A half-duplex system uses the same frequencies at least at two-time slots in both directions to provide exchanging of information between end-users, where only one direction can be used at a time. But a full-duplex system uses the same frequencies at the same time in both directions to convey the information to end-users. This means capacity is theoretically doubled since the full bandwidth can be used in both directions simultaneously. However, SI lowers this gain. In this thesis, both of FD and HD transmission protocols are investigated for bidirectional and unidirectional relayed networks. HD transmission is accomplished in two-time slots.

2.3. Forwarding Protocols

There are three forwarding strategies, namely, compress-and-forward (CF), decode-and-forward (DF), and amplify-and-forward (AF) [68]. CF method quantizes the received signal and after mapping, forwards it to the destination. DF, also known as detect-and-forward in case of usage of uncoded modulation, means that the relay in between decodes and re-encodes the received signal, and then transmits it to the destination. AF is the power normalization process of the receipt signal at the relay without any decoding/detecting process. Firstly, the power of the received signal is normalized so that it has unit power, and thereafter, it is amplified to maintain a fixed average transmit power. While compares to DF and CF forwarding protocols, in addition to the need for less processing power, AF scheme also requires much less processing delay.

DF and AF protocols are used in this dissertation.

2.4. Multiple Access Techniques

Sharing of the resource blocks such as frequency band and time slots between distinct users is described as a multiple access technique (MAT). MAT allows for many users

at one time by sharing finite resource blocks [16]. MAT can be done in three domains, namely, code, frequency, and time. The well known two basic multiple access methods are frequency division multiple access (FDMA) and time division multiple access (TDMA). In FDMA, the total bandwidth is divided into many narrower bands and each user is allocated a unique band. Similarly, in TDMA, a period is subdivided into smaller time slots where each of them is assigned to unique users. Wavelength division multiple access (WDMA), which is related to FDMA, used in optical fiber communication systems to partition channels. Another type of MAT is spatial division multiple access (SDMA), where sectored base station antenna is used as multiple radiators to simultaneously form multiple beams. The last and most used technique is orthogonal frequency division multiple access (OFDMA) where users' signals are orthogonal in the frequency and/or time domains. OFDMA is an extension of the orthogonal frequency division multiplexing (OFDM) architecture. Multiple access is achieved in OFDMA by assigning subsets of subcarriers to individual users. The methods mentioned so far are identified as orthogonal multiple access (OMA) techniques. The orthogonality of the physical (PHY) layer is the underlying design principle of today's standards up to 5G. However, orthogonality poses significant challenges to 5G systems and beyond in which a massive number of users have to be served. Hence, non-orthogonal multiple access (NOMA) technique is offered for 5G networks and beyond. Note that code division multiple access (CDMA) is a NOMA method which utilizes codes to separate the users over the same channel [69]. The basic concept behind NOMA is to serve more than one user in the same resource block, e.g., a time slot, subcarrier, spreading code, or space. With this, NOMA promotes massive connectivity, lowers latency, improves user fairness and spectral efficiency, and increases reliability compared to OMA techniques [70].

Both of OMA and NOMA are used in this dissertation. Power domain NOMA is implemented, especially, quality of service (QoS), i.e., fixed power allocation (PA) NOMA is used in the systems under consideration in this dissertation. PA in NOMA depends on what point (rate pair) in the capacity region is being targeted, and depending on that specific point, the amount of power allocated to the user with the weaker channel can be higher than, equal to, or less than that of the other user [70].

2.5. Diversity Techniques

Both fading and shadowing lead to increased outage and error rate. Using the fact that multiple independent copies of the same signals are unlikely to face deep

fading simultaneously, i.e., it is statistically unlikely that all of them would have a low signal-to-noise ratio (SNR) / signal-to-interference-plus-noise ratio (SINR), thereby, diversity techniques are developed to mitigate detrimental effects of fading and shadowing. Diversity techniques constitute multiple versions of the transmitted signals. Thus, the basic idea of diversity is a repetition or redundancy of information. The improvement in performance obtained through diversity techniques depends on the modulation and coding techniques used for data transmission. In short, diversity implies a set of versions of the transmitted signal, and this set is accomplished through space (spatial), frequency, polarization, time (signal repetition), and multipath/Rake (a form of time diversity) diversity. The uncorrelatedness/independence of received signals is the key factor for the improvement in performance expected from diversity schemes. The main diversity techniques are summarized below:

Space Diversity: Spatial diversity is accomplished by multiple transmitters or receivers placed at different spatial locations, resulting in different received signals, which are desired to be independent or uncorrelated. This can be reached by sufficiently separated transmitters or receivers. Multi-antenna networks are important examples of spatial diversity method, which are investigated through this dissertation.

Frequency Diversity: Frequency diversity is attained by transmitting the same information signal on different carriers. The separation between the carriers must be at least equal or larger than the coherence bandwidth of the channel to ensure uncorrelatedness/independence of the received signals. But larger separations implies a reduction in bandwidth available for data transmission. Therefore, a trade-off between maximum available bandwidth for transmission and several diversity branches comes out.

Polarization Diversity: Polarization diversity depends on the orthogonality of the electric and magnetic fields of the signal carrying the information, which is modified to send the same information. These orthogonal fields provide uncorrelated behavior and hence independence of the received signals. Therefore, designing the receiver with two antennas for each polarization results in a diversity of order two. Unlike space diversity, a separation between antennas is not required since the two polarizations are orthogonal and ensure uncorrelatedness/independence of the received signals.

Time Diversity: Time diversity is applied by multiple times transmission of the same information signal. The separation between the transmission times should be greater than

the coherence time, which is dependent on the speed of the transmitter/receiver, to get uncorrelated/independent versions of the transmitted signal. Repeated transmission of the same information and subsequent processing produces time delay. Because of this, time diversity is not much preferable to other schemes and often used sparingly.

Multipath/Rake Diversity: This diversity scheme practically becomes applicable by the aid of Rake receiver. Well known that fading results in multipath signals at the receiver which are normally not resolvable. Fortunately, these signals can be resolvable by increasing the signal bandwidth further than channel bandwidth, hence, the width of the transmitted signals is small enough so that the received multipath signals become resolvable at the receiver side. These resolvable multipath signals result in a form of time diversity providing uncorrelated copies without the cost of time delay, i.e., without suffering from the latency effects associated with conventional time diversity [71].

In addition to the implementation of the space diversity methods, namely, antenna and relay diversities, in the HD/FD systems through this thesis, multipath diversity is also applied for the FD transmission over the multi-relay unidirectional system with generalized relay section where the direct path between the source and destination is not omitted, leading to the cooperative diversity [1].

2.6. Combining Methods

Implementation of diversity schemes results in many versions of the transmitted or received signal at the receiver. Diversity can be employed at the transmitter site as shown in Fig. 2.1 and similarly at the receiver site as illustrated in Fig. 2.2, namely, transmit and receive diversities are elaborated for spatial diversity. To maximize e2e SNR/SINR, the maximal ratio transmission (MRT) scheme is applied in conjunction with transmit diversity where the same signal is weighted on each branch and then broadcasted to the receiver. The weighting process is also demonstrated by multiplication of the input signal with a weight coefficient of w_i for i^{th} path in Fig. 2.1, where its value is the normalized complex conjugate of channel gain between transmit and receive antenna (of the sources and relay) in point to point networks (two-way relayed networks) and again normalized complex conjugate of the product of first and second hop channel gains in unidirectional relayed networks. These are the examples demonstrated in this dissertation. Different choices of weighting coefficients are dependent on the design of the system under consideration.

By the way, to enhance the performance, various signal processing methods should

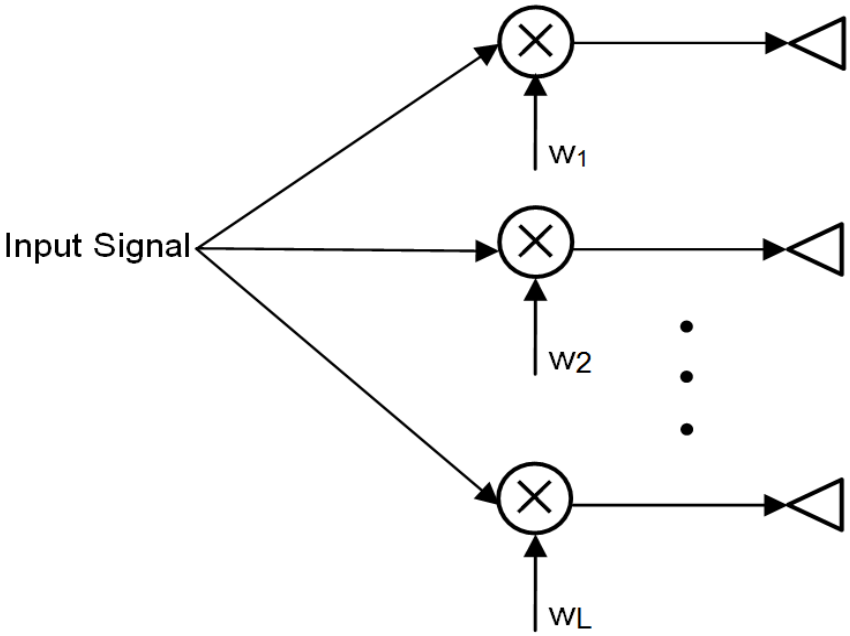

Figure 2.1: Transmit diversity and maximal-ratio transmission concept are shown.

be developed and implemented together with diversity techniques to merge these multiple copies to lower the error rate and OP. The combining process takes place on the receiver site, hence, it is embodied in conjunction with receive diversity in Fig. 2.2, where g_i is the i^{th} branch weighting factor and its value depends on the utilized combining technique. Combining methods are selection combining (SC), maximal ratio combining (MRC), equal gain combining (EGC), and switch and stay combining (SSC) [72–74].

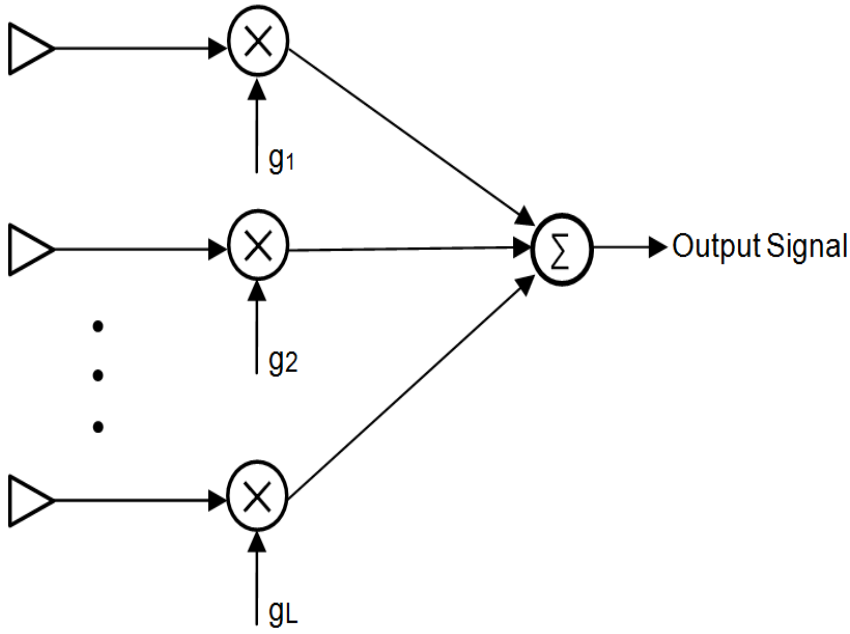

Figure 2.2: Receive diversity and combining concept are illustrated.

Maximal Ratio Combining: The incoming signals are combined so that the output SNR/SINR is maximized. The weight of each path is made proportional to the rms signal level and inversely proportional to the mean square noise/interference-plus-noise level in that channel [72]. In order to apply MRC, all channel fading parameters have to be known to the receiver. Although this scheme can be used for coherent modulations with unequal energy signals, it is not practical for differentially coherent and non-coherent detection.

Equal–Gain Combining: In this scheme, each received signal is weighted with the same gain. Although knowledge of the fading amplitudes is not required unless unequal energy signals are transmitted, co-phasing of all signals is needed to avoid signal cancellation. While compares to MRC scheme, complexity is reduced but it can only be implemented with coherent modulations having equal-energy symbols.

Selection Combining: SC chooses the branch with the maximum SNR/SINR. Therefore, it is the simplest and most commonly used scheme. Since it processes only one of the diversity branches, unlike MRC and EGC, the need for more RF chains is omitted. In addition to coherent modulations, it can be implemented with differentially coherent and non-coherent modulations.

Switch and Stay Combining: Unlike SC, the receiver does not continuously choose the path with the maximum SNR/SINR, it selects a particular path until SNR/SINR drops below a predetermined threshold. Hence, the implementation of SSC is practical in the systems using uninterrupted transmission such as FDMA systems. This makes SSC more preferable than SC.

Types of selection schemes vary with the number of selected antennas/relays, namely, single transmit/receive antenna or relay selection (TAS, RAS, RS), joint transmit and receive antenna selection (JTRAS), generalized transmit-antenna/relay selection known as generalized selection transmission (GST), generalized receive antenna selection described as generalized selection combining (GSC), and many combinations of them take place such as TAS/GSC and GST/RAS. Nearly all the mentioned methods are examined through this thesis in conjunction with MRC and SC schemes.

2.7. Performance Measures

In this dissertation, quantitative performance measures are limited to SER, OP, and ergodic capacity. Improvements in second-order statistical characteristics such as amount of crossings and fade duration are not covered.

To quantify the stated measures, the equivalent overall SNR/SINR of the network under the consideration, its PDF and CDF are represented as γ_{eq}, $f_{\gamma_{eq}}(x)$, and $F_{\gamma_{eq}}(x)$, respectively.

2.7.1. Ergodic Capacity

The normalized Shannon capacity for FD and HD systems is

$$C(\gamma_{eq}) = \frac{1}{R_0}\log_2(1+\gamma_{eq}). \tag{2.10}$$

In (2.10), $R_0 = 1$ and $R_0 = 2$ for FD and HD transmissions, respectively. The average capacity, i.e., ergodic capacity is derived based on CDF method as [75, eq. (38)]

$$\begin{aligned} R_{avg.} &= \mathbb{E}[\frac{1}{R_0}\log_2(1+\gamma_{eq})] \\ &= \frac{1}{R_0}\int_0^\infty \log_2(1+x) f_{\gamma_{eq}}(x)dx \\ &= \frac{\log_2(e)}{R_0}\int_0^\infty \frac{1-F_{\gamma_{eq}}(x)}{x+1}dx, \end{aligned} \tag{2.11}$$

where $\mathbb{E}[\cdot]$ denotes the expectation operator.

2.7.2. Outage Probability

The overall system is in outage if instantaneous capacity is less than a minimum required data rate, R_{th}, in turn, the instantaneous equivalent SNR/SINR, γ_{eq}, is less than a SNR/SINR threshold, γ_{th}. In other words, outage happens when instantaneous equivalent SNR/SINR is lower than the minimum SNR/SINR required to maintain an acceptable level of the average probability of error. Mathematically, OP is

Table 2.1: Modulation type dependent parameters for M-AM, M-QAM, and M-PSK SER calculations.

Parameter	M-AM	M-QAM	M-PSK
a_1	$\frac{2(M-1)}{\pi M}$	$\frac{\pi}{4}\left(1-\frac{1}{\sqrt{M}}\right)$	$\frac{1}{\pi}$
a_2	0	$-\frac{\pi}{4}\left(1-\frac{1}{\sqrt{M}}\right)^2$	0
θ_1	$\frac{\pi}{2}$	$\frac{\pi}{2}$	$\frac{(M-1)\pi}{M}$
θ_2	0	$\frac{\pi}{4}$	0
λ_{mod}	$\frac{3}{(M^2-1)}$	$\frac{3}{2(M-1)}$	$\sin^2(\pi/M)$
Q	1	2	1

$$\begin{aligned} P(\gamma_{th}) &= Pr(\frac{1}{R_0}\log_2(1+\gamma_{eq}) < R_{th}) \\ &= Pr(\gamma_{eq} < \gamma_{th} = 2^{R_0 R_{th}-1}) \\ &= \int_0^{\gamma_{th}} f_{\gamma_{eq}}(x)dx \\ &= F_{\gamma_{eq}}(\gamma_{th}), \end{aligned} \tag{2.12}$$

where $Pr(\cdot)$ stands for probability and note that $\gamma_{th} = 2^{R_0 R_{th}-1}$ is straightforward.

2.7.3. Symbol Error Rate

Average SER of slow-fading channels for coherent modulations is only aimed which can be derived based on Gaussian Q-function and equivalent PDF of the overall system which is transformed into form of moment generating function (MGF) [74, eq. (5.2)]. Average SER of M-ary phase shift keying (M-PSK), M-ary amplitude modulation (M-AM), and square M-ary quadrature amplitude modulation (M-QAM) can be evaluated based on MGF method as

$$P_{M,SER} = \sum_{q=1}^{Q} a_q \int_0^{\theta_q} M_{\gamma_{eq}}\left(-\frac{\lambda_{\text{mod}}}{\sin^2(\theta)}\right) d\theta, \tag{2.13}$$

where the equivalent MGF, $M_{\gamma_{eq}}(s) = \int_0^\infty f_{\gamma_{eq}}(x)e^{sx}dx$. a_q, θ_q, and λ_{mod} are modulation type dependent parameters given in Table 2.1.

Additionally, average SER of exact binary phase keying (BPSK) and approximated M-PSK is also computed based on CDF method as follows:

$$P_{C,SER} = \frac{a\sqrt{b}}{2\pi}\int_0^\infty x^{-1/2}e^{-bx}F_{\gamma_{eq}}(x)dx, \tag{2.14}$$

where $a = 1$ and $b = 1$ for BPSK, and for approximated M-PSK, $a = 2$ and $b = \sin^2(\pi/M)$.

Two type modulations, namely, M–PSK and M–QAM are investigated through this dissertation.

3. TWO-WAY RELAY NETWORKS WITH GENERALIZED TRANSMIT AND RECEIVE ANTENNA SELECTION OVER RAYLEIGH FADING CHANNELS

3.1. Introduction

In wireless communications, fading is the main impairment that deteriorates system performance. Diversity is an effective way to combat fading since diversity makes several replicas of the same information bearing signal available for the receiver to utilize in order to increase signal-to-noise ratio (SNR). For this reason, multi-antenna diversity schemes, i.e., multi-input multi-output (MIMO) transmission techniques are used in wireless communication systems [6, 7]. MIMO transmission techniques enhance error performance and capacity. Meanwhile, recently in order to have coverage extension and power reduction, cooperative relaying has been offered for wireless communications [76]. Although half-duplex one way relaying systems improve aforementioned parameters, they cause some reduction of spectral efficiency since two time slots are required per single transmission. Two way relaying network (TWRN) was proposed to overcome this reduction of spectral efficiency [8], which can be recovered by simultaneously exchanging information between two sources via a relay in two time slots. Moreover, when two way transmission is carried out at the region of high spectral efficiency, it also provides higher energy efficiency than direct transmission and one-way relay transmission [9].

In order to increase the communication quality in TWRNs, MIMO transmission can be used. The performance of TWRN with multi-antenna sources has been investigated in several publications [17–21]. Beamforming, where the signal from multiple antennas are weighted according to the instantaneous channel coefficients, is applied at end sources to benefit from advantages of MIMO communications in order to enhance performance and reliability of communication between end sources [22–24]. However, beamforming needs radio frequency (RF) chain for each antenna and complex signal processing techniques which mean high cost and complexity. In order to decrease complexity and cost by reducing number of RF chains, and use advantages of multiple antennas, antenna selection strategy was also proposed [25]. Antenna selection reduces complexity and power requirements of the MIMO transmitter [26]. Several studies have focused on a single antenna selection in sources or relay selection [26–34]. However, to the best of our

knowledge, generalized antenna selection, which is a compromise between beamforming and single antenna selection, at TWRN has not been examined yet. Thus, we propose to use generalized transmit antenna selection (GTAS) for transmission and generalized receive antenna selection (GRAS) for reception at sources of TWRN whose relay is with single antenna as depicted in Fig. 3.1. By GTAS and GRAS we mean combined transmit antenna selection (TAS)/maximal ratio transmission (MRT) [77] and generalized selection combining (GSC) [78], respectively.

In this chapter, we consider a MIMO TWRN where an N_A-antenna source A and an N_B-antenna source B exchange information via single antenna relay R using amplify-and-forward (AF) protocol. L_i, $i \in \{A, B\}$, antennas are selected at each source for transmission and reception, i.e., this TWRN is examined for two phases by using GTAS and GRAS for transmission and reception, respectively at sources over Rayleigh fading channels. The main contributions of this chapter can be summarized as follows:

- The exact and asymptotic sum outage probability (SOP), moment generating function (MGF), and sum symbol error rate (SSER) for M-ary phase shift keying (M-PSK) and M-ary quadrature amplitude modulation (M-QAM) are derived.
- It is proven that the diversity order of the proposed antenna selection strategy is $\min(N_A, N_B)$.
- The number of RF chains is reduced from $N_A + N_B$ to $L_A + L_B$ with respect to beamforming, i.e., hardware complexity is reduced.
- The dependency of SSER on power allocation, relay location, and total number of antennas and number of selected antennas at each source is illustrated. It is shown that an increment in the number of selected or total number of antennas for any source causes some shift in optimum relay location towards other source with fewer number of selected antennas or total number of antennas. Similarly, assigning more power to any source also causes some shift in optimum relay location towards the other one. Furthermore, it is presented that assigning equal power to the sources and less or more power to the relay has no effect on optimum relay location but it affects SSER.

The rest of this chapter is organized as follows. The system model and the proposed antenna selection strategy are presented in Section 3.2. In Section 3.3, the exact and asymptotic cumulative distribution functions (CDF) of end-to-end (e2e) SNR are derived. The exact and asymptotic expressions for SSER are also derived. Numerical results are presented in Section 3.4 and we conclude our work in Section 3.5.

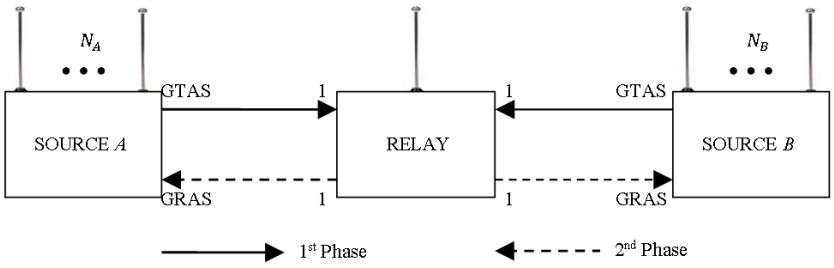

Figure 3.1: The proposed generalized antenna selection scheme.

3.2. System Model

We focus on an AF MIMO TWRN with an N_A-antenna source A and an N_B-antenna source B which communicate via a single antenna relay R. We assume that there is no direct link between these two sources because of heavy channel conditions. All nodes are assumed to be half-duplex and also let h_m^i be the complex channel gain between the relay and the m^{th} transmit antenna of source i, where $i \in \{A, B\}$. We assume that $\{h_m^i, m = 1, \ldots, N_i\}$ are independent identically distributed (i.i.d.) and circularly symmetric Gaussian random variables which are modeled as $h_m^i \sim CN(0, d_{iR}^{-f_i})$, where d_{iR} is the normalized distance between source i and the relay (i.e., $d_{AR} + d_{BR} = 1$) and f_i is the path loss exponent between source i and the relay. We assume errorless estimation of channel coefficients at the relay and error free feedback channels. Channels of source i–relay R and relay R–source i, $i \in \{A, B\}$ are also assumed to be reciprocal for two consecutive phases and channels between the source A and B are independent from each other. The additive noise at all the receivers is assumed to be zero mean complex Gaussian noise with variance σ_x^2, where $x \in \{A, R, B\}$. Let us define SNR between the relay and the m^{th} transmit antenna of source i to be $\lambda_m^i = |h_m^i|^2 E_s/\sigma_R^2$, where E_s is the average energy of transmitted symbols and is assumed to be 1 and $|\cdot|$ represents absolute value. Let $\lambda_{1:N_i}^i \geq \lambda_{2:N_i}^i \geq \cdots \geq \lambda_{N_i:N_i}^i$ be the order statistics obtained by arranging $\{\lambda_m^i\}_{m=1}^{N_i}$ in decreasing order of magnitude in the first phase. The antennas for the first L_i of these ordered statistics are selected to obtain maximum SNR between source i and relay R. Then the signals for the selected antennas are weighted based on the channel coefficients between source i and the relay in order to maximize instantaneous SNR at the relay. This means that GTAS is carried out in the first phase and since channels are reciprocal, GRAS is carried out in the second phase. Then, by using the same approach in [27], the received signal at R for GTAS can be given as

$$Y_R = \sqrt{P_A} w_A^T h_A s_A + \sqrt{P_B} w_B^T h_B s_B + n_R \tag{3.1}$$

where s_i is the transmitted signal at source i, P_i is the transmit power at source i, $(\cdot)^T$ denotes transpose, $h_i = [h^i_{1:N_i}; h^i_{2:N_i}; \cdots; h^i_{L_i:N_i}]$ is the $L_i \times 1$ channel vector of GTAS between source i and the relay, $w_i = h_i^*/\|h_i\|$, where $(\cdot)^*$ denotes complex conjugate, $\|\cdot\|$ denotes Euclidean norm, and n_R is the additive Gaussian noise at the relay with zero mean and variance σ_R^2. In the second phase, Y_R is multiplied by $G = \sqrt{P_R/(P_A\|h_A\|^2 + P_B\|h_B\|^2 + \sigma_R^2)}$, where P_R is the relay power, and is broadcasted to each source. The received signals at the sources are weighted and combined to obtain received signals of GRAS:

$$Y_i = G w_i^T h_i Y_R + w_i^T n_i \tag{3.2}$$

In (3.2), n_i is the $L_i \times 1$ additive Gaussian noise vector at source i with zero mean and mean power $I_{L_i}\sigma_i^2$ where I_{L_i} denotes an identity matrix of order L_i. Since each source knows its own transmitted signal and channel state information, after canceling self-interference, the remained signal is

$$\tilde{Y}_i = G\sqrt{P_j}\|h_j\|\|h_i\|s_j + G\|h_i\|n_R + w_i^T n_i \tag{3.3}$$

where $(i, j) \in \{(A, B), (B, A)\}$. Then, as in [27], the e2e SNR at source i can be derived as follows:

$$\gamma_i = \frac{\alpha_i \Upsilon_i \Upsilon_j}{(\alpha_i + 1)\Upsilon_i + \Upsilon_j + \rho} \tag{3.4}$$

where $(i, j) \in \{(A, B), (B, A)\}$ and $\alpha_i = P_R\sigma_R^2/(P_i\sigma_i^2)$. In (3.4), $\Upsilon_i = P_i\|h_i\|^2/\sigma_R^2$ and $\Upsilon_j = P_j\|h_j\|^2/\sigma_R^2$ are the instantaneous SNRs of the $i - R$ link and the $j - R$ link, respectively. In (3.4), setting $\rho = 1$ and 0 correspond to channel-noise-assisted (CNA) AF relaying, and channel-assisted (CA) AF relaying, respectively.

3.3. Performance Analysis

In this section, we derive exact and asymptotic SOP, MGF, and SSER expressions, respectively.

3.3.1. Exact Analysis

In this section exact CDF and SER expression are obtained.

3.3.1.1. Exact CDF of the e2e SNR

In order to derive SOP and SSER, it is essential to derive CDF of the e2e SNR. The CDF of the instantaneous e2e SNR γ_i in (3.4) can be expressed as [27, eq. (61)]

$$F_{\gamma_i}(\gamma) = 1 - \int_{\varsigma_i\gamma}^{\infty} \tilde{F}_{\Upsilon_i}(\nu_i) f_{\Upsilon_j}(\Upsilon_j) d\Upsilon_j \tag{3.5}$$

where $\tilde{F}_{\Upsilon_i}(\gamma) = 1 - F_{\Upsilon_i}(\gamma)$, $\varsigma_i = (\alpha_i + 1)/\alpha_i$, and $\nu_i = \gamma(\Upsilon_j + \rho)/(\alpha_i \Upsilon_j - \gamma(\alpha_i + 1))$. Using [79, eq. (4)], the CDF of Υ_i can be expressed as

$$F_{\Upsilon_i}(\gamma) = 1 + \sum_{l_i=1}^{L_i} \frac{\hat{c}_{l_i} \gamma^{l_i - 1}}{(l_i - 1)!} e^{-\gamma/\bar{\Upsilon}_i} + \sum_{l_i=L_i+1}^{N_i} \hat{c}_{l_i} e^{-l_i \gamma/(L_i \bar{\Upsilon}_i)} \tag{3.6}$$

where $\bar{\Upsilon}_i = P_i d^{-f_i}/\sigma_R^2$ is the average SNR of the $i - R$ link and the coefficients $\hat{c}_{l_i}$ are given by [79, eq. (3)]

$$\hat{c}_{l_i} = \begin{cases} 1 & l_i = 0 \\ \bar{\Upsilon}_i^{-l_i+1}[-1 + \delta_{l_i k_i}] & 1 \le l_i < L_i \\ -\bar{\Upsilon}_i^{-l_i+1} \binom{N_i}{N_i - L_i} & l_i = L_i \\ \frac{(-1)^{l_i} \binom{N_i}{N_i - l_i} \binom{l_i - 1}{l_i - L_i - 1}}{(\frac{l_i}{L_i} - 1)^{L_i}} & L_i < l_i \le N_i \end{cases} \tag{3.7}$$

where $\delta_{l_i k_i} = \sum_{k_i=L_i+1}^{N_i} \frac{(-1)^{k_i - l_i} \binom{N_i}{N_i - k_i} \binom{k_i - 1}{k_i - L_i - 1}}{(\frac{k_i}{L_i} - 1)^{L_i - l_i + 1}}$. For simplicity we rephrase $F_{\Upsilon_i}(\gamma)$ as

$$F_{\Upsilon_i}(\gamma) = 1 + \sum_{l_i=1}^{N_i} C_{l_i} \gamma^{\omega_{l_i}} e^{-\gamma \Omega_{l_i}} \tag{3.8}$$

where $C_{l_i} = \hat{c}_{l_i}/(l_i - 1)!$ if $1 \le l_i \le L_i$ and $C_{l_i} = \hat{c}_{l_i}$ if $L_i < l_i \le N_i$, $\omega_{l_i} = l_i - 1$ if $1 \le l_i \le L_i$ and $\omega_{l_i} = 0$ if $L_i < l_i \le N_i$, $\Omega_{l_i} = 1/\bar{\Upsilon}_i$ if $1 \le l_i \le L_i$ and $\Omega_{l_i} = l_i/(L_i \bar{\Upsilon}_i)$ if $L_i < l_i \le N_i$. Now we can give the probability density function (PDF) of Υ_j as

$$f_{\Upsilon_j}(\gamma) = \sum_{l_j=1}^{N_j} C_{l_j} \omega_{l_j} \gamma^{\omega_{l_j} - 1} e^{-\gamma \Omega_{l_j}} - \sum_{l_j=1}^{N_j} C_{l_j} \Omega_{l_j} \gamma^{\omega_{l_j}} e^{-\gamma \Omega_{l_j}}. \tag{3.9}$$

To derive the CDF of the instantaneous e2e SNR γ_i, we substitute (3.8) and (3.9) into (3.5) and obtain $F_{\gamma_i}(\gamma)$ as

$$F_{\gamma_i}(\gamma) = 1 - \sum_{l_i=1}^{N_i}\sum_{l_j=1}^{N_j} \Omega_{l_j} C_{l_i} C_{l_j} I_1(\omega_{l_j}) + \sum_{l_i=1}^{N_i}\sum_{l_j=1}^{N_j} \omega_{l_j} C_{l_i} C_{l_j} I_1(\omega_{l_j} - 1) \tag{3.10}$$

where

$$I_1(m) = \int_{\varsigma_i\gamma}^{\infty} x^m \left(\frac{\gamma(x+\rho)}{\alpha_i x - \gamma(\alpha_i+1)}\right)^{\omega_{l_i}} e^{-\left(\Omega_{l_j} x + \frac{\Omega_{l_i}\gamma(x+\rho)}{\alpha_i x - \gamma(\alpha_i+1)}\right)} dx. \tag{3.11}$$

To solve $I_1(m)$, we make change of variable as $x = t + \varsigma_i\gamma$. After changing of variable, we apply binomial expansion given by [65, eq. (1.111)] to $(t+\varsigma_i\gamma)^m$ and $(t+\varsigma_i\gamma+\rho)^{\omega_{l_i}}$. Then we obtain

$$\begin{aligned} I_1(m) = \left(\frac{\gamma}{\alpha_i}\right)^{\omega_{l_i}} e^{-\left(\Omega_{l_j}\varsigma_i + \frac{\Omega_{l_i}}{\alpha_i}\right)\gamma} \sum_{p=0}^{\omega_{l_i}}\sum_{q=0}^{m} \binom{\omega_{l_i}}{p}\binom{m}{q} (\varsigma_i\gamma+\rho)^p (\varsigma_i\gamma)^{m-q} \\ \int_0^{\infty} t^{q-p} e^{-\left(\Omega_{l_j} t + \frac{\Omega_{l_i}\gamma(\varsigma_i\gamma+\rho)}{\alpha_i t}\right)} dt. \end{aligned} \tag{3.12}$$

To solve the integral in (3.12), we use the identity [65, eq. (3.471.9)] and obtain

$$\begin{aligned} I_1(m) = 2\left(\frac{\gamma}{\alpha_i}\right)^{\omega_{l_i}} e^{-\left(\Omega_{l_j}\varsigma_i + \frac{\Omega_{l_i}}{\alpha_i}\right)\gamma} \sum_{p=0}^{\omega_{l_i}}\sum_{q=0}^{m} \binom{\omega_{l_i}}{p}\binom{m}{q} (\varsigma_i\gamma+\rho)^p (\varsigma_i\gamma)^{m-q} \\ \left(\frac{\Omega_{l_i}\gamma(\varsigma_i\gamma+\rho)}{\Omega_{l_j}\alpha_i}\right)^{\frac{q-p+1}{2}} K_{q-p+1}\left(2\sqrt{\frac{\Omega_{l_i}\Omega_{l_j}\gamma(\varsigma_i\gamma+\rho)}{\alpha_i}}\right) \end{aligned} \tag{3.13}$$

where $K_\nu(x)$ is the ν^{th}-order modified Bessel Function of the second kind [65, eq. (8.407)], which is available in well known software programs such as MATHEMATICA and MAPLE. We substitute (3.13) into (3.10) and get closed-form CDF expression of the e2e SNR γ_i as

$$F_{\gamma_i}(\gamma) = 1 + 2\sum_{l_i=1}^{N_i}\sum_{l_j=1}^{N_j}\Big[\omega_{l_j} H_1(\omega_{l_j} - 1) - \Omega_{l_j} H_1(\omega_{l_j})\Big] \tag{3.14}$$

where

$$H_1(m) = \sum_{p=0}^{\omega_{l_i}} \sum_{q=0}^{m} \binom{\omega_{l_i}}{p} \binom{m}{q} C_{l_i} C_{l_j} \left(\frac{\gamma}{\alpha_i}\right)^{\omega_{l_i}} e^{-\left(\Omega_{l_j}\varsigma_i + \frac{\Omega_{l_i}}{\alpha_i}\right)} (\varsigma_i\gamma + \rho)^p (\varsigma_i\gamma)^{m-q} \left(\frac{\Omega_{l_i}\gamma(\varsigma_i\gamma+\rho)}{\Omega_{l_j}\alpha_i}\right)^{\frac{q-p+1}{2}} K_{q-p+1}\left(2\sqrt{\frac{\Omega_{l_i}\Omega_{l_j}\gamma(\varsigma_i\gamma+\rho)}{\alpha_i}}\right). \tag{3.15}$$

In order to obtain a simpler equation for the CDF of CA-AF, instead of setting $\rho = 0$ in (3.14) and (3.15), we reproduce it by setting $\rho = 0$ and continue from the beginning as in derivation of the CDF of γ_i in (3.14). Then, the CDF of γ_i for CA-AF is derived as

$$F_{\gamma_i}(\gamma) = 1 + 2\sum_{l_i=1}^{N_i} \sum_{l_j=1}^{N_j} \Big[\omega_{l_j} H_2(\omega_{l_j} - 1) - \Omega_{l_j} H_2(\omega_{l_j})\Big] \tag{3.16}$$

where

$$H_2(m) = \sum_{q=0}^{\omega_{l_i}+m} \binom{\omega_{l_i}+m}{q} C_{l_i} C_{l_j} \alpha_i^{-\omega_{l_i}} \varsigma_i^{\frac{m+q+1}{2}} \gamma^{\omega_{l_i}+m+1} \left(\frac{\Omega_{l_i}}{\alpha_i\Omega_{l_j}}\right)^{\frac{m-q+1}{2}} e^{-\left(\Omega_{l_j}\varsigma_i + \frac{\Omega_{l_i}}{\alpha_i}\right)} K_{m-q+1}\left(\gamma\sqrt{\frac{4\Omega_{l_i}\Omega_{l_j}\varsigma_i}{\alpha_i}}\right). \tag{3.17}$$

For a threshold γ_{th}, the exact e2e SOP can be evaluated by using (3.14) and (3.16) as $F_{\gamma_A}(\gamma_{th}) + F_{\gamma_B}(\gamma_{th})$ for CNA-AF and CA-AF cases, respectively.

3.3.1.2. Exact SSER

We use SSER to evaluate error performance of two-way relaying which is defined as the summation of the SERs of two sources [80]. For CA-AF case, we can use (3.16) to derive closed-form expression for MGF of γ_i, however, it is not easy to obtain closed-form expression of SSER from MGF based analysis. Hence we use CDF based method [81] to derive closed-form expression of SSER of M-PSK. For numerical calculations of SSER based on MGF method, it is useful to give MGF expression of γ_i. MGF of γ_i can be obtained as

$$M_{\gamma_i}(-s) = s\int_0^\infty e^{-sx} F_{\gamma_i}(x)dx. \tag{3.18}$$

We substitute (3.16) into (3.18) and use the identity [67, eq. (2.16.6.3)] to derive MGF as

$$M_{\gamma_i}(-s) = 1 + 2s \sum_{l_i=1}^{N_i} \sum_{l_j=1}^{N_j} \Big[\omega_{l_j} H_2(\omega_{l_j} - 1, s) - \Omega_{l_j} H_2(\omega_{l_j}, s) \Big] \tag{3.19}$$

$H_2(m, s)$ in (3.19) is given below

$$H_2(m,s) = \sqrt{\pi} \sum_{q=0}^{\omega_{l_i}+m} \Delta^{ij} {}_2F_1\Bigg(\frac{\omega_{l_i}+q+1}{2}, \frac{\omega_{l_i}+q+2}{2}; \omega_{l_i}+m+\frac{5}{2}, 1 - \frac{\frac{4\Omega_{l_i}\Omega_{l_j}\varsigma_i}{\alpha_i}}{\Big(\omega_{l_j}\varsigma_i + \frac{\Omega_{l_i}}{\alpha_i} + s\Big)^2} \Bigg) \tag{3.20}$$

where

$$\Delta^{ij} = \frac{\binom{\omega_{l_i}+m}{q} C_{l_i} C_{l_j} \alpha_i^{-\omega_{l_i}} \varsigma_i^q \Omega_{l_j}^{-(m-q+1)} \Gamma(\omega_{l_i}+q+1)\Gamma(\omega_{l_i}+2m-q+3)}{2^{(\omega_{l_i}+2m-q+3)} \Gamma(\omega_{l_i}+m+\frac{5}{2}) \Big(\Omega_{l_j}\varsigma_i + \frac{\Omega_{l_i}}{\alpha_i} + s\Big)^{(\omega_{l_i}+q+1)}}. \tag{3.21}$$

${}_2F_1(\iota, \tau; w; z)$ in (3.20) is the Gauss hypergeometric function [65, eq. (9.111)] and $\Gamma(\iota)$ is Gamma function [65, eq. (8.310.1)], which are available in well known software programs such as MATHEMATICA and MAPLE.

Based on (3.19), SSER can be expressed as

$$P_{SSER,M} = \sum_{q=1}^{Q} a_q \int_0^{\theta_q} \left[M_{\gamma_A}\left(-\frac{\lambda_{mod}}{\sin^2(\theta)} \right) + M_{\gamma_B}\left(-\frac{\lambda_{mod}}{\sin^2(\theta)} \right) \right] d\theta. \tag{3.22}$$

The modulation dependent parameters in (3.22) for M-PSK and M-QAM are given in Table 2.1.

It is difficult to derive a closed-form expression for SSER based on MGF, but the integrals in (3.22) can be evaluated numerically. The closed-form expression for exact SSER based on CDF can be derived as

$$P_{SSER,C} = P_{A,SER} + P_{B,SER} \tag{3.23}$$

where $P_{i,SER} = \frac{a\sqrt{b}}{2\pi} \int_0^\infty x^{-1/2} e^{-bx} F_{\gamma_i}(x) dx$, $i \in \{A, B\}$ [81]. a and b are modulation dependent parameters. For Binary PSK (BPSK) $a = 1$ and $b = 1$, and for approximated

M-PSK $a = 2$ and $b = \sin^2(\pi/M)$. To derive $P_{i,SER}$, we concentrate on CA-AF with $\rho = 0$. We substitute (3.16) into $P_{i,SER}$ and use the identity [67, eq. (2.16.6.3)] to derive $P_{i,SER}$ as

$$P_{i,SER} = \frac{a}{2} + a\sqrt{b}\sum_{l_i=1}^{N_i}\sum_{l_j=1}^{N_j}[\omega_{l_j} H_{SER}(\omega_{l_j} - 1) - \Omega_{l_j} H_{SER}(\omega_{l_j})] \tag{3.24}$$

$H_{SER}(m)$ in (3.24) is given as

$$H_{SER}(m) = \sum_{q=0}^{\omega_{l_i}+m} \binom{\omega_{l_i}+m}{q} \frac{C_{l_i} C_{l_j} \alpha_i^{-\omega_{l_i}} \varsigma_i^q}{\Omega_{l_j}^{m-q+1}} I_{SER}(m) \tag{3.25}$$

where

$$\begin{aligned} I_{SER}(m) = & \frac{\Gamma\left(\omega_{l_i} + q + \frac{1}{2}\right)\Gamma\left(\omega_{l_i} + 2m - q + \frac{5}{2}\right)}{2^{(\omega_{l_i}+2m-q+\frac{5}{2})}\left(\Omega_{l_j}\varsigma_i + \frac{\Omega_{l_i}}{\alpha_i} + b\right)^{(\omega_{l_i}+q+\frac{1}{2})}\Gamma\left(\omega_{l_i}+m+2\right)} \\ & {}_2F_1\left(\frac{\omega_{l_i}+q+\frac{1}{2}}{2}, \frac{\omega_{l_i}+q+\frac{3}{2}}{2}; \omega_{l_i}+m+2; 1 - \frac{\Omega_{l_i}\Omega_{l_j}\varsigma_i/\alpha_i}{\left(\Omega_{l_j}\varsigma_{l_i} + \Omega_{l_i}/\alpha_i + b\right)^2}\right). \end{aligned} \tag{3.26}$$

3.3.2. Asymptotic Analysis

At high SNR, the e2e SOP and SSER can be characterized by diversity gain and array gain [82]. Hence, it is essential to obtain asymptotic CDF of the e2e SNR and SSER.

3.3.2.1. Asymptotic CDF of the e2e SNR

At high SNR, the asymptotic e2e $F_{\gamma_i}(\gamma)$ can be given by

$$F_{\gamma_i}^{\infty}(\gamma) \approx \hat{G}_{a,i}\left(\frac{\bar{\Upsilon}_i}{\gamma}\right)^{-\hat{G}_{d,i}} + o\left(\bar{\Upsilon}_i^{-\hat{G}_{d,i}}\right) \tag{3.27}$$

where $(\cdot)$ denotes higher order terms.

Clearly, it is not easy to determine array gain $\hat{G}_{a,i}$ and diversity gain $\hat{G}_{d,i}$ directly from (3.14). To overcome this difficulty, we use single term polynomial approximation

of the PDF and CDF of Rayleigh fading and the inequality $\alpha_i\Upsilon_i\Upsilon_j/((\alpha_i+1)\Upsilon_i+\Upsilon_j+\rho) < \min(\alpha_i\Upsilon_i, \alpha_i\Upsilon_j/(\alpha_i+1))$ to derive asymptotic CDF [83]. The single term polynomial approximation for the PDF and CDF of Rayleigh fading are $f(x) = 1/\bar{\Upsilon}_i$ and $F(x) = x/\bar{\Upsilon}_i$, respectively [82]. We derive approximated MGF of Υ_i by substituting these approximated PDF and CDF in [74, eq. (508)] and [74, eq. (510)]: $M^{\infty}_{\Upsilon_i}(s) = \frac{N_i}{L_i! L_i^{N_i-L_i+1}} \frac{N_i! \bar{\Upsilon}_i^{-N_i}}{s^{N_i}}$. The asymptotic CDF of Υ_i is derived by taking inverse Laplace transform of $\frac{M^{\infty}_{\Upsilon_i}(s)}{s}$:

$$F^{\infty}_{\Upsilon_i}(\gamma) = \frac{N_i}{L_i! L_i^{N_i-L_i+1}} \left(\frac{\gamma}{\bar{\Upsilon}_i}\right)^{N_i}. \tag{3.28}$$

Now we consider the aforementioned inequality to find asymptotic CDF of the e2e SNR γ_i [83]: $F^{\infty}_{\gamma_i}(\gamma) = Pr(\min(\alpha_i\Upsilon_i, \frac{\alpha_i\Upsilon_j}{(\alpha_i+1)}) < \gamma)$. Hence $F^{\infty}_{\gamma_i}(\gamma) = 1 - Pr(\min(\alpha_i\Upsilon_i, \frac{\alpha_i\Upsilon_j}{(\alpha_i+1)}) > \gamma)$. Since Υ_i and Υ_j are independent, $Pr(\min(\alpha_i\Upsilon_i, \frac{\alpha_i\Upsilon_j}{(\alpha_i+1)}) > \gamma) = Pr(\alpha_i\Upsilon_i > \gamma) Pr(\frac{\alpha_i\Upsilon_j}{(\alpha_i+1)} > \gamma)$. $Pr(\alpha_i\Upsilon_i > \gamma) = 1 - F_{\Upsilon_i}(\frac{\gamma}{\alpha_i})$ and $Pr(\frac{\alpha_i\Upsilon_j}{(\alpha_i+1)} > \gamma) = 1 - F_{\Upsilon_j}(\frac{(\alpha_i+1)\gamma}{\alpha_i})$. Therefore, the asymptotic CDF is found as

$$F^{\infty}_{\gamma_i}(\gamma) = F_{\Upsilon_i}(\frac{\gamma}{\alpha_i}) + F_{\Upsilon_j}(\frac{(\alpha_i+1)\gamma}{\alpha_i}) - F_{\Upsilon_i}(\frac{\gamma}{\alpha_i}) F_{\Upsilon_j}(\frac{(\alpha_i+1)\gamma}{\alpha_i}). \tag{3.29}$$

If we ignore the third term in (3.29) and substitute (3.28) into (3.29), and define $\kappa_i = \bar{\Upsilon}_i/\bar{\Upsilon}_j$, then $\hat{G}_{d,i}$ and $\hat{G}_{a,i}$ in (3.27) are respectively obtained as

$$\hat{G}_{d,i} = \min(N_i, N_j) \tag{3.30}$$

and

$$\hat{G}_{a,A} = \begin{cases} \frac{N_A \alpha_A^{-N_A}}{L_A! L_A^{N_A-L_A+1}} & N_A < N_B \\ \frac{N_B \varsigma_A^{N_B} \kappa_A^{N_B}}{L_B! L_B^{N_B-L_B+1}} & N_A > N_B \\ \frac{N_A \alpha_A^{-N_A}}{L_A! L_A^{N_A-L_A+1}} + \frac{N_B \varsigma_A^{N_B} \kappa_A^{N_B}}{L_B! L_B^{N_B-L_B+1}} & N_A = N_B \end{cases}$$

$$\hat{G}_{a,B} = \begin{cases} \frac{N_A \varsigma_B^{N_A}}{L_A! L_A^{N_A-L_A+1}} & N_A < N_B \\ \frac{N_B \alpha_B^{-N_B} \kappa_A^{N_B}}{L_B! L_B^{N_B-L_B+1}} & N_A > N_B \\ \frac{N_A \varsigma_B^{N_A}}{L_A! L_A^{N_A-L_A+1}} + \frac{N_B \alpha_B^{-N_B} \kappa_A^{N_B}}{L_B! L_B^{N_B-L_B+1}} & N_A = N_B \end{cases}. \tag{3.31}$$

The asymptotic e2e SOP can be evaluated by using (3.27) as $F^{\infty}_{\gamma_A}(\gamma_{th}) + F^{\infty}_{\gamma_B}(\gamma_{th})$.

3.3.2.2. Asymptotic SSER

In the high-SNR region, SSER can be represented in terms of diversity gain and array gain [82]. We obtain two asymptotic SSER expressions: First one depends on CDF based analysis and second one depends on MGF based analysis. For CDF based analysis, we substitute (3.27) into (3.23) and derive asymptotic SSER as

$$P_{SSER,C}^{\infty} \approx \left(G_{a,C}\bar{\Upsilon}_A\right)^{-G_d} + o\left(\bar{\Upsilon}_A^{-G_d}\right) \tag{3.32}$$

where $G_d = \hat{G}_{d,A} = \hat{G}_{d,B} = \min(N_A, N_B)$ and $G_{a,C} = \left(\frac{ab^{-G_d}}{2\sqrt{\pi}}\Gamma\left(G_d + \frac{1}{2}\right)\Psi_C\right)^{-1/G_d}$. Ψ_C is given as

$$\Psi_C = \begin{cases} \frac{N_A}{L_A! L_A^{N_A - L_A + 1}}\left(\alpha_A^{-N_A} + \varsigma_B^{N_A}\right) & N_A < N_B \\ \frac{N_B \kappa_A^{N_B}}{L_B! L_B^{N_B - L_B + 1}}\left(\varsigma_A^{N_B} + \alpha_B^{-N_B}\right) & N_A > N_B \\ \frac{N_A}{L_A! L_A^{N_A - L_A + 1}}\left(\alpha_A^{-N_A} + \varsigma_B^{N_A}\right) + \frac{N_B \kappa_A^{N_B}}{L_B! L_B^{N_B - L_B + 1}}\left(\alpha_B^{-N_B} + \varsigma_A^{N_B}\right) & N_A = N_B \end{cases} . \tag{3.33}$$

To obtain asymptotic SSER based on MGF analysis, we firstly derive asymptotic MGF of e2e SNR by substituting (3.27) into (3.18):

$$M_{\gamma_i}^{\infty}(-s) \approx \frac{\hat{G}_{a,i}\Gamma(G_d + 1)}{\left(s\bar{\Upsilon}_i\right)^{G_d}} + o\left(\bar{\Upsilon}_i^{-G_d}\right) \tag{3.34}$$

Then, we substitute (3.34) into (3.22) and derive asymptotic SSER as

$$P_{SSER,M}^{\infty} = \frac{\Gamma\left(G_d + 1\right)\bar{\Upsilon}_A^{-G_d}}{\lambda_{mod}^{G_d}}\left(\sum_{q=1}^{Q} a_q I_2(G_d, \theta_q)\right)\left(\hat{G}_{a,A} + \hat{G}_{a,B}\right) \tag{3.35}$$

where

$$\begin{aligned} I_2(G_d, \theta_q) &= \int_0^{\theta_q} \sin^{2G_d}(x)dx \\ &= \begin{cases} \int_0^{\theta_q} \sin^{2G_d}(x)dx = \int_0^{\pi/2} \sin^{2G_d}(x)dx \\ \qquad\qquad - \int_{\theta_q}^{\pi/2} \sin^{2G_d}(x)dx, \quad 0 \le \theta_q \le \pi/2 \\ \int_0^{\theta_q} \sin^{2G_d}(x)dx = \int_0^{\pi/2} \sin^{2G_d}(x)dx \\ \qquad\qquad + \int_{\pi/2}^{\theta_q} \sin^{2G_d}(x)dx, \quad \pi/2 < \theta_q \le \pi \end{cases} \end{aligned} \tag{3.36}$$

and $0 \leq \theta_q \leq \pi$. To solve the integrals in (3.36), we make change of variable as $y = \sin^2(x)$ where $dy = 2\sin(x)\cos(x)dx = 2\sqrt{y}\sqrt{1-y}$ for $0 \leq \theta_q \leq \pi/2$ and $dy = 2\sin(x)\cos(x)dx = -2\sqrt{y}\sqrt{1-y}$ for $\pi/2 < \theta_q \leq \pi$. After proper arrangements, the integral becomes

$$I_2(G_d, \theta_q) = \begin{cases} \frac{1}{2}\int_0^1 g(y)dy - \frac{1}{2}\int_{\sin^2(\theta_q)}^1 g(y)dy, & 0 \leq \theta_q \leq \pi/2 \\ \frac{1}{2}\int_0^1 g(y)dy + \frac{1}{2}\int_{\sin^2(\theta_q)}^1 g(y)dy, & \pi/2 < \theta_q \leq \pi \end{cases} . \tag{3.37}$$

The function in this integral is $g(y) = y^{N-1/2}(1-y)^{-1/2}$. The integrals in (3.37) can be represented by incomplete Beta function, $B_x(p,q) = \int_0^x t^{p-1}(1-t)^{q-1}dt$. To solve these integrals, we make change of variable as $t = 1-y$, use the facts $\cos^2(x) = 1 - \sin^2(x)$ and $\sqrt{\cos^2(x)} = |\cos(x)|$ where $|\cos(x)| = -\cos(x)$ for $\pi/2 < \theta_q \leq \pi$ together with properties given in [65, eq. 8.384.1 and 8.391]. Then, we obtain the integral as follows, which is valid for for $G_d > -1/2$ and $\sin(\theta_q) \geq 0$:

$$I_2(G_d, \theta_q) = \frac{\sqrt{\pi}\Gamma\left(G_d + \frac{1}{2}\right)}{2\Gamma\left(G_d + 1\right)} - \cos(\theta_q){}_2F_1\left(\frac{1}{2}, \frac{1}{2} - G_d; \frac{3}{2}; \cos^2(\theta_q)\right). \tag{3.38}$$

Now we can rephrase (3.35) as

$$P_{SSER,M}^{\infty} \approx \left(G_{a,M}\bar{\Upsilon}_A\right)^{-G_d} + o\left(\bar{\Upsilon}_A^{-G_d}\right) \tag{3.39}$$

where $G_d = \hat{G}_{d,A} = \hat{G}_{d,B} = \min(N_A, N_B)$ and $G_{a,M} = \left(\Phi_M \Psi_C\right)^{-1/G_d}$. Φ_M is given below

$$\Phi_M = \frac{\Gamma\left(G_d + 1\right)}{\lambda_{mod}^{G_d}} \left(\sum_{q=1}^{Q} a_q I_2(G_d, \theta_q)\right). \tag{3.40}$$

Although asymptotic SSER expressions are derived for different methods they are equivalent. It is easy to see that for BPSK, however, it is not easy for M-PSK.

3.4. Numerical Results

In this section, we present numerical and simulation results in order to illustrate proposed antenna selection strategy. We also illustrate the effects of different power

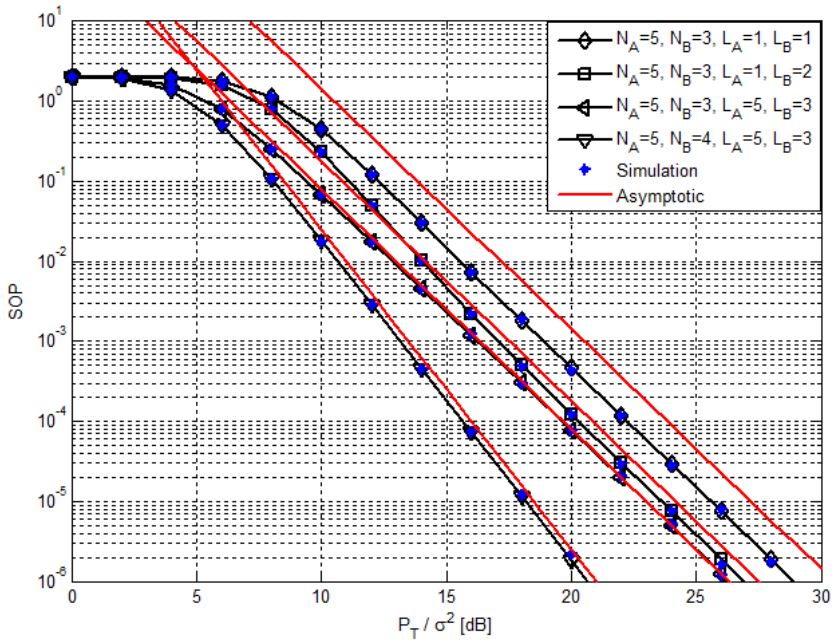

Figure 3.2: SOP for different numbers of selected antennas and diversity orders.

allocations, total number of antennas, and number of selected antennas on optimum relay location. We assume that total power $P_T = 1$ and $\sigma^2 = \sigma_A^2 = \sigma_B^2 = \sigma_R^2$. We also assume $P_A = P_B = P_R = P_T/3$ and $d_{AR} = d_{BR} = 0.5$ unless otherwise is stated. The path loss exponent f_i is taken to be 3 which represents heavy urban environment. The curves are plotted versus P_T/σ^2. We use (3.14) and (3.27) to plot the exact and asymptotic e2e SOP curves, respectively and (3.22) and (3.24) to obtain exact SSER curves for M-QAM and M-PSK, respectively. For asymptotic curves, we use (3.32) and (3.39) for M-PSK and M-QAM respectively. Note that exact e2e SOP is calculated for CNA-AF, i.e., $\rho = 1$ and exact SSER is calculated for CA-AF, i.e., $\rho = 0$, and simulations are done accordingly by using Monte Carlo simulation technique.

Fig. 3.2 plots SOP curves for a threshold of 10 dB with $N_A = 5$, $N_B = 3$ and 4, and $L_A = 1$ and 5, $L_B = 1$, 2, and 3. Diversity order is 4 for the lowest curve and 3 for other 3 upper curves. Asymptotic and exact curves have a precise agreement and get closer as the number of selected antennas is increased for the source whose total number of antennas equals to the diversity order. In addition, simulation results coincide with theoretical results exactly. Selecting all antennas of the source having total number of antennas equal to the diversity order results in an SNR gain of about 2.7 dB at a SOP of 10^{-5} with respect to a single antenna selection at sources. An increment of 1 for the diversity order with the same number of selected antennas results in an SNR gain of 7.5 dB at the same SOP. We also note that increasing the number of selected antennas for the source having the total number of antennas equal to the diversity order is more effective

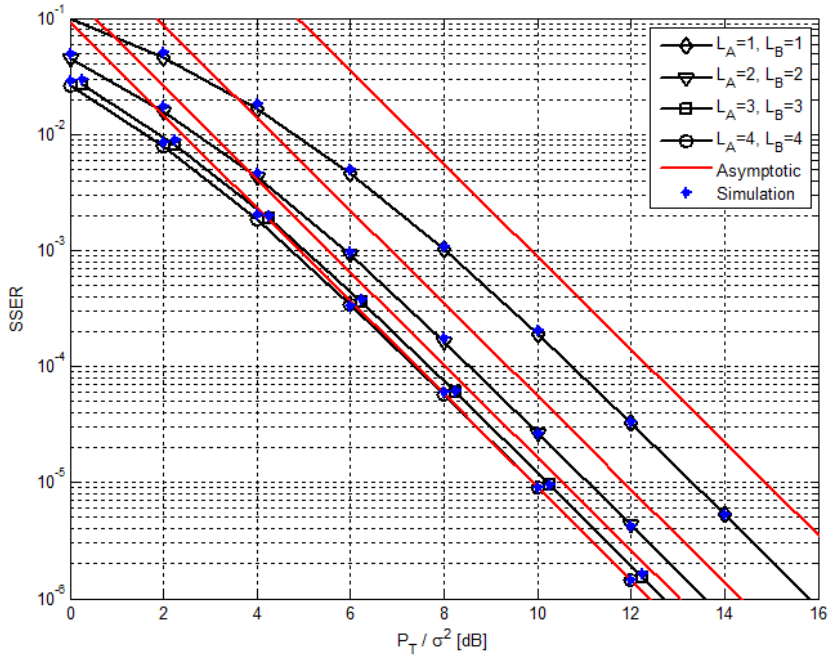

Figure 3.3: SSER of BPSK for different numbers of selected antennas.

than that for the other source.

Fig. 3.3 plots SSER (in this case sum bit error rate (SBER)) curves of BPSK with $N_A = N_B = 4$ and $L_A = L_B = 1$, 2, 3, and 4. As seen in Fig. 3.3, as the number of selected antennas increases, the gap among exact and asymptotic curves diminishes and precisely overlap with each other. Selecting all antennas approximately results in an SNR gain of 3.6 dB for an SSER of 10^{-5} with respect to a single antenna selection at sources. On the other hand, this gain is only about 1 dB and 0.17 dB when compared to the cases of two and three antenna selections at sources, respectively. This means complexity can be reduced with a small degradation in performance.

Fig. 3.4 plots SSER curves of 8-PSK with $N_A = 3$, 4, $N_B = 4$, $L_A = 1$, 2 and 3, and $L_B = 1$ and 3. As also seen in Fig. 3.3, the gap among exact and asymptotic curves decreases when the number of selected antennas increases. This shows the effect of diversity gain together with the number of selected antennas for the source dominating SSER. Increasing diversity order from 3 to 4 with an increment in number of selected antennas from 1 to 3 at both sources results in an SNR gain of more than 5 dB at an SSER of 10^{-5}.

Fig. 3.5 plots SSER curves of 16-QAM with $N_A = 2$ and 4, $N_B = 3$ and 5, and $L_A = L_B = 2$. Diversity order is 2 for the upper curve, 3 for the middle one, and 4 for the lower one. An increment in diversity order from 2 to 3 gives an SNR gain more than 7 dB at an SSER of 10^{-5}. On the other hand, this gain is about 4 dB when the diversity order is

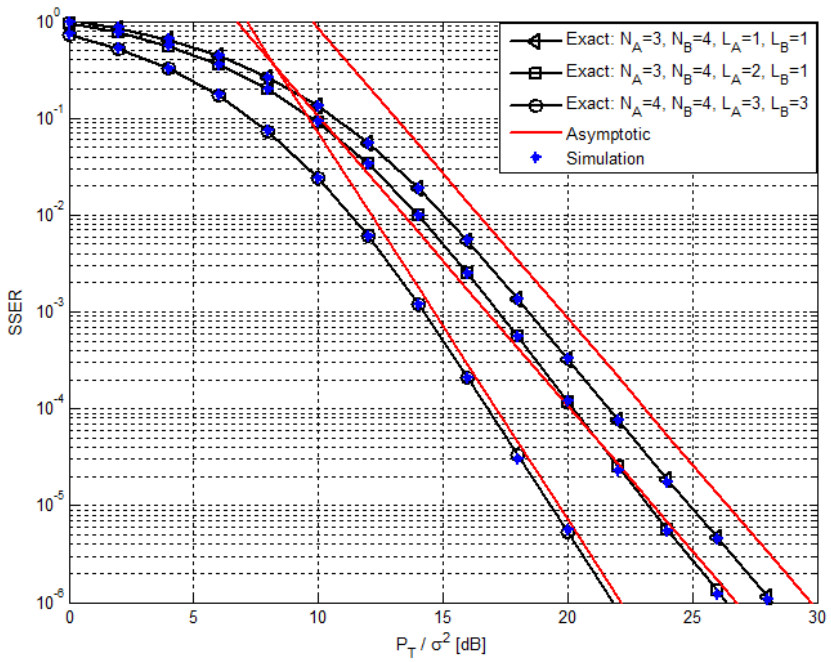

Figure 3.4: SSER of 8-PSK for different diversity gains and numbers of selected antennas.

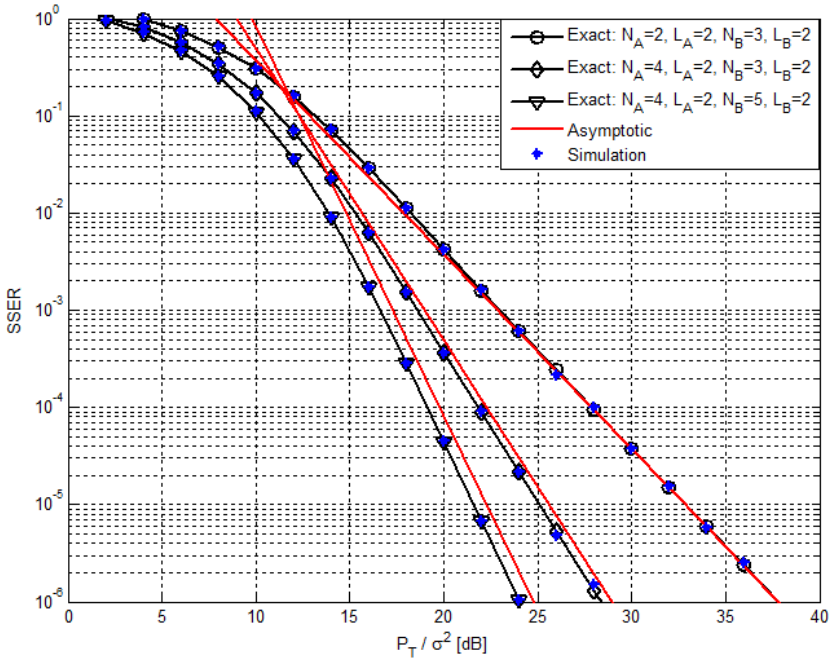

Figure 3.5: SSER of 16-QAM for different diversity gains.

increased from 3 to 4.

Fig. 3.6 plots exact SSER curves of 16-QAM versus normalized distance between source A and the relay for two different SNR values with $N_A = 4$, $N_B = 4$ and 5, $L_A = 2$ and 3, and $L_B = 2$. Upper curves are obtained by assigning the same power to both sources and the relay for an SNR of 10 dB. Lower curves with an SNR of 12 dB are

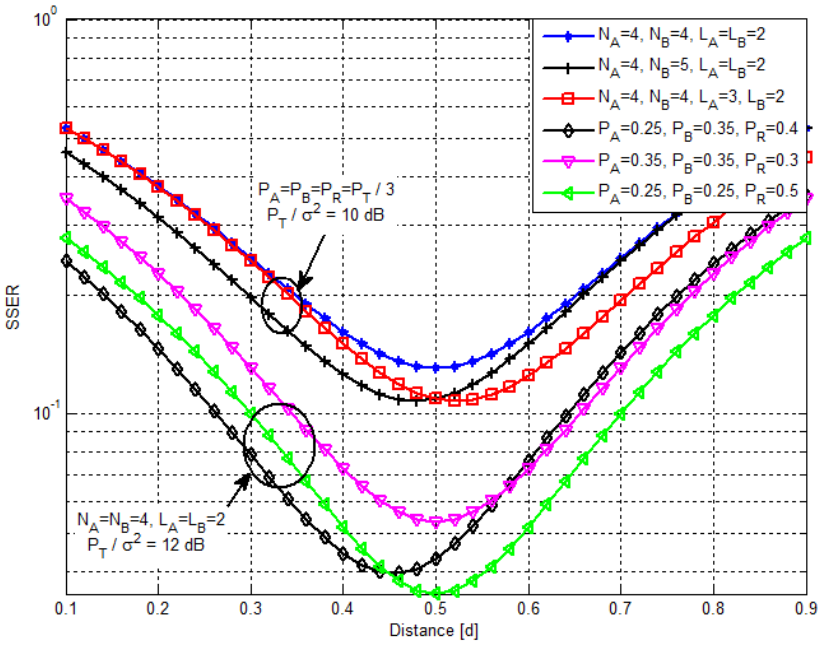

Figure 3.6: Exact SSER of 16-QAM versus normalized distance between source A and the relay.

plotted for three different power allocation cases, namely, 1) $P_A = 0.25$, $P_B = 0.35$, $P_R = 0.40$, 2) $P_A = 0.35$, $P_B = 0.35$, $P_R = 0.30$, and 3) $P_A = 0.25$, $P_B = 0.25$, $P_R = 0.50$. As seen in Fig. 3.6, optimum relay location (the relay location that provides the lowest achievable SSER at a specific SNR value) depends on diversity order, number of selected antennas, and power assigned to each source. When all parameters (the total number of antennas, number of selected antennas, and assigned power) are the same at both sources, the expected optimum relay location is 0.5, which is also validated by two curves given in Fig. 3.6. So, locating the relay at any other point produces a SSER value which is greater than the SSER value obtained at relay location of 0.5. On the other hand, an inequality of one of these parameters deviates optimum relay location from 0.5. When powers of sources are equal, increasing or decreasing relay power does not affect relay location. An increment in the number of selected or total number of antennas for any source causes some shift in optimum relay location towards other source with fewer number of selected antennas or total number of antennas. Assigning more power to any source also causes some shift in optimum relay location towards the other one. Furthermore, while considering all curves in Fig. 3.6, dependency of SSER on power allocation, relay location, total number of antennas and number of selected antennas at each source is demonstrated.

3.5. Conclusion

We have examined generalized transmit and receive antenna selection at sources in MIMO TWRN over flat Rayleigh fading channel. We have derived exact and asymptotic SOP, MGF, and SSER expressions for M-PSK and M-QAM. We have shown that the diversity order is minimum of the numbers of transmit antennas available at the sources and does not depend on the number of selected antennas. Secondly, we have shown that complexity can be reduced, which also means reduction of cost, with a negligible performance deviation from that of beamforming. Thirdly, we have observed that an increment in the number of selected antennas for the source having total number of antennas equal to the diversity order is more effective than that for the other source. Finally, we have demonstrated that optimum relay location shifts away from any source when its selected or total number of antennas is increased. The same observation is also valid when more power is assigned to it than the other source. Hence, the dependency of SSER on both relay location and power allocation is illustrated.

4. PERFORMANCE OF TWO-WAY AF MIMO RELAY NETWORKS WITH SINGLE AND MULTIPLE ANTENNA SELECTION SCHEMES

4.1. Introduction

In wireless communications, cooperative relaying has been offered to enhance capacity, coverage extension, and power reduction [76]. However in half-duplex one way relaying systems, spectral efficiency is reduced since two time slots are required per single transmission. The reduction in spectral efficiency can be recovered by simultaneously exchanging information between two sources via a relay in two phases. For this reason, two way relaying networks (TWRNs) have attracted much attention in recent years [8, 84]. Moreover, transmission reliability can be enhanced between the end sources and the relay by usage of multi-input multi-output (MIMO) transmission technique in TWRNs [17–21, 85, 86]. Among MIMO techniques, beamforming uses all channel state information to improve reliability and performance of the TWRN [22–24], however, it also increases complexity of the system which means high cost. To overcome this disadvantaging factor of the systems using MIMO transmission technique, fewer radio frequency (RF) chains can be used by selecting antennas at the sources and the relay to reduce the complexity and power requirements [25]. Performance of single antenna selection at the sources or the relay is studied in many works [26–31, 87–90] over Rayleigh and Nakagami-m fading channels. A comparison of beamforming and single antenna selection at the sources over Nakagami-m fading channel is done in [27]. In that work it is proven that at two special cases, where one of the sources is equipped with single antenna, beamforming and antenna selection provide the same sum symbol error rate (SSER). In [26], joint transmit and receive antenna selection at the sources and the relay is performed based on the minimization of overall outage probability and maximization of sum rate. Since max-min criterion is used for overall outage probability minimization, an exhaustive search increasing the complexity, has to be carried out to find triple antennas for transmission and reception, and the same deduction is also valid for sum rate maximization. An antenna selection scheme at the relay based on sum rate maximization which reduces search complexity for amplify-and-forward (AF) MIMO TWRN is proposed in [90]. However, to the best of our knowledge, multiple antenna selection at the sources accompanying with single antenna selection at a multi antenna

relay has not been analyzed yet. Therefore, We propose an antenna selection scheme where firstly a single antenna selection at relay and generalized antenna selection at the source equipped with fewer number of antennas is committed for both transmission and reception and secondly generalized antenna selection at the other source is carried out by using the selected relay antenna. So, as depicted in Fig. 4.1, in the first phase of the communication, generalized transmit antenna selection or generalized selection transmission (GST), i.e, combined transmit antenna selection (TAS) and beamforming (maximal ratio transmission) for transmission at the sources and receive antenna selection (RAS) at the relay for reception between the relay and the source with fewer number of antennas are committed (Note that there is no RAS between the relay and the source having larger number of antennas). On the other hand, since we assume perfect reciprocity of channels between the sources and the relay, in the second phase, generalized receive antenna selection at the sources (well known as generalized selection combining (GSC) [78]) for reception and TAS at the relay for transmission between the relay and the source with fewer number of antennas are performed. The total number of antennas at the source A, the source B, and the relay are assumed to be N_A, N_B, and N_R, respectively. Without loss of generality, it is assumed that $N_A \leq N_B$. The main contributions of this chapter can be summarized as follows:

- It is proven that the diversity order of the proposed antenna selection strategy is $min(N_A N_R, N_B)$.
- The exact and asymptotic expressions of sum outage probability (SOP), moment generating function (MGF), and SSER for M-ary phase shift keying (M-PSK) and M-ary quadrature amplitude modulation (M-QAM) are derived.
- The ratio of the new and previous asymptotic SSER after an increment (decrement) of L_Δ in the number of selected antennas for the source dominating SSER at high signal-to-noise ratio (SNR) regime is defined as selection attenuation (amplification) factor (SAF) and is shown to be $\frac{(L_A! L_A^{N_A - L_A})^{N_R}}{\left((L_A \pm L_\Delta)! (L_A \pm L_\Delta)^{N_A - (L_A \pm L_\Delta)}\right)^{N_R}}$ if $N_A N_R < N_B$, otherwise it is $\frac{L_B! L_B^{N_B - L_B}}{(L_B \pm L_\Delta)! (L_B \pm L_\Delta)^{N_B - (L_B \pm L_\Delta)}}$.
- A smart antenna selection, where more antennas can be selected at low SNR region and a single antenna can be selected at high SNR regime for the source having larger number of antennas, is investigated to reduce the complexity further.
- It is illustrated that an increment in the number of antennas or power of any source produces a shift in optimum relay location towards the other source. An increment in the number of relay antennas shifts the optimum relay location towards the source with larger number of antennas. Furthermore, it is presented that assigning equal

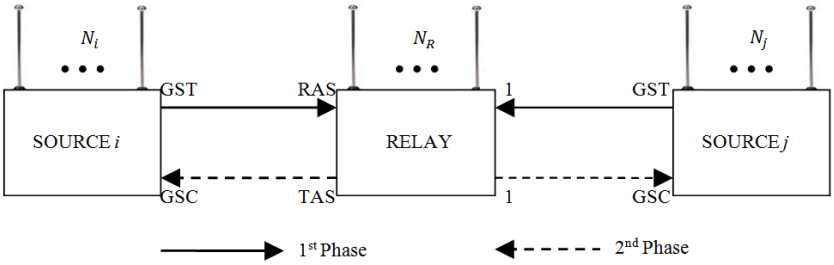

Figure 4.1: The proposed single and generalized antenna selection scheme.

power to the sources and less or more power to the relay has no effect on optimum relay location but it affects SSER.

The rest of this chapter is presented in four sections: In Section 4.2, the details of the system model and the proposed antenna selection strategy are given. The derivations of the exact and asymptotic cumulative distribution functions (CDF) of end-to-end (e2e) SNR and SSER expressions are presented in Section 4.3. In Section 4.4, numerical results supported by Monte-Carlo simulations are given. Finally, Section 4.5 concludes the work.

4.2. System Model

In this chapter we consider an AF MIMO TWRN which consists of two multi antenna sources, namely an N_A-antenna source A and an N_B-antenna source B, and an N_R-antenna relay R. We assume that all nodes are half-duplex, no direct link between the sources due to deep fading and signal blockage periods, errorless estimation of channel coefficients at the relay and error free feedback channels. Besides, the sources are equipped with L_i RF chains, where $i \in \{A, B\}$ and the relay is equipped with single RF chain. We represent the complex channel gain between the r^{th} antenna of the relay and the m^{th} transmit antenna of source i as $h^r_{i,m}$, where $i \in \{A, B\}$ and assume that $\{h^r_{i,m}, m = 1, \ldots, N_i$ and $r = 1, \ldots, N_R\}$ are independent identically distributed (i.i.d.) and circularly symmetric Gaussian random variables. We model these random variables as $h^r_{i,m} \sim CN(0, d_{iR}^{-f_i})$, where d_{iR} is the normalized distance between source i and the relay (i.e., $d_{AR} + d_{BR} = 1$) and f_i is the path loss exponent between source i and the relay. We also assume perfect channel reciprocity between channels of source i–relay R and relay R–source i, $i \in \{A, B\}$ and the additive noise at all the receivers is zero mean complex Gaussian noise with variance σ^2_x, where $x \in \{A, R, B\}$.

Selection Strategy: Without loss of generality, we suppose that $N_A \leq N_B$, single antenna is selected at the relay for source $A - R$ (and $R-$source A) link, and L_i antennas are selected at the sources, where $i \in \{A, B\}$. Antenna selection is carried out at the relay in two time slots during training period: In the first time slot, L_A antennas of the source A and an antenna of the relay which maximize SNR between the source A and the relay are selected. In this time slot only source A communicates with the relay. In the second time slot, only source B communicates with the relay and L_B antennas of the source B are selected to maximize SNR between the source B and the selected antenna of the relay in the first time slot. To clarify the selection strategy, let us define SNR between the r^{th} antenna of the relay and the m^{th} transmit antenna of source i to be $\alpha^r_{i,m} = \|h^r_{i,m}\|^2 E_s/\sigma^2_R$, where E_s is the average energy of transmitted symbols and is assumed to be 1. Let $\alpha^r_{m_i,1:N_i} \geq \alpha^r_{m_i,2:N_i} \geq \cdots \geq \alpha^r_{m_i,N_i:N_i}$ be the order statistics obtained by arranging $\{\alpha^r_{i,m}\}_{m=1}^{N_i}$ in decreasing order of magnitude in the first time slot. To obtain the maximum SNR between the r^{th} antenna of the relay and the source A, the first L_A antennas are selected. In order to find the relay antenna that maximizes the SNR between the relay and the source A, first L_A variable(s) in the order statistics are summed up and the antenna of the relay which maximizes total SNR is selected, namely, $k_{MR} = argmax \left\{ \sum_{l_A=1}^{L_A} \alpha^r_{m_A,l_A:N_A} \right\}_{r=1}^{N_R}$. In this way, GST is done at the source A and RAS is carried out at the relay R. In the second time slot of selection, k^{th}_{MR} antenna of the relay is used to communicate with the source B and the first L_B antennas of the source B are selected to maximize the SNR between k^{th}_{MR} antenna of the relay and the source B. Hence, GST is carried out at the source B. Since perfect channel reciprocity is assumed, GSC is committed at the sources and TAS and single antenna transmissions are performed at the relay for the $R-$source A link and the $R-$source B link, respectively, in the second phase of the transmission.

In the first phase of transmission, each source weights signals of selected antennas to maximize instantaneous SNR at the relay and broadcasts the signals to the relay. Then, the received signal at R via k^{th}_{MR} antenna of the relay for GST/RAS of source A and GST of source B can be given as

$$Y_R = \sqrt{P_A} w_A^T h_A s_A + \sqrt{P_B} w_B^T h_B s_B + n_R \tag{4.1}$$

where s_i, where $i \in \{A, B\}$, is the transmitted signal at source i with unit energy, P_i is the transmit power at source i, $(\cdot)^T$ denotes transpose, $h_i = [h^i_{1:N_i}; h^i_{2:N_i}; \cdots; h^i_{L_i:N_i}]$ is the $L_i \times 1$ channel vector between source i and k^{th}_{MR} antenna of the relay, $w_i = h_i^*/\|h_i\|$, where $(\cdot)^*$ denotes complex conjugate, is the transmission weight vector, $\|\cdot\|$ denotes Euclidean norm, and n_R is the additive Gaussian noise component at the relay with zero mean and variance

σ_R^2. In the second phase, Y_R is scaled by $G = \sqrt{P_R/(P_A\|h_A\|^2 + P_B\|h_B\|^2 + \sigma_R^2)}$, where P_R is the relay power, and is broadcasted to each source. The received signals at the sources are weighted and combined to obtain received signals of TAS/GSC and GSC at the sources A and B, respectively:

$$Y_i = G w_i^T h_i Y_R + w_i^T n_i \tag{4.2}$$

In (4.2), n_i is the $L_i \times 1$ additive Gaussian noise vector at source i with zero mean and mean power $I_{L_i}\sigma_i^2$ where I_{L_i} denotes an identity matrix of order L_i. Since each source knows its own transmitted signal and channel state information, after self-interference subtraction , the intended signal at the source i is given by

$$\tilde{Y}_i = G\sqrt{P_j}\|h_j\|\|h_i\|s_j + G\|h_i\|n_R + w_i^T n_i \tag{4.3}$$

where $(i, j) \in \{(A, B), (B, A)\}$. Then, the e2e SNR at source i can be expressed as

$$\gamma_i = \frac{\alpha_i \Upsilon_i \Upsilon_j}{(\alpha_i + 1)\Upsilon_i + \Upsilon_j + \rho} \tag{4.4}$$

where $(i, j) \in \{(A, B), (B, A)\}$ and $\alpha_i = P_R\sigma_R^2/(P_i\sigma_i^2)$. In (4.4), $\Upsilon_i = P_i\|h_i\|^2/\sigma_R^2$ and $\Upsilon_j = P_j\|h_j\|^2/\sigma_R^2$ are the instantaneous SNRs of the $i - R$ link and the $j - R$ link, respectively. In (4.4), setting $\rho = 1$ and 0 correspond to channel-noise-assisted (CNA) AF relaying, and channel-assisted (CA) AF relaying, respectively.

4.3. Performance Analysis

Derivations of exact and asymptotic SOP, MGF, and SSER expressions are elaborated in this section.

4.3.1. Exact Analysis

In this section derivation of exact CDF and SER expressions are provided.

4.3.1.1. Exact CDF of the e2e SNR

The proposed selection strategy results in two different random variables. In other words, γ_A and γ_B have different statistical properties since Υ_A and Υ_B do not have the same probability density functions (PDF). Because of that, derivations of CDF, MGF, and SOP for one of these random variables, γ_A and γ_B are not valid for the other one. So we have to derive them separately. The CDF of the instantaneous e2e SNR γ_i in (4.4) is given as [27, eq. (61)]

$$F_{\gamma_i}(\gamma) = 1 - \int_{\varsigma_i\gamma}^{\infty} \tilde{F}_{\Upsilon_i}(\nu_i) f_{\Upsilon_j}(\Upsilon_j) d\Upsilon_j \tag{4.5}$$

where $\tilde{F}_{\Upsilon_i}(\gamma) = 1 - F_{\Upsilon_i}(\gamma)$, $\varsigma_i = (\alpha_i + 1)/\alpha_i$, and $\nu_i = \gamma(\Upsilon_j + \rho)/(\alpha_i \Upsilon_j - \gamma(\alpha_i + 1))$. The random variable Υ_A (the instantaneous SNR of the $A - R$ link) is obtained after GST/RAS (GSC/TAS) and Υ_B (the instantaneous SNR of the $B - R$ link) is obtained after GST (GSC). Their CDFs are given in [79, eq. (5) and eq. (4)], respectively. Using [79, eq. (4)], the CDF of Υ_B can be expressed as

$$F_{\Upsilon_B}(\gamma) = 1 + \sum_{l_B=1}^{L_B} \frac{\hat{c}_{l_B} \gamma^{l_B - 1}}{(l_B - 1)!} e^{-\gamma/\bar{\Upsilon}_B} + \sum_{l_B = L_B + 1}^{N_B} \hat{c}_{l_B} e^{-l_B \gamma/(L_B \bar{\Upsilon}_B)} \tag{4.6}$$

where $\bar{\Upsilon}_B = P_B d_{BR}^{-f_B}/\sigma_R^2$ is the average SNR of the $B - R$ link and the coefficients $\hat{c}_{l_B}$ are given by [79, eq. (3)]

$$\hat{c}_{l_B} = \begin{cases} 1 & l_B = 0 \\ \bar{\Upsilon}_B^{-l_B+1}[-1 + \delta_{l_B k_B}] & 1 \le l_B < L_B \\ -\bar{\Upsilon}_B^{-l_B+1} \binom{N_B}{N_B - L_B} & l_B = L_B \\ \frac{(-1)^{l_B} \binom{N_B}{N_B - l_B} \binom{l_B - 1}{l_B - L_B - 1}}{(\frac{l_B}{L_B} - 1)^{L_B}} & L_B < l_B \le N_B \end{cases} \tag{4.7}$$

where $\delta_{l_B k_B} = \sum_{k_B = L_B + 1}^{N_B} \frac{(-1)^{k_B - l_B} \binom{N_B}{N_B - k_B} \binom{k_B - 1}{k_B - L_B - 1}}{(\frac{k_B}{L_B} - 1)^{L_B - l_B + 1}}$. For simplicity, we rephrase $F_{\Upsilon_B}(\gamma)$ as

$$F_{\Upsilon_B}(\gamma) = 1 + \sum_{l_B=1}^{N_B} C_{l_B} \gamma^{\omega_{l_B}} e^{-\gamma \Omega_{l_B}} \tag{4.8}$$

where $C_{l_B} = \hat{c}_{l_B}/(l_B - 1)!$ if $1 \le l_B \le L_B$ and $C_{l_B} = \hat{c}_{l_B}$ if $L_B < l_B \le N_B$, $\omega_{l_B} = l_B - 1$ if $1 \le l_B \le L_B$ and $\omega_{l_B} = 0$ if $L_B < l_B \le N_B$, $\Omega_{l_B} = 1/\bar{\Upsilon}_B$ if $1 \le l_B \le L_B$ and

$\Omega_{l_B} = l_B/(L_B\bar{\Upsilon}_B)$ if $L_B < l_B \leq N_B$. Therefore, PDF of Υ_B can be expressed as

$$f_{\Upsilon_B}(\gamma) = \sum_{l_B=1}^{N_B} C_{l_B}\omega_{l_B}\gamma^{\omega_{l_B}-1}e^{-\gamma\Omega_{l_B}} - \sum_{l_B=1}^{N_B} C_{l_B}\Omega_{l_B}\gamma^{\omega_{l_B}}e^{-\gamma\Omega_{l_B}}. \tag{4.9}$$

Although the CDF of Υ_A is given in [79, eq. (5)], we use another compact expression for this CDF. To obtain the mentioned expression, let us define $\lambda_A = \sum_{l_A=1}^{L_A} \alpha^r_{m_A,l_A:N_A}$ which has the same CDF as Υ_B and can be rephrased as

$$F_{\lambda_A}(\gamma) = 1 + e^{-\gamma/\bar{\lambda_A}} \sum_{l_A=0}^{L_A-1} \frac{\hat{c}_{l_A+1}}{l_A!}\gamma^{l_A} + e^{-(L_A+1)\gamma/(L_A\bar{\lambda_A})} \sum_{l_A=0}^{N_A-L_A-1} \hat{c}_{l_A+L_A+1}e^{-l_A\gamma/(L_A\bar{\lambda}_A)} \tag{4.10}$$

where $\bar{\lambda}_A = P_A d_{AR}^{-f_A}/\sigma_R^2$ is the average SNR of the $A-R$ link and the coefficients $\hat{c}_{l_A+1}$ and $\hat{c}_{l_A+L_A+1}$ are calculated from (4.7) but using $\bar{\lambda}_A$ instead of $\bar{\Upsilon}_B$. The CDF of Υ_A is equal to $F_{\lambda_A}^{N_R}(\gamma)$. To derive the CDF of the Υ_A, in [79] multinomial theorem is directly applied to expand $F_{\lambda_A}^{N_R}(\gamma)$. Instead of applying multinomial theorem directly, binomial theorem can be applied twice (firstly two summation terms taken as one term) and then power of the series of finite terms is expanded using [65, eq. (0.314)]. When power of a series of finite terms is expanded, the following expression is obtained:

$$\left(\sum_{n=0}^{m-1} c_n x^n\right)^p = \sum_{q=0}^{p(m-1)} \mu(q,p,m-1)x^q \tag{4.11}$$

where $\mu(0,p,m-1) = c_0^p$ and $\mu(q,p,m-1) = \frac{1}{qc_0}\sum_{k=1}^{q}(k(p+1)-q)c_k\mu(q-k,p,m-1)$. Note that $c_k = 0$ for $k > m-1$. Hence, CDF of the Υ_A can be given as

$$F_{\Upsilon_A}(\gamma) = \sum_{m_A=0}^{N_R}\sum_{k_A=0}^{m_A}\sum_{l_{1A}=0}^{k_A(L_A-1)}\sum_{l_{2A}=0}^{(m_A-k_A)(N_A-L_A-1)} C_{l_A}\gamma^{\omega_{l_A}}e^{-\Omega_{l_A}\gamma}, \tag{4.12}$$

where $C_{l_A} = \binom{N_R}{m_A}\binom{m_A}{k_A}\mu_{1A}(l_{1A},k_A,L_A-1)\mu_{2A}(l_{2A},m_A-k_A,N_A-L_A-1)$, $\omega_{l_A} = l_{1A}$, and $\Omega_{l_A} = \frac{m_A(L_A+1)-k_A+l_{2A}}{L_A\Upsilon_A}$. The coefficients $\mu_{1A}(l_{1A},k_A,L_A-1)$ and $\mu_{2A}(l_{2A},m_A-k_A,N_A-L_A-1)$ are obtained when the expansion in (4.11) is applied to the first and second summations of (4.10) after two binomial expansions, respectively. For $\mu_{1A}(l_{1A},k_A,L_A-1)$, $c_n = \frac{\hat{c}_{l_A+1}}{l_A!}$ and for $\mu_{2A}(l_{2A},m_A-k_A,N_A-L_A-1)$, $c_n = \hat{c}_{l_A+L_A+1}$. To avoid ambiguity when binomial theorem is applied to the expressions such as $(x+0)^N$, we

define 0^0 to be 1 (This case occurs when all antennas are selected for the source A which has fewer total number of antennas than source B). For the sake of simplicity, we let $\sum_{\Upsilon_A(m_A=1)} = \sum_{m_A=1}^{N_R} \sum_{k_A=0}^{m_A} \sum_{l_{1A}=0}^{k_A(L_A-1)} \sum_{l_{2A}=0}^{(m_A-k_A)(N_A-L_A-1)}$ and restate the CDF of the Υ_A as

$$F_{\Upsilon_A}(\gamma) = 1 + \sum_{\Upsilon_A(m_A=1)} C_{l_A} \gamma^{\omega_{l_A}} e^{-\Omega_{l_A}\gamma}. \tag{4.13}$$

Furthermore, by taking derivative of (4.13), we find the PDF of the Υ_A as follows

$$f_{\Upsilon_A}(\gamma) = \sum_{\Upsilon_A(m_A=1)} \omega_{l_A} C_{l_A} \gamma^{\omega_{l_A}-1} e^{-\gamma\Omega_{l_A}} - \sum_{\Upsilon_A(m_A=1)} C_{l_A} \Omega_{l_A} \gamma^{\omega_{l_A}} e^{-\gamma\Omega_{l_A}}. \tag{4.14}$$

The CDF of the instantaneous e2e SNR γ_A, $F_{\gamma_A}(\gamma)$, is obtained after substitution of (4.9) and (4.13) into (4.5) as

$$F_{\gamma_A}(\gamma) = 1 - \sum_{\Upsilon_A(m_A=1)} \sum_{l_B=1}^{N_B} \Omega_{l_B} C_{l_A} C_{l_B} I_1(\omega_{l_B}) + \sum_{\Upsilon_A(m_A=1)} \sum_{l_B=1}^{N_B} \omega_{l_B} C_{l_A} C_{l_B} I_1(\omega_{l_B} - 1) \tag{4.15}$$

where

$$I_1(m) = \int_{\varsigma_A\gamma}^{\infty} x^m \left(\frac{\gamma(x+\rho)}{\alpha_A x - \gamma(\alpha_A+1)} \right)^{\omega_{l_A}} e^{-\left(\Omega_{l_B} x + \frac{\Omega_{l_A}\gamma(x+\rho)}{\alpha_A x - \gamma(\alpha_A+1)}\right)} dx. \tag{4.16}$$

The integral given in (4.16) is reformulated by a changing of variable as $x = t + \varsigma_A\gamma$ and then binomial expansion given by [65, eq. (1.111)] is applied to the resulting two terms, namely $(t+\varsigma_A\gamma)^m$ and $(t+\varsigma_A\gamma+\rho)^{\omega_{l_A}}$. Consequently, the integral is reformulated as

$$I_1(m) = \left(\frac{\gamma}{\alpha_A}\right)^{\omega_{l_A}} e^{-\left(\Omega_{l_B}\varsigma_A + \frac{\Omega_{l_A}}{\alpha_A}\right)\gamma} \sum_{p=0}^{\omega_{l_A}} \sum_{q=0}^{m} \binom{\omega_{l_A}}{p} \binom{m}{q} (\varsigma_A\gamma+\rho)^p (\varsigma_A\gamma)^{m-q} \int_0^{\infty} t^{q-p} e^{-\left(\Omega_{l_B} t + \frac{\Omega_{l_A}\gamma(\varsigma_A\gamma+\rho)}{\alpha_A t}\right)} dt. \tag{4.17}$$

The identity [65, eq. (3.471.9)] is applied to the integral in (4.17) and $I_1(m)$ is obtained as

$$I_1(m) = 2\left(\frac{\gamma}{\alpha_A}\right)^{\omega_{l_A}} e^{-\left(\Omega_{l_B}\varsigma_A+\frac{\Omega_{l_A}}{\alpha_A}\right)\gamma} \sum_{p=0}^{\omega_{l_A}} \sum_{q=0}^{m} \binom{\omega_{l_A}}{p} \binom{m}{q} (\varsigma_A\gamma+\rho)^p (\varsigma_A\gamma)^{m-q} \left(\frac{\Omega_{l_A}\gamma(\varsigma_A\gamma+\rho)}{\Omega_{l_B}\alpha_A}\right)^{\frac{q-p+1}{2}} K_{q-p+1}\left(2\sqrt{\frac{\Omega_{l_A}\Omega_{l_B}\gamma(\varsigma_A\gamma+\rho)}{\alpha_A}}\right). \tag{4.18}$$

$K_\nu(x)$ in (4.18) is the ν^{th}-order modified Bessel Function of the second kind [65, eq. (8.407)], which is available in well known software programs such as MATHEMATICA and MAPLE.

The closed form for $F_{\gamma_A}(\gamma)$, after substituting (4.18) into (4.15), is

$$F_{\gamma_A}(\gamma) = 1 + 2 \sum_{\Upsilon_A(m_A=1)} \sum_{l_B=1}^{N_B} \Big[\omega_{l_B} H_{1A}(\omega_{l_B}-1) - \Omega_{l_B} H_{1A}(\omega_{l_B})\Big]. \tag{4.19}$$

$H_{1A}(m)$ in (4.19) is

$$H_{1A}(m) = \sum_{p=0}^{\omega_{l_A}} \sum_{q=0}^{m} \binom{\omega_{l_A}}{p} \binom{m}{q} C_{l_A} C_{l_B} \left(\frac{\gamma}{\alpha_A}\right)^{\omega_{l_A}} e^{-\left(\Omega_{l_B}\varsigma_A+\frac{\Omega_{l_A}}{\alpha_A}\right)} (\varsigma_A\gamma+\rho)^p (\varsigma_A\gamma)^{m-q} \left(\frac{\Omega_{l_A}\gamma(\varsigma_A\gamma+\rho)}{\Omega_{l_B}\alpha_A}\right)^{\frac{q-p+1}{2}} K_{q-p+1}\left(2\sqrt{\frac{\Omega_{l_A}\Omega_{l_B}\gamma(\varsigma_A\gamma+\rho)}{\alpha_A}}\right). \tag{4.20}$$

The CDF for CA-AF can be found by setting $\rho = 0$ in (4.19) and (4.20). However, a simpler expression can be obtained by letting $\rho = 0$ and following the same derivation steps as the CDF of the γ_A in (4.19):

$$F_{\gamma_A}(\gamma) = 1 + 2 \sum_{\Upsilon_A(m_A=1)} \sum_{l_B=1}^{N_B} \Big[\omega_{l_B} H_{2A}(\omega_{l_B}-1) - \Omega_{l_B} H_{2A}(\omega_{l_B})\Big]. \tag{4.21}$$

$H_{2A}(m)$ in (4.21) is

$$H_{2A}(m) = \sum_{q=0}^{\omega_{l_A}+m} \binom{\omega_{l_A}+m}{q} C_{l_A} C_{l_B} \alpha_A^{-\omega_{l_A}} \varsigma_A^{\frac{m+q+1}{2}} \gamma^{\omega_{l_A}+m+1} \left(\frac{\Omega_{l_A}}{\alpha_A\Omega_{l_B}}\right)^{\frac{m-q+1}{2}} e^{-\left(\Omega_{l_B}\varsigma_A+\frac{\Omega_{l_A}}{\alpha_A}\right)} K_{m-q+1}\left(\gamma\sqrt{\frac{4\Omega_{l_A}\Omega_{l_B}\varsigma_A}{\alpha_A}}\right). \tag{4.22}$$

To derive the CDF of the instantaneous e2e SNR γ_B, $F_{\gamma_B}(\gamma)$, we substitute (4.8) and (4.14) into (4.5) but subscripts A and B in (4.5) are swapped. Tracking the same steps for derivation of $F_{\gamma_A}(\gamma)$, the following expression is extracted:

$$F_{\gamma_B}(\gamma) = 1 + 2 \sum_{\Upsilon_A(m_A=1)} \sum_{l_B=1}^{N_B} \Big[\omega_{l_A} H_{1B}(\omega_{l_A} - 1) - \Omega_{l_A} H_{1B}(\omega_{l_A}) \Big]. \tag{4.23}$$

$H_{1B}(m)$ in (4.23) is equal to the $H_{1A}(m)$ in (4.20) when subscripts A and B are interchanged. The CDF of CA-AF for γ_B can also be derived as that of γ_B and it is obtained as

$$F_{\gamma_B}(\gamma) = 1 + 2 \sum_{\Upsilon_A(m_A=1)} \sum_{l_B=1}^{N_B} \Big[\omega_{l_A} H_{2B}(\omega_{l_A} - 1) - \Omega_{l_A} H_{2B}(\omega_{l_A}) \Big] \tag{4.24}$$

where $H_{2B}(m)$ equal to $H_{2A}(m)$ when subscripts A and B are swapped in (4.22).

The exact e2e SOP for CNA-AF is evaluated for a threshold γ_{th} as $F_{\gamma_B}(\gamma_{th}) + F_{\gamma_B}(\gamma_{th})$ by using (4.19) and (4.23) and it is evaluated for CA-AF case by (4.21) and (4.24).

4.3.1.2. Exact SSER

In this section, we derive closed-form expressions of SSER which is defined as summation of the SERs of two sources [80] based on the CDF method for M-PSK [81]. On the other hand, although it is hard to obtain closed-form expression of SSER from MGF based analysis, we derive closed-form expressions for MGF of γ_A and γ_B which can be used to calculate SSER numerically for M-PSK and M-QAM. Therefore, we firstly give MGFs of γ_A and γ_B and secondly derive closed-form expressions of SSER based on CDF analysis. The derivations based on both analysis methods are carried out for CA-AF case. We use the CDF of the γ_A in (4.21) (γ_B in (4.24)), $F_{\gamma_A}(\gamma)(F_{\gamma_B}(\gamma))$, and express its MGF as

$$M_\gamma(-s) = s \int_0^\infty e^{-sx} F_\gamma(x) dx. \tag{4.25}$$

After substituting (4.21) into (4.25) and using the identity [67, eq. (2.16.6.3)], $M_{\gamma_A}(-s)$ is obtained as

$$M_{\gamma_A}(-s) = 1 + 2s \sum_{\Upsilon_A(m_A=1)} \sum_{l_B=1}^{N_B} \Big[\omega_{l_B} H_{2A}(\omega_{l_B} - 1, s) - \Omega_{l_B} H_{2A}(\omega_{l_B}, s)\Big] \tag{4.26}$$

$H_{2A}(m,s)$ in (4.26) is

$$H_{2A}(m,s) = \sqrt{\pi} \sum_{q=0}^{\omega_{l_A}+m} \Delta^{AB}\, {}_2F_1\Bigg(\frac{\omega_{l_A}+q+1}{2}, \frac{\omega_{l_A}+q+2}{2}; \omega_{l_A}+m+\frac{5}{2}, 1 - \frac{\frac{4\Omega_{l_A}\Omega_{l_B}\varsigma_A}{\alpha_A}}{\Big(\omega_{l_B}\varsigma_A + \frac{\Omega_{l_A}}{\alpha_A} + s\Big)^2}\Bigg) \tag{4.27}$$

where

$$\Delta^{AB} = \frac{\binom{\omega_{l_A}+m}{q} C_{l_A} C_{l_B} \alpha_A^{-\omega_{l_A}} \varsigma_A^q \Omega_{l_B}^{-(m-q+1)} \Gamma(\omega_{l_A}+q+1)\Gamma(\omega_{l_A}+2m-q+3)}{2^{(\omega_{l_A}+2m-q+3)}\Gamma(\omega_{l_A}+m+\frac{5}{2})\Big(\Omega_{l_B}\varsigma_A + \frac{\Omega_{l_A}}{\alpha_A} + s\Big)^{(\omega_{l_A}+q+1)}}. \tag{4.28}$$

${}_2F_1(\iota,\tau;w;z)$ in (4.27) is the Gauss hypergeometric function [65, eq. (9.111)], which is available in well known software programs such as MATHEMATICA and MAPLE.

Similarly, the MGF of γ_B based on (4.24) is

$$M_{\gamma_B}(-s) = 1 + 2s \sum_{\Upsilon_A(m_A=1)} \sum_{l_B=1}^{N_B} \Big[\omega_{l_A} H_{2B}(\omega_{l_A} - 1, s) - \Omega_{l_A} H_{2B}(\omega_{l_A}, s)\Big] \tag{4.29}$$

where $H_{2B}(m,s)$ is the same as $H_{2A}(m,s)$ in (4.27) when subscripts A and B are interchanged with each other. Thereby, SSER based on MGF analysis can be expressed by using (4.26) and (4.29) as

$$P_{SSER,M} = \sum_{q=1}^{Q} a_q \int_0^{\theta_q} \left[M_{\gamma_A}\left(-\frac{\lambda_{mod}}{\sin^2(\theta)}\right) + M_{\gamma_B}\left(-\frac{\lambda_{mod}}{\sin^2(\theta)}\right)\right] d\theta. \tag{4.30}$$

Q, a_q, λ_{mod}, and θ_q in (4.30) are modulation dependent parameters. For M-PSK and M-QAM, these parameters are given in Table 2.1.

Although it is not easy to derive closed-form expression for SSER based on MGF analysis, (4.30) can be used to calculate SSER numerically. On the other hand, SSER can be derived in closed form for M-PSK by using CDF based analysis as

$$P_{SSER,C} = P_{A,SER} + P_{B,SER} \tag{4.31}$$

$P_{A,SER}$ and $P_{B,SER}$ in (4.31) are SER at sources A and B and can be evaluated from the integral $\frac{a\sqrt{b}}{2\pi}\int_0^\infty x^{-1/2}e^{-bx}F_\gamma(x)dx$ [81] where a and b are modulation dependent parameters. $a = 1$ and $b = 1$ for Binary PSK (BPSK) and $a = 2$ and $b = \sin^2(\pi/M)$ for approximated SER of M-PSK. Firstly, let us consider $P_{A,SER} = \frac{a\sqrt{b}}{2\pi}\int_0^\infty x^{-1/2}e^{-bx}F_{\gamma_i}(x)dx$: To solve this integral, the CDF of γ_i in (4.21), $F_{\gamma_A}(\gamma)$, is substituted into $P_{A,SER}$ and then the identity [67, eq. (2.16.6.3)] is used to obtain the $P_{A,SER}$ as

$$P_{A,SER} = \frac{a}{2} + a\sqrt{b}\sum_{\Upsilon_A(m_A=1)}\sum_{l_B=1}^{N_B}[\omega_{l_B}H_{SER_A}(\omega_{l_B}-1) - \Omega_{l_B}H_{SER_A}(\omega_{l_B})], \tag{4.32}$$

$H_{SER_A}(m)$ in (4.32) is given as

$$H_{SER_A}(m) = \sum_{q=0}^{\omega_{l_A}+m}\binom{\omega_{l_A}+m}{q}\frac{C_{l_A}C_{l_B}\alpha_A^{-\omega_{l_A}}\varsigma_A^q}{\Omega_{l_B}^{m-q+1}}I_{SER_A}(m) \tag{4.33}$$

where

$$\begin{aligned} I_{SER_A}(m) = {} & \frac{\Gamma\left(\omega_{l_A}+q+\frac{1}{2}\right)\Gamma\left(\omega_{l_A}+2m-q+\frac{5}{2}\right)}{2^{(\omega_{l_A}+2m-q+\frac{5}{2})}\left(\Omega_{l_B}\varsigma_A+\frac{\Omega_{l_A}}{\alpha_A}+b\right)^{(\omega_{l_A}+q+\frac{1}{2})}\Gamma\left(\omega_{l_A}+m+2\right)} \\ & {}_2F_1\left(\frac{\omega_{l_A}+q+\frac{1}{2}}{2},\frac{\omega_{l_A}+q+\frac{3}{2}}{2};\omega_{l_A}+m+2;1-\frac{\Omega_{l_A}\Omega_{l_B}\varsigma_A/\alpha_A}{\left(\Omega_{l_B}\varsigma_{l_A}+\Omega_{l_A}/\alpha_A+b\right)^2}\right). \end{aligned} \tag{4.34}$$

$P_{B,SER}$ can be derived by tracking the same steps and it is obtained as

$$P_{B,SER} = \frac{a}{2} + a\sqrt{b}\sum_{\Upsilon_A(m_A=1)}\sum_{l_B=1}^{N_B}[\omega_{l_A}H_{SER_B}(\omega_{l_A}-1) - \Omega_{l_A}H_{SER_B}(\omega_{l_A})]. \tag{4.35}$$

$H_{SER_B}(m)$ in (4.35) is equal to $H_{SER_A}(m)$ in (4.33) when subscripts A and B are swapped.

4.3.2. Asymptotic Analysis

Exact SOP and SSER can be represented as asymptotic SOP and SSER at high SNR, namely these two performance metrics are characterized by diversity order and array gain [82]. Therefore, it is useful to derive asymptotic SOP and SSER for system performance analysis at high SNR as given in this section.

4.3.2.1. Asymptotic CDF of the e2e SNR

The asymptotic e2e CDF of the γ_A and γ_B can be represented in terms of their diversity order and array gain at high SNR as given below:

$$F_{\gamma_A}^{\infty}(\gamma) \approx \hat{G}_{a,A} \left(\frac{\bar{\Upsilon}_A}{\gamma} \right)^{-\hat{G}_{d,A}} + o\left(\bar{\Upsilon}_A^{-\hat{G}_{d,A}} \right) \tag{4.36}$$

and

$$F_{\gamma_B}^{\infty}(\gamma) \approx \hat{G}_{a,B} \left(\frac{\bar{\Upsilon}_B}{\gamma} \right)^{-\hat{G}_{d,B}} + o\left(\bar{\Upsilon}_B^{-\hat{G}_{d,B}} \right), \tag{4.37}$$

$o(\cdot)$ in (4.36) and (4.37) denotes higher order terms.

An asymptotic expression of e2e CDF of the γ_A, $F_{\gamma_A}(\gamma)$ can be obtained from asymptotic expressions of the $F_{\Upsilon_B}(\gamma)$ and $F_{\lambda_B}(\gamma)$ in (4.6) and (4.10), respectively, where they are derived from single term polynomial approximation of the PDF and CDF of Rayleigh fading [82]. However, they lose their tightness as the number of selected antennas decreases. To obtain a tighter asymptotic CDF for $F_{\Upsilon_B}(\gamma)$ and $F_{\lambda_B}(\gamma)$, we apply the Taylor series expansion of the exponential function given by the identity [65, eq. (1.211.1)] to the CDFs in (4.6) and (4.10) and we observe that the dominant components of these two CDFs are as follows, respectively:

$$F_{\Upsilon_B}^{\infty}(\gamma) = \frac{1}{L_B! L_B^{N_B - L_B}} \left(\frac{\gamma}{\bar{\Upsilon}_B} \right)^{N_B} \tag{4.38}$$

and

$$F_{\lambda_A}^{\infty}(\gamma) = \frac{1}{L_A! L_A^{N_A - L_A}} \left(\frac{\gamma}{\bar{\lambda}_A} \right)^{N_A}. \tag{4.39}$$

Since $F_{\Upsilon_A}(\gamma) = F_{\lambda_A}(\gamma)^{N_R}$, $F_{\Upsilon_A}^{\infty}(\gamma)$ is found to be

$$F_{\Upsilon_A}^{\infty}(\gamma) = \left(\frac{1}{L_A! L_A^{N_A - L_A}} \right)^{N_R} \left(\frac{\gamma}{\bar{\Upsilon}_A} \right)^{N_A N_R}. \tag{4.40}$$

In order to derive asymptotic CDF for $F_{\gamma_A}(\gamma)$ and $F_{\gamma_B}(\gamma)$, we use the inequality $\alpha_A \Upsilon_A \Upsilon_B / ((\alpha_A + 1)\Upsilon_A + \Upsilon_B + \rho) < min(\alpha_A \Upsilon_A, \alpha_A \Upsilon_B / (\alpha_A + 1))$ and obtain $F_{\gamma_A}^{\infty}(\gamma) = F_{\Upsilon_A}^{\infty}(\frac{\gamma}{\alpha_A}) + F_{\Upsilon_B}^{\infty}(\frac{(\alpha_A+1)\gamma}{\alpha_A}) - F_{\Upsilon_A}^{\infty}(\frac{\gamma}{\alpha_A}) F_{\Upsilon_B}^{\infty}(\frac{(\alpha_A+1)\gamma}{\alpha_A})$. We ignore the term

$F^{\infty}_{\Upsilon_A}(\frac{\gamma}{\alpha_A})F^{\infty}_{\Upsilon_B}(\frac{(\alpha_A+1)\gamma}{\alpha_A})$ and write $F^{\infty}_{\gamma_A}(\gamma)$ and $F^{\infty}_{\gamma_B}(\gamma)$ as in (4.41) and (4.42), respectively:

$$F^{\infty}_{\gamma_A}(\gamma) = F^{\infty}_{\Upsilon_A}(\frac{\gamma}{\alpha_A}) + F^{\infty}_{\Upsilon_B}(\varsigma_A\gamma) \tag{4.41}$$

and

$$F^{\infty}_{\gamma_B}(\gamma) = F^{\infty}_{\Upsilon_A}(\varsigma_B\gamma) + F^{\infty}_{\Upsilon_B}(\frac{\gamma}{\alpha_B}). \tag{4.42}$$

By substituting (4.38) and (4.40) into (4.41) and (4.42) and defining $\kappa_A = \bar{\Upsilon}_A/\bar{\Upsilon}_B$, diversity order and array gain in (4.36) and (4.37) are found respectively, as

$$\hat{G}_{d,A} = \hat{G}_{d,B} = min(N_A N_R, N_B) \tag{4.43}$$

and

$$\begin{aligned}
\hat{G}_{a,A} &= \begin{cases}
\frac{\alpha_A^{-N_A N_R}}{\left(L_A! L_A^{N_A - L_A}\right)^{N_R}} & N_A N_R < N_B \\
\frac{\varsigma_A^{N_B} \kappa_A^{N_B}}{L_A! L_B^{N_B - L_B}} & N_A N_R > N_B \\
\frac{\alpha_A^{-N_A N_R}}{\left(L_A! L_A^{N_A - L_A}\right)^{N_R}} + \frac{\varsigma_A^{N_B} \kappa_A^{N_B}}{L_A! L_B^{N_B - L_B}} & N_A N_R = N_B
\end{cases} \\
\hat{G}_{a,B} &= \begin{cases}
\frac{\varsigma_B^{N_A N_R}}{\left(L_A! L_A^{N_A - L_A}\right)^{N_R}} & N_A N_R < N_B \\
\frac{\alpha_B^{-N_B} \kappa_A^{N_B}}{L_B! L_B^{N_B - L_B}} & N_A N_R > N_B \\
\frac{\varsigma_B^{N_A N_R}}{\left(L_A! L_A^{N_A - L_A}\right)^{N_R}} + \frac{\alpha_B^{-N_B} \kappa_A^{N_B}}{L_B! L_B^{N_B - L_B}} & N_A N_R = N_B
\end{cases}
\end{aligned} . \tag{4.44}$$

For evaluation of asymptotic SOP (4.41) and (4.42) can be used and it can be calculated as $F^{\infty}_{\gamma_A}(\gamma_{th}) + F^{\infty}_{\gamma_B}(\gamma_{th})$.

4.3.2.2. Asymptotic SSER

In this section, two different asymptotic expressions are presented, namely, one of them is derived for the asymptotic SSER expression which is obtained by using the CDF based analysis method for M-PSK and the second one is for the MGF based analysis for both M-PSK and M-QAM.

To obtain asymptotic SSER based on the CDF based analysis method, (4.36) and (4.37) are substituted into (4.31) and the result is found as

$$P_{SSER,C}^{\infty} \approx \left(G_{a,C}\bar{\Upsilon}_A\right)^{-G_d} + o\left(\bar{\Upsilon}_A^{-G_d}\right). \tag{4.45}$$

The diversity gain G_d is found as $G_d = \hat{G}_{d,i} = \hat{G}_{d,A} = min(N_A N_R, N_B)$ and the array gain is obtained as $G_{a,C} = \left(\frac{ab^{-G_d}}{2\sqrt{\pi}}\Gamma\left(G_d + \frac{1}{2}\right)\Psi_C\right)^{-1/G_d}$, where Ψ_C is given as

$$\Psi_C = \begin{cases} \frac{\left(\alpha_A^{-N_A N_R} + \varsigma_B^{N_A N_R}\right)}{\left(L_A! L_A^{N_A - L_A}\right)^{N_R}}, & N_A N_R < N_B \\ \frac{\kappa_A^{N_B}\left(\varsigma_A^{N_B} + \alpha_B^{-N_B}\right)}{L_B! L_B^{N_B - L_B}}, & N_A N_R > N_B \\ \frac{\left(\alpha_A^{-N_A N_R} + \varsigma_B^{N_A N_R}\right)}{\left(L_A! L_A^{N_A - L_A}\right)^{N_R}} + \frac{\kappa_A^{N_B}\left(\varsigma_A^{N_B} + \alpha_B^{-N_B}\right)}{L_B! L_B^{N_B - L_B}}, & N_A N_R = N_B \end{cases}. \tag{4.46}$$

To find asymptotic SSER based on MGF analysis method, we have to find asymptotic MGFs of γ_A and γ_B. We substitute (4.36) and (4.37) into (4.25) and derive asymptotic MGFs for γ_A and γ_B as follows:

$$M_{\gamma_{A(B)}}^{\infty}(-s) \approx \frac{\hat{G}_{a,A(B)}\Gamma(G_d + 1)}{\left(s\bar{\Upsilon}_{A(B)}\right)^{G_d}} + o\left(\bar{\Upsilon}_{A(B)}^{-G_d}\right) \tag{4.47}$$

Now, asymptotic SSER based on MGF analysis can be attained by substituting MGFs of γ_A and γ_B in (4.47) into (4.30):

$$P_{SSER,M}^{\infty} = \frac{\Gamma\left(G_d + 1\right)\bar{\Upsilon}_A^{-G_d}}{\lambda_{mod}^{G_d}}\left(\sum_{q=1}^{Q} a_q I_2(G_d, \theta_q)\right)\left(\hat{G}_{a,A} + \hat{G}_{a,B}\right). \tag{4.48}$$

The $I_2(G_d, \theta_q)$ is given as

$$I_2(G_d, \theta_q) = \int_0^{\theta_q} \sin^{2G_d}(x)dx. \tag{4.49}$$

The integral in (4.49), which is is valid for $G_d > -1/2$ and $\sin(\theta_q) \geq 0$, is found as

$$I_2(G_d, \theta_q) = \frac{\sqrt{\pi}\Gamma\left(G_d + \frac{1}{2}\right)}{2\Gamma\left(G_d + 1\right)} - \cos(\theta_q)\,{}_2F_1\left(\frac{1}{2}, \frac{1}{2} - G_d; \frac{3}{2}; \cos^2(\theta_q)\right). \tag{4.50}$$

Consequently, the asymptotic SSER based on MGF analysis method can be reorganized as

$$P_{SSER,M}^{\infty} \approx \left(G_{a,M}\bar{\Upsilon}_A\right)^{-G_d} + o\left(\bar{\Upsilon}_A^{-G_d}\right). \tag{4.51}$$

The diversity gain G_d is found as $G_d = \hat{G}_{d,A} = \hat{G}_{d,A} = min(N_A N_R, N_B)$ and the array gain $G_{a,M}$ is derived as $G_{a,M} = (\Phi_M \Psi_C)^{-1/G_d}$, where

$$\Phi_M = \frac{\Gamma(G_d + 1)}{\lambda_{mod}^{G_d}} \left(\sum_{q=1}^{Q} a_q I_2(G_d, \theta_q) \right). \tag{4.52}$$

Let us consider increasing or decreasing the number of selected antennas for the source contributing to asymptotic SSER by L_Δ, i.e, let $\hat{L}_i \leftarrow L_i \pm L_\Delta$, where $i \in \{A, B\}$ and consider the ratio of new and previous asymptotic SSERs by using (4.45) or (4.51). The ratio is obtained as

$$R_{SSER} = \begin{cases} \frac{(L_A! L_A^{N_A - L_A})^{N_R}}{\left((L_A \pm L_\Delta)! (L_A \pm L_\Delta)^{N_A - (L_A \pm L_\Delta)}\right)^{N_R}} & N_A N_R < N_B \\ \frac{L_B! L_B^{N_B - L_B}}{(L_B \pm L_\Delta)! (L_B \pm L_\Delta)^{N_B - (L_B \pm L_\Delta)}} & N_A N_R \geq N_B \end{cases}. \tag{4.53}$$

Hence, we conclude that an increment (decrement) of L_Δ in the number of selected antennas for the source dominating asymptotic SSER reduces (increases) SSER by a factor of R_{SSER}. We call this ratio selection attenuation (amplification) factor (SAF). However, increasing the number of selected antennas for the other source does not affect SSER in the high-SNR region.

4.4. Numerical Results

In this section, numerical results and Monte Carlo simulations are provided to validate the obtained analytical expressions for the proposed selection scheme. It is assumed that total power $P_T = 1$, $\sigma^2 = \sigma_A^2 = \sigma_B^2 = \sigma_R^2$, power of the sources and relay are equal, $P_A = P_B = P_R = P_T/3$, and the relay is in the middle of the sources, namely, $d_{AR} = d_{BR} = 0.5$. The path loss exponent f_i is taken to be 3 which represents heavy urban environment. Different power allocations and relay locations will be stated if they are used. SOP, SSER, and SAF curves are plotted versus P_T/σ^2. The SSER expressions are ploted for the CA-AF case, i.e., $\rho = 0$, for which they are derived only.

Fig. 4.2 validates analytical expressions of the exact and asymptotic SOP for a threshold of 10 dB and several diversity orders, namely 2, 3, 4, and 5. The exact SOP curves are plotted from (4.19) and (4.23) which means CNA-AF case, i.e. $\rho = 1$. The asymptotic ones are plotted from (4.41) and (4.42). Total and selected number of antennas are taken as $N_R \in \{1, 2\}$, $N_A \in \{2, 3\}$, $N_B \in \{3, 5\}$, $L_A \in$

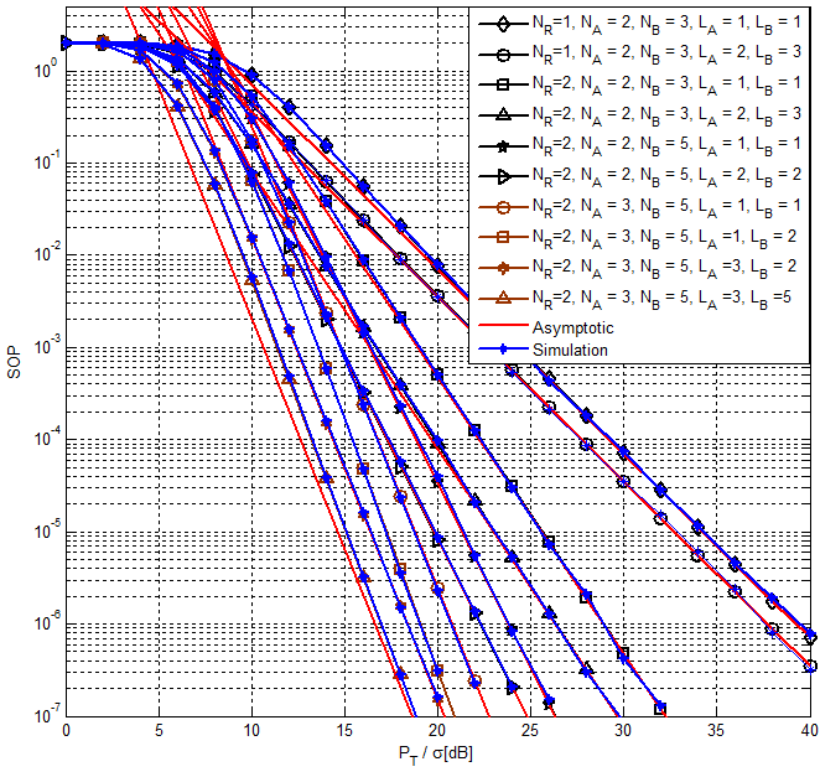

Figure 4.2: SOP of the proposed selection strategy for different numbers of selected antennas and diversity orders.

$\{1, 2, 3\}$, and $L_B \in \{1, 2, 3, 5\}$. Analytical results coincide with the simulations results. Increasing N_R from 1 to 2, increases diversity order from 2 to 3 for $(N_A, N_B, L_A, L_B) \in \{(2, 3, 1, 1), (2, 3, 2, 3)\}$ and also this results in an SNR gain of about 8.8 dB at a SOP of 10^{-5} for $(N_A, N_B, L_A, L_B) = (2, 3, 1, 1)$. When $N_R = 1$, the SNR gap between $(N_A, N_B, L_A, L_B) = (2, 3, 1, 1)$ and $(N_A, N_B, L_A, L_B) = (2, 3, 2, 3)$ at a SOP of 10^{-5} is about 1.7 dB, however, the gap becomes 2.7 dB when N_R is set to 2. This is because of the source dominating the SOP is changed from the source A to the source B whose total number of active antennas becomes 3. Furthermore, at the same SOP value, an SNR gain of about 4.4 dB is obtained when increasing the diversity order from 3 to 4 (the SNR gap between $(N_R, N_A, N_B, L_A, L_B) = (2, 2, 3, 1, 1)$ and $(N_R, N_A, N_B, L_A, L_B) = (2, 2, 5, 1, 1)$). Increasing diversity order by 1 results in an SNR gain of about 2.5 dB (the SNR gap between $(N_R, N_A, N_B, L_A, L_B) = (2, 2, 5, 1, 1)$ and $(N_R, N_A, N_B, L_A, L_B) = (2, 3, 5, 1, 1)$). Now let us consider the curves given for $(N_R, N_A, N_B, L_A, L_B) = (2, 3, 5, 1, 2)$ and $(N_R, N_A, N_B, L_A, L_B) = (2, 3, 5, 3, 2)$: The diversity orders of these two curves are the same, namely 5, and their asymptotic curves are also the same. This situation leads us to a smart antenna selection strategy such that at high SNRs only one antenna can be selected for the source not dominating the asymptotic SOP and at low SNR region more antennas can be selected. This selection strategy decreases

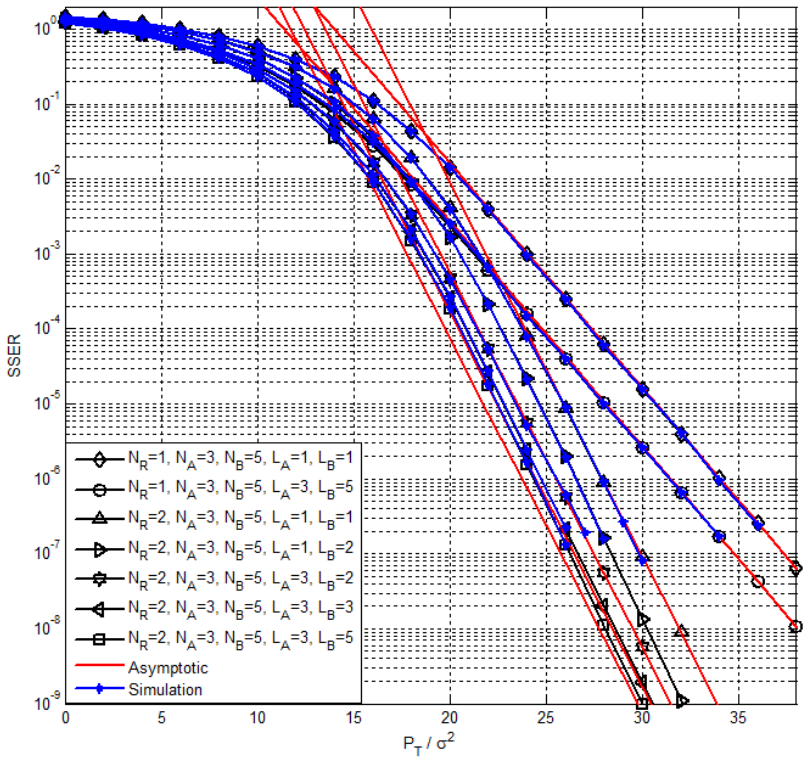

Figure 4.3: SSER of 16-PSK for different diversity gains and numbers of selected antennas.

complexity further.

Fig. 4.3 shows curves of the SSER of 16-PSK for analytical, simulation, and asymptotic results. The exact SSER for M-PSK are plotted from (4.31) and the asymptotic ones are plotted based on (4.45). The curves are plotted for $N_R \in \{1, 2\}$, $N_A = 3$, $N_B = 5$, $L_A \in \{1, 3\}$, and $L_B \in \{1, 2, 3, 5\}$. There is a precise agreement between simulation and exact results which validates the accuracy of analytical expressions derived. Furthermore, the agreement between exact and asymptotic curves at high SNR regime is also nearly excellent. The SNR gap between $(N_R, N_A, N_B, L_A, L_B) = (1, 3, 5, 1, 1)$ and $(N_R, N_A, N_B, L_A, L_B) = (2, 3, 5, 1, 1)$ at an SSER of 10^{-5} is about 4.9 dB. When considering the lower 4 curves, which have diversity order 5, and taking the $(N_R, N_A, N_B, L_A, L_B) = (2, 3, 5, 1, 1)$ as the reference curve, the SNR gaps are about 1.4 dB, 2.6 dB, 3.2 dB, and 3.9 dB at an SSER of 10^{-5} for $(N_R, N_A, N_B, L_A, L_B) = (2, 3, 5, 1, 2)$, $(N_R, N_A, N_B, L_A, L_B) = (2, 3, 5, 3, 2)$, $(N_R, N_A, N_B, L_A, L_B) = (2, 3, 5, 3, 3)$, and $(N_R, N_A, N_B, L_A, L_B) = (2, 3, 5, 3, 5)$ curves, respectively. Hence, we observe that the SNR gain between successive curves decreases as the number of selected antennas increases. So, we can conclude that antenna selection can be performed to reduce complexity with a negligible loss in performance. The aforementioned smart selection strategy can be seen from the curves of

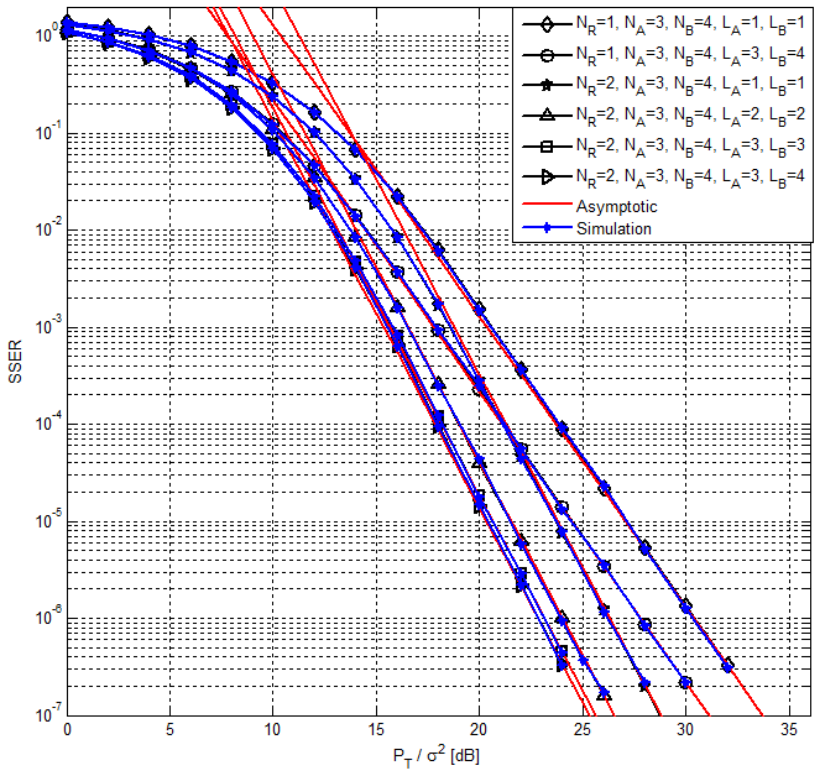

Figure 4.4: SSER of 16-QAM for different diversity gains.

$(N_R, N_A, N_B, L_A, L_B) = (2, 3, 5, 1, 2)$ and $(N_R, N_A, N_B, L_A, L_B) = (2, 3, 5, 3, 2)$ which have the same asymptotic curve.

Fig. 4.4 verifies accuracy of expressions derived for SSER of M-QAM. It plots the SSER of 16-QAM for analytical, simulation, and asymptotic results. The exact SSER for M-QAM are plotted from (4.30) and the asymptotic ones are plotted based on (4.51). The parameters used are $N_R \in \{1, 2\}$, $N_A = 3$, $N_B = 4$, $L_A \in \{1, 3\}$, and $L_B \in \{1, 2, 3, 4\}$. The numerical results and simulation results have an excellent agreement. The asymptotic results and exact ones precisely coincide with each other. An SNR gain of about 3.4 dB at an SSER of 10^{-5} is obtained when increasing the diversity order from 3 to 4 and considering the case of selecting a single antenna at each source. Now let us take $(N_R, N_A, N_B, L_A, L_B) = (2, 3, 4, 1, 1)$ curve as reference and consider the SNR gains for the lower 3 curves at an SSER of 10^{-5}: The gains are nearly $2, 2$ dB for the upper one, 3.0 dB for the middle one, and 3.2 dB for the lowest one. This also supports that a significant reduction in complexity can be reached with inconsiderable loss in performance.

Fig. 4.5 compares the ratio of SSERs for 16-PSK using exact expression, equation (4.31), and the SAF expression, equation (4.53). It plots SAF of 16-PSK for $(N_R, N_A, N_B, L_A, L_B) = (2, 3, 4, 1, L_B)$, where $L_B \in \{1, 2, 3, 4\}$. For the sake of simplicity, we represent ratios as SAF$(L_i/(L_i \pm L_\Delta))$. Five different ratios of SSER

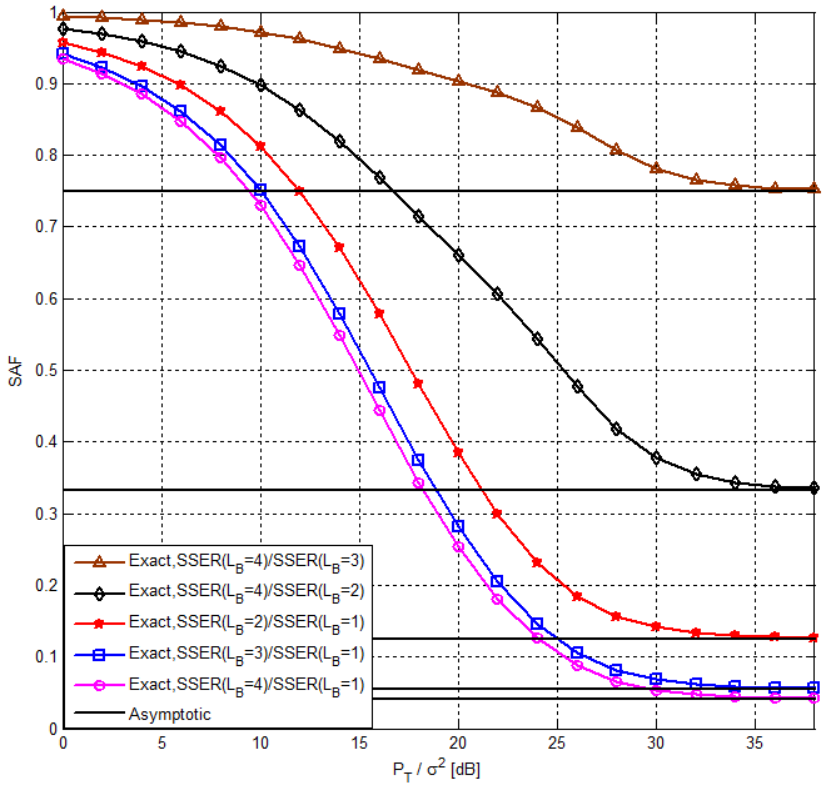

Figure 4.5: SAF of 16-PSK for different numbers of selected antennas.

are plotted, namely SAF$(4/3)$, SAF$(4/2)$, SAF$(2/1)$, SAF$(3/1)$, and SAF$(4/1)$. The asymptotic ratios, i.e., SAFs are 0.7500, 0.3333, 0.1250, 0.0556, 0.0417 for SAF$(4/3)$, SAF$(4/2)$, SAF$(2/1)$, SAF$(3/1)$, and SAF$(4/1)$, respectively. As expected, the exact ratios reach the asymptotic ones at high SNRs which verify the accuracy of the derived SAF expression.

Fig. 4.6 illustrates effects of primary factors that shift the optimum relay location. To investigate effects of different parameters such as different power allocations, total number of antennas, and number of selected antennas on optimum relay location, exact SSER curves are plotted by using (4.31). The exact SSER curves of QPSK with an SNR of 15 dB are plotted for 4 different power allocation cases, $(P_A, P_B, P_R) \in \{(\frac{1}{3}, \frac{1}{3}, \frac{1}{3}), (0.1, 0.45, 0.45), (0.3, 0.3, 0.4), (0.4, 0.4, 0.2)\}$, with $(N_R, N_A, N_B, L_A, L_B) = (N_R, 3, 4, L_A, 4)$ where $N_R \in \{1, 2\}$ and $L_A \in \{1, 3\}$. Increasing diversity order of the link between the relay and a source (in this example source A) shifts the optimum relay location towards the other source (source B). The same deduction is valid in case of increasing the number of selected antennas for any source (number of selected antennas for source A is changed from 1 to 3) or assigning more power to any source ($P_A = 0.1$ and $P_B = 0.45$). Increasing or decreasing the relay power but allocating equal powers to the sources does not have any effect on optimum relay location ($P_A = P_B = 0.3$ and

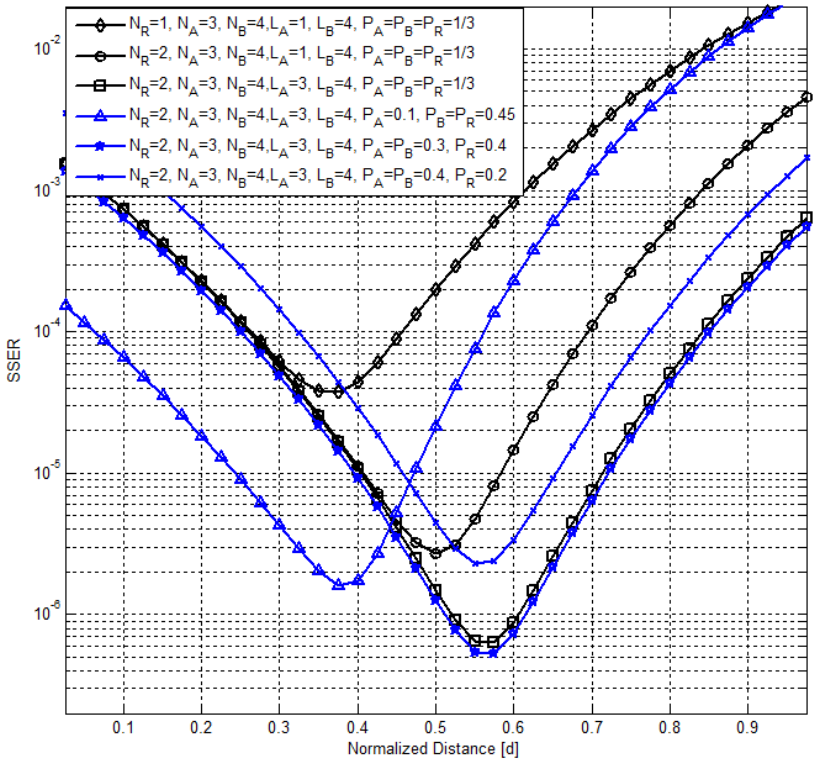

Figure 4.6: Exact SSER of QPSK versus normalized distance between source A and the relay.

$P_A = P_B = 0.4$). Assigning more power to the relay only decreases SSER but does not causes a shift in relay location when the sources are of equal power.

4.5. Conclusion

A generalized antenna selection strategy where multi antennas are selected at the sources and a single antenna is selected at relay is proposed in AF MIMO TWRNs over flat Rayleigh fading channel. The exact and asymptotic SOP, MGF, and SSER for M-PSK and M-QAM are derived and validated through Monte Carlo simulations. The diversity order of selection scheme is proven to be the minimum of the total number of antennas of the sources with more antennas and the product of the total number of relay antennas with the total number of antennas of the source having fewer antennas. It is shown that fewer antennas can be selected to reduce the complexity without a significant loss in performance with respect to full antenna selection at the sources, i.e., with respect to beamforming. It is observed that a smart antenna selection strategy, where more antennas are selected at the source with the larger number of antennas at the low SNR regime and only one antenna is selected at the high SNR regime, can be performed to decrease complexity further.

Furthermore, a ratio expression between asymptotic SSERs, which is called SAF, for any increment or decrement in the number of selected antennas at the source contributing to the diversity order is derived and its accuracy is verified by comparing it to the ratio of exact SSERs. Finally, primary factors which affect optimum relay location are examined: It is observed that increasing the total number of antennas of any source or assigning more power to any source causes a shift in relay location towards the other source. Increasing the total number of antennas of the relay shifts the relay location towards the source with larger number of antennas. On the other hand, allocating equal power to the sources and less or more power to the relay than the sources does not change the relay location.

5. PERFORMANCE OF TRANSCEIVER ANTENNA SELECTION IN TWO WAY FULL-DUPLEX RELAY NETWORKS OVER RAYLEIGH FADING CHANNELS

5.1. Introduction

Cooperative relay networks transmit data from the terminal sources to destinations to gain extended coverage, high throughput and reduction in energy consumption [76]. However, reduction of spectral efficiency is a major weakness of half-duplex (HD) one way cooperative relay networks. Hence, HD bidirectional end-to-end wireless communications systems are offered to transmit and receive data in different time slots or frequency subbands as a solution to improve spectral efficiency. In addition to compensation of fading channel impairments and improvement of reception reliability, Multi-input multi-output (MIMO) technique increases data rate [91]. Like MIMO, orthogonal frequency division multiplexing is another advanced technique which transfer ever-increasing data rates but this is not sufficient. Hence, new systems which improve spectral efficiency further and compensate for the shortcomings of HD systems should be adapted. For this reason, full-duplex (FD) systems are offered to improve achievable spectral efficiency by always transmitting and receiving in the entire bandwidth [10]. Theoretically, this means doubling capacity as compared to HD systems. However, as a drawback, this gain is limited by self-interference (SI) due to the large power difference between the power imposed by own transmissions and the low-power received signals arriving from remote transmit antennas. This SI may result in lower capacity than that of HD systems. Therefore, SI cancellation is a critical issue, which is usually classified into passive such as antenna separation, and active suppression such as analog and digital cancellation [11]. Generally, applying single SI cancellation is not adequate, therefore, two or more techniques are used together for improving system performance.

Although HD two way relay networks (TWRNs) are well studied in the literature [26, 27, 87], recently FD TWRNs are offered to overcome HD constraints to enhance spectral efficiency further [92–100]. In [92], outage probability of a single antenna FD two way system is analyzed under imperfect channel state information. In [93], FD two way and one way systems are compared in terms of average rate and outage probability. In [94], relay power control for two way FD network is investigated. In

[95], an FD TWRN where relay is equipped with multiple antennas, instead of a pure SI suppression, end-to-end (e2e) performance is maximized by jointly optimizing the beamforming matrix at the relay. Hence, the offered design claims that the total number of radio frequency (RF) chains at the relay and sources is $N^r_{T_X} + N^r_{R_X} + 4$, where $N^r_{T_X}$ and $N^r_{R_X}$ are total number of transmit and receive antennas at the relay, respectively. In [96], an FD amplify-and-forward (AF) TWRN with imperfect cancellation of loopback SI is considered and joint design of relay and receive beamforming for minimizing the mean square error under a relay transmit power constraint is investigated, where the total number of RF chains is $2N^s_{T_X} + 2N^s_{R_X} + N^r_{T_X} + N^r_{R_X}$ where $N^s_{T_X}$ and $N^s_{R_X}$ are the number of transmit and receive antennas at the sources, respectively, and $N^s_{T_X} = N^s_{R_X}$, $N^r_{T_X} = N^r_{R_X}$ are assumed. In [101], an FD TWRN with multi-antenna nodes employing spatial modulation technique is investigated and an upper bound on the average bit error probability is proposed. The investigated system is also compared with an HD TWRN counterpart. In [102], an FD AF TWRN with multi relays, two antennas at each node, is presented and a relay is selected based on maximum paths between the end nodes and relays. Moreover, although equivalent (reciprocal) paths are assumed between the relay and nodes, an antenna is selected at the relay for transmission which maximizes the SNR between a node and the relay. The selected antenna is used to transmit data to the other node without any maximization which makes antenna selection absolutely senseless for the other node. In [97], spectral and energy efficiency of a multi-pair two way FD relay system is studied, where relay is equipped with multi transmit and receive antennas to exchange data among many users. Antenna selection for a bidirectional FD MIMO systems is investigated in [98] where a pair of transmit and receive antennas at both ends for communications in each direction is selected to maximize the weighted sum rate or minimize the weighted sum symbol error rate. In [99], a bidirectional FD MIMO system with transmit or receive antenna selection is investigated to maximize the average sum-rate where total number of RF chains is four. In [100], relay selection is investigated to maximize effective e2e signal to self-interference-plus-noise ratio (SINR).

Although, some aforementioned studies consider forward and backward paths between the sources and relay as different ones [95, 96], there are many works related to AF FD networks which ignore this practical case by assuming reciprocal channel gains [92, 93, 100]. This reciprocity assumption causes that the considered systems are asymptotically analyzed. For non-fading SIs together with reciprocity assumption, e2e SINR of FD networks can be expressed as that of HD AF networks. Hence, analyzing such problems becomes easy but practical cases are ignored, which is not the case in this

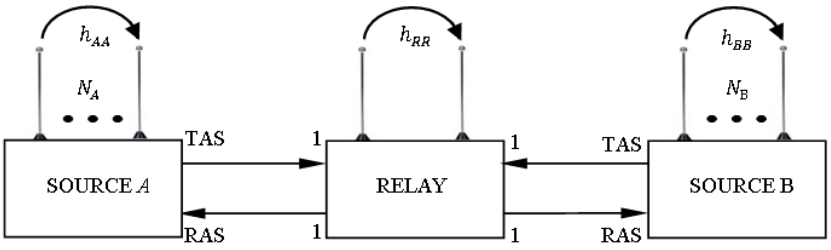

Figure 5.1: The proposed antenna selection scheme.

work.

To the best of our knowledge, antenna pair (transmit and receive antennas) selection at terminal sources, where SIs are also taken into consideration, and forward and backward paths between the sources and relay are assumed to be different, while the relay is equipped with a single antenna, i.e. transmit and receive antenna pair, has not been investigated yet. Therefore, we propose an AS scheme where pairs of antennas are selected at multi-antenna sources for transmission and reception. In order to avoid the use of larger number of antennas at the sources, the paths with maximum and second maximum effective SINRs between the sources and relay are used for transmission and reception. Hence, the proposed AS strategy means that transmit antenna selection (TAS) and receive antenna selection (RAS) are performed at the sources for transmission and reception, respectively. Furthermore, since a pair of antennas is selected at each source and FD transmission is used, the selection scheme is a transceiver antenna selection (TRAS). Since path with maximum SINR and path with maximum or second maximum SINR for transmission or reception are used at the sources, there are four possible cases. We analyze and compare all of these cases. The proposed AS scheme is depicted in Fig. 1.

In this chapter, an FD AF TWRN communication system with all FD nodes where source A with N_A antennas and source B with N_B antennas exchange information via a relay having a pair of antennas over Rayleigh fading channels is considered. The main contributions of this work can be summarized as follows:

- Compact e2e SINR expressions for both fading and non-fading SI are provided.
- The exact sum outage probability (SOP) for fading SI and the exact, approximated, and asymptotic SOP expressions for non-fading SI are derived and validated by means of Monte-Carlo simulation technique.
- The diversity order at the high SINR regime is proven to be $G_d = (1 - \lambda) \times \min(N_A - 1, N_B - 1)$ where variance of SI channels is modelled as $\kappa P^{\lambda-1}$, κ and λ are linear and exponential attenuation factors depicting dependence of SI on transmitted power, P, from each node and both vary between 0 and 1 [103–105].

This result implies that the diversity order is dependent on SI and varies between 0 and minimum of the total number of antennas of two end sources minus 1, i.e., $\min(N_A, N_B) - 1$.

- The number of RF chains (sum of transmit and receive RF chains at all nodes) is reduced from $N_A + N_B + 2$ to 6 if the same system was considered to perform beamforming.
- The proposed AS strategy uses all antenna space for both transmission and reception which decreases total number of antennas used in each terminal node, i.e., since antenna space is not divided into two subsets, where one subset is used for transmission and the other one is used for reception, each antenna can be selected for transmission or reception. Furthermore, the obtained analytical expressions are also valid for the case where antenna set of any source is divided into two subsets, i.e., $N_i = N_{T_x}^i + N_{R_x}^i$ where $N_{T_x}^i$ and $N_{R_x}^i$ antennas can be used for transmission and reception, respectively, and then one antenna is selected from each subset, based on maximum path selection. But in that case, all antennas can not be used for both transmission and reception.
- It is shown that an increment (decrement) in the number of antennas of any source produces a shift in optimum relay location towards the other source (itself). Assigning equal SI to the sources and less or more SI to the relay has no effect on optimum relay location but it affects SOP. Furthermore, increasing (decreasing) SI value at any source shifts the optimum relay location towards the other source (itself).

The rest of this chapter is presented in five sections: In Section 5.2, the details of the system model and the proposed AS strategy are given. The derivation of the exact, approximated, and asymptotic cumulative distribution functions (CDFs) of e2e SINR are presented in Section 5.3. In Section 5.4, case selection criterion is introduced. In Section 5.5, numerical results supported by Monte-Carlo simulations are given. Finally, Section 5.6 concludes the work.

5.2. System Model

We focus on an FD AF MIMO TWRN with an N_A-antenna source A and an N_B-antenna source B which communicate via the relay R having a pair of antennas over Rayleigh fading channels. We assume no direct link can be established between these

two sources because of heavy channel conditions. All nodes are assumed to be FD and also let h_m^i, g_m^i be the complex channel gains between the m^{th} antenna of the source i and the receive and transmit antennas of the relay, respectively, where $i \in \{A, B\}$. h_m^i and g_m^i are assumed to be independent. We assume that $\{h_m^i, m = 1, \ldots, N_i\}$ and $\{g_m^i, m = 1, \ldots, N_i\}$ are independent identically distributed (i.i.d.) and circularly symmetric Gaussian random variables, i.e., $|h_m^i|$ and $|g_m^i|$ are Rayleigh distributed, which are modelled as $h_m^i \sim CN(0, \Omega_{iR})$ and $g_m^i \sim CN(0, \Omega_{Ri})$, where CN stands for complex normal. We let $\Omega_{iR} = \Omega_{Ri} = d_{iR}^{-f_i}$, where d_{iR} is the distance between the source i and the relay and f_i is the path loss exponent between the source i and the relay R. We assume errorless estimation of channel coefficients and error free feedback channels. We also represent SI channels between transmit and receive antennas of the sources and the relay as h_{ii}, where $i \in \{A, B, R\}$. Variances of SI channels are modelled as $\kappa_i P_i^{\lambda_i - 1}$, where κ_i and λ_i are linear and exponential attenuation factors representing dependence of SI on transmitted power, these two parameters vary between 0 and 1, respectively [103–105] and P_i is the transmitted power of i^{th} node. A critical issue that should be clarified is that SI channels can not be estimated but only their instantaneous power is detectable. Furthermore, when fading SI channels are considered, $|h_{ii}|$s are assumed to be Rayleigh distributed and SI channels are distributed with zero mean Gaussian noise in case of non-fading SIs [106]. In addition, SI channels and channels between the sources and relay are assumed to be mutually independent. The additive noise at all the receivers is assumed to be zero mean complex Gaussian noise with variance σ_x^2, where $x \in \{A, R, B\}$.

Selection Strategy: Antenna set of any source can be divided into two subsets, i.e. $N_i = N_{T_x}^i + N_{R_x}^i$ where $N_{T_x}^i$ and $N_{R_x}^i$ antennas can be used for transmission and reception, respectively and then a pair of antennas, one for transmission and one for reception, can be selected from these two subsets. But doing that requires using more antennas. To avoid usage of more antennas at the sources, we assume any antenna can be used for transmission or reception. For this reason, AS can be done during two training periods at the sources and relay. Since only transmission or reception is conducted during the training periods, there is no SI. So signal-to-noise ratios (SNRs) of each path can be represented as $|h_m^i|^2 E_s/\sigma_R^2$ and $|g_m^i|^2 E_s/\sigma_i^2$, where $i \in \{A, B\}$ and E_s is the average energy of transmitted symbols and is assumed to be 1. During the first training period, paths having maximum and second maximum SNRs between transmit antenna of the relay and the sources are determined at the sources, namely, $g_M^i = \max \{|g_m^i|^2 E_s/\sigma_i^2\}_{m=1}^{N_i}$ and $g_{SM}^i = \text{secondmax} \{|g_m^i|^2 E_s/\sigma_i^2\}_{m=1}^{N_i}$ are found. Similarly, during the second period of

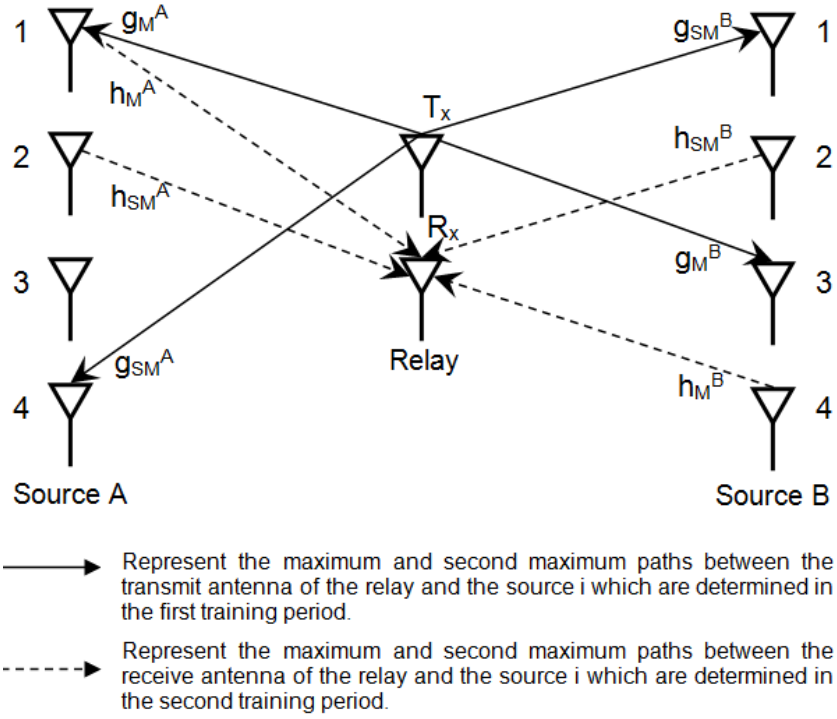

Figure 5.2: Representation of training periods.

training, $h_M^i = \max\{|h_m^i|^2 E_s/\sigma_R^2\}_{m=1}^{N_i}$ and $h_{SM}^i = \text{secondmax}\{|h_m^i|^2 E_s/\sigma_R^2\}_{m=1}^{N_i}$, the paths having maximum and second maximum SNRs between receive antenna of the relay and the sources, are determined at the relay. During the second training period, the paths between the relay and sources (the transmit antennas at the sources) can be determined at the relay simultaneously or in order to reduce complexity, they can be decided separately, however in that case three training periods are needed. These two training periods are illustrated in Fig. 5.2. Furthermore, let $I_M^i = \text{argmax}\{|h_m^i|^2 E_s/\sigma_R^2\}_{m=1}^{N_i}$ and $I_{SM}^i = \text{argsecondmax}\{|h_m^i|^2 E_s/\sigma_R^2\}_{m=1}^{N_i}$ represent indices of the selected antennas between the receive antenna of the relay and the source i, which are assumed to be transmitted to the source i without feedback error. Let $J_M^i = \text{argmax}\{|g_m^i|^2 E_s/\sigma_i^2\}_{m=1}^{N_i}$ and $J_{SM}^i = \text{argsecondmax}\{|g_m^i|^2 E_s/\sigma_i^2\}_{m=1}^{N_i}$ be the indices of reverse paths, i.e., the indices of the selected antennas for the maximum and second maximum paths between the transmit antenna of the relay and the source i. Clearly, it is possible $I_M^i = J_M^i$ with a probability of $1/N_i$, for example the first antenna of source A in Fig. 5.2: If this happens, second maximum antenna, whose index is represented by I_{SM}^i or J_{SM}^i is used for reverse path (If the path where $I_M^i = J_M^i$ is used for transmission from the source i to the relay, the reverse path is used for reception at the source i, and vice versa). The probability of selecting $(I_{SM}^i)^{th}$ or $(J_{SM}^i)^{th}$ antenna for the reverse path is $1 - 1/N_i$. For simultaneous antenna selection during the second training period, firstly, indices of maximum paths

can be determined by $(I_M^A, I_M^B) = \text{argmax}\left\{(|h_m^A|^2 + |h_n^B|^2)E_s/\sigma_R^2\right\}$ where $m \in \{1, 2, \ldots, N_A\}$ and $n \in \{1, 2, \ldots, N_B\}$. Similarly, indices of second maximum paths can be determined by $(I_{SM}^A, I_{SM}^B) = \text{argsecondmax}\left\{(|h_m^A|^2 + |h_n^B|^2)E_s/\sigma_R^2\right\}$ where $m \in \{1, 2, \ldots, N_A\}/\{I_M^A\}$ and $n \in \{1, 2, \ldots, N_B\}/\{I_M^B\}$ and / stands for exclusion. As mentioned before determination of antennas in this way results in an exhaustive search increasing complexity. Therefore, separated decision is more preferable than simultaneous one. Although AS is conducted without considering SIs, the selected antennas still maximize e2e SINR. AS in this manner is not optimum but it is a suboptimal one [107]. Selection of two antennas at each source in this way means that RAS is conducted in the first training period and TAS is carried out in the second training period.

The whole antenna set at any source is used for both transmission and reception. Therefore, it is possible for an antenna being selected as maximum (the antenna with the link producing maximum SNR between the source and the relay) for both forward and backward paths between a source and the relay. Then, if selected antenna is used for transmission (reception), second maximum antenna (the antenna with the link producing second maximum SNR between the source and the relay) will be used for reception (transmission). But, it is also possible that another antenna is selected as maximum for reverse path. In that case, the reverse path becomes a mixture path (It becomes sometimes maximum path and sometimes second maximum path). We name this path as the path with mix SINR or mix path. So, depending on using path with maximum or mix SINR for transmission or reception at the sources, there are four possible schemes:

- First Case: Both sources A and B use the paths having maximum SINRs for transmission and mix paths for reception.
- Second Case: Both sources A and B use the paths having maximum SINRs for reception and mix paths for transmission.
- Third Case: The source A uses the path with maximum SINR for transmission and mix path for reception, but the source B uses the path having maximum SINR for reception and mix path for transmission.
- Fourth Case: The source A uses the mix path for transmission and path with maximum SINR for reception, but the source B uses the mix path for reception and the path having maximum SINR for transmission.

Single antennas are selected for transmission and reception, hence, let h_{iR} be the path between transmit antenna of the source i and the receive antenna of the relay after AS. We also represent the reverse path, i.e., the path between the transmit antenna of the relay and

Table 5.1: Antenna selection possibilities for proposed selection strategy.

Case	Channel Gains	Case	Channel Gains
First	$h_{iR} = h_M^i$ $g_{Ri} = \begin{cases} g_M^i & I_M^i \neq J_M^i \\ g_{SM}^i & I_M^i = J_M^i \end{cases}$ where $i \in \{A, B\}$	Second	$h_{iR} = \begin{cases} h_M^i & I_M^i \neq J_M^i \\ h_{SM}^i & I_M^i = J_M^i \end{cases}$ $g_{Ri} = g_M^i$ where $i \in \{A, B\}$
Third	$h_{AR} = h_M^A$ $g_{RA} = \begin{cases} g_M^A & I_M^A \neq J_M^A \\ g_{SM}^A & I_M^A = J_M^A \end{cases}$ $h_{BR} = \begin{cases} h_M^B & I_M^B \neq J_M^B \\ h_{SM}^B & I_M^B = J_M^B \end{cases}$ $g_{RB} = g_M^B$	Fourth	$h_{AR} = \begin{cases} h_M^A & I_M^A \neq J_M^A \\ h_{SM}^A & I_M^A = J_M^A \end{cases}$ $g_{RA} = g_M^A$ $h_{BR} = h_M^B$ $g_{RB} = \begin{cases} g_M^B & I_M^B \neq J_M^B \\ g_{SM}^B & I_M^B = J_M^B \end{cases}$

the receive antenna of the source i by g_{Ri} after AS. These four cases are summarized in Table 5.1. Although, there are four cases, third and fourth cases are symmetrical. Because of that, we will only consider the first three cases.

Hence, for all cases, the received signal at the relay R can be given as

$$Y_R = h_{AR}\sqrt{P_A}s_A + h_{BR}\sqrt{P_B}s_B + h_{RR}s_R + n_R \tag{5.1}$$

where s_i, $i \in \{A, B\}$, is the transmitted signal at the source i and s_R, which is updated for each transmission time slot as $s_R = \beta Y_R$, is the new transmitted signal at the relay R, P_i is the transmit power at the source i or the relay R, n_R is the additive Gaussian noise at the relay with zero mean and variance σ_R^2. Y_R is multiplied by $\beta = \sqrt{\frac{P_R}{\left(|h_{AR}|^2 P_A + |h_{BR}|^2 P_B + |h_{RR}|^2 P_R + \sigma_R^2\right)}}$ and is broadcasted to each source. So the received signals at the sources are expressed as

$$Y_i = \beta g_{Ri}\Big(h_{iR}\sqrt{P_i}s_i + h_{jR}\sqrt{P_j}s_j + h_{RR}s_R + n_R\Big) + h_{ii}\sqrt{P_i}\tilde{s}_i + n_i \tag{5.2}$$

where $(i, j) \in \{(A, B), (B, A)\}$ and $\tilde{s}_i$ is the new transmitted signal at the source i.

Since channel state information and previously transmitted signals are known, the components including these parts of information are canceled out from (5.2) and the remaining signals are given as

$$Z_i = \beta g_{Ri} h_{jR}\sqrt{P_j}s_j + \beta g_{Ri}\Big(h_{RR}s_R + n_R\Big) + h_{ii}\sqrt{P_i}\tilde{s}_i + n_i, \tag{5.3}$$

where $(i, j) \in \{(A, B), (B, A)\}$. The e2e SINR expression for each source can be obtained as

$$\gamma_i = \frac{\frac{P_R|g_{Ri}|^2}{P_i|h_{ii}|^2+\sigma_i^2}\frac{P_j|h_{jR}|^2}{P_R|h_{RR}|^2+\sigma_R^2}}{\frac{P_R|g_{Ri}|^2}{P_i|h_{ii}|^2+\sigma_i^2}+\frac{P_i|h_{iR}|^2}{P_R|h_{RR}|^2+\sigma_R^2}+\frac{P_j|h_{jR}|^2}{P_R|h_{RR}|^2+\sigma_R^2}+\rho}, \tag{5.4}$$

where $(i,j) \in \{(A,B),(B,A)\}$. In (5.4), $\rho = 1$ and 0 correspond to channel-self-interference-noise-based (CINB) FD AF relaying, and channel-assisted (CA) FD AF relaying, respectively. Since, we focus on both fading and non-fading SIs, the e2e SINR expression for both cases are presented.

5.2.1. The e2e SINR Expression for Fading SIs

When SIs are modelled as fading ones, we rephrase e2e SINR expression in (5.4) as

$$\gamma_i^F = \frac{\frac{\Upsilon_{Ri}^F}{\Upsilon_{ii}+1}\frac{\Upsilon_{jR}^F}{\Upsilon_{RR}+1}}{\frac{\Upsilon_{Ri}^F}{\Upsilon_{ii}+1}+\frac{\Upsilon_{iR}^F}{\Upsilon_{RR}+1}+\frac{\Upsilon_{jR}^F}{\Upsilon_{RR}+1}+\rho} \tag{5.5}$$

where $(i,j) \in \{(A,B),(B,A)\}$, $\Upsilon_{Ri}^F = \frac{P_R|g_{Ri}|^2}{\sigma_i^2}$, $\Upsilon_{ii} = \frac{P_i|h_{ii}|^2}{\sigma_i^2}$, $\Upsilon_{jR}^F = \frac{P_j|h_{jR}|^2}{\sigma_R^2}$, $\Upsilon_{RR} = \frac{P_R|h_{RR}|^2}{\sigma_R^2}$, and $\Upsilon_{iR}^F = \frac{P_i|h_{iR}|^2}{\sigma_R^2}$. Υ_{Ri}^F, Υ_{iR}^F , and Υ_{jR}^F are SNR expressions and Υ_{ii} and Υ_{RR} are interference to noise ratios (INRs). For CA FD AF relaying, the e2e SINR expression in (5.5) turns into

$$\gamma_i^{FCA} = \frac{Z_{Ri}\Upsilon_{jR}^F}{Z_{Ri}(\Upsilon_{RR}+1)+\Upsilon_{iR}^F+\Upsilon_{jR}^F} \tag{5.6}$$

where $(i,j) \in \{(A,B),(B,A)\}$ and $Z_{Ri} = \frac{\Upsilon_{Ri}^F}{\Upsilon_{ii}+1}$. γ_i^{FCA} can also be rephrased as $\gamma_i^{FCA} = \frac{Z_{Ri}Z_{jR}}{Z_{Ri}+Z_{iR}+Z_{jR}}$, where $Z_{iR} = \frac{\Upsilon_{iR}^F}{\Upsilon_{RR}+1}$ and $Z_{jR} = \frac{\Upsilon_{jR}^F}{\Upsilon_{RR}+1}$, but in that case Z_{iR} and Z_{jR} become dependent random variables (RVs).

5.2.2. The e2e SINR Expression for Non-Fading SIs

To obtain a compact e2e SINR expression for non-fading SIs case, the following definitions are given: Since SIs are assumed to be non-fading, the powers of SI-plus-noise at the sources and relay are given as

$$K_i = |h_{ii}|^2 P_i + \sigma_i^2 \tag{5.7}$$

where $i \in \{A, B, R\}$ and SINRs of the paths are defined as

$$\Upsilon_{iR}^{NF} = \frac{P_i|h_{iR}|^2}{K_R}, \quad \Upsilon_{Ri}^{NF} = \frac{P_i|g_{Ri}|^2}{K_R} \tag{5.8}$$

where $i \in \{A, B\}$. After all, e2e SINR expression for each source can be obtained as [54]

$$\gamma_i^{NF} = \frac{\alpha_i \Upsilon_{Ri}^{NF} \Upsilon_{jR}^{NF}}{\alpha_i \Upsilon_{Ri}^{NF} + \Upsilon_{iR}^{NF} + \Upsilon_{jR}^{NF} + \rho} \tag{5.9}$$

where $\alpha_i = \frac{K_R P_R}{K_i P_i}$ and $(i, j) \in \{(A, B), (B, A)\}$.

5.3. Performance Analysis

The two-way relaying system is a special case of multi-user system. Therefore, the considered FD AF TWRN is in outage if any end terminal is in outage [91, eq. (25)], [108], namely, the overall outage probability (OOP) is

$$\begin{aligned} \text{OOP}(\gamma_{th}) &= Pr\left(\gamma_A^r \leq \gamma_{th} \quad \text{or} \quad \gamma_B^r \leq \gamma_{th}\right) \\ &= Pr\left(\gamma_A^r \leq \gamma_{th}\right) + Pr\left(\gamma_B^r \leq \gamma_{th}\right) - Pr\left(\gamma_A^r \leq \gamma_{th} \quad \text{and} \quad \gamma_B^r \leq \gamma_{th}\right) \end{aligned} \tag{5.10}$$

where $r \in \{F, NF\}$, γ_A^r and γ_B^r are the instantaneous e2e SINRs in (5.5) for fading SIs and in (5.9) for non-fading SIs. However, for FD case, it is mathematically challenging to get simplified expressions for the third term in (5.10). An HD AF TWRN is explored in [109] and exact expression can be given in double-integral-form, but closed-form is provided only for asymptotic expression. Similar difficulties are stated for FD AF TWRNs [110]. Additionally, OOP is useful for focusing on individual traffic flow of two-way relaying transmission but it is also essential to focus on the total traffic flows of two-way relaying transmission [111]. Furthermore, the SOP, $Pr\left(\gamma_A^r \leq \gamma_{th}\right) + Pr\left(\gamma_B^r \leq \gamma_{th}\right)$, is a tight upper bound of OOP which means all conclusions related to the SOP are also valid for OOP. For these reasons, derivations of exact SOP of fading SIs case; exact, approximated, and asymptotic SOP of non-fading case for all selection cases are detailed in this section.

There are four different RVs for the proposed selection strategy, i.e. four different SINRs for selected paths between the sources and relay which are illustrated in Table 5.1 for each case. To obtain CDFs, since CDF of maximum path is evident, we should

introduce CDFs of conditional selection, namely, CDFs of RVs (SNRs in fading case and SINRs in non-fading case) depending on conditional channel gains as g_{RA} and g_{RB} in the first selection case or h_{AR} and h_{BR} in the second selection case. In order to find the CDFs of SNRs/SINRs belonging to mix paths, we suggest the following proposition and provide its proof:

Theorem 5.1. Let X_i, $i \in \{1, 2, \ldots, N\}$, be i.i.d. RVs with CDF of $F_{X_i}(x)$, $X_M = \max\{X_i\}$, and $X_{SM} = \text{secondmax}\{X_i\}$. Define X_{MIX} conditioning on event Y which is independent from X_i's with its occurrence probability being $\frac{1}{N}$ as follows:

$$X_{MIX} = \begin{cases} X_{SM}, & \text{if } Y \text{ occurs} \\ X_M, & \text{otherwise} \end{cases}$$

The CDF of X_{MIX} can be found as $F_{X_{MIX}}(x) = F_{X_i}(x)^{N-1}$.

Proof: It is evident that $F_{X_{MIX}}(x) = \frac{N-1}{N} F_{X_M}(x) + \frac{1}{N} F_{X_{SM}}(x)$. Since $F_{X_M}(x) = F_{X_i}(x)^N$ and $F_{X_{SM}}(x) = N\left[F_{X_i}(x)\right]^{N-1} - (N-1)\left[F_{X_i}(x)\right]^N$, $F_{X_{MIX}}(x)$ can be obtained as $F_{X_{MIX}}(x) = F_{X_i}(x)^{N-1}$.

5.3.1. Exact SOP of the e2e SINR For Fading SIs

There are five independent RVs in SINR expression given in (5.5). To proceed further, we should introduce CDFs of these RVs. Therefore, we define the following SNRs of each path between the source i and the relay R:

$$\Upsilon_{iR}^{F,m} = \frac{P_i |h_m^i|^2}{\sigma_R^2}, \quad \Upsilon_{Ri}^{F,m} = \frac{P_R |g_m^i|^2}{\sigma_i^2} \tag{5.11}$$

where $i \in \{A, B\}$ and $m \in \{1, 2, \ldots, N_i\}$. Since h_m^i and g_m^i are circularly symmetric Gaussian RVs, which means that $|h_m^i|$ and $|g_m^i|$ are Rayleigh distributed RVs and therefore, $\Upsilon_{iR}^{F,m}$ and $\Upsilon_{Ri}^{F,m}$ are exponential distributed RVs. Hence, we can give their CDFs as

$$F_{\Upsilon_{iR}^{F,m}}(x) = 1 - e^{-x/\bar{\Upsilon}_{iR}^F}, \quad F_{\Upsilon_{Ri}^{F,m}}(x) = 1 - e^{-x/\bar{\Upsilon}_{Ri}^F} \tag{5.12}$$

where $\bar{\Upsilon}_{iR}^F = \frac{P_i \Omega_{iR}}{\sigma_R^2}$ and $\bar{\Upsilon}_{Ri}^F = \frac{P_R \Omega_{Ri}}{\sigma_i^2}$ are average SNRs of the link between the m^{th} antenna of the source i and the receive antenna of the relay and the link between the m^{th} antenna of source i and the transmit antenna of the relay, respectively.

After all details and derivations given until now and by considering Proposition 5.1, the CDFs of the SNRs depending on maximum and mix paths given in (5.5), namely, CDFs

of Υ_{Ri}^F and Υ_{iR}^F, for all cases can be expressed by using binomial theorem as

$$F_{\Upsilon_{ij}^F}(x) = 1 + \sum_{m=1}^{N_{ij}} C_{\Upsilon_{ij}^F}^m e^{-\omega_{\Upsilon_{ij}^F}^m x} \tag{5.13}$$

where $(i,j) \in \{(A,R),(B,R),(R,A),(R,B)\}$, $C_{\Upsilon_{ij}^F}^m = \binom{N_{ij}}{m}(-1)^m$, $\omega_{\Upsilon_{ij}^F}^m = m/\bar{\Upsilon}_{ij}^F$, and N_{ij} is the order of each CDF given in Table 5.2. The probability density function (PDF) of Υ_{ij}^F can be easily obtained by taking derivation of (5.13):

$$f_{\Upsilon_{ij}^F}(x) = \sum_{m=1}^{N_{ij}} C_{\Upsilon_{ij}^F}^m (-\omega_{\Upsilon_{ij}^F}^m) e^{-\omega_{\Upsilon_{ij}^F}^m x}. \tag{5.14}$$

Since SI magnitudes, i.e., $|h_{ii}|$s, are assumed to be Rayleigh distributed, PDF of Υ_{ii} is

$$f_{\Upsilon_{ii}}(x) = \omega_{\Upsilon_{ii}} e^{-\omega_{\Upsilon_{ii}} x}, \tag{5.15}$$

where $i \in \{A,B,R\}$, $\omega_{\Upsilon_{ii}} = 1/\bar{\Upsilon}_{ii}$, and $\bar{\Upsilon}_{ii} = \kappa_i P_i^{\lambda_i}/\sigma_i^2$.

While considering the CINB FD AF relaying SINR expression in (5.5), it is a bit difficult to obtain CDF of γ_i^F. Therefore, we focus on the e2e SINR expression of CA FD AF relaying in (5.6), i.e., γ_i^{FCA}. To derive CDF of γ_i^{FCA}, we need PDF of $Z_{Ri} = \frac{\Upsilon_{Ri}^F}{\Upsilon_{ii}+1}$ which is obtained from $F_{Z_{Ri}}(z) = \int_0^\infty F_{\Upsilon_{Ri}^F}(z(y+1)) f_{\Upsilon_{ii}}(y) dy$ by derivation as

$$f_{Z_{Ri}}(z) = \sum_{m=1}^{N_{Ri}} \left(-C_{\Upsilon_{Ri}^F}^m \omega_{\Upsilon_{Ri}^F}^m \omega_{\Upsilon_{ii}} (\omega_{\Upsilon_{Ri}^F}^m z + \omega_{\Upsilon_{ii}} + 1) \frac{e^{-\omega_{\Upsilon_{Ri}^F}^m z}}{(\omega_{\Upsilon_{Ri}^F}^m z + \omega_{\Upsilon_{ii}})^2} \right). \tag{5.16}$$

Since CDFs and PDFs of all random varibles in (5.6) are avaliable, CDF of γ_i^{FCA} can be obtained as (See Appendix 5.7.1.)

$$\begin{aligned} F_{\gamma_i^{FCA}}(\gamma) = 1 + \sum_{k=1}^{N_{jR}} \sum_{p=1}^{N_{iR}} \sum_{m=1}^{N_{Ri}} \frac{C_{\Upsilon_{Ri}^F}^m C_{\Upsilon_{iR}^F}^p C_{\Upsilon_{jR}^F}^k \omega_{\Upsilon_{ii}} \omega_{\Upsilon_{RR}}}{\omega_{\Upsilon_{jR}^F}^k \gamma + \omega_{\Upsilon_{RR}}} e^{-(\omega_{\Upsilon_{Ri}^F}^m + \omega_{\Upsilon_{jR}^F}^k)\gamma} \\ \int_0^\infty \left[\frac{z^2 \left(z + \frac{\omega_{\Upsilon_{Ri}^F}^m \gamma + \omega_{\Upsilon_{ii}} + 1}{\omega_{\Upsilon_{Ri}^F}^m} \right)}{\left(z + \frac{\omega_{\Upsilon_{jR}^F}^k \gamma^2}{\omega_{\Upsilon_{jR}^F}^k \gamma + \omega_{\Upsilon_{RR}}} \right) \left(z + \frac{\omega_{\Upsilon_{jR}^F}^k \gamma}{\omega_{\Upsilon_{iR}^F}^p} \right)} \frac{e^{-\omega_{\Upsilon_{Ri}^F}^m z - \frac{\omega_{\Upsilon_{jR}^F}^k \gamma^2}{z}}}{\left(z + \frac{\omega_{\Upsilon_{Ri}^F}^m \gamma + \omega_{\Upsilon_{ii}}}{\omega_{\Upsilon_{Ri}^F}^m} \right)^2} \right] dz. \end{aligned} \tag{5.17}$$

Table 5.2: CDF orders for all cases.

Case	CDF Order	Case	CDF Order
First	$N_{AR} = N_A$ $N_{RA} = N_A - 1$ $N_{BR} = N_B$ $N_{RB} = N_B - 1$	Second	$N_{AR} = N_A - 1$ $N_{RA} = N_A$ $N_{BR} = N_B - 1$ $N_{RB} = N_B$
Third	$N_{AR} = N_A$ $N_{RA} = N_A - 1$ $N_{BR} = N_B - 1$ $N_{RB} = N_B$	Fourth	$N_{AR} = N_A - 1$ $N_{RA} = N_A$ $N_{BR} = N_B$ $N_{RB} = N_B - 1$

To the best of our knowledge, the integral in (5.17) does not have a closed-form. Since we can not proceed further, we focus on non-fading SIs case in next section for the sake of mathematical tractability.

The SOP of the proposed AS strategy for fading SIs case can be calculated at a specified threshold, γ_{th}, as $F_{\gamma_A^{FCA}}(\gamma_{th}) + F_{\gamma_B^{FCA}}(\gamma_{th})$.

5.3.2. SOP of the e2e SINR for Non-Fading SIs

In this section, we introduce exact, approximate, and asymptotic derivation of CDF of SINRs for non-fading SIs case.

5.3.2.1. Exact and Approximate SOP

Similar to fading SIs case, we define the following SINRs for each path between the sources and the relay:

$$\Upsilon_{iR}^{m} = \frac{P_i |h_m^i|^2}{K_R}, \quad \Upsilon_{Ri}^{m} = \frac{P_i |g_m^i|^2}{K_R} \tag{5.18}$$

where $i \in \{A, B\}$ and $m \in \{1, 2, \ldots, N_i\}$. Since Υ_{iR}^{m} and Υ_{Ri}^{m} are exponential distributed RVs, we can give their CDFs as

$$F_{\Upsilon_{iR}^{m}}(x) = 1 - e^{-x/\bar{\Upsilon}_{iR}}, \quad F_{\Upsilon_{Ri}^{m}}(x) = 1 - e^{-x/\bar{\Upsilon}_{Ri}} \tag{5.19}$$

where $\bar{\Upsilon}_{iR} = \frac{P_i \Omega_{iR}}{K_R}$ and $\bar{\Upsilon}_{Ri} = \frac{P_i \Omega_{Ri}}{K_R}$ are average SINRs of the link between the m^{th} antenna of the source i and the receive antenna of the relay and the link between the transmit antenna of the relay and the m^{th} antenna of source i , respectively. By using

Proposition 5.1, the CDFs of the SINRs given in (5.8) for all cases can be expressed by using binomial theorem as

$$F_{\Upsilon_{ij}^{NF}}(x) = 1 + \sum_{m=1}^{N_{ij}} C_{\Upsilon_{ij}^{NF}}^{m} e^{-\omega_{\Upsilon_{ij}^{NF}}^{m} x} \tag{5.20}$$

where $(i,j) \in \{(A,R),(B,R),(R,A),(R,B)\}$, $C_{\Upsilon_{ij}^{NF}}^{m} = \binom{N_{ij}}{m}(-1)^m$, $\omega_{\Upsilon_{ij}^{NF}}^{m} = m/\bar{\Upsilon}_{ij}$, and N_{ij} is the order of each CDF given in Table 5.2. The PDF of Υ_{ij} is obtained by taking derivation of (5.20):

$$f_{\Upsilon_{ij}^{NF}}(x) = \sum_{m=1}^{N_{ij}} C_{\Upsilon_{ij}^{NF}}^{m} (-\omega_{\Upsilon_{ij}^{NF}}^{m}) e^{-\omega_{\Upsilon_{ij}^{NF}}^{m} x}. \tag{5.21}$$

Following similar steps used in derivation of CDFs of fading SIs case, CDFs of the e2e SINR expressions given in (5.9), i.e., the CDFs of γ_A^{NF} and γ_B^{NF} are derived as (See Appendix 5.7.2.)

$$\begin{aligned} F_{\gamma_i^{NF}}(\gamma) = 1 + \sum_{k=1}^{N_i}\sum_{p=1}^{N_i}\sum_{m=1}^{N_j} 2\epsilon_{ij} C_{\Upsilon_{jR}^{NF}}^{m} C_{\Upsilon_{Ri}^{NF}}^{p} C_{\Upsilon_{iR}^{NF}}^{k} e^{\omega_{\Upsilon_{iR}^{NF}}^{k}(\gamma+\rho)} \\ e^{-\gamma\left(\omega_{\Upsilon_{jR}^{NF}}^{m} + \frac{\omega_{\Upsilon_{Ri}^{NF}}^{p}}{\alpha_i}\right)} \int_{u_{ij}}^{\infty} y^2 K_1(y) e^{-\epsilon_{ij} y^2} dy. \end{aligned} \tag{5.22}$$

It is not tractable to take integral in (5.22). So, instead of exact derivation, we provide an approximated closed form for $F_{\gamma_i^{NF}}(\gamma)$. To proceed further, we use the approximated first-order modified Bessel Function of the second kind as [65, eq. (8.446) and (8.451.6)]

$$\hat{K}_1(x) = \begin{cases} \Bigg[\dfrac{1}{x} + \displaystyle\sum_{h=0}^{20} \frac{2^{-2h-1}}{h!(h+1)!} \ln(x) x^{2h+1} \\ \quad - \displaystyle\sum_{h=0}^{20} \frac{\psi(h+2)2^{-2h-2}}{h!(h+1)!} x^{2h+1} & x \le 15.7 \\ \quad - \displaystyle\sum_{h=0}^{20} \frac{2\ln(2) + \psi(h+1)}{2h!(h+1)!} \left(\frac{x}{2}\right)^{2h+1} \Bigg], \\ \sqrt{\frac{\Pi}{2x}} e^{-x}, & x > 15.7 \end{cases} \tag{5.23}$$

where $\psi(z)$ is digamma function [65, eq. (8.360.1)], i.e., logarithmic derivative of gamma function $\Gamma(z) = \int_0^\infty t^{z-1} e^{-t} dt$ [65, eq. (8.310.1)]. Approximation error is maximum

around 15.7, which is about 2.33 %. The approximation for $x > 15.7$ leads to another intractable integral. However, for any possible combination of u_{ij} and ϵ_{ij} (u_{ij} and ϵ_{ij} are inversely related to each other), we find out that the effect of $\int_{u_{ij}}^{\infty} y^2 K_1(y) e^{-\epsilon_{ij} y^2} dy$ (if $u_{ij} > 15.7$) or $\int_{15.7}^{\infty} y^2 K_1(y) e^{-\epsilon_{ij} y^2} dy$ (if $u_{ij} < 15.7$) is negligible. Hence, we only focus on the integrals where $u_{ij} \leq 15.7$.

We define $\hat{I}_{mpk} = \int_{u_{ij}}^{u_{up}} y^2 \hat{K}_1(y) e^{-\epsilon_{ij} y^2} dy$, where $u_{up} = 15.7$, and reformulate it as

$$\begin{aligned} \hat{I}_{mpk} = & \underbrace{\int_{u_{ij}}^{u_{up}} y e^{-\epsilon_{ij} y^2} dy}_{I_3} + \sum_{h=0}^{20} \frac{2^{-2h-1}}{h!(h+1)!} \underbrace{\int_{u_{ij}}^{u_{up}} \ln(y) y^{2h+3} e^{-\epsilon_{ij} y^2} dy}_{I_1} \\ & - \sum_{h=0}^{20} \frac{(2\ln(2) + \psi(h+1) + \psi(h+2)) 2^{-2h-2}}{h!(h+1)!} \underbrace{\int_{u_{ij}}^{u_{up}} y^{2h+3} e^{-\epsilon_{ij} y^2} dy}_{I_2} \end{aligned} \tag{5.24}$$

To obtain the integrals I_1, I_2, and I_3, we make change of variable as $x = \epsilon_{ij} y^2$ and the resulting integrals become (See Appendix 5.7.3. for derivation of I_1)

$$\begin{aligned} I_1 = \frac{\epsilon_{ij}^{-h-2}}{4} \Big[& \Gamma(h+2, \epsilon_{ij} {u_{ij}}^2) \ln(u_{ij}^2) - \Gamma(h+2, \epsilon_{ij} {u_{up}}^2) \ln(u_{up}^2) \\ & + G^{3\,0}_{2\,0} \left({}^{1,1}_{0,0,h+2} \middle| \epsilon_{ij} {u_{ij}}^2 \right) - G^{3\,0}_{2\,0} \left({}^{1,1}_{0,0,h+2} \middle| \epsilon_{ij} {u_{up}}^2 \right) \Big], \end{aligned} \tag{5.25}$$

$$I_2 = \frac{\epsilon_{ij}^{-h-2}}{2} \Big[\Gamma(h+2, \epsilon_{ij} {u_{ij}}^2) - \Gamma(h+2, \epsilon_{ij} {u_{up}}^2) \Big], \tag{5.26}$$

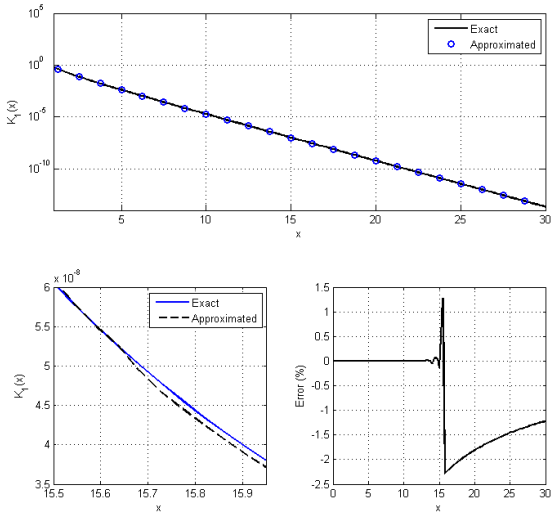

Figure 5.3: Approximation of the first order modified Bessel function of second type and its error.

and

$$I_3 = \frac{e^{-\epsilon_{ij}{u_{ij}}^2} - e^{-\epsilon_{ij}{u_{up}}^2}}{2\epsilon_{ij}}. \tag{5.27}$$

Therefore, the approximated $F_{\gamma_i^{NF}}(\gamma)$ becomes

$$\hat{F}_{\gamma_i^{NF}}(\gamma) = 1 + \sum_{k=1}^{N_i}\sum_{p=1}^{N_i}\sum_{m=1}^{N_j} 2\epsilon_{ij} C^m_{\Upsilon^{NF}_{jR}} C^p_{\Upsilon^{NF}_{Ri}} C^k_{\Upsilon^{NF}_{iR}} e^{\omega^k_{\Upsilon^{NF}_{iR}}(\gamma+\rho)} e^{-\gamma\left(\omega^m_{\Upsilon^{NF}_{jR}} + \frac{\omega^p_{\Upsilon^{NF}_{Ri}}}{\alpha_i}\right)} \hat{I}_{mpk}. \tag{5.28}$$

The approximated SOP of the proposed AS strategy can be calculated at a specified threshold, γ_{th}, as $\hat{F}_{\gamma_A^{NF}}(\gamma_{th}) + \hat{F}_{\gamma_B^{NF}}(\gamma_{th})$.

5.3.2.2. Asymptotic SOP for Non-Fading SIs

At high SINR, exact SOP can be characterized by diversity order and array gain [82]. Hence, these two parameters are derived to examine SOP at high SINR. The asymptotic e2e SINR can be expressed as

$$F^{\infty}_{\gamma_i^{NF}}(\gamma) \approx G_{a,i}\left(\frac{P_i}{\gamma}\right)^{-G_{d,i}} + o\left(\bar{\Upsilon}_i^{-G_{d,i}}\right) \tag{5.29}$$

where P_i is the transmitted power of the source i, $(\cdot)$ denotes higher order terms, $G_{a,i}$ is the array gain, and $G_{d,i}$ is the diversity gain.

In HD TWRNs, there are only two RVs in e2e SNR expressions. However, in FD TWRNs, there are three RVs. So it is a bit more difficult to obtain asymptotic CDFs. To obtain asymptotic expressions, we consider the SINR expression of CA FD AF relaying, i.e. we set $\rho = 0$: $\gamma_i^{NF} = \frac{\alpha_i \Upsilon^{NF}_{Ri}\Upsilon^{NF}_{jR}}{\alpha_i\Upsilon^{NF}_{Ri} + \Upsilon^{NF}_{iR} + \Upsilon^{NF}_{jR}}$. For the sake of simplicity, we let $\Upsilon^{NF}_{iR} = \Upsilon^{NF}_{Ri}$, i.e., we assume forward and backward paths between the source i and the relay are reciprocal, which will give us asymptotic results. Consequently, e2e SINR expression reduces to

$$\gamma_i^{NF} = \frac{\alpha_i \Upsilon^{NF}_{Ri}\Upsilon^{NF}_{jR}}{(\alpha_i+1)\Upsilon^{NF}_{Ri} + \Upsilon^{NF}_{jR}} \tag{5.30}$$

where $(i,j) \in \{(A,B),(B,A)\}$. This result is well known from the analysis of HD CA AF TWRNs. This assumption produces four candidate asymptotic SINRS, namely, for both

Υ_{Ri}^{NF} and Υ_{jR}^{NF}, there are two CDF possibilities. While considering e2e SINR expressions in (5.9), we should let one of Υ_{Ri}^{NF} and Υ_{jR}^{NF} be SINR of the maximum path and the other one should be the mix one. To obtain a valid expression for all selection cases, we let Υ_{Ri}^{NF} be the path with maximum SINR and Υ_{jR}^{NF} be the path with the mix SINR, which produces a suitable solution. The single term polynomial approximation of the CDFs can be obtained as

$$F_{\Upsilon_{Ri}^{NF}}^{\infty}(\gamma) \approx \left(\frac{\gamma}{\bar{\Upsilon}_{Ri}}\right)^{N_i}, \quad F_{\Upsilon_{jR}^{NF}}^{\infty}(\gamma) \approx N_j \left(\frac{\gamma}{\bar{\Upsilon}_{jR}}\right)^{N_j-1} \tag{5.31}$$

where $i \in \{A, B\}$. The e2e asymptotic CDF for SINR expression in (5.30) is obtained as [52, eq. 29]

$$F_{\gamma_i^{NF}}^{\infty}(\gamma) = F_{\Upsilon_{Ri}^{NF}}(\frac{\gamma}{\alpha_i}) + F_{\Upsilon_{jR}^{NF}}(\frac{(\alpha_i+1)\gamma}{\alpha_i}). \tag{5.32}$$

Since no assumption is made on total number of antennas at the sources, assigned powers, SI values, and noise variances at all nodes, it is not easy to obtain diversity order, $G_{d,i}$, and array gain, $G_{a,i}$. For this reason, we assume that $P_A = P_B = P_R$, $|h_{AA}| = |h_{BB}| = |h_{RR}|$, and $\sigma_A = \sigma_B = \sigma_R$. Furthermore, at high SINR, we can ignore the noise variance at the denominators of $\bar{\Upsilon}_{Ri}^{NF}$ and $\bar{\Upsilon}_{jR}^{NF}$ and for simplicity take $\kappa_A = \kappa_B = \kappa_R = 1$. In addition, we assume equal SIs, i.e., $\lambda_A = \lambda_B = \lambda_R = \lambda$. Hence, $G_{d,i}$ and $G_{a,i}$ in (5.29) are respectively obtained as in (5.33) and (5.34).

$$G_{d,i} = (1-\lambda) \times min(N_i, N_j - 1). \tag{5.33}$$

$$G_{a,i} = \begin{cases} (\alpha_i \Omega_{Ri})^{-N_i} & N_i < N_j - 1 \\ N_j \left(\frac{(\alpha_i+1)\Omega_{jR}}{\alpha_i}\right)^{N_j-1} & N_i > N_j - 1 \\ (\alpha_i \Omega_{Ri})^{-N_i} + N_j \left(\frac{(\alpha_i+1)\Omega_{jR}}{\alpha_i}\right)^{N_j-1} & N_i = N_j - 1 \end{cases}. \tag{5.34}$$

Therefore, the diversity order of SOP becomes $G_d = (1-\lambda) \times min(N_i - 1, N_j - 1)$ which implies that diversity order varies between 0 and $min(N_i, N_j) - 1$. Zero diversity order means variances of SI channels are not dependent on transmitted power, i.e., SI powers are linearly dependent on transmitted powers and $min(N_i - 1, N_j - 1)$ means there is no SI. Effect of SI on diversity order is illustrated in many works but not provided in closed-form [112].

The asymptotic e2e SOP can be evaluated at a specific value, γ_{th}, by using (5.29) as $F^{\infty}_{\gamma_A^{NF}}(\gamma_{th}) + F^{\infty}_{\gamma_B^{NF}}(\gamma_{th})$.

5.4. Case Selection

The proposed selection scheme produces four different selection cases. Therefore, it is a necessity to provide a case selection criterion in order to make selection strategy being optimal for different network settings. Since exact SOP can be characterized by diversity order and array gain at high SINRs, two reasonable parameters for case selection are diversity order and array gain. Unfortunately, since all cases have the same diversity order, the only remained candidate is array gain. Meanwhile, the obtained array gain is only for non-fading SIs and derived based on some assumptions such as equal powers at each node, hence, it can not be used as a criterion. But we can use the instantaneous e2e SINR dominating SOP for case decision. Firstly, minimum instantaneous e2e SINR of two end nodes can be determined for each selection case and then the maximum of these minima is determined to decide the case for communication:

$$case = \text{argmax} \left\{ \min\{\gamma^r_{A,c}, \gamma^r_{B,c}\} \right\}_{c=1}^{4} \tag{5.35}$$

where $r \in \{F, NF\}$, $\gamma^r_{A,c}$ and $\gamma^r_{B,c}$ are the instantaneous e2e SINRs in (5.5) for fading SIs and in (5.9) for non-fading SIs. This criterion can be simplified further as

$$case = \text{argmax} \left\{ \min\{\bar{\gamma}^{P,r}_{A,c}, \bar{\gamma}^{P,r}_{B,c}\} \right\}_{c=1}^{4} \tag{5.36}$$

where $\bar{\gamma}^{P,r}_{A,c}$ and $\bar{\gamma}^{P,r}_{B,c}$ are pseudo-expected values of e2e SINRs and calculated at a predetermined high SINR value as

$$\begin{aligned} \bar{\gamma}^{P,F}_{i,c} &= \frac{\frac{\mu_{\Upsilon^F_{Ri}}}{\mu_{\Upsilon_{ii}}+1}\frac{\mu_{\Upsilon^F_{jR}}}{\mu_{\Upsilon_{RR}}+1}}{\frac{\mu_{\Upsilon^F_{Ri}}}{\mu_{\Upsilon_{ii}}+1} + \frac{\mu_{\Upsilon^F_{iR}}}{\mu_{\Upsilon_{RR}}+1} + \frac{\mu_{\Upsilon^F_{jR}}}{\mu_{\Upsilon_{RR}}+1} + \rho}, \\ \bar{\gamma}^{P,NF}_{i,c} &= \frac{\alpha_i \mu_{\Upsilon^{NF}_{Ri}} \mu_{\Upsilon^{NF}_{jR}}}{\alpha_i \mu_{\Upsilon^{NF}_{Ri}} + \mu_{\Upsilon^{NF}_{iR}} + \mu_{\Upsilon^{NF}_{jR}} + \rho} \end{aligned} \tag{5.37}$$

where $\mu_{\Upsilon_{ij}^r} = \sum_{m=1}^{N_{ij}} \left(-C_{\Upsilon_{ij}^r}^m / \omega_{\Upsilon_{ij}^r}^m\right)$ is the expected value of Υ_{ij}^r at the predetermined high SINR value, $(i,j) \in \{(A,R),(B,R),(R,A),(R,B)\}$ and $r \in \{F, NF\}$. $\mu_{\Upsilon_{ii}}$ and $\mu_{\Upsilon_{RR}}$ are the expected value of INRs at the source i and the relay R, respectively.

The simplified criterion in (5.36) is merely dependent on average power of SNRs and INRs for fading SIs and average power of SINRs for non-fading SIs. Therefore, if there are no serious deviations in network settings, there is no need to search an optimum selection case for long durations. So a selection case can be determined by considering current network settings and then it can be used for block transmission. A wrong case selection decision does not omit advantages of the proposed AS strategy except an allowable performance loss. Proceeding in this way reduces frequency of training periods.

5.5. Numerical Results

In order to illustrate performance of the proposed AS strategy, numerical and simulation results are presented in this section. It is assumed that $P_A = P_B = P_R = P_T/3$ where P_T is total power and $\sigma^2 = \sigma_A^2 = \sigma_B^2 = \sigma_R^2 = 1$. We let $d_{AR} = d_{BR} = 1$ for fading SIs and $d_{AR} = d_{BR} = 0.5$ for non-fading SIs. The path loss exponent f_i is taken to be 3 which represents heavy urban environment. Furthermore, SI values at all nodes are assumed to be equal and $\kappa_A = \kappa_B = \kappa_R = 1$. Other assignments for different relay locations, SI values, and power allocations are separately given in the explanation of each figure. The curves are plotted versus P_T/σ^2. We use (5.17) to obtain exact SOP curves for fading SI case and (5.28) and (5.29) to plot the approximate (Since exact curves are equal to approximated ones, for the sake of clarity and simplicity, they are not provided) and asymptotic e2e SOP curves for non-fading SI case, respectively, and also provide simulations.

Fig. 5.4 plots fading SI SOP curves for the first three selection cases, where whole antenna set is used for both transmission and reception, and maximum selection case, where antenna sets of the sources are divided into two equal subsets and the maximum paths are used for transmission and reception. The curves are produced for a threshold of 6 dB with equal SIs where $\lambda_A = \lambda_B = \lambda_R = 0.2, 0.5$. It also depicts SOP curve of no selection case where each node has a pair of antennas, i.e., $N_A = N_B = 2$ and one antenna is always used for transmission and the other one is used for reception. The exact curve of no selection case is obtained from (5.17) by letting $N_{AR} = N_{RA} = N_{BR} = N_{RB} = 1$. The total number of antennas at each source are $N_A = N_B = 3, 4, 5$ for the proposed AS

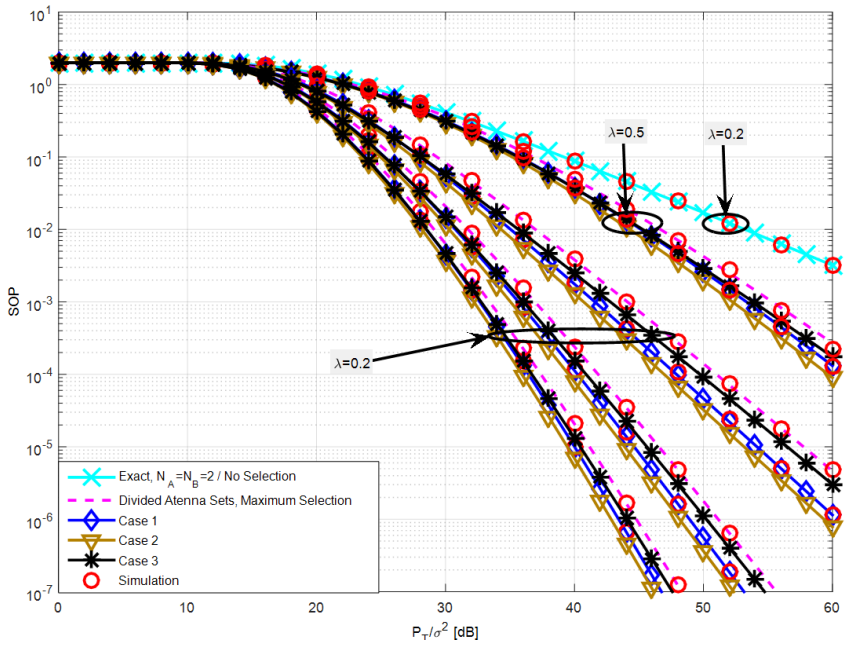

Figure 5.4: SOP for different number of antennas and fading SIs.

strategy using whole antenna space and $N_A = N_B = 4, 6, 8$ for maximum selection case with divided antenna sets. Choosing number of total antennas at each source in this way means diversity orders of SOPs are proportional to 2, 3, and 4 for both selection strategies, i.e., for selection strategy using whole antenna space and selection strategy using divided antenna space into two subsets. The exact curves of divided antenna sets with maximum path selection are obtained from (5.17) by letting $N_{AR} = N_{RA} = N_{BR} = N_{RB} = N_A/2 = N_B/2$. Although we divide the antenna sets of two sources into equal antenna subsets, the total number of antennas of each subset can be set arbitrarily. At SI value of $\lambda = 0.5$, curves of selection strategy using whole antenna space are given for $N_A = N_B = 4$ and curve of divided antenna set strategy is given for $N_A = N_B = 6$. For SI value of $\lambda = 0.2$, upper, middle, and lower curves which demonstrate proposed AS strategy using whole antenna sets are for $N_A = N_B = 3$, $N_A = N_B = 4$, and $N_A = N_B = 5$, respectively. Similarly, upper, middle, and lower curves which verify divided antenna set selection strategy are for $N_A = N_B = 4$, $N_A = N_B = 6$, and $N_A = N_B = 8$, respectively. For the sake of clarity, simulation results of selection strategy using whole antenna sets are only provided for first selection case. Simulation and exact results overlap perfectly for both selection strategies. The selection strategy using all antennas for both transmission and reception outperforms, although it uses fewer antennas, the selection strategy dividing antenna space into two subsets while the same diversity orders are considered. Besides the performance gain in SOP, the reduction in total number of antennas is 2, 4, and 6 while diversity order proportionality (SI effect is not considered) changes from 2 to 4,

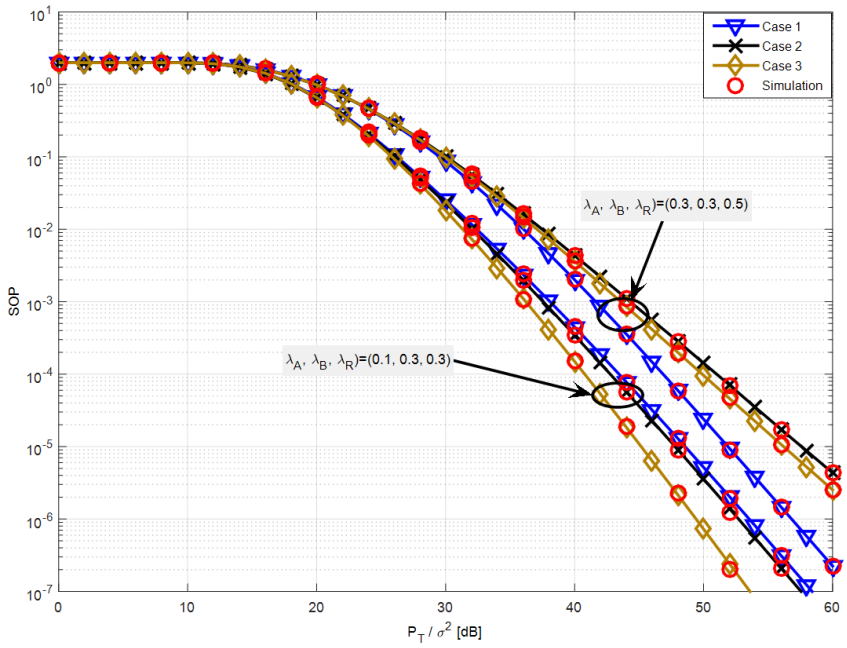

Figure 5.5: SOP of three selection cases for different fading SI values at each node.

respectively. The curves of the first and second selection cases get closer to each other, and the gap between these curves and the curve of the third selection case becomes larger as SI value and the total number of antennas becomes smaller. While considering the curves of SI values for $\lambda = 0.2$, for a SOP value of 10^{-2}, the gain in P_T/σ^2 with respect to no selection case is nearly 17 dB, 22 dB, and 25 dB as total number of antennas changes from 3 to 5, respectively. The gain in P_T/σ^2 with respect to $N_A = N_B = 3$ curves at a SOP value of 10^{-5} is nearly 10 dB and 15 dB as total number of antennas changes to 4 and 5, respectively. Also, as considering the curves for $N_A = N_B = 3$ at a SOP value of 10^{-5}, the gain in P_T/σ^2 with respect to third selection case is about 2 dB and 3 dB for the first and second selection cases, respectively. These gains reduce to 1 dB and 2 dB for the curves of $N_A = N_B = 4$. For the curves of $N_A = N_B = 5$, the gain in P_T/σ^2 reduces further and becomes about 0.5 dB and 1 dB for the first and second selection cases, respectively.

Fig. 5.5 illustrates effect of experiencing different fading SI values at each node for three selection cases for a threshold of 6 dB. $N_A = N_B = 4$ and the SI values for each assignment are given in a triple tuple as $(\lambda_A, \lambda_B, \lambda_R) \in \{(0.1, 0.3, 0.3), (0.3, 0.3, 0.5)\}$. For the curves where $\lambda_A = \lambda_B = \lambda_R = 0.2$ in Fig. 5.4, the second selection case results in smaller SOP than the other selection cases. So if all the nodes have equal SI values and total number of antennas, and also all nodes have equal powers, using the second selection case produces smaller SOP values. The smaller SOP can be obtained by using the third selection case if the relay and one of the sources have equal SI and the other source has smaller SI (consider the lower three curves). Note that about 5.6 dB gain in

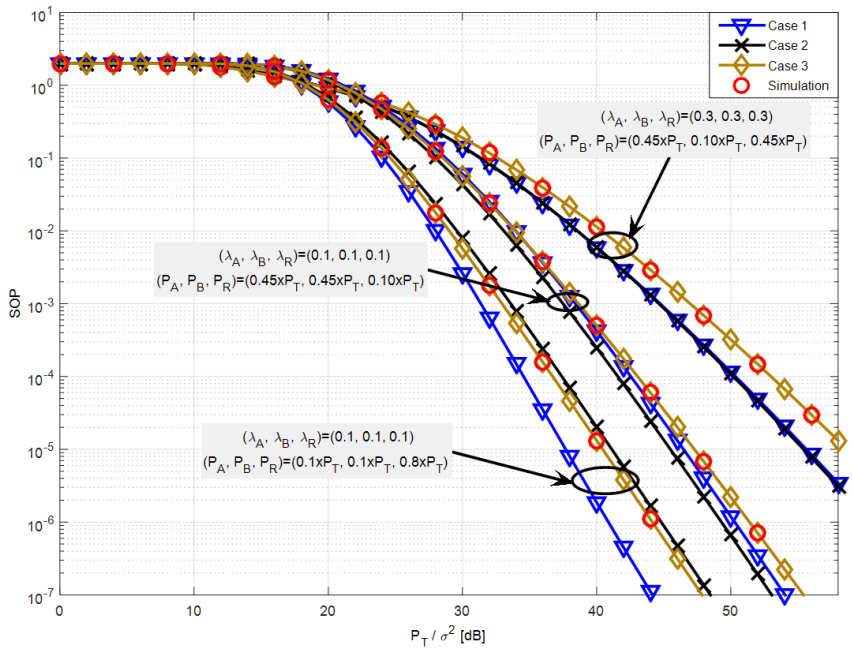

Figure 5.6: SOP of fading SIs for different power allocations at each node.

P_T/σ^2 is obtained with respect to the first selection case at a SOP of 10^{-5}. In case of equal SI values at the terminal nodes and higher SI value at the relay, using the first selection case results in the smallest SOP (consider the upper three curves). Note also that about 3.4 dB gain in P_T/σ^2 is obtained with respect to the second selection case at a SOP of 10^{-5}. Consequently, each selection case produces the smallest SOP for different SI occurrences.

Fig. 5.6 plots curves of three different power allocations for fading SI values where $\lambda_A = \lambda_B = \lambda_R = 0.1, 0.3$, $N_A = N_B = 4$, and $(P_A, P_B, P_R) \in \{(0.45 \times P_T, 0.10 \times P_T, 0.45 \times P_T), (0.45 \times P_T, 0.45 \times P_T, 0.10 \times P_T), (0.1 \times P_T, 0.1 \times P_T, 0.8 \times P_T)\}$. The threshold is taken as 6 dB. For the sake of clarity, simulation results are provided only for the third selection case. The overlapping of exact and simulation results is excellent. For equal number of total antennas and SI values, assigning equal and more power to the sources than the relay causes the second selection case produce smaller SOP (middle three curves), assigning equal and less power to the sources than the relay makes the first selection case produce smaller SOP (lower three curves), letting one of the sources and the relay have the same power which is bigger than the other source's power causes the first and second selection cases produce the same SOP, which is lower than that of the third selection case (upper three curves). Hence, each selection case is suitable and dominant for each power allocation choice. It means an optimum SOP can be obtained by using one of the selection cases for different power allocations.

To validate the correctness and robustness of the proposed simplified case selection criterion in (5.36), we represent the pseudo-expected values of e2e SINRs for any case in a

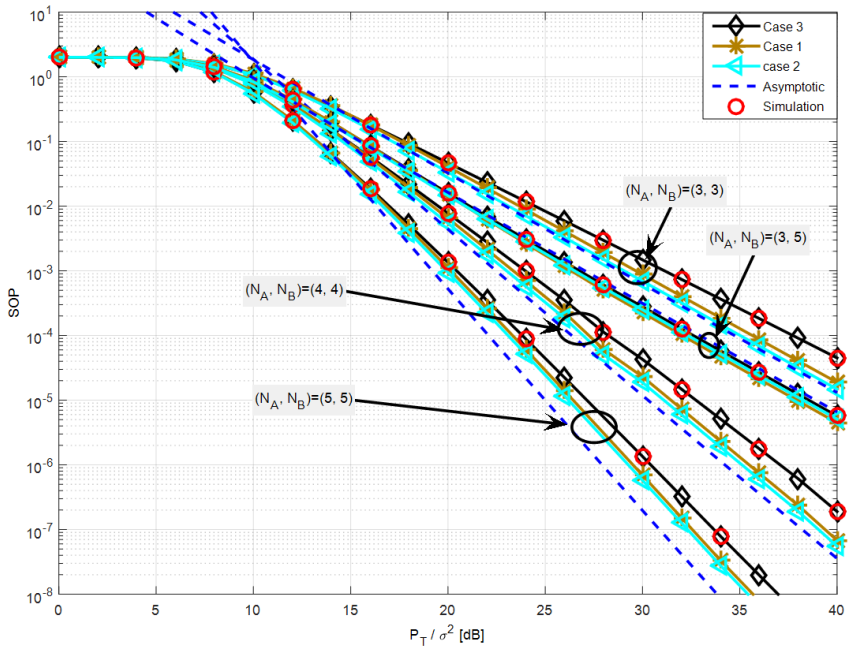

Figure 5.7: SOP of three selection cases for different total number of antennas at non-fading SI

triple form as $(\min(\bar{\gamma}_{A,1}^{P,F}, \bar{\gamma}_{B,1}^{P,F}), \min(\bar{\gamma}_{A,2}^{P,F}, \bar{\gamma}_{B,2}^{P,F}), \min(\bar{\gamma}_{A,3}^{P,F}, \bar{\gamma}_{B,3}^{P,F}))$ and consider the curves of $N_A = N_B = 4$ where $(\lambda_A, \lambda_B, \lambda_R) \in \{(0.1, 0.1, 0.1), (0.2, 0.2, 0.2), (0.1, 0.3, 0.3), (0.3, 0.3, 0.3), (0.3, 0.3, 0.5)\}$ and $(P_A, P_B, P_R) \in \{(1/3\times P_T, 1/3\times P_T, 1/3\times P_T), (0.45\times P_T, 0.10\times P_T, 0.45\times P_T), (0.45\times P_T, 0.45\times P_T, 0.10\times P_T), (0.1\times P_T, 0.1\times P_T, 0.8\times P_T)\}$ in Fig. 5.4, 5.5, and 5.6. The pseudo-expected values are calculated at $P_T/\sigma^2 = 30$ dB. If equal powers and SIs occur, the optimum selection case is decided as the second one since $\text{argmax}(\min(66.3, 66.3), \min(69.2, 69.2), \min(60.9, 75.3)) = 2$ which is the same as the result of curves for $N_A = N_B = 4$ in Fig. 5.4. In case of equal powers and unequal SIs, we can consider curves in Fig. 5.5: For $(\lambda_A, \lambda_B, \lambda_R) = (0.1, 0.3, 0.3)$, $\text{argmax}(\min(70.9, 37.0), \min(37.0, 68.9), \min(64.0, 42.1)) = 3$ and for $(\lambda_A, \lambda_B, \lambda_R) = (0.3, 0.3, 0.5)$, $\text{argmax}(\min(22.1, 22.1), \min(21.5, 21.5), \min(19.9, 23.8)) = 1$. The decisions of optimum cases correspond to the results produced in Fig. 5.5. Validity of optimum case selection criterion for unequal power assignments can be verified by considering the curves in Fig. 5.6. For $(P_A, P_B, P_R) = (0.45 \times P_T, 0.10 \times P_T, 0.45 \times P_T)$, $\text{argmax}\left(\min(13.9, 79.4), \min(14.1, 78.1), \min(12.4, 84.9)\right) = 2$, for $(P_A, P_B, P_R) = (0.45 \times P_T, 0.45 \times P_T, 0.10 \times P_T)$, $\text{argmax}\left(\min(45.9, 45.9), \min(51.0, 51.0), \min(42.7, 54.6)\right) = 2$, and for $(P_A, P_B, P_R) = \left(0.10 \times P_T, 0.10 \times P_T, 0.80 \times P_T\right)$, $\text{argmax}(\min(86.7, 86.7), \min(79.7, 79.7), \min(77.1, 89.6)) = 1$ which overlap with the results of Fig. 5.6. Therefore, the proposed simplified case selection criterion is the best choice for optimum selection.

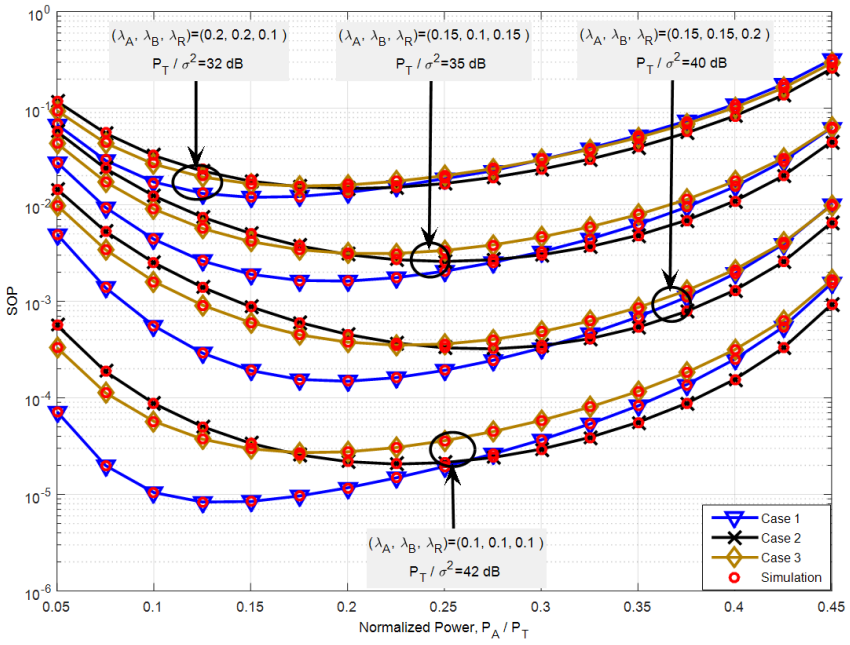

Figure 5.8: Optimum SOP for different fading SI values and power allocations.

Fig. 5.7 plots SOP curves of the three selection cases for a threshold of 6 dB with non-fading SI values for $\lambda = 0.2$. The curves are plotted for various values of (N_A, N_B). The diversity order of the curves obtained for $(N_A, N_B) = (3, 3)$ and $(N_A, N_B) = (3, 5)$ is the same and equals to 1.6 but performances of the curves for $(N_A, N_B) = (3, 5)$ are better than those of $(N_A, N_B) = (3, 3)$ and they get closer to each other. The reason for this situation is the increment in total number of antennas of the source B. The diversity orders of curves for $(N_A, N_B) = (5, 5)$, $(N_A, N_B) = (4, 4)$, $(N_A, N_B) = (3, 5)$, and $(N_A, N_B) = (3, 3)$ are 3.2, 2.4, 1.6, and 1.6, respectively. For the sake of the clarity, simulation results are only provided for the third selection case. Simulation and analytical results properly coincide with each other. Asymptotic curves follow analytical and simulation curves, and demonstrate effect of diversity order. Taking curves of $(N_A, N_B) = (3, 3)$ as reference, the gains in P_T/σ^2 at a SOP value of 10^{-5} are more than 8.5 dB and 14 dB for curves of $(N_A, N_B) = (4, 4)$ and $(N_A, N_B) = (5, 5)$, respectively.

Fig. 5.8 plots fading SI SOP curves of different SI values for tuples $(\lambda_A, \lambda_B, \lambda_R)$, versus normalized power P_A/P_T for a threshold of 10 dB and $N_A = N_B = 4$ where $P_T/\sigma^2 \in \{32, 35, 40, 42\}$ dB. The powers of nodes are assigned as $P_A = P_B = P_T \times (0.05 + 0.025 \times p)$ and $P_R = P_T \times (0.9 - 0.05 \times p)$ where p changes from 0 to 16. For all λ tuples (i.e. all SI tuples), the optimum SOP of each selection case occurs at different power allocations. Furthermore, the first selection case results in smaller SOP for all SI combinations. These results demonstrate the importance of power allocation for optimum SOP .

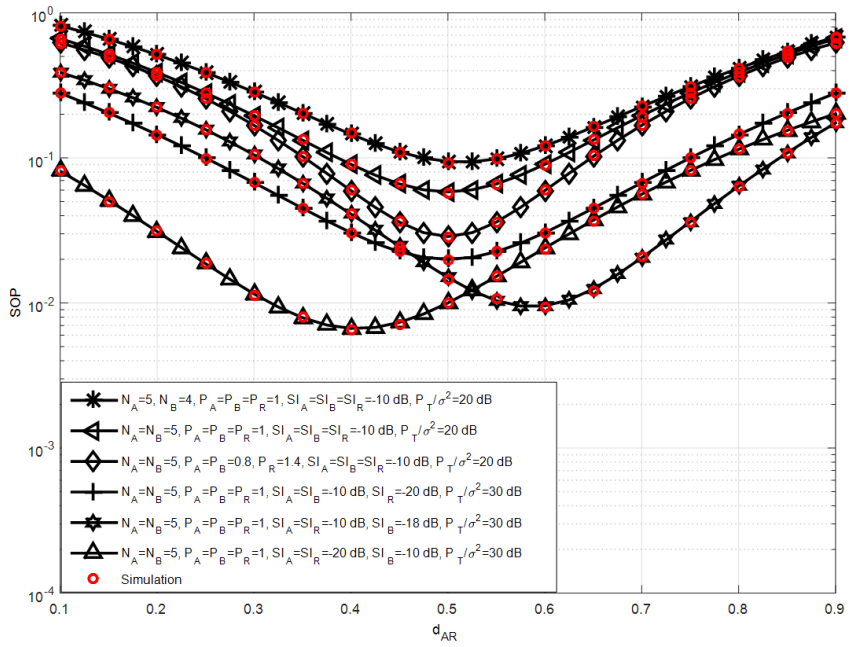

Figure 5.9: Optimum relay location for different non-fading SI values and power allocations.

Fig. 5.9 illustrates effects of primary factors that shift the optimum relay location for the first selection case (non-fading case is considered). The linear attenuation factor values are obtained as $10\log_{10}(\kappa_i)$ dB and $\lambda_i = 1$ where $i \in A, B, R$. The curves are plotted for $(\kappa_A, \kappa_B, \kappa_R) \in \{(-10,-10,-10),(-10,-10,-20),(-10,-18,-10),(-20,-10,-20)\}$, $P_T = 3$, $(P_A, P_B, P_R) \in \{(1,1,1),(0.8,0.8,1.4)\}$, $P_T/\sigma^2 \in \{20, 30\}$ dB, $(N_A, N_B) = (5,5)$, and $(N_A, N_B) = (5,4)$ for a threshold of 10 dB. Initial location is $(d_{AR}, d_{BR}) = (0.1, 0.9)$. The curves for the second and third selection cases are not provided but results obtained for the first selection case are also valid for these two cases. For the sake of clarity, curves for assigning more/less power and more total antennas to a source are not provided where we observe the same results available in the literature as HD TWRNs. As expected, for equal powers and SIs at all nodes, and antennas at end nodes, the optimum relay location is 0.5 for the first and second selection cases, but it is 0.575 for the third selection case, where distance increment (decrement) step is 0.025 (As stated, although curves are provided for the first selection case, they are similar for other two cases and are not provided for the sake of clarity). This result is because of unsymmetrical e2e SINRs at the end nodes for the third selection case, where, for equal distance, SINR of source B is bigger than that of source A. Assigning more (less) antennas to a source shifts the optimum relay location towards the other source (itself). Assigning equal powers (SIs) to the sources and different power (SI) to the relay does not change the optimum relay

location. Decreasing SI at a source causes a deviation in optimum relay location towards itself, however, increasing SI at a source shifts the optimum relay location towards the other source.

5.6. Conclusion

We proposed a novel transceiver AS strategy in an FD AF MIMO TWRN where a pair of antennas is selected at each end terminal based on maximum and second maximum SINRs for transmission and reception. The exact SOP expression for fading SI and exact, approximated, and asymptotic SOP expressions for non-fading SI are derived and validated through Monte Carlo simulation technique when forward and backward paths between the sources and the relay are different. The proposed AS strategy uses all antenna space for either transmission or reception, thus reduces total number of antennas at the sources. The offered selection strategy improves performance significantly. For all selection cases, the diversity order of the proposed selection strategy depends on SI and varies between 0 and minimum of the total number of antennas of two end sources minus 1. For different SI values, optimum power allocation is illustrated and the factors effecting optimum relay location are also elaborated.

5.7. Appendix: Derivations for CDFs and the integral I_1

Detailed derivation of CDFs for fading and non-fading SIs and closed form derivation of I_1 are given in this section.

5.7.1. CDF Derivation of Fading SIs

All RVs given in (5.6) are mutually independent. Hence the CDF of γ_i^{FCA}, $F_{\gamma_i^{FCA}}(\gamma)$, can be expressed as

$$
\begin{aligned}
F_{\gamma_i^{FCA}}(\gamma) &= Pr\left(\frac{Z_{Ri}\Upsilon_{jR}^{F}}{Z_{Ri}(\Upsilon_{RR}+1)+\Upsilon_{iR}^{F}+\Upsilon_{jR}^{F}} \leq \gamma\right) \\
&= \underbrace{Pr\left(\Upsilon_{jR}^{F} \leq \eta_i^{F}, Z_{Ri} \geq \gamma\right)}_{P_1} \\
&+ \underbrace{Pr\left(\Upsilon_{jR}^{F} \geq \eta_i^{F}, Z_{Ri} \leq \gamma\right)}_{P_2}
\end{aligned}
\tag{5.38}
$$

where $\eta_i^F = \gamma\left(Z_{Ri}(\Upsilon_{RR}+1)+\Upsilon_{iR}^{F}\right)/(Z_{Ri}-\gamma)$. Since Z_{Ri}, Υ_{jR}^{F}, Υ_{RR}, and Υ_{iR}^{F} are mutually independent RVs, P_1 can be written as

$$
P_1 = \int_{\gamma}^{\infty}\int_{0}^{\infty}\int_{0}^{\infty}\left(F_{\Upsilon_{jR}^{F}}\left(\eta_i^{F}\right) f_{\Upsilon_{iR}^{F}}(x) f_{\Upsilon_{RR}}(y) f_{Z_{Ri}}(z)\right)dxdydz. \tag{5.39}
$$

For $Z_{Ri} \leq \gamma$, $\frac{\gamma\left(Z_{Ri}(\Upsilon_{RR}+1)+\Upsilon_{iR}^{F}\right)}{Z_{Ri}-\gamma} < 0$ but Υ_{jR}^{F} is an exponential RV which means $\Upsilon_{jR}^{F} \geq 0$, so P_2 is derived as

$$
\begin{aligned}
P_2 &= Pr\left(\Upsilon_{jR}^{F} \geq 0, Z_{Ri} \leq \gamma\right) \\
&= \int_{0}^{\gamma}\int_{0}^{\infty} f_{\Upsilon_{jR}^{F}}(w)\, f_{Z_{Ri}}(z)dwdz \\
&= F_{Z_{Ri}}(\gamma) \\
&= 1 - \int_{\gamma}^{\infty} f_{Z_{Ri}}(z)dz.
\end{aligned}
\tag{5.40}
$$

After insertion of (5.39) and (5.40) in (5.38), $F_{\gamma_i^{FCA}}(\gamma)$ can be rephrased as

$$
F_{\gamma_i^{FCA}}(\gamma) = 1 - \int_{\gamma}^{\infty}\left[\int_{0}^{\infty}\int_{0}^{\infty}\left(1 - F_{\Upsilon_{jR}^{F}}\left(\eta_i^{F}\right)\right) f_{\Upsilon_{iR}^{F}}(x) f_{\Upsilon_{RR}}(y)dxdy\right] f_{Z_{Ri}}(z)dz. \tag{5.41}
$$

$F_{\gamma_i^{FCA}}(\gamma)$ is simplified by using (5.13), (5.14), (5.15), and (5.16) such that (5.17) is obtained.

5.7.2. CDF Derivation of Non-Fading SIs

To obtain CDFs of the e2e SINR expressions in (5.9), i.e., the CDFs of γ_A^{NF} and γ_B^{NF}, since Υ_{AR}^{NF}, Υ_{BR}^{NF}, Υ_{RA}^{NF}, and Υ_{RB}^{NF} are independent RVs, by following the same steps in Appendix 5.7.1., we obtain

$$
\begin{aligned}
F_{\gamma_i^{NF}}(\gamma) &= Pr\left(\frac{\alpha_i \Upsilon_{Ri}^{NF}\Upsilon_{jR}^{NF}}{\alpha_i \Upsilon_{Ri}^{NF}+\Upsilon_{iR}^{NF}+\Upsilon_{jR}^{NF}+\rho} \leq \gamma\right) \\
&= Pr\left(\Upsilon_{jR}^{NF} \leq \eta_i, \Upsilon_{Ri}^{NF} \geq \frac{\gamma}{\alpha_i}\right) + Pr\left(\Upsilon_{jR}^{NF} \geq \eta_i, \Upsilon_{Ri}^{NF} \leq \frac{\gamma}{\alpha_i}\right) \\
&= 1 - \int_0^{\infty}\left[\int_{\frac{\gamma}{\alpha_i}}^{\infty}\Big(1 - F_{\Upsilon_{jR}^{NF}}(\eta_i)\Big) f_{\Upsilon_{Ri}^{NF}}(z)dz\right] f_{\Upsilon_{iR}^{NF}}(x)dx
\end{aligned}
\tag{5.42}
$$

where $\eta_i = \gamma\left(\alpha_i \Upsilon_{Ri}^{NF} + \Upsilon_{iR}^{NF} + \rho\right)/(\alpha_i \Upsilon_{Ri}^{NF} - \gamma)$. Using CDFs and PDFs for Υ_{iR}^{NF}, Υ_{Ri}^{NF}, and Υ_{jR}^{NF} from (5.20) and (5.21), $F_{\gamma_i^{NF}}(\gamma)$ is rephrased as

$$
\begin{aligned}
F_{\gamma_i^{NF}}(\gamma) = 1 + \sum_{k=1}^{N_{iR}}\sum_{p=1}^{N_{Ri}}\sum_{m=1}^{N_{jR}} C^m_{\Upsilon_{jR}^{NF}} C^p_{\Upsilon_{Ri}^{NF}} C^k_{\Upsilon_{iR}^{NF}} \omega^k_{\Upsilon_{iR}^{NF}} \omega^p_{\Upsilon_{Ri}^{NF}} \\
\int_0^{\infty}\left[\int_{\frac{\gamma}{\alpha_i}}^{\infty} e^{-\left(\omega^m_{\Upsilon_{jR}^{NF}} \frac{\alpha_i\gamma z + \gamma(x+\rho)}{\alpha_i z - \gamma} + \omega^p_{\Upsilon_{Ri}^{NF}} z + \omega^k_{\Upsilon_{iR}^{NF}} x\right)} dz\right] dx.
\end{aligned}
\tag{5.43}
$$

By change of variable $z = t + \frac{\gamma}{\alpha_i}$ and proper rearrangements, $F_{\gamma_i^{NF}}(\gamma)$ becomes

$$
\begin{aligned}
F_{\gamma_i^{NF}}(\gamma) = 1 + \sum_{k=1}^{N_i}\sum_{p=1}^{N_i}\sum_{m=1}^{N_j} C^m_{\Upsilon_{jR}^{NF}} C^p_{\Upsilon_{Ri}^{NF}} C^k_{\Upsilon_{iR}^{NF}} \omega^k_{\Upsilon_{iR}^{NF}} \omega^p_{\Upsilon_{Ri}^{NF}} e^{-\gamma\left(\omega^m_{\Upsilon_{jR}^{NF}} + \frac{\omega^p_{\Upsilon_{Ri}^{NF}}}{\alpha_i}\right)} \\
\int_0^{\infty}\left[\int_0^{\infty} e^{-\omega^k_{\Upsilon_{iR}^{NF}} x} e^{-\left(\frac{\gamma\omega^m_{\Upsilon_{jR}^{NF}} x + \omega^m_{\Upsilon_{jR}^{NF}}\gamma(\gamma+\rho)}{\alpha_i t} + \omega^p_{\Upsilon_{Ri}^{NF}} t\right)} dt\right] dx.
\end{aligned}
\tag{5.44}
$$

We define the double integral in (5.44) as I_{mpk}, use [65, eq. (3.324)], and obtain the integral as

$$
\begin{aligned}
I_{mpk} = \int_0^{\infty}\left[2\sqrt{\frac{\gamma\omega^m_{\Upsilon_{jR}^{NF}}}{\alpha_i \omega^p_{\Upsilon_{Ri}^{NF}}}\Big(x + (\gamma+\rho)\Big)} e^{-\omega^k_{\Upsilon_{iR}^{NF}} x}\right. \\
\left. K_1\left(2\sqrt{\frac{\gamma\omega^m_{\Upsilon_{jR}^{NF}}\omega^p_{\Upsilon_{Ri}^{NF}}}{\alpha_i}\Big(x + (\gamma+\rho)\Big)}\right)\right] dx
\end{aligned}
\tag{5.45}
$$

where $K_1(x)$ is the first-order modified Bessel Function of the second kind [65, eq. (8.407)], which is available in well known software programs such as MATHEMATICA and MAPLE.

We make change of variable as $y^2 = \frac{4\gamma\omega^m_{\Upsilon_{jR}^{NF}}\omega^p_{\Upsilon_{Ri}^{NF}}}{\alpha_i}(x + (\gamma+\rho))$, define $u_{ij} = \sqrt{\frac{4\omega^m_{\Upsilon_{jR}^{NF}}\omega^p_{\Upsilon_{Ri}^{NF}}\gamma(\gamma+\rho)}{\alpha_i}}$, $\epsilon_{ij} = \frac{\alpha_i\omega^k_{\Upsilon_{iR}^{NF}}}{4\gamma\omega^m_{\Upsilon_{jR}^{NF}}\omega^p_{\Upsilon_{Ri}^{NF}}}$, and make proper rearrangements such that (5.22) is obtained.

5.7.3. Derivation of Integral in the Approximation of CDF of Non-Fading SIs

$I_1 = \int_{u_{ij}}^{u_{up}} \ln(y) y^{2h+3} e^{-\epsilon_{ij} y^2} dy$ is rephrased by making change of variable as $x = \epsilon_{ij} y^2$:

$$\begin{aligned} I_1 &= \int_{u_{ij}}^{u_{up}} \ln(y) y^{2h+3} e^{-\epsilon_{ij} y^2} dy \\ &= \frac{\epsilon_{ij}^{-h-2}}{4} \int_{\epsilon_{ij} {u_{ij}}^2}^{\epsilon_{ij} {u_{up}}^2} \ln(\frac{x}{\epsilon_{ij}}) x^{h+1} e^{-x} dx \\ &= \frac{\epsilon_{ij}^{-h-2}}{4} \Big[\int_0^{\epsilon_{ij} {u_{up}}^2} \ln(\frac{x}{\epsilon_{ij}}) x^{h+1} e^{-x} dx - \int_0^{\epsilon_{ij} {u_{ij}}^2} \ln(\frac{x}{\epsilon_{ij}}) x^{h+1} e^{-x} dx \Big], \end{aligned} \tag{5.46}$$

To obtain a closed form of I_1, we define $I = \int_0^a \ln(x/M) x^K e^{-x} dx$ and derive it by the aid of [65, eq. (4.352.1) and (4.358.1)] as

$$\begin{aligned} I = -\Gamma(K+1, a)[\ln(a) - \ln(M)] - G_{2\ 0}^{3\ 0}\left({}_{0,0,K+1}^{1,1} \Big| a \right) \\ + \Gamma(K+1)[\psi(K+1) - \ln(M)], \end{aligned} \tag{5.47}$$

where $K > -1$ and $G_{p\ q}^{m\ n}\left({}_{b_1,\ldots,b_q}^{a_1,\ldots,a_p} \Big| z \right)$ is Meijer's G function [65, eq. (9.301)], which is available in well known software programs such as MATHEMATICA and MAPLE. Hence, by using the result given in (5.47), I_1 becomes as in (5.25).

6. RELAY SELECTION FOR COOPERATIVE FD AF RELAY NETWORKS

6.1. Introduction

Improvement of coverage area, reduction of power consumption, effective utilization of bandwidth, and high data rates are the most important system parameters required to be provided by the next generation wireless communication systems. Relaying transmission, which has recently been accepted by several standards such as IEEE 802.11s, IEEE 802.16j and long term evolution-advanced (LTE-advanced), is offered to broad the coverage area, consume less power and overcome channel impairments due to fading in a wireless communications system [1], where unlicensed users can also be used as cooperative relays [113]. Although half-duplex (HD) relaying offers performance gains, it suffers from inherent spectral efficiency loss due to the allocation of orthogonal listening and forwarding phases. Full-duplex (FD) transmission, which allows simultaneously transmission and reception on the same channel, is introduced to increase the spectral efficiency and thus has received considerable attention recently [10, 114–116].

Relay selection (RS) is an attractive and effective technique to enhance the performance of multi-relay communication systems in terms of lower power consumption and better symbol error rate (SER). It has been shown that RS significantly improves system performance since number of relays increases diversity order and selection introduces lower hardware complexity [35]. Additionally, relayed communication is an attractive method for secure communication and different RS schemes are offered to analyze security-reliability trade-off, where it is proven that offered RS strategies outperform opportunistic RS in terms of security-reliability trade-off analysis [36–40]. The intermediate relays in [36–40] are assumed to be trustworthy relays, i.e., they are trusted at both service and data levels, where service level trustworthiness means accurate channel state information (CSI) of the communication links are shared with the source through relays and transmission confidentiality is not violated at the data level. Moreover, unselected relays accepting collaboration are used for friendly jammer-based jamming to disturb the eavesdropper by sending artificial noise, which boosts transmission security further [40]. RS in case of untrusted relays, actually semi-trusted (trusted at the service level but untrusted at the data level), has also been deeply studied for different communications systems to improve transmission security [117–120].

Utilization of direct-path (DP) signals improves reliability of the communication systems since it increases diversity order of the considered system by 1 [121]. In reality, ignoring DP is not a practical approach even if its signal-to-noise ratio (SNR) is too low at the destination. Furthermore, FD RS is also studied deeply in the literature for both decode-and-forward (DF) and amplify-and-forward (AF) protocols [106, 122–128]. In [106], for a cooperative DF system without DP, RS based on max-min criterion is investigated for non-fading self-interference (SI) at the relays and closed-form expressions for average capacity and SER are derived over an independent and identically distributed (i.i.d.) Rayleigh fading channel. The same system in the presence of DP is analyzed in [124]. In [122], five different RS schemes based on instantaneous channel gains and SI gains are proposed for FD transmission and analyzed over slow Rayleigh fading channels. The closed-form expressions of outage probability (OP) can not be derived except max-min RS criterion without SI. On the other hand, the asymptotic expressions are provided for all criteria. An analytical framework combining stochastic geometry and semi-Markov processes is offered in [123] to account for the cost of a suitable RS. In [126], the secrecy OP of an FD two-way relay network with RS scheme in the presence of an eavesdropper is studied by implementing DF protocol over Rayleigh fading channels and a closed form expression of sum OP is derived. FD RS with DP is elaborated in [128] for DF protocols over Nakagami-m fading, where authors derive exact expressions of OPs together with asymptotic ones. In [127], OP of a FD system using DF protocol without a DP over i.i.d. Rayleigh fading environment is analyzed, where all relays attempt to decode new message even if they do not transmit it except selected relay. OP analysis is done based on a Markov chain-based analytical model, where inter-relay interference is also considered.

For HD relaying, generalized selection transmission (GST) for multi-relay networks, i.e., generalized relay selection (GRS), is investigated over i.i.d. Rayleigh fading environment for different RS schemes without DP in [129]. The diversity orders of all selection schemes are derived and numerically verified. GRS (GST) with DP (GSTDP) is also studied in [130], where asymptotic OP and SER expressions are derived for Nakagami-m fading channels. Although both these works claim that an array / coding gain is obtained for multi-relay selections or usage of all relays (beamforming), i.e. maximum ratio transmission (MRT), their comparisons are not fair. The results are not plotted versus total consumed power but the transmitted power of the source. If the results were plotted versus total consumed power, it would be seen that performance is nearly the same for all RS choices or degrades as number of selected relays increases. Unlike antenna

selection strategies, increasing number of selected relays does not keep decreasing OP or SER, i.e. array / coding gain does not increase as total number of used relays increases. Besides, although MRT technique without RS is more complex due to the usage of all the relays, the disadvantage of the RS schemes with respect to MRT technique is the need of feedback. In case of any feedback error, the performance of the RS schemes degrades severely [131, 132]. On the other hand, MRT without RS provides close performance to single RS.

6.1.1. Motivation

Analysis of DF relaying is mathematically tractable, however, reality of power-limited and/or complexity-limited nodes may hinder practical implementation of DF relaying. Moreover, AF relaying has no decoding/re-encoding module to detect received signals, which means a much simpler amplifying and forwarding process can be achieved by AF relaying [133, 134]. Therefore, for easy and practical implementation, AF protocol is preferred in the system under consideration. Moreover, nearly all RS analyses for FD relaying are based on i.i.d. fading channels except [128] where DF protocol is used, however, i.i.d. fading channels are rare owing to the insuficient physical separations among relays [135].

It is well known that RS significantly improves system performance and reduces hardware complexity but feedback error and exhaustive searching are drawbacks of RS. Nevertheless, MRT is used without any selection to overcome feedback error and exhaustive searching complexity. Moreover, by including DP signals, cooperative diversity improves reliability of the communication systems. To the best of our knowledge, single RS schemes are investigated over i.i.d. Rayleigh fading environment without DP for FD AF transmission, however, there is no work considering single RS over independent but not identically distributed (i.n.i.d.) Rayleigh fading environment without DP although i.n.i.d. fading channels are more practical. In addition, single RS with DP is not investigated over both i.i.d. and i.n.i.d. Rayleigh fading channels for FD AF transmission. Furthermore, MRT for FD AF networks has not been studied yet, either. Therefore, as depicted in Fig. 6.1, we focus on an FD AF multi-relay cooperative-diversity system consisting of a source S, L intermediate relays, and a destination D where there exists a DP between the source S and destination D. In this system, a single relay is selected out of L relays in order to maximize effective signal-to-interference-plus-noise ratio (SINR) between the source and destination or MRT is performed without RS, i.e. all the relays

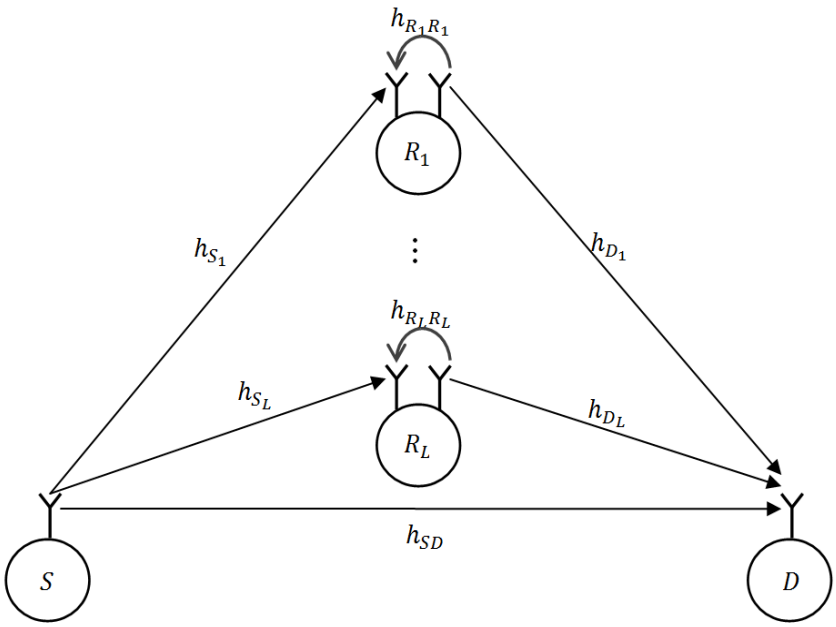

Figure 6.1: An FD AF multi-relay cooperative-diversity system.

are used for transmission via MRT, where weighting is done at the relays by using both first and second hop channel gains (Note that selecting more relays means increment of computational complexity but no array / coding gain or a negligible array / coding gain is attained in performance, therefore, only two special cases are worth considering). Due to the mathematical intractability, researchers have been using max-min criterion in order to get some closed form of the upper bounds of the investigated system performance parameters and, in sequence, they have been trying to find asymptotic expressions. However, in this chapter, we derive approximated and asymptotic expressions of OP and SER for both GST (GRS without DP) and GSTDP (GRS with DP). Although our aim is to focus on single RS and MRT without RS, it is reasonable to use the term GST since single RS and MRT without RS are two special cases of GST (Note that the signals are transmitted after weighted by channel gains even if a single relay is used). Moreover, OP and SER expressions are also provided as if GST was conducted but derived results can be used for any number of selected relays. Unlike the available approximations in the literature where max-min criterion is used to get a closed form expression for upper bound of the performance evaluation parameters such as OP and SER, the proposed approximation in this chapter is directly based on exact expression of probability density function (PDF) of end-to-end (e2e) SINR.

6.1.2. Contributions

The main contributions of this chapter can be summarized as follows:

- RS for an FD AF multi-relay cooperative-diversity system without a DP between the source and destination over i.i.d. slow Rayleigh fading channels is revised, MRT for the same system is introduced. Additionally, RS and MRT for the considered system are presented over i.n.i.d. slow Rayleigh fading channels. Furthermore, the same system with a DP between the source and destination is analyzed over both i.i.d. and i.n.i.d. slow Rayleigh fading channels for both RS and MRT techniques.
- Unlike common approach, the approximated PDF and cumulative distribution function (CDF) of a dual-hop link with FD relay are derived from exact expressions for Rayleigh fading channels.
- Using the fact that PDF and CDF of an exponential random variable can be characterized by its expected value which is equivalent to its PDF value evaluated at zero, we propose an adopted approximated PDF for e2e SINR of a dual-hop link with FD relay and validate its correctness and robustness via exact and simulation results. This proposed robust approximation of PDF facilitates the analyses of the systems with FD relay.
- Based on the derived adopted approximation, we derive closed-form approximated and asymptotic CDF, moment generating function (MGF), and SER expressions for both GST and GSTDP over both i.i.d and i.n.d Rayleigh fading channels. The theoretical findings are verified by numerical simulations via Monte-Carlo simulation technique.
- The diversity order at the high SNR regime is proven to be $G_{\text{d.GST}} = (L - \sum_{l=1}^{L} \vartheta_l)$ and $G_{\text{d.GSTDP}} = (L + 1 - \sum_{l=1}^{L} \vartheta_l)$ for GST and GSTDP, respectively, where variance of SI channels is modelled as $\kappa_l P_{R_i}^{\vartheta_l - 1}$, κ_l and ϑ_l are linear and exponential cancellation/attenuation factors depicting dependence of SI on the transmitted power, P_{R_i}, from each relay and both vary between 0 and 1. This result implies the diversity is dependent on SI and varies between 0 and $L - \sum_{l=1}^{L} \vartheta_l$ / $L + 1 - \sum_{l=1}^{L} \vartheta_l$ for GST/GSTDP.
- Closed-form approximated ergodic capacity expressions for both i.i.d. GST and GSTDP are provided and verified.
- OP, SER, and achievable rate results show that RS and MRT provide close performance, however, RS and MRT attain significant performance gains with

respect to single relay case. In addition, for the same rates, FD transmission outperforms HD one.

The remainder of this chapter is organized as follows. In Section 6.2, details of system model are provided. Section 6.3 includes derivations of approximated and asymptotic OP, MGF, and SER for both GST and GSTDP. Ergodic capacity expressions are provided in Section 6.4. Numerical results are detailed in Section 6.5. Finally, we conclude our work in Section 6.6.

6.2. System Model

As mentioned in Introduction, the main aim of this chapter is to provide analysis of a single RS (Opportunistic RS, i.e., the best relay is selected to maximize the received SINR) and MRT without RS (conventional transmission, i.e., all the relays participate the transmission) with(out) a DP between the source, S, and destination, D. RS or MRT is applied at the relays and in the presence of DP, maximal ratio combining (MRC) technique is used to combine the received signals from DP and GST link at the destination by aid of the rake receiver which is not needed if no DP exists. MRT is accomplished by using first and second hop channel gains together and each relay only needs to know its first and second hop CSI. Additionally, the source and relays transmit their signals at the same time slot by a processing delay greater than the symbol period to guarantee that the relays receive and transmit uncorrelated symbols at a certain moment [136–138]. It is also assumed that signal replicas received from the relays through GST link and DP are fully resolvable by the destination, D such that they can be appropriately co-phased and merged via MRC based on the operation of rake receivers [137, 139, 140] and more detailed discussion can be found therein. Rake receiver implementation on the receiver side is only needed in case of existence of a DP between the source and destination and it constitutes a theoretical performance benchmark for practical systems. Another critical point is about the interference stemming from other relays: Since nearly the same replicas are received, the amount of total received power increases, which is a desirable result for active SI cancellation [103]. On the other hand, SI cancellation for the proposed network is out of scope of this work. A block transmission is considered.

Let us denote the link between the source and relay R_i by h_{S_i}, the link between the relay R_i and destination D by h_{D_i}, the source-destination link by h_{SD} , and the SI channel at each relay by $h_{R_iR_i}$ (This link is also assumed to include effect of all interferences from

the other relays), where $i \in \{1, 2, \ldots, L\}$. A critical issue that should be clarified is that SI channels can not be estimated but only their instantaneous power is detectable. We assume that h_{S_i}, h_{D_i}, h_{SD}, and $h_{R_iR_i}$ are mutually independent and noise components at the relays and destination are zero mean additive Gaussian. Since we assume slow Rayleigh fading channels, SNRs and interference-to-noise ratios (INRs) are exponentially distributed random variables. The total power is denoted by $P_T = P_S + \sum_{i=1}^{L_c} P_{R_i}$, where P_S and P_{R_i} represent the source and relay powers, respectively. The instantaneous SNRs of the $S-D$, $S-R_i$, and R_i-D links are $\gamma_{DP} = \frac{P_S|h_{SD}|^2}{\sigma_D^2}$, $\gamma_{S_i} = \frac{P_S|h_{S_i}|^2}{\sigma_{R_i}^2}$, and $\gamma_{D_i} = \frac{P_{R_i}|h_{D_i}|^2}{\sigma_D^2}$, respectively. σ_D^2 and $\sigma_{R_i}^2$ are the noise variances at the D and the relay R_i, respectively. The instantaneous INR at each relay is $\gamma_{R_i} = \frac{P_{R_i}|h_{R_iR_i}|^2}{\sigma_{R_i}^2}$. For the sake of clarity and simplicity, time indexing is intentionally ignored but one can refer to [139] for more details. The received signal at the relay R_i can be given as

$$Y_{R_i} = h_{S_i}\sqrt{P_S}x_S + h_{R_iR_i}x_{R_i} + n_{R_i}, \tag{6.1}$$

where x_S is the transmitted signal at the source S with unit energy and x_{R_i}, which is updated for each transmission time slot as $x_{R_i} = \beta Y_{R_i}$, is the new transmitted signal at the relay R_i, n_{R_i} is the additive Gaussian noise at the R_i with zero mean and variance $\sigma_{R_i}^2$. Conducting GST at the relays and resolving the received signals at the destination by means of a rake receiver is the way to cope with co-phasing and merging problem on the receiver side when DP exists. Hence, Y_{R_i} is scaled by $\omega_{D_i} = \frac{h_{S_i}^* h_{D_i}^*}{|h_{D_i}||h_{S_i}|}$ and $\beta_{R_i} = \sqrt{P_{R_i}/\left(|h_{S_i}|^2 P_S + |h_{R_iR_i}|^2 P_{R_i} + \sigma_{R_i}^2\right)}$, where $(.)^*$ represents the complex conjugate, and then broadcasted to the destination D. At the D, the received signals through GST and DP are

$$\begin{aligned} Y_{D_{GST}} &= \textstyle\sum_{i=1}^{L_c} Y_{D_i} = \sum_{i=1}^{L_c}\left(h_{D_i}\beta_{R_i}\omega_{D_i}Y_{R_i} + n_{D_i}\right) \\ Y_{DP} &= \sqrt{P_s}h_{SD}x_s + n_{D_{DP}} \end{aligned}, \tag{6.2}$$

where n_{D_i} and $n_{D_{DP}}$ are the additive Gaussian noises at the D with zero mean and variance σ_D^2. The signals given in (6.2) are combined by MRC technique to obtain the signal of GSTDP as

$$Y_{D_{GSTDP}} = \frac{h_{SD}^*}{|h_{SD}|}Y_{DP} + Y_{D_{GST}} \ . \tag{6.3}$$

Since GST technique is used at the relays, MRC technique treats the signals of the relays as if only one signal comes to the D and can combine this signal with that of DP by the

aid of rake receiver. The SINR of the link $S - R_i - D$ is expressed in terms of SNRs (γ_{S_i} and γ_{D_i}) and INR (γ_{R_i}) as

$$\gamma_{SR_iD} = \frac{\gamma_{D_i}\gamma_{S_i}}{(\gamma_{D_i}+1)(\gamma_{R_i}+1)+\gamma_{S_i}}. \tag{6.4}$$

By rearranging $\{\gamma_{SR_iD}\}_{i=1}^{L}$ in decreasing order of magnitude, the order statistics $\gamma_{SR_{(1)}D} \geq \gamma_{SR_{(2)}D} \geq \ldots \geq \gamma_{SR_{(L)}D}$ are obtained. Note that this representation is used for analytical purposes of GST but only single RS and MRT are considered. The first L_c of these order statistics and instantaneous SNR of the DP are added up to carry out GST with/out DP, where $L_c = 1$ or $L_c = L$:

$$\begin{aligned} \gamma_{\mathrm{GST}} &= \sum_{\mathrm{i=1}}^{\mathrm{L_c}} \gamma_{\gamma_{\mathrm{SR_{(i)}D}}} \\ \gamma_{\mathrm{GSTDP}} &= \gamma_{\mathrm{DP}} + \gamma_{\mathrm{GST}} \end{aligned} \tag{6.5}$$

6.3. Performance Analysis

6.3.1. Equivalent PDF and CDF of Dual Hop Link

The notion of approximating the PDF of the link $S - R_i - D$ for HD transmission as an exponential random variable for Rayleigh fading is discussed in [1, eq. (46)], however, this result can be used if the combined random variable can be expressed as a harmonic mean of exponential random variables. Alternatively, equivalent or approximated PDF of the link $S - R_i - D$ can be assumed as an exponential distributed one and represented by its expected value for Rayleigh fading channels. But this approach can be used only if the expected value of the SINR of the link $S - R_i - D$ is available. For FD relaying, it is not tractable to derive closed form of the expected value of the SINR of the link $S - R_i - D$. Therefore, we propose an adopted[1] approximated PDF and CDF of a dual hop link as (See Appendix 6.7.)

$$\begin{aligned} f^{\mathrm{Eq}}_{\gamma_{SR_iD}}(x) &= \lambda_{\mathrm{E_i}} e^{-\lambda_{\mathrm{E_i}} x} \\ F^{\mathrm{Eq}}_{\gamma_{SR_iD}}(x) &= 1 - e^{-\lambda_{\mathrm{E_i}} x} \end{aligned} \tag{6.6}$$

[1] The term "adopted" is used to emphasize the difference of the proposed approximation from the available approaches.

provided that $\lambda_{E_i} = \frac{(\lambda_{D_i}+\lambda_{S_i})\lambda_{R_i}+\lambda_{S_i}}{\lambda_{R_i}} \leq 1$. Inserting equivalences of λ_{D_i}, λ_{S_i}, and λ_{R_i} into λ_{E_i}, we get

$$\begin{aligned} \lambda_{E_i} &= \left[\frac{\sigma_D^2 P_T^{-\vartheta_i}}{\Omega_{D_i} p_{f_{R_i}}} + \frac{\sigma_{R_i}^2 P_T^{-\vartheta_i} + \kappa_i p_{f_{R_i}}^{\vartheta_i}}{\Omega_{S_i} p_{f_S}}\right] P_T^{\vartheta_i - 1} \\ &= \Psi_{E_i} P_T^{\vartheta_i - 1} \end{aligned}, \tag{6.7}$$

where the power allocation factors $p_{f_{R_i}}$ and p_{f_S} are defined as $p_{f_{R_i}} = P_{R_i}/P_T$ and $p_{f_S} = P_S/P_T$, respectively. This representation implies that the diversity order and array gain of dual-hop link are $G_d = 1 - \vartheta_i$ and $G_a = \Psi_{E_i}$, respectively. The asymptotic PDF and CDF are [82]

$$\begin{aligned} f_{\gamma_{SR_iD}}^{\text{Eq},\infty}(x) &= \lambda_{E_i} \\ F_{\gamma_{SR_iD}}^{\text{Eq},\infty}(x) &= \lambda_{E_i} x \end{aligned}. \tag{6.8}$$

6.3.2. MGF and CDF of GSC

MGF and CDF for i.n.i.d. and i.i.d. cases are provided in this section.

6.3.2.1. i.n.i.d. case

Inserting (6.6) in [141, eq. (3) and eq. (4)], the MGF of GST for i.n.i.d. channel and SI gains is obtained as

$$\begin{aligned} M_{\gamma_{\text{GST}}}^{\text{ind}}(-s) = \sum_{\substack{n_1,\ldots,n_{L_c-1} \\ n_1<n_2<\ldots<n_{L_c-1}}} \sum_{n_{L_c}} \left[\frac{\prod_{l=1}^{L_c} \lambda_{E_{n_l}}}{\prod_{l=1}^{L_c-1}\left(s+\lambda_{E_{n_l}}\right)}\right] \\ \int_0^\infty e^{-\left(L_c s + \sum_{l=1}^{L_c} \lambda_{E_{n_l}}\right)x} \prod_{l'=L_c+1}^{L} \left(1 - e^{-\lambda_{E_{n_{l'}}} x}\right) dx \end{aligned}, \tag{6.9}$$

where $\sum_{\substack{n_1,\ldots,n_{L_c-1} \\ n_1<n_2<\ldots<n_{L_c-1}}}$ denotes the $\binom{L}{L_c-1}$ possible combinations of selecting the (L_c-1) largest SINR branches out of the L branches, $\sum_{n_{L_c}}$ denotes the index n_{L_c} chosen from the remaining $L - L_c + 1$ branches. Using the fact that there are $L_c\binom{L}{L_c}$ terms in (6.9) and substituting (6.8) into [141, eq. (3) and eq. (4)], the asymptotic MGF of the GST for i.n.i.d. case is derived as

$$M_{\gamma_{\text{GST}}}^{\text{ind},\infty}(-s) \approx \frac{\Gamma[L+1]}{\Gamma[L_c+1]L_c^{L-L_c}} \frac{\prod_{l=1}^{L}\lambda_{E_l}}{s^L}. \tag{6.10}$$

The asymptotic CDF of i.n.d case is obtained by using inverse Laplace transform [65, eq. (17.13.26)]:

$$\begin{aligned} F_{\gamma_{\text{GST}}}^{\text{ind},\infty}(x) &\approx \frac{\prod_{l=1}^{L}\lambda_{E_l}}{\Gamma[L_c+1]L_c^{L-L_c}}x^L \\ &\approx \frac{P_T^{-L+\sum_{l=1}^{L}\vartheta_l}\prod_{l=1}^{L}\Psi_{E_l}}{\Gamma[L_c+1]L_c^{L-L_c}}x^L \end{aligned}. \tag{6.11}$$

The result in (6.11) implies that the diversity order and array gain of GST are $G_{\text{d.GSC}} = (L - \sum_{l=1}^{L}\vartheta_l)$ and $G_{\text{a.GST}} = \frac{\prod_{l=1}^{L}\Psi_{E_l}}{\Gamma[L_c+1]L_c^{L-L_c}}$, respectively.

6.3.2.2. i.i.d. case

Since it is not tractable to derive MGF expression in (6.9) in closed form for i.n.i.d. case, we assume SI and channel gains are i.i.d., namely, we assume that $\lambda_E = \lambda_{E_l}$, $l = 1, \ldots, L$. We use this assumption together with the Binomial Theorem in (6.9), then the resulting MGF of the GST for i.i.d. assumption becomes

$$M_{\gamma_{\text{GST}}}^{\text{iid}}(-s) = \sum_{k=1}^{L-L_c} \frac{\binom{L}{L_c}\binom{L-L_c}{k}(-1)^k\lambda_E^L}{\left(s + \frac{(L_c+k)\lambda_E}{L_c}\right)(s+\lambda_E)^{L_c-1}} + \frac{\binom{L}{L_c}\lambda_E^{L_c}}{(s+\lambda_E)^{L_c}}. \tag{6.12}$$

The same result is derived in [78, eq. (13)]. By the aid of partial fraction decomposition, $M_{\gamma_{GST}}(-s)$ is reformulated as

$$M_{\gamma_{\text{GST}}}^{\text{iid}}(-s) = \sum_{k=1}^{L-L_c} \frac{C_{\lambda_k}^G}{s+\lambda_k} + \sum_{m=1}^{L_c} \frac{C_{\lambda_E}^G}{(s+\lambda_E)^m}, \tag{6.13}$$

where $\lambda_k = \frac{(L_c+k)\lambda_E}{L_c}$, $C_{\lambda_k}^G$ and $C_{\lambda_E}^G$ are expressed as

$$\begin{aligned} C_{\lambda_k}^G =& \binom{L}{L_c}\binom{L-L_c}{k}\left(\frac{L_c}{k}\right)^{L_c-1}(-1)^{k-L_c+1}\lambda_E \\ C_{\lambda_E}^G =& \binom{L}{L_c}\lambda_E^{L_c}u[m-L_c] + \sum_{k=1}^{L-L_c}\binom{L}{L_c}\binom{L-L_c}{k}. \\ & \left(\frac{L_c}{k}\right)^{L_c-m}(-1)^{L_c+k-m-1}\lambda_E^m u[L_c-m-1] \end{aligned} \tag{6.14}$$

In (6.14), $u[n]$ represents the unit-step function. Using inverse Laplace transform of (6.13), the closed form PDF of the GST is obtained

$$f_{\gamma_{GST}}^{\text{iid}}(x) = \sum_{k=1}^{L-L_c} C_{\lambda_k}^{G} e^{-\lambda_k x} + \sum_{m=1}^{L_c} \frac{C_{\lambda_E}^{G} x^{m-1} e^{-\lambda_E x}}{\Gamma[m]}. \tag{6.15}$$

Using the identity [65, eq. (2.321.2)], the CDF of γ_{GST} derived as

$$\begin{aligned} F_{\gamma_{GST}}^{\text{iid}}(x) = &\sum_{k=1}^{L-L_c} \frac{C_{\lambda_k}^{G}}{\lambda_k} + \sum_{m=1}^{L_c} \frac{C_{\lambda_E}^{G}}{\lambda_E^{m}} - \sum_{k=1}^{L-L_c} \frac{C_{\lambda_k}^{G} e^{-\lambda_k x}}{\lambda_k} \\ &- \sum_{m=1}^{L_c} \sum_{k=0}^{m-1} \frac{C_{\lambda_E}^{G} \binom{m-1}{k} \lambda_E^{-(k+1)} \Gamma[k+1] x^{m-k-1} e^{-\lambda_E x}}{\Gamma[m]}. \end{aligned} \tag{6.16}$$

The constant terms in (6.16) equal 1. Furthermore (6.10) and (6.11) reduce to

$$M_{\gamma_{GST}}^{\text{iid},\infty}(-s) \approx \frac{\Gamma[L+1]}{\Gamma[L_c+1] L_c^{L-L_c}} \frac{\lambda_E^{L}}{s^{L}} \tag{6.17}$$

and

$$\begin{aligned} F_{\gamma_{GST}}^{\text{iid},\infty}(x) &\approx \frac{\lambda_E^{L}}{\Gamma[L_c+1] L_c^{L-L_c}} x^{L} \\ &\approx \frac{P_T^{(\vartheta-1)L} \Psi_E^{L}}{\Gamma[L_c+1] L_c^{L-L_c}} x^{L} \end{aligned}. \tag{6.18}$$

For i.i.d. case, the diversity order of GST reduces to $G_{\text{d.GST}} = (1-\vartheta)L$.

6.3.3. MGF and CDF of GSTDP

Based on the independence of DP and relaying channels, the MGF of γ_{GSTDP} for both i.i.d. and i.n.i.d. cases can be derived as

$$M_{\gamma_{GSTDP}}(-s) = M_{\gamma_{GST}}(-s) M_{\gamma_{DP}}(-s). \tag{6.19}$$

The MGF of the direct path between the S and D is $M_{\gamma_{DP}}(-s) = \frac{\lambda_{DP}}{s+\lambda_{DP}}$ [74, eq. (5.5)]. Inserting $M_{\gamma_{DP}}(-s)$ into (6.19), $M_{\gamma_{GSTDP}}(-s)$ becomes

$$M_{\gamma_{GSTDP}}(-s) = \frac{\lambda_{DP}}{s+\lambda_{DP}} M_{\gamma_{GST}}(-s). \tag{6.20}$$

6.3.3.1. i.n.i.d. case

Substituting (6.9) into (6.20) results in

$$M_{\text{GSTDP}}^{\text{ind}}(-s) = \sum_{\substack{n_1,\ldots,n_{L_c-1} \\ n_1<n_2<\ldots<n_{L_c-1}}} \sum_{n_{L_c}} \left[\frac{\prod_{l=1}^{L_c} \lambda_{E_{n_l}}}{\prod_{l=1}^{L_c-1} \left(s+\lambda_{E_{n_l}}\right)} \right] \frac{\lambda_{DP}}{(s+\lambda_{DP})} \int_0^\infty e^{-\left(L_c s+\sum_{l=1}^{L_c} \lambda_{E_{n_l}}\right)x} \prod_{l'=L_c+1}^{L} \left(1-e^{-\lambda_{E_{n_{l'}}} x}\right) dx. \tag{6.21}$$

To obtain the asymptotic CDF of γ_{GSTDP} for i.n.i.d. case, we substitute asymptotic MGF of γ_{DP}, $M_{\gamma_{DP}}^{\infty}(-s) = \frac{\lambda_{DP}}{s}$ and asymptotic MGF of i.n.i.d. GST given in (6.10) into (6.19) and get

$$M_{\text{GSTDP}}^{\text{ind},\infty}(-s) \approx \frac{\Gamma[L+1]}{\Gamma[L_c+1] L_c^{L-L_c}} \frac{\lambda_{DP} \prod_{l=1}^{L} \lambda_{E_l}}{s^{L+1}}. \tag{6.22}$$

The asymptotic CDF of i.n.i.d. case is obtained by using inverse Laplace transform:

$$\begin{aligned} F_{\gamma_{\text{GSTDP}}}^{\text{ind},\infty}(x) &\approx \frac{\lambda_{DP} \prod_{l=1}^{L} \lambda_{E_l}}{(L+1)\Gamma[L_c+1] L_c^{L-L_c}} x^{L+1} \\ &\approx \frac{P_T^{-1-L+\sum_{l=1}^{L} \vartheta_l} \Psi_{DP} \prod_{l=1}^{L} \Psi_{E_l}}{(L+1)\Gamma[L_c+1] L_c^{L-L_c}} x^{L+1} \end{aligned}, \tag{6.23}$$

where $\lambda_{DP} = \frac{\sigma_D^2}{p_{f_S} \Omega_{SD}} P_T^{-1} = \Psi_{DP} P_T^{-1}$, and the diversity order and array gain of GSTDP are $G_{\text{d.GSTDP}} = (L+1-\sum_{l=1}^{L} \vartheta_l)$ and $G_{\text{a.GSTDP}} = \frac{\Psi_{DP} \prod_{l=1}^{L} \Psi_{E_l}}{(L+1)\Gamma[L_c+1] L_c^{L-L_c}}$, respectively.

6.3.3.2. i.i.d. case

Inserting $M_{\gamma_{\text{GST}}}^{\text{iid}}(-s)$ given in (6.12) and $M_{\gamma_{DP}}(-s)$ into (6.19) and carrying a partial fraction decomposition between the terms with the poles $-\lambda_k$ and $-\lambda_{DP}$, $M_{\gamma_{GSTDP}}(-s)$ results in

$$\begin{aligned} M_{\gamma_{\text{GSTDP}}}^{\text{iid}}(-s) = \sum_{k=1}^{L-L_c} \Bigg[\frac{\binom{L}{L_c}\binom{L-L_c}{k}(-1)^k \lambda_{DP} \lambda_E^{L_c}}{(\lambda_k - \lambda_{DP})} \frac{1}{(s+\lambda_E)^{L_c-1}} \left(\frac{1}{s+\lambda_{DP}} - \frac{1}{s+\lambda_k} \right) \Bigg] \\ + \frac{\binom{L}{L_c} \lambda_{DP} \lambda_E^{L_c}}{(s+\lambda_{DP})(s+\lambda_E)^{L_c}}. \end{aligned} \tag{6.24}$$

The partial fraction decomposition is valid if λ_{DP} is not an integer multiple of λ_E or vice versa. Applying second partial fraction decomposition and making proper rearrangements produces

$$M^{\text{iid}}_{\gamma_{\text{GSTDP}}}(-s) = \frac{C_{DP}}{(s+\lambda_{DP})} - \sum_{k=1}^{L-L_c} \frac{C_k}{(s+\lambda_k)} + \sum_{m=1}^{L_c} \frac{C_m}{(s+\lambda_E)^m}. \tag{6.25}$$

The coefficients in (6.25) are

$$\begin{aligned}
C_k &= \frac{\binom{L}{L_c}\binom{L-L_c}{k}\left(\frac{L_c}{k}\right)^{L_c-1}(-1)^{k-L_c+1}\lambda_{DP}\lambda_E}{\lambda_{DP}-\lambda_k} \\
C_{DP} &= \sum_{k=0}^{L-L_c}\Bigg(\frac{\binom{L}{L_c}\lambda_{DP}\lambda_E^{L_c}}{(\lambda_E-\lambda_{DP})^{L_c}}u[-k] \\
&\quad + \frac{\binom{L}{L_c}\binom{L-L_c}{k}(-1)^k\lambda_{DP}\lambda_E^{L_c}}{(\lambda_k-\lambda_{DP})(\lambda_E-\lambda_{DP})^{L_c-1}}u[k-1]\Bigg) \\
C_m &= \sum_{k=1}^{L-L_c}\Bigg[\frac{\binom{L}{L_c}\binom{L-L_c}{k}\lambda_{DP}\lambda_E^{L_c}(-1)^{L_c+k-m-1}}{(\lambda_k-\lambda_{DP})}\Bigg(\frac{1}{(\lambda_{DP}-\lambda_E)^{L_c-m}} \\
&\quad - \left(\frac{L_c}{k\lambda_E}\right)^{L_c-m}\Bigg)u[L_c-m-1]\Bigg] + \frac{\binom{L}{L_c}\lambda_{DP}\lambda_E^{L_c}(-1)^{L_c-m}}{(\lambda_{DP}-\lambda_E)^{L_c-m+1}}
\end{aligned} \tag{6.26}$$

Taking the inverse Laplace transform of (6.25) gives the PDF of GSTDP

$$f^{\text{iid}}_{\gamma_{\text{GSTDP}}}(x) = C_{DP}e^{-\lambda_{DP}x} - \sum_{k=1}^{L-L_c} C_k e^{-\lambda_k x} + \sum_{m=1}^{L_c}\frac{C_m}{\Gamma[m]}x^{m-1}e^{-\lambda_E x} \tag{6.27}$$

and CDF of γ_{GSTDP} is obtained by using the identity [65, eq. (2.321.2)] as

$$\begin{aligned}
F^{\text{iid}}_{\gamma_{\text{GSTDP}}}(x) = \frac{C_{DP}}{\lambda_{DP}} + \sum_{m=1}^{L_c}\frac{C_m}{\lambda_E^m} - \sum_{k=1}^{L-L_c}\frac{C_k}{\lambda_k} - \frac{C_{DP}e^{-\lambda_{DP}x}}{\lambda_{DP}} + \sum_{k=1}^{L-L_c}\frac{C_k e^{-\lambda_k x}}{\lambda_k} \\
- \sum_{m=1}^{L_c}\sum_{k=0}^{m-1}\frac{\binom{m-1}{k}\Gamma[k+1]C_m}{\Gamma[m]\lambda_E^{k+1}}x^{m-k-1}e^{-\lambda_E x}.
\end{aligned} \tag{6.28}$$

The constant terms in (6.28) equal 1.

Asymptotic expressions for MGF and CDF of i.i.d. assumption are the same as those of the i.n.i.d. case in (6.22) and (6.23), where the term $\prod_{l=1}^{L}\lambda_{E_l}$ simplifies to λ_E^L and the diversity order returns to $G_{\text{d.GSTDP}} = (1-\vartheta)L + 1$.

6.3.4. SER Analysis

In this section, SER analysis of GST and GSTDP are provided based on MGF approach [74, eq. (5.3)]. For i.n.i.d. case only asymptotic expressions are derived. The SER of GST can be derived from $\sum_{q=1}^{Q} a_q \int_0^{\theta_q} M_{\gamma_{\text{GST}}}^{\text{iid}} \left(-\frac{\lambda_{\text{mod}}}{\sin^2(\theta)}\right) d\theta$ by using (6.13)

$$\begin{aligned} P_{\text{SER}}^{\text{GST,iid}} = &\sum_{q=1}^{Q} \sum_{k=1}^{L-L_c} \frac{a_q C_{\lambda_k}^G}{\lambda_k} \int_0^{\theta_q} \frac{\sin^2(\theta)}{\sin^2(\theta) + \frac{\lambda_{\text{mod}}}{\lambda_k}} d\theta \\ &+ \sum_{q=1}^{Q} \sum_{k=1}^{L-L_c} \frac{a_q C_{\lambda_E}^G}{\lambda_E^m} \int_0^{\theta_q} \left(\frac{\sin^2(\theta)}{\sin^2(\theta) + \frac{\lambda_{\text{mod}}}{\lambda_E}} \right)^m d\theta. \end{aligned} \tag{6.29}$$

Similarly, by using (6.25), the SER of GSTDP becomes

$$\begin{aligned} P_{\text{SER}}^{\text{GSTDP,iid}} = &\sum_{q=1}^{Q} \frac{a_q C_{DP}}{\lambda_{DP}} \int_0^{\theta_q} \frac{\sin^2(\theta)}{\sin^2(\theta) + \frac{\lambda_{\text{mod}}}{\lambda_{DP}}} d\theta \\ &- \sum_{q=1}^{Q} \sum_{k=1}^{L-L_c} \frac{a_q C_k}{\lambda_k} \int_0^{\theta_q} \frac{\sin^2(\theta)}{\sin^2(\theta) + \frac{\lambda_{\text{mod}}}{\lambda_k}} d\theta \\ &+ \sum_{q=1}^{Q} \sum_{k=1}^{L-L_c} \frac{a_q C_m}{\lambda_E^m} \int_0^{\theta_q} \left(\frac{\sin^2(\theta)}{\sin^2(\theta) + \frac{\lambda_{\text{mod}}}{\lambda_E}} \right)^m d\theta. \end{aligned} \tag{6.30}$$

The modulation dependent parameters in (6.29) and (6.30) for M-ary PSK (M-PSK) and M-ary quadrature amplitude modulation (M-QAM) are given in Table 2.1.

All the integrals in (6.29) and (6.30) can be represented by a single integral, namely,

$$I_{\text{m}}(\theta_q; c) = \int_0^{\theta_q} \left(\frac{\sin^2(\theta)}{\sin^2(\theta) + c} \right)^m d\theta. \tag{6.31}$$

The closed form of the integral, $I_m(\theta_q; c)$, in (6.31) is derived in [74, eq.(5A.24) and (5A.35)]. However, for the sake of easy implementation, we solve this integral in another form. Using [74, (5A.33)], $I_m(\theta_q; c)$ can be expressed as

$$I_{\mathrm{m}}(\theta_q;c)=\sqrt{\frac{c}{c+1}}\Bigg[\int_0^T\frac{1}{2(1+a\sin(x))}dx+\int_0^T\frac{1}{2(1-a\sin(x))}dx - \sum_{k=0}^{m-1}a^{2k}\int_0^T\sin^{2k}(x)dx\Bigg], \tag{6.32}$$

where $a=\sqrt{\frac{1}{c+1}}$, $T=\tan^{-1}\frac{N_T}{D_T}+\frac{1}{\pi}\left(1-\mathrm{sign}(N_T)\frac{1+\mathrm{sign}(D_T)}{2}\right)$, $N_T=2\sqrt{c(c+1)}$ $\sin(2\theta_q)$, and $D_T=(2c+1)\cos(2\theta_q)-1$ [74, eq. (5A.31) and (5A.32)]. The closed form of the first two integrals in (6.32) can be found by making a change of variable as $y=\frac{a\pm\tan(x/2)}{\sqrt{1-a^2}}$. Third integral is obtained in [52, eq. (37)]. Hence, the integral in (6.32) has the following closed form:

$$\begin{aligned}I_{\mathrm{m}}(\theta_q;c)=&\tan^{-1}\left[\frac{a+\tan(T/2)}{\sqrt{1-a^2}}\right]-\tan^{-1}\left[\frac{a-\tan(T/2)}{\sqrt{1-a^2}}\right]\\&-\sqrt{\frac{c}{c+1}}\sum_{k=0}^{m-1}a^{2k}\left[\frac{\sqrt{\pi}\Gamma[k+1/2]}{\Gamma[k+1]}-\cos(T){}_2F_1(\frac{1}{2},\frac{1}{2}-k;\frac{3}{2};\cos^2(T))\right].\end{aligned} \tag{6.33}$$

which is valid for $0<\theta_q<\pi$. ${}_2F_1(\iota,\tau;w;z)$ in (6.33) is the Gauss hypergeometric function [65, eq. (9.111)], which is available in well known mathematical software programs such as MATHEMATICA and MAPLE.

Using (6.10) and [52, eq. (37)], asymptotic SER for both i.i.d. and i.n.i.d. GST is derived as

$$\begin{aligned}P_{SER}^{GST,\infty}(-s)&=\sum_{q=1}^{Q}a_q\int_0^{\theta_q}M_{\gamma_{GST}}^{\infty}\left(-\frac{\lambda_{\mathrm{mod}}}{\sin^2(\theta)}\right)d\theta\\&=\sum_{q=1}^{Q}\frac{a_q\Gamma[L+1]\prod_{l=1}^{L}\lambda_{E_l}}{\Gamma[L_c+1]L_c^{L-L_c}\lambda_{\mathrm{mod}}^{L}}\int_0^{\theta_q}\sin^{2L}(\theta)d\theta\\&=\sum_{q=1}^{Q}\frac{a_q\Gamma[L+1]\prod_{l=1}^{L}\lambda_{E_l}}{\Gamma[L_c+1]L_c^{L-L_c}\lambda_{\mathrm{mod}}^{L}}\left[\frac{\sqrt{\pi}\Gamma[L+1/2]}{\Gamma[L+1]}\right.\\&\quad\left.-\cos(\theta_q){}_2F_1(\frac{1}{2},\frac{1}{2}-L;\frac{3}{2};\cos^2(\theta_q))\right]\end{aligned}. \tag{6.34}$$

Similarly, by using (6.22), asymptotic SER for i.n.i.d. and i.i.d. GSTDP is

$$\begin{aligned}P_{\mathrm{SER}}^{\mathrm{GSTDP},\infty}(-s)=&\sum_{q=1}^{Q}\left[\frac{a_q\Gamma[L+1]\lambda_{DP}\prod_{l=1}^{L}\lambda_{E_l}}{\Gamma[L_c+1]L_c^{L-L_c}\lambda_{\mathrm{mod}}^{L+1}}\right.\\&\left.\left(\frac{\sqrt{\pi}\Gamma[L+3/2]}{\Gamma[L+2]}-\cos(\theta_q){}_2F_1(\frac{1}{2},-\frac{1}{2}-L;\frac{3}{2};\cos^2(\theta_q))\right)\right]\end{aligned}. \tag{6.35}$$

Clearly, as expected, the diversity order for SER of GST and GSTDP are $G_{\text{d.GST}} = (L - \sum_{l=1}^{L} \vartheta_l)$ and $G_{\text{d.GSTDP}} = (L + 1 - \sum_{l=1}^{L} \vartheta_l)$, respectively. For i.i.d. case, $\prod_{l=1}^{L} \lambda_{E_l}$ reduces to λ_E^L in (6.34) and (6.35), and diversity orders of GST and GSTDP become $G_{\text{d.GST}} = (1 - \vartheta)L$ and $G_{\text{d.GSTDP}} = (1 - \vartheta)L + 1$, respectively.

6.4. Ergodic Capacity

In this section, we only give the achievable rate expressions for i.i.d. case. The achievable rates can be computed based on CDF approach [75, eq. (38)]:

$$R^{\text{iid}}_{\gamma_{GST}/\gamma_{\text{GSTDP}}} = \log_2(e) \int_0^{\infty} \frac{1 - F^{\text{iid}}_{\gamma_{GST}/\gamma_{\text{GSTDP}}}(x)}{x+1} dx. \tag{6.36}$$

Using the fact that constant terms in (6.16) and (6.28) are equal to 1, the rates can be calculated as

$$\begin{aligned} R^{\text{iid}}_{\gamma_{GST}} = \log_2(e) \Bigg(& \sum_{k=1}^{L-L_c} \frac{C^G_{\lambda_k}}{\lambda_k} I_0(\lambda_k) \\ & + \sum_{m=1}^{L_c} \sum_{k=0}^{m-1} \frac{C^G_{\lambda_E} \binom{m-1}{k} \lambda_E^{-(k+1)} \Gamma[k+1]}{\Gamma[m]} I_{m-k-1}(\lambda_E) \Bigg) \end{aligned} \tag{6.37}$$

and

$$\begin{aligned} R^{\text{iid}}_{\gamma_{\text{GSTDP}}} = \log_2(e) \Bigg(& \frac{C_{DP}}{\lambda_{DP}} I_0(\lambda_{DP}) - \sum_{k=1}^{L-L_c} \frac{C_k}{\lambda_k} I_0(\lambda_k) \\ & + \sum_{m=1}^{L_c} \sum_{k=0}^{m-1} \frac{\binom{m-1}{k} \Gamma[k+1] C_m}{\Gamma[m] \lambda_E^{k+1}} I_{m-k-1}(\lambda_E) \Bigg). \end{aligned} \tag{6.38}$$

The integral in (6.37) and (6.38) is defined and solved as

$$\begin{aligned} I_m(\lambda) &= \int_0^{\infty} \frac{x^m e^{-\lambda x}}{x+1} dx \\ &= e^{\lambda} \Gamma[m+1] \Gamma[-m, \lambda] \end{aligned}, \tag{6.39}$$

where $\lambda > 0$, $m > -1$, and $\Gamma[m, \lambda]$ is incomplete gamma function [65, eq. (8.350.2)]. For integer m values, as in our case, this integral is also solved in [65, eq. (3.353.5)] where it includes an exponential integral.

Table 6.1: Simulation Parameters.

Parameters	Fig. 6.2	Fig. 6.3	Fig. 6.4	Fig. 6.5	Fig. 6.6
Powers	$P_S = P_{R_l} = P_T/(L_c+1)$				
Noise Variances	$\sigma^2 = \sigma^2_{R_l} = \sigma^2_D = 1$				
Total Number of Relays (L)	1	{2, 3, 4}	{1, 2, 3}	{1, 3}	{1, 3, 4}
Number of Selected Relays (L_c)	1	{1, 2, 3, 4}	{1, 3}	{1, 3}	{1, 3, 4}
Linear SI Cancellation Factor (κ_l)	1	1	$\{10^{-10}, 1\}$	$\{10^{-10}, 1\}$	$\{10^{-10}, 1\}$
Exponential SI Cancellation Factor (ϑ_l)	{0.2,0.5, 0.8, 1}	0.2	{0, 0.2}	{0, 0.2}	{0, 0.2}
SINR Threshold (γ_{th})	{6 dB, 10 dB}	6 dB	6 dB	-	-
Distances ($d_{SR_l}, d_{R_lD}, d_{SD}$)	(0.5, 0.5, -)	(0.5, 0.5, -)	(0.5, 0.5, 1)	(0.5, 0.5, 1)	(1, 1, 2)
Path Loss Exponent (α)	3	3	3	3	3

6.5. Numerical Results

In this section, numerical results for OP and SER of M-PSK and M-QAM are provided to validate the derived expressions for each measurement quantity. It is assumed that $P_S = P_{R_l} = P_T/(L_c+1)$, where P_T is total power and $\sigma^2 = \sigma^2_{R_l} = \sigma^2_D = 1$. We assume normalized distances and let $d_{SR_l} = d_{R_lD} = 1/2$ and also $d_{SD} = 1$ but exceptions will be given where necessary. The path loss exponent α is taken to be 3 which represents heavy urban environment. Furthermore, SI values at all relays are assumed to be equal. The curves are plotted versus P_T/σ^2. Furthermore, simulation parameters for each figure are provided in Table 6.1 for easy referring, where simulation results are derived after 10^8 iterations at each SINR value.

Fig. 6.2 shows validity of approximated and adopted approximation expressions of OP for a dual-hop link, which are given in (6.43) and (6.6), respectively. The exact results are produced by taking numerical integration given in (6.42). Linear SI cancellation/attenuation factor $\kappa_l = 1$, the exponential one $\vartheta_l \in \{0.2, 0.5, 0.8, 1\}$, and threshold $\gamma_{\text{th}} \in \{6 \text{ dB}, 10 \text{ dB}\}$ are used, where the data rate thresholds become $\log_2(10^{6/10}+1) = 2.32$ bits/s/Hz and $\log_2(10^{10/10}+1) = 3.46$ bits/s/Hz. Although there

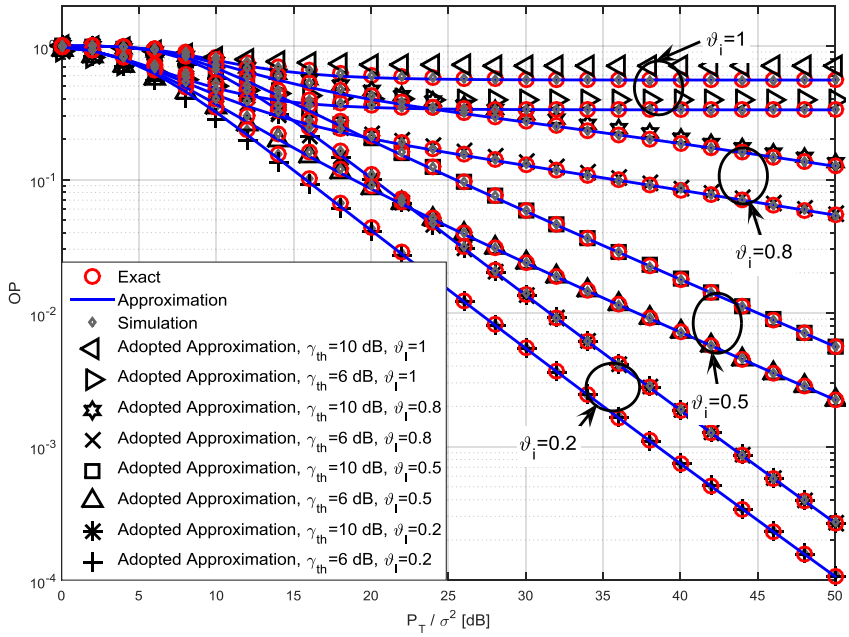

Figure 6.2: Exact, approximated, asymptotic, and simulation OPs of a dual-hop link.

are small differences at low P_T/σ^2 values, the overlap at the high P_T/σ^2 values is almost excellent, which verifies correctness of the derived adopted approximation. The deviation occurs for high thresholds, γ_{th}, and high exponential attenuation/cancellation factors of SI, ϑ_l, which may happen in case of insufficient SI cancellation. Setting $\kappa_l = \vartheta_l = 1$ means that SI power equals to relay power, and shows the worst case.

Fig. 6.3 illustrates OP of GST for $(\kappa_l, \vartheta_l) = (1, 0.2)$, $L \in \{2, 3, 4\}$, $L_c \in \{1, 2, 3, 4\}$,

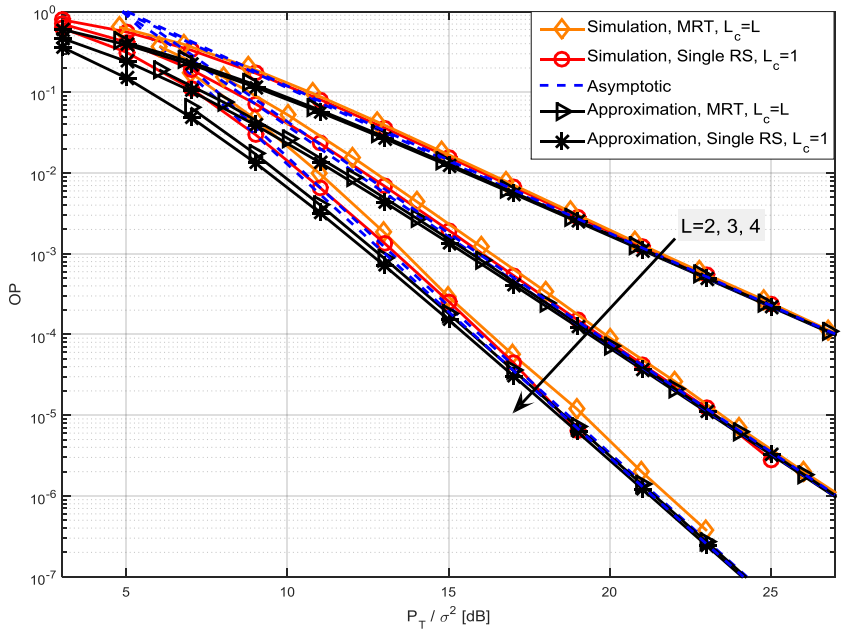

Figure 6.3: OP of GST for different diversity orders.

and a threshold of 6 dB. The exact (adopted approximated) curves are generated from (6.16), and asymptotic ones from (6.18). The gap between the approximated and simulation results reduces and finally becomes negligible at high P_T/σ^2 values. Similarly, asymptotic curves follow the simulation and approximated curves. Approximation error demonstrates its effect at low P_T/σ^2 values and increases as total number of relays increases. Increment in error stems from integration over adopted approximated PDF and CDF of a dual-hop link. The gain in P_T/σ^2 with respect to single relay transmission (consider Fig. 6.2) is about 22 dB, 30 dB, and 34 dB at an OP value of 10^{-4} as total number of relays changes from 2 to 4, respectively. To observe the diversity order, one can consider the OP values at 15 dB and 23 dB for $(L, L_c) = (3, 1)$, which are about 10^{-3} and 10^{-5}. Therefore, the diversity order is about $2/0.8 \approx 2.5$ which coincides with the nominal one, namely, $L \times (1 - \vartheta_l) = 2.4$. Although single RS and MRT schemes have nearly the same performance at high P_T/σ^2 values, single RS scheme outperforms MRT scheme at low P_T/σ^2 values especially as total number of relays increases.

Fig. 6.4 demonstrates numerical results of OP for GSTDP, where approximated and asymptotic OPs are obtained from (6.28) and (6.23), respectively. The curves are plotted for $L \in \{1, 2, 3\}$, $L_c \in \{1, 3\}$, threshold $\gamma_{\text{th}} = 6$ dB, and $(\kappa_l, \vartheta_l) \in \{(10^{-10}, 0), (1, 0.2)\}$. The adopted approximation curves coincide with the simulation ones. At high P_T/σ^2 regime, the overlap among approximated, asymptotic, and simulation curves is nearly perfect. While considering the two upper curves, as expected, HD one outperforms FD one and the gain in P_T/σ^2 is more than 3 dB at an OP value of 10^{-6}. This result is valid

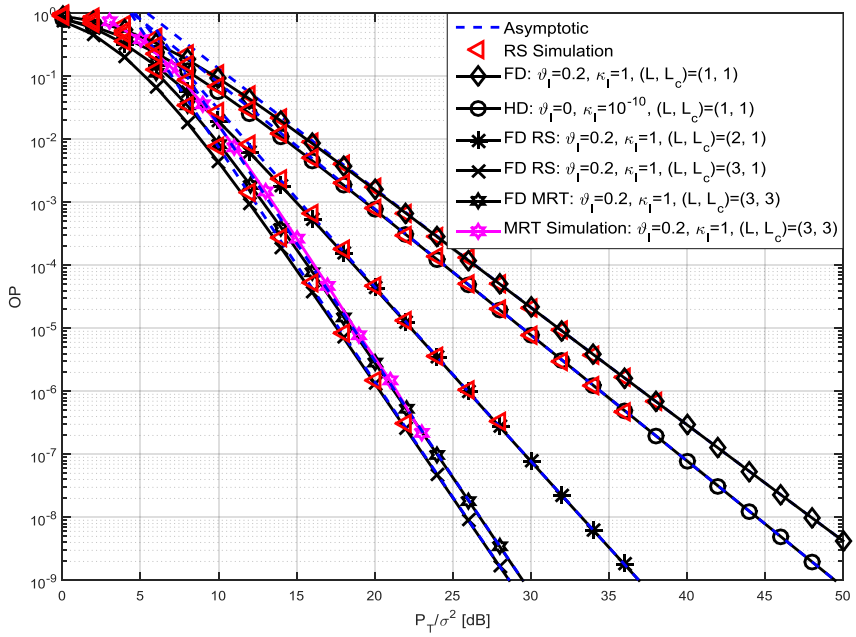

Figure 6.4: OP of GSTDP.

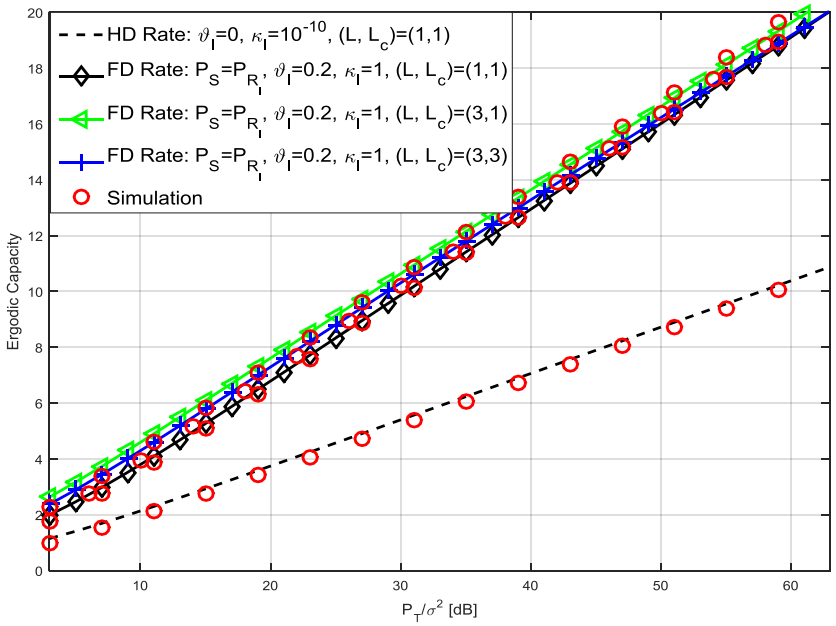

Figure 6.5: Ergodic capacity of GSTDP.

for equal thresholds but not for equal data rates. For equal data rates, the SINR threshold of HD transmission can be obtained as $\frac{1}{2}\log_2(10^{\gamma_{\text{th}}^{HD}/10}+1) = 2.32$ bits/s/Hz, therefore, $\gamma_{\text{th}}^{HD} = 10 \times \log_{10}(2^{4.64}-1) = 13.73$ dB, which means the HD curve shift towards right and its performance becomes worse. The diversity orders, from upper to lower curves, are 1.8, 2, 2.6, 3.4, and 3.4, respectively. For single RS, the gains in P_T/σ^2 at an OP value of 10^{-6} with respect to the curve $(L, L_c) = (1, 1)$ are about 11 dB and 17 dB for the curves $(L, L_c) = (2, 1)$ and $(L, L_c) = (3, 1)$, respectively. Considering the two lower curves, unlike multi-antenna case, there is no gain in P_T/σ^2 when all the relays are used as compared to single RS case.

Fig. 6.5 verifies the ergodic capacity expression given in (6.38), i.e., ergodic capacity of GSTDP. The curves are provided for $(\kappa_l, \vartheta_l) \in \{(10^{-10}, 0), (1, 0.2)\}$, $L \in \{1, 3\}$, $L_c \in \{1, 3\}$. The ratios between the achievable rates of FD cases and rate of HD case with $(L, L_c) = (1, 1)$ at $P_T/\sigma^2 = 49.01$ dB from upper curve to lower one are about 1.91, 1.86, and 1.84. The theoretical value of ratios between the achievable rates is 2, however, these values are not reachable in practice due to SI effect as illustrated. Furthermore, using all the relays does not provide any gain as in OP.

Fig. 6.6 plots SERs of GSTDP using QPSK for FD transmission and 16-PSK for HD transmission, where $(\kappa_l, \vartheta_l) = (1, 0.2)$ for FD transmission, $(\kappa_l, \vartheta_l) = (10^{-10}, 0)$ for HD transmission, $L \in \{1, 3, 4\}$, and $L_c \in \{1, 3, 4\}$. The exact and asymptotic curves are obtained from (6.30), (6.33) and (6.35), respectively. Choice of QPSK for FD transmission and 16-PSK for HD transmission is necessary for a fair comparison, which results in the

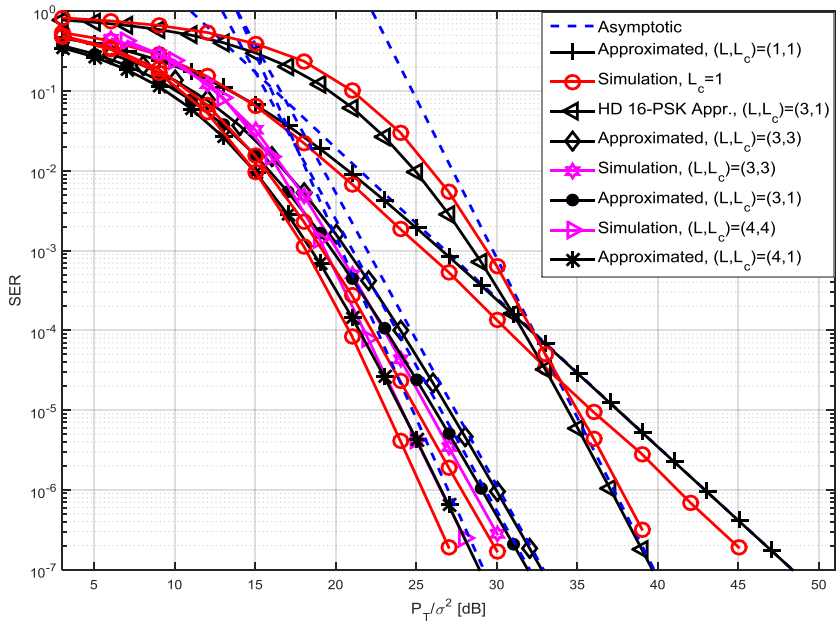

Figure 6.6: SERs of GSTDP.

same data rate. The distances between the nodes are selected as $d_{SR_l} = d_{R_lD} = 1$ and $d_{SD} = 2$. The approximated and asymptotic curves of $(L, L_c) = (4, 4)$ are not provided for the sake of figure clarity, since their behavior is the same as those of $(L, L_c) = (3, 3)$. Approximated results follow the simulation ones. For FD transmission, the gains in P_T/σ^2 with respect to single relay case, i.e., $(L, L_c) = (1, 1)$ for 3 and 4 total number of relays, i.e., $(L, L_c) = (3, 1)$ and $(L, L_c) = (4, 1)$ are about 14 dB and 16 dB at a SER value of 10^{-6}, respectively. To observe the diversity order of FD transmission, one can consider the SER values at 23 dB and 29 dB for $(L, L_c) = (3, 1)$, which are about 10^{-4} and 10^{-6}. Therefore, the slope is about $2/0.6 \approx 3.33$ which coincides with the nominal slope, namely, $L \times (1 - \vartheta_l) + 1 = 3 \times (1 - 0.2) + 1 = 3.4$. SER of HD transmission, i.e, 16-PSK, is only plotted for $(L, L_c) = (3, 1)$. At a SER value of 10^{-6}, the gain in P_T/σ^2 obtained by FD transmission with respect to HD transmission is 8 dB. For $P_T/\sigma^2 = 25$ dB, SER of FD transmission is 2×10^{-5} but HD SER is just 10^{-2}. Note that FD transmission outperforms HD transmission significantly for equal data rates, and with respect to single relay case, significant performance gains are obtained for FD transmission as the number of relays increases.

6.6. Conclusion

In this chapter, two extreme cases of GST (opportunistic RS and conventional relaying, i.e., MRT) over i.i.d. (i.n.i.d.) non-selective Rayleigh fading channels are investigated in (non-)existence of a DP between the source and the destination for an FD AF multi-relay cooperative-diversity system. RS or MRT is applied at the FD relays and the rake receiver with MRC is used to overcome with the problem of co-phasing and merging of the received signals at the destination when DP exists. The proposed robust approximations of PDF and CDF for dual-hop link with FD relay facilitate OP and SER analyses of GST for FD AF multi-relay cooperative-diversity systems. Additionally, ergodic capacity of the considered system is also analyzed over i.i.d. channels. Furthermore, SI effect on diversity order is revealed and all analytic findings are verified via Manto-Carlo simulation technique. Also, as compared to single relay case significant performance gains are achieved by RS and MRT, which have close performance. Although MRT provides worse performance than RS, it does not need searching and any feedback, thus keeps its performance in case of any feedback error. Numerical results reveals that substantial reduction in SER can be reached by FD transmission as compared to HD one for equal rates.

6.7. CDF and PDF Derivations of $S - R_i - D$ Link

Using [55, eq. (B.1)], the CDF of the $S - R_i - D$ link can be expressed as

$$F_{\gamma_{SR_iD}}(\gamma_{\text{th}}) = 1 - \int_0^\infty \int_{\gamma_{\text{th}}}^\infty \Big(1 - F_{\gamma_{S_i}}(\eta)\Big) f_{\gamma_{D_i}}(x) f_{\gamma_{R_i}}(y) dx dy \tag{6.40}$$

where $\eta = \frac{\gamma_{\text{th}}(x+1)(y+1)}{x-\gamma_{\text{th}}}$. For Rayleigh fading channels, CDFs and PDFs of SNRs (γ_{S_i} and γ_{D_i}) and INR (γ_{R_i}) are

$$\begin{aligned} f_{\gamma_{\zeta_i}}(x) &= \lambda_{\zeta_i} e^{-\lambda_{\zeta_i} x} \\ F_{\gamma_{\zeta_i}}(x) &= 1 - e^{-\lambda_{\zeta_i} x} \end{aligned} \tag{6.41}$$

where $\zeta \in \{S, D, R\}$, $\lambda_{S_i} = \frac{\sigma_{R_i}^2}{P_S \Omega_{S_i}}$, $\lambda_{D_i} = \frac{\sigma_D^2}{P_{R_i} \Omega_{D_i}}$, and $\lambda_{R_i} = \frac{\sigma_{R_i}^2}{P_{R_i} \Omega_{R_i}}$. Ω_{ζ_i}s are the variances of the corresponding channels, defined as $\Omega_{D_i} = (1 - d_f)^{-\alpha}$, $\Omega_{S_i} = d_f^{-\alpha}$, $0 < d_f < 1$, α is path loss factor, and d_f is the distance between the S and each relay. For the sake of simplicity, we use d_f as if all the relays are approximately at the

same point. We let $\Omega_{R_i} = \kappa_i P_{R_i}^{\vartheta_i - 1}$ where $0 \leq \kappa_i, \vartheta_i \leq 1$. κ_i and ϑ_i are linear and exponential attenuation/cancellation factors demonstrating dependence of SI variance on the transmitted relay power [103–105].

Inserting (6.41) in (6.40) results in

$$F_{\gamma_{SR_iD}}(\gamma_{\text{th}}) = 1 - \frac{\lambda_{D_i}\lambda_{R_i} e^{-(\lambda_{D_i}+\lambda_{S_i})\gamma_{\text{th}}}}{\lambda_{R_i} + \lambda_{S_i}\gamma_{\text{th}}} \int_0^\infty \left(1 - \frac{\frac{\lambda_{S_i}\gamma_{\text{th}}(\gamma_{\text{th}}+1)}{\lambda_{R_i}+\lambda_{S_i}\gamma_{\text{th}}}}{z + \frac{\lambda_{S_i}\gamma_{\text{th}}(\gamma_{\text{th}}+1)}{\lambda_{R_i}+\lambda_{S_i}\gamma_{\text{th}}}}\right) e^{-\frac{\lambda_{S_i}\gamma_{\text{th}}(\gamma_{\text{th}}+1)}{z} - \lambda_{D_i} z} dz \tag{6.42}$$

The same result is derived in [122, eq. (15)] where the number of random variables in SINR expression is reduced from three to two by defining an intermediate random variable. We ignore the rational term inside the integral in (6.42), which means the integral stemming from this term is omitted, use identity [65, eq. (3.324)] and then get

$$F_{\gamma_{SR_iD}}(\gamma_{\text{th}}) \approx 1 - \frac{2\lambda_{R_i}\sqrt{\lambda_{D_i}\lambda_{S_i}\gamma_{\text{th}}(\gamma_{\text{th}}+1)}}{\lambda_{R_i} + \lambda_{S_i}\gamma_{\text{th}}} e^{-(\lambda_{D_i}+\lambda_{S_i})\gamma_{\text{th}}} K_1\left(2\sqrt{\lambda_{D_i}\lambda_{S_i}\gamma_{\text{th}}(\gamma_{\text{th}}+1)}\right), \tag{6.43}$$

where $K_1(x)$ is the first-order modified Bessel Function of the second kind [65, eq. (8.407)], which is available in well known software programs such as MATHEMATICA and MAPLE.

Derivative of (6.42) with respect to γ_{th} gives the PDF of γ_{SR_iD} as in (6.44) and using the same reasons as in the derivation of approximated $F_{\gamma_{SR_iD}}(\gamma_{\text{th}})$, $f_{\gamma_{SR_iD}}(\gamma_{\text{th}})$ reduces to (6.45).

$$\begin{aligned} f_{\gamma_{SR_iD}}(\gamma_{\text{th}}) = {} & \lambda_{D_i}\lambda_{R_i} e^{-(\lambda_{D_i}+\lambda_{S_i})\gamma_{\text{th}}} \int_0^\infty \frac{((\lambda_{D_i}+\lambda_{S_i})z + \lambda_{S_i}(2\gamma_{\text{th}}+1))}{\lambda_{S_i}\gamma_{\text{th}}(\gamma_{\text{th}}+1) + (\lambda_{R_i}+\lambda_{S_i}\gamma_{\text{th}})z} \\ & e^{-\frac{\lambda_{S_i}\gamma_{\text{th}}(\gamma_{\text{th}}+1)}{z} - \lambda_{D_i} z} dz \\ & + \lambda_{D_i}\lambda_{R_i}\lambda_{S_i} e^{-(\lambda_{D_i}+\lambda_{S_i})\gamma_{\text{th}}} \int_0^\infty \frac{z(2\gamma_{\text{th}}+z+1)\, e^{-\frac{\lambda_{S_i}\gamma_{\text{th}}(\gamma_{\text{th}}+1)}{z} - \lambda_{D_i} z}}{(\lambda_{S_i}\gamma_{\text{th}}(\gamma_{\text{th}}+1) + (\lambda_{R_i}+\lambda_{S_i}\gamma_{\text{th}})z)^2} dz \end{aligned} \tag{6.44}$$

and

$$\begin{aligned} f_{\gamma_{SR_iD}}(\gamma_{\text{th}}) \approx {} & \frac{2\lambda_{R_i}(\lambda_{D_i}+\lambda_{S_i})\sqrt{\lambda_{D_i}\lambda_{S_i}\gamma_{\text{th}}(\gamma_{\text{th}}+1)}}{\lambda_{R_i}+\lambda_{S_i}\gamma_{\text{th}}} e^{-(\lambda_{D_i}+\lambda_{S_i})\gamma_{\text{th}}} \\ & K_1\left(2\sqrt{\lambda_{D_i}\lambda_{S_i}\gamma_{\text{th}}(\gamma_{\text{th}}+1)}\right) + \frac{2\lambda_{S_i}\lambda_{R_i}\sqrt{\lambda_{D_i}\lambda_{S_i}\gamma_{\text{th}}(\gamma_{\text{th}}+1)}}{(\lambda_{R_i}+\lambda_{S_i}\gamma_{\text{th}})^2} \\ & e^{-(\lambda_{D_i}+\lambda_{S_i})\gamma_{\text{th}}} K_1\left(2\sqrt{\lambda_{D_i}\lambda_{S_i}\gamma_{\text{th}}(\gamma_{\text{th}}+1)}\right). \end{aligned} \tag{6.45}$$

Considering the fact that as $x \to 0^+$, $e^{-x} \approx 1$ and $K_1(x) \approx \frac{1}{x}$, asymptotic PDF and CDF of γ_{SR_iD} are obtained as

$$\begin{aligned} f^{\infty}_{\gamma_{SR_iD}}(\gamma_{\text{th}}) &\approx \frac{(\lambda_{D_i}+\lambda_{S_i})\,\lambda_{R_i}}{\lambda_{R_i}+\lambda_{S_i}\gamma_{\text{th}}} + \frac{\lambda_{S_i}\lambda_{R_i}}{(\lambda_{R_i}+\lambda_{S_i}\gamma_{\text{th}})^2} \\ F^{\infty}_{\gamma_{SR_iD}}(\gamma_{\text{th}}) &\approx 1 - \frac{\lambda_{R_i}}{\lambda_{R_i}+\lambda_{S_i}\gamma_{\text{th}}} \end{aligned} \quad . \tag{6.46}$$

The SINR of the single branch in (6.4) can be rephrased as

$$\gamma_{SR_iD} = \frac{\gamma_{D_i}\frac{\gamma_{S_i}}{\gamma_{R_i}+1}}{\gamma_{D_i}+\frac{\gamma_{S_i}}{\gamma_{R_i}+1}+1} < \frac{\gamma_{D_i}\frac{\gamma_{S_i}}{\gamma_{R_i}+1}}{\gamma_{D_i}+\frac{\gamma_{S_i}}{\gamma_{R_i}+1}} = \frac{1}{\frac{1}{\gamma_{D_i}}+\frac{\gamma_{R_i}+1}{\gamma_{S_i}}}. \tag{6.47}$$

This representation means the γ_{SR_iD} is upper bounded by a random variable, which is harmonic mean of two other random variables. Approximating the PDF of a random variable, which is expressed as a harmonic mean of exponential random variables, as an exponential random variable is previously discussed in [1, eq. (46)] and thereafter, this result is used in [48, 142]. Although the expression of γ_{SR_iD} is not simply a harmonic mean of exponential random variables, it is a bit more complicated, but we can still assume that it can be approximated as an exponential random variable at high SINRs. We focus on the high SINR region and the asymptotic PDF derived in (6.46) where $f^{\infty}_{\gamma_{SR_iD}}(0) = \frac{(\lambda_{D_i}+\lambda_{S_i})\lambda_{R_i}+\lambda_{S_i}}{\lambda_{R_i}}$. Considering this equality with exponential approximation assumption facilitates the problem since PDF of an exponential random variable can only be characterized by its expected value, namely, by its value at zero. Moreover, we define the right hand side of (6.47) as $\gamma^{\text{up}}_{SR_iD}$ and its inverse is

$$\frac{1}{\gamma^{\text{up}}_{SR_iD}} = \frac{1}{\gamma_{D_i}} + \frac{1}{\gamma_{S_i}} + \frac{\gamma_{R_i}}{\gamma_{S_i}}. \tag{6.48}$$

On the other hand, it is well known that the expected value of inverse of an exponential random variable γ_{ζ_i} can be expressed as $\frac{\int_0^{\infty} e^{-x}/x dx}{\mathbb{E}[\gamma_{\zeta_i}]}$, where $\mathbb{E}[\cdot]$ is expected value operator. So, if we assume $\gamma^{\text{up}}_{SR_iD}$ can be approximated as an exponential random variable, we should have $\mathbb{E}[1/\gamma^{\text{up}}_{SR_iD}] = \frac{\int_0^{\infty} e^{-x}/x dx}{E[\gamma^{\text{up}}_{SR_iD}]} = \frac{\int_0^{\infty} e^{-x}/x dx}{E[\gamma_{D_i}]} + \frac{\int_0^{\infty} e^{-x}/x dx}{E[\gamma_{S_i}]} + \frac{\int_0^{\infty} e^{-x}/x dx E[\gamma_{R_i}]}{E[\gamma_{S_i}]}$. Therefore, we get $\frac{1}{E[\gamma^{\text{up}}_{SR_iD}]} = \lambda_{D_i} + \lambda_{S_i} + \frac{\lambda_{S_i}}{\lambda_{R_i}}$. Using this fact together with equality $\frac{1}{E[\gamma^{\text{up}}_{SR_iD}]} = f^{\infty}_{\gamma_{SR_iD}}(0)$, the equivalent PDF and CDF of γ_{SR_iD} can be approximated as

$$\begin{aligned} f^{Eq}_{\gamma_{SR_iD}}(\gamma_{\text{th}}) &= \lambda_{Eq_i} e^{-\lambda_{Eq_i}\gamma_{\text{th}}} \\ F^{Eq}_{\gamma_{SR_iD}}(\gamma_{\text{th}}) &= 1 - e^{-\lambda_{Eq_i}\gamma_{\text{th}}} \end{aligned} \quad , \tag{6.49}$$

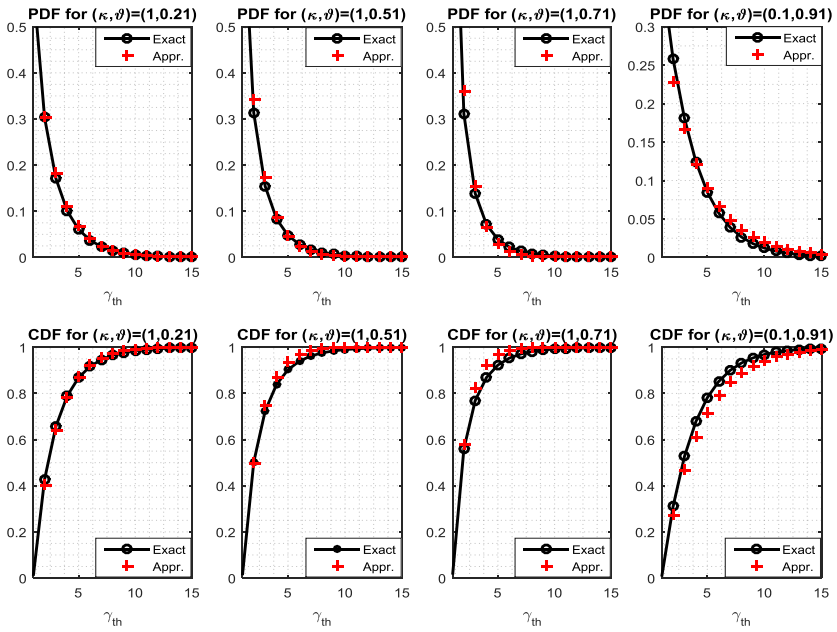

Figure 6.7: Exact and approximated PDF and CDF of a dual-hop link with FD relay.

where $\lambda_{Eq_i} = \frac{(\lambda_{D_i}+\lambda_{S_i})\lambda_{R_i}+\lambda_{S_i}}{\lambda_{R_i}} \leq 1$. Fig. 6.7 illustrates three different examples of this approximation, where $P_S = P_{R_i} = P_T/2 = 5$, $\alpha = 0$, $\sigma_{R_i} = \sigma_D = \Omega_{S_i} = \Omega_{D_i} = 1$, $\kappa \in \{0.1, 1\}$, and $\vartheta \in \{0.21, 0.51, 0.71, 0.91\}$. The exact and approximated results are produced by (6.42) and (6.44), and (6.49), respectively. It is shown that a value of 0.21 for ϑ can be reached after active analog SI cancellation and a value of 0.12 can be obtained after a combined active analog and digital cancellation [103]. As the exponential attenuation/cancellation factor ϑ increases, the success of our approximation decreases but, especially at high SINRs, OPs are calculated at low γ_{th} values, where the match between the exact and approximated CDF values is nearly excellent. Finally, usage of small exponential attenuation/cancellation factors ϑ together with the small values of linear attenuation/cancellation factors κ increases robustness of the proposed approximation since contribution of SI on the SINR decreases.

7. RELAY SELECTION FOR NOMA BASED COOPERATIVE NETWORKS OVER NAKAGAMI-*m* FADES

7.1. Introduction

Effective resource utilization of the communication resources such as latency, power and spectrum are essential and critical issues that should be handled out carefully. A promising technique to satisfy massive connectivity, low latency, and high spectral efficiency for the fifth generation (5G) and beyond networks is non-orthogonal multiple access (NOMA), which also achieves higher user fairness [12–15, 143, 144]. In NOMA, all resource blocks, i.e., non-orthogonal resources can be used by each user; therefore, as compared to traditional orthogonal multiple access (OMA) techniques where available resource blocks are occupied separately, spectrum efficiency is improved [143, 145]. Application of NOMA can be implemented in different domains such as code and power domains or mixed of them [16], where superposed signals can be simultaneously received (up-link NOMA) or transmitted (down-link NOMA). In code domain, a unique spreading code is assigned to each user, similarly, a portion of the total power is assigned to each user in power domain. Successive interference cancellation (SIC) is used to separate the superposed signals. However, due to the limited processing power at the end users, power domain NOMA seems to be the dominant choice and gain more attention in the literature: Two different power allocation (PA) strategies, namely, assigning more power to the users having poor channel conditions or allocating power in accordance with quality of service (QoS) requirements, where PA factors may be independent of channel state information (CSI) or not. Considering CSI during PA means always assigning more power to the user facing worse fading, on the other hand, more power is assigned to a user with QoS priority where CSI is not considered.

Cooperative NOMA is first introduced in [143] for a system consisting of multiple-users and a base station (BS) over Rayleigh fading channels, where less power is allocated to the users with better channel conditions. Each user applies SIC and decodes its signal and thereafter, they share decoded signals via short range communication channels to avoid use of extra time slots. Since cooperative relaying networks (CRN) extend coverage area, consume less power, and improve reliability and security; their application on NOMA based transmission systems over many fading environment and forwarding

protocols, namely, amplify/decode-and-forward (AF/DF) protocols with both half-duplex (HD) and full-duplex (FD) relays has been deeply investigated in terms of ergodic capacity and outage probability (OP) with adaptive and fixed PAs [41–48, 146–159]. Contrary to OMA based systems [56,122], opportunistic relay selection (RS) is not possible for NOMA based systems due to the fact that at least two users are served and a single selected relay can not enhance reliability for all users. Therefore, other approaches such as sub-optimum [45, 47, 152], buffer-aided [149], partial [46, 153], and multi-level (two-stage) [41–43, 48] RS schemes are offered and analyzed. Sub-optimum selection strategies are based on conventional max-min criterion, partial relay selection (PRS) strategies are based on selecting a relay with the maximum channel gain between the source (BS) and relays, two stage RS (TSRS) schemes are based on selecting a relay from a predetermined subset of relays realizing an assigned condition such as priority of a user or sum of users' data rates, which has also been proposed for OMA based physical layer security [38–40,160,161]. RS in case of buffer-aided transmission is done in accordance with a number of predetermined conditions where not only relay link between the BS and relay providing target data rate but also transmission mode (NOMA, time-division-multiple-access) is also selected, which only implements downlink NOMA in the second hop (between the selected relay and users) [149]. Additionally, TSRS scheme with the condition that at least N relays should be in the predetermined subset is known as N^{th} best RS scheme [151]. Without loss of generality, hereinafter, we use the term CRN to emphasize a cooperative relaying network consisting of a BS, multiple-relays, and two end users (destinations).

In [47], a sub-optimum RS based on max-min criterion for a CRN with HD relays is offered over non-selective Rayleigh fade but the implementation is like FD relaying operation except that the selected relay is not used in the subsequent transmission but a relay is selected from the remaining set, where all the relays keep receiving transmitted signals of the BS during broadcasting time slot of the selected relay. Therefore, self (loop)-interference (SI) effect is eliminated but inter-relay interference due to previously selected relay is not taken into account and it is not possible to conceal out this interference as in FD relaying. By implementing fixed PA policy and giving priority to the far user, OP and ergodic sum rate are analyzed. The proposed selection method outperforms existing HD RS schemes but due to FD operation, comparisons are not fair. A comprehensive comparison with FD RS schemes will complete the analysis of proposed RS method. Another, sub-optimum RS using max-min strategy is investigated for a two-way transmission system consisting of two pairs of NOMA users exchanging data via multiple relays by implementing the downlink and uplink NOMA protocols [152]. OP

performance is illustrated together with hardware impairments for fixed power factors and slow Rayleigh fading environment, where DF relays are used.

Conventional max-min (sub-optimum) RS and TSRS schemes are introduced and compared for a CRN over slow Rayleigh fading channels to select an HD DF relay in [41]. In this work, users are not ordered by their CSI but rather categorized by QoS requirements, i.e., fixed PA is used and priority is given to user 1. Firstly an HD subset of relays guaranteeing user 1's target data rate at all nodes (relay, user 1, and user 2) is determined and thereafter, a relay maximizing data rate of user 2 is determined. OP is analyzed and it is proven that offered TSRS scheme outperforms conventional max-min RS scheme. A similar system is considered in [42] and a slightly different condition is assigned to determine the subset of HD AF/DF relays: The set of relays realizing data rate of both users at relays and user 1 are determined, i.e., subset of relays satisfies QoS requirements of user 1 is detected and then, the best relay is selected out of this subset to serve user 2, where realization of data rate of user 1 at user 2 is not ensured. The results demonstrate that offered selection criterion has better performance as compared to previous works. In [45], two TSRS strategies termed as two-stage weighted–max–min (WMM) and max–weighted–harmonic–mean (MWHM), are proposed for cooperative NOMA with fixed and adaptive PAs at the relays, respectively. Since NOMA is only applied in the second hop, in the first hop a coded message including data of both users is transmitted so no need of SIC at the relay, relay-subset is determined based on the relays achieving sum data rate of two users. The results demonstrate that the proposed RS schemes outperform the existing TSRS schemes. OP of another different TSRS strategy is studied in [154], where PAs are dynamically done in accordance with poorness of CSI, i.e., more power is allocated to the poor link between the relay and users. Relay subset is determined by taking the sum of data rates as a threshold, where a relay is in the selected subset if its capacity is larger than or equal to sum of the data rates but additionally, QoS priority for user 1 is also ensured. Similar to the work in [45], the considered CRN has multiple HD DF relays and the BS transmitting a superposed signal produced by Gray mapping based joint-modulation [162] so that both users' messages can be decoded simultaneously without the complicated SIC. Besides, such a coding strategy also leads to lower OP than superposition coding at the relays. Furthermore, nearly the same TSRS scheme is simultaneously investigated in spatially random CRN over non-selective block Rayleigh fading with fixed PAs and QoS requirement for user 1 and the same condition is applied to determine relay subset in [43,48] except that work in [43] considers DF HD/FD relays but that of [48] focuses on DF/AF HD relays. A critical issue that should be pointed

out is the dilemma of zero/non-zero diversity order between these two works; non-zero diversity order for HD transmission is claimed in the former one but zero-diversity order is in the later one. In the context of this work, the reason for that dilemma is also clarified. Finally, physical-layer security based on NOMA protocol is also deeply examined as OMA counterpart based on TSRS schemes in [155–159].

In this chapter, two different relay selection schemes, namely, single-stage relay selection (SSRS) and TSRS strategies in accordance with service quality priority are applied to a system consisting of two sources and two users (destinations) over independent non-identically distributed (i.n.i.d.) slow Nakagami-m fading channels. A single relay using DF is selected out of a set of FD/HD multiple relays in accordance with the quality of service criterion, where first user is assumed to have service priority. Both perfect SIC (pSIC) and imperfect SIC (ipSIC) situations are considered. For practical approaches, it is reasonable and more comprehensive to investigate such systems over Nakagami-m fading channel since it covers many fading environments such as Rayleigh and Rician. Moreover, pSIC is difficult to achieve in practical applications, i.e., not possible in reality, therefore, ipSIC should be analyzed to shed light on such communication systems.

7.1.1. Contributions

The main contributions of this chapter can be summarized as follows:

- Exact and asymptotic OP expressions for both RS strategies, namely, SSRS for the user 1 and TSRS for the user 2 are derived over i.n.i.d. slow Nakagami-m fading channels with not only pSIC but also ipSIC, and their validity is verified via Monte Carlo simulation technique. Unlike existing works, our expressions are unique and valid for all cases such as FD and HD together with pSIC and ipSIC, i.e., expressions are not given separately but in a single compact form.
- At the high signal-to-noise (SNR), asymptotic expression of SSRS explicitly reveals that throughput is almost not affected by PA factors at the selected relay and characteristics (shaping and scaling factors) of the channels among the selected relay and the two end users. However, it is dominated by PA factors at the sources and characteristics of the channels among the sources and selected relay and that of SI channel for FD transmission. For TSRS scheme, previously mentioned deductions are also valid for pSIC case but characteristics of the channel between the selected relay and user 2 and ipSIC at user 2 become effective on throughput when ipSIC

takes place. Additionally, characteristics of ipSIC at the selected relay are also other substantial factors dominating throughput at the high SNR.

- Optimum relay location for many scenarios consisting of different PA factors, data rates, SIs for FD transmission, total transmitted powers, and ipSIC at the relays / user 2 are handled out and illustrated. The results demonstrate that relay location changes toward to the second source for FD transmission to eliminate SI effect and toward to the first source for HD transmission to eliminate SIC effect.
- Modeling of SI variance as $\kappa_l P_{R_i}^{\vartheta_l - 1}$, where κ_l and ϑ_l are linear and exponential cancellation/attenuation factors depicting dependence of SI on the transmitted power, P_{R_i}, from each relay and both vary between 0 and 1, allows to individually investigate effect of SIC, SI, and ipSIC on error floors.
- At high SNR regions, signal-to-interference-plus-noise ratios (SINRs) approach constant values, in turn, error floors, i.e., equal probabilities occur for the communication systems using NOMA or FD protocol where SI power is only linearly dependent on transmitted power. Therefore, dividing logarithm of the error (OP or symbol error rate (SER)) by logarithm of transmitted power or SNR and then letting power or SNR approach to infinity causes limit of this ratio to be zero, which is commonly accepted as zero-diversity order. Actually, treating the slope of log – log plot as diversity order is a common myth based on the work of Wang and Giannakis, where even no diversity technique is used, slope of log – log plot is considered as diversity order for Nakagami-m fade [82, eq. (6)]. The diversity order is the number of independent paths between the source and destination, i.e., number of independent scaled copies of a transmitted signal arriving to the destination but not the slope of the log – log plot which is just only valid over Rayleigh fading channels for HD/FD transmission over Rayleigh fading channels, where SI variance dependence on transmitted power is assumed to be exponentially. But this approach is not suitable to determine diversity order of HD analysis of this work. To be more precise, a robust and comprehensive solution has already been offered but does not attract attention in recent researches, especially on those of FD and NOMA based transmission systems [163, eq. (1)], where diversity order is determined by comparing probabilities for the system with a diversity technique and that without any diversity technique. It is worth noting that diversity order and independent number of channels are not always corresponding to each other [164].

The remainder of this chapter is organized as follows. In Section 7.2, details of system model are provided. RS criteria are provided in Section 7.3. Section 7.4 includes

derivations of approximated and asymptotic OP. Numerical results are detailed in Section 7.5. Finally, we conclude our work in Section 7.6.

7.2. System Model

We consider a multiple relay system with two sources and two users as depicted in Fig. 7.1. Due to deep fading and shadowing, no direct link is assumed among the sources (S_1 ve S_2) and users (D_1 ve D_2) and the communication is conducted via L FD/HD multi-relays with DF protocol. The information signals are assumed to have unit energy. A relay is selected to provide service quality priority for the user 1, D_1. The transmission from the sources to the selected relay and from the selected relay to the users is done via uplink and downlink NOMA, respectively. Without loss of generality, relays are assumed to be clustered such that they are at the origin of the cartesian system and have equal distance to each node. Position of each node, the sources and users is represented as (x_j, y_j), $j \in \{S_1, S_2, D_1, D_2\}$ with respect to this origin. To investigate the best relay location, the assumed origin is kept fixed and positions of relays are denoted as $\left(x_{R_i}, y_{R_i}\right) = \left(r\cos(\theta), r\sin(\theta)\right)$. Whereby, distance between the node j and relays is $d_{jR_i} = \sqrt{(x_j - r\cos(\theta))^2 + (y_j - r\sin(\theta))^2}$. As in [165], the sources are assumed to collaborate for PA. The PA coefficients at the S_1 and S_2 are represented as a_1 and a_2, where $a_1 + a_2 = 1$ and $a_1 > a_2$. Similarly, after DF process at the selected relay, detected signals are weighted in accordance with the service quality priority by PA coefficients a_3 and a_4, where $a_3 + a_4 = 1$ and $a_3 > a_4$. The relays are equipped with one transmit and one receive antennas. All channel gains are assumed to have Nakagami-m distribution. Therefore, square amplitudes of channel gains are Gamma distributed. The channel gains of the links S_1—i^{th} relay, S_2—i^{th} relay, i^{th} relay—D_1, i^{th} relay—D_2, ipSIC at the i^{th} relay, ipSIC at the D_2, and SI are g_{S_i}, h_{S_i}, $g_{R_{i1}}$, $h_{R_{i2}}$, $\tilde{g}_{S_i}$, $\tilde{h}_{R_{i2}}$ and $h_{R_iR_i}$, respectively. The shape and scale parameters of the stated links are $(m_{S_{1i}}, \Omega_{S_{1i}} = \Omega^0_{S_{1i}} d^{-\alpha}_{S_1R_i})$, $(m_{S_{2i}}, \Omega_{S_{2i}} = \Omega^0_{S_{2i}} d^{-\alpha}_{S_2R_i})$, $(m_{D_{1i}}, \Omega_{D_{1i}} = \Omega^0_{D_{1i}} d^{-\alpha}_{R_iD_1})$, $(m_{D_{2i}}, \Omega_{D_{2i}} = \Omega^0_{D_{2i}} d^{-\alpha}_{R_iD_2})$, $(\tilde{m}_{R_i}, 1)$, $(\tilde{m}_{D_{2i}}, 1)$, and $(m_{R_iR_i}, \Omega_{R_iR_i}\kappa_l P_{R_i}^{\vartheta_l - 1})$, respectively, where α is path loss exponent. Terms with superscript 0 in the definition of scale parameters represent values where distances among nodes are not considered or taken to be 1. Total power at the sources and i^{th} relay are P_S and P_{R_i}, respectively.

The received signal at the i^{th} relay, by omitting time indexing for the sake of the simplicity, is

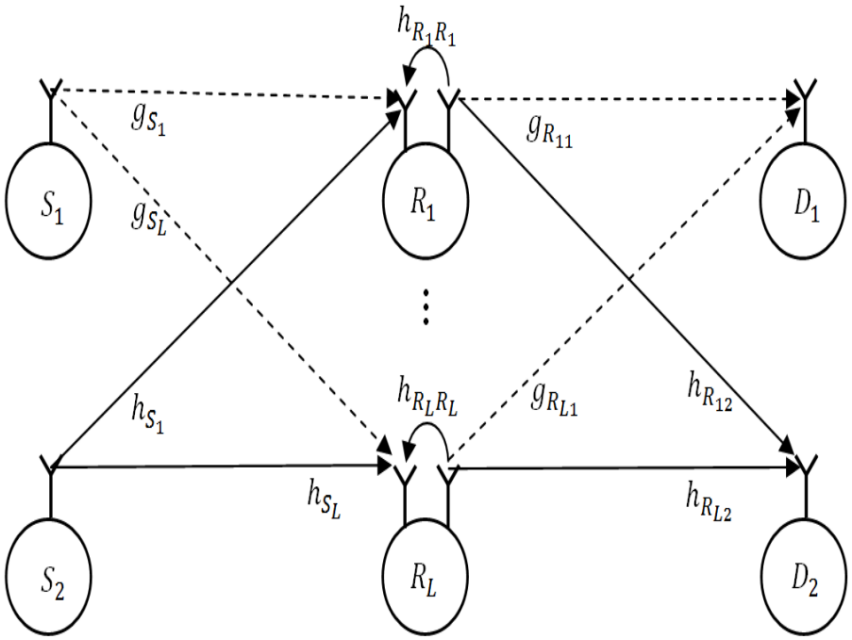

Figure 7.1: Multi-relay system.

$$Y_{R_i} = \sqrt{a_1 P_S} g_{S_i} x_1 + \sqrt{a_2 P_S} h_{S_i} x_2 + \varpi_i h_{R_i R_i} x_{R_i} + n_{R_i}, \tag{7.1}$$

where $x_{R_i} = \sqrt{a_3 P_{R_i}} \hat{x}_1 + \sqrt{a_4 P_{R_i}} \hat{x}_2$, $\hat{x}_1$ and $\hat{x}_2$ are previously decoded signals by SIC process. ϖ_i is 0 for HD and 1 for FD transmission. n_{R_i} is the additive Gaussian noise at the relay i. Decoded signals are weighted in accordance with the service quality priority and retransmitted. SINR related to the signal of the first source at the i^{th} relay is

$$\gamma_{D_1}^{R_i} = \frac{a_1 \rho_{S_i} |g_{S_i}|^2}{a_2 \rho_{S_i} |h_{S_i}|^2 + \varpi_i \rho_{R_i} |h_{R_i R_i}|^2 + 1}, \tag{7.2}$$

where $\rho_{S_i} = \frac{P_S}{\sigma_{R_i}^2}$, $\rho_{R_i} = \frac{P_{R_i}}{\sigma_{R_i}^2}$, and $\sigma_{R_i}^2$ is the variance of the additive Gaussian noise at the relay i. Absolute value operator is represented by $|\cdot|$. SINR related to the signal of the second source at the i^{th} relay is

$$\gamma_{D_2}^{R_i} = \frac{a_2 \rho_{S_i} |h_{S_i}|^2}{a_1 \epsilon_{R_i} \rho_{S_i} |\tilde{g}_{S_i}|^2 + \varpi \rho_{R_i} |h_{R_i R_i}|^2 + 1}, \tag{7.3}$$

where ϵ_{R_i} models the amount of the ipSIC at the i^{th} relay and $0 \leq \epsilon_{R_i} \leq 1$.

The received signals at the destinations are

$$Y_{D_1} = \sqrt{a_3 P_{R_i}} g_{R_{i1}} \hat{x}_1 + \sqrt{a_4 P_{R_i}} g_{R_{i1}} \hat{x}_2 + n_{D_1} \tag{7.4}$$

and

$$Y_{D_2} = \sqrt{a_3 P_{R_i}} h_{R_{i2}} \hat{x}_1 + \sqrt{a_4 P_{R_i}} h_{R_{i2}} \hat{x}_2 + n_{D_2}. \tag{7.5}$$

n_{D_1} and n_{D_2} are the additive Gaussian noise at the destinations. The SINR related to the first source at the user 1 is

$$\gamma_{D_{1i}}^{D_1} = \frac{a_3 \rho_{D_{1i}} |g_{R_{i1}}|^2}{a_4 \rho_{D_{1i}} |g_{R_{i1}}|^2 + 1}, \tag{7.6}$$

where $\rho_{D_{1i}} = \frac{P_{R_i}}{\sigma_{D_1}^2}$ and $\sigma_{D_1}^2$ is the noise variance at the user 1. Similarly, SINR related to the the first source at the user 2 is

$$\gamma_{D_{1i}}^{D_2} = \frac{a_3 \rho_{D_{2i}} |h_{R_{i2}}|^2}{a_4 \rho_{D_{2i}} |h_{R_{i2}}|^2 + 1}, \tag{7.7}$$

and SINR related to the second source at user 2 is

$$\gamma_{D_{2i}}^{D_2} = \frac{a_4 \rho_{D_{2i}} |h_{R_{i2}}|^2}{a_3 \epsilon_{D_2} \rho_{D_{2i}} |\tilde{h}_{R_{i2}}|^2 + 1}. \tag{7.8}$$

$\rho_{D_{2i}} = \frac{P_{R_i}}{\sigma_{D_2}^2}$, $\sigma_{D_2}^2$ is the variance of the noise at the user 2, ϵ_{D_2} models the amount of the ipSIC at the user 2 and $0 \leq \epsilon_{D_2} \leq 1$.

7.3. Relay Selection

RS is carried out in two different methods, namely SSRS and TSRS, as offered in [43].

SSRS is done by maximizing data rate of user 1 at the relay i and two users:

$$i_S = \arg\max_i \{\min\{\log(1+\gamma_{D_1}^{R_i}), \log(1+\gamma_{D_{1i}}^{D_1}), \log(1+\gamma_{D_{1i}}^{D_2})\}, i \in \{1, \cdots, L\}\}. \tag{7.9}$$

TSRS firstly determines a set of relays ensuring service quality for user 1 and then selecting a relay maximizing data rate of user 2. So the set of relays providing service quality priority condition is determined as follows:

$$K_R = \{\log(1+\gamma_{D_1}^{R_i}) \geq R_{D_1}, \log(1+\gamma_{D_1 i}^{D_1}) \geq R_{D_1}, \log(1+\gamma_{D_1 i}^{D_2}) \geq R_{D_1}\}, \quad i \in \{1, \cdots, L\}\}. \tag{7.10}$$

R_{D_1} is the data rate of the D_1. Then, the relay maximizing data rate of D_2 is found as

$$i_T = \arg\max_i \{\min\{\log(1+\gamma_{D_2}^{R_i}), \log(1+\gamma_{D_{2i}}^{D_2})\}, i \in K_R\}. \tag{7.11}$$

Since a decision is made on selected relay in (7.9), (7.10), and (7.11), the prefactor $1/2$, which does not have any impact on the selected relay, is omitted for HD transmission.

7.4. Outage Probability Analysis

OP of both selection strategies is given in this section.

7.4.1. Outage Probability of Single Stage Relay Selection

The OP of SSRS is (Please refer to Appendix A)

$$\begin{aligned} P_{SSRS}(\gamma_{th_1}) &= Pr(\min\{\gamma_{D_1}^{R_{i_S}}, \gamma_{D_{1i_S}}^{D_1}, \gamma_{D_{1i_S}}^{D_2}\} < \gamma_{th_1}) \\ &= \prod_{i=1}^{L}\Big(1 - Pr(R_i \in K_R)\Big), \end{aligned} \tag{7.12}$$

where $\gamma_{th_1} = 2^{2R_{D_1}} - 1$ for HD and $\gamma_{th_1} = 2^{R_{D_1}} - 1$ for FD. K_R represents the set of relays providing service quality priority expressed in (7.10), a relay in that set satisfies $\min\{\gamma_{D_1}^{R_i}, \gamma_{D_{1i}}^{D_1}, \gamma_{D_{1i}}^{D_2}\} > \gamma_{th_1}$ which is expressed as $R_i \in K_R$. Then, $Pr(R_i \in K_R)$ is

$$\begin{aligned} P_{R_i \in K_R}(\gamma_{th_1}) = {} & \frac{\Gamma\left(m_{D_{1i}}, \frac{m_{D_{1i}}\gamma_{th_1}}{\Omega_{D_{1i}}\rho_{D_{1i}}(a_3 - \gamma_{th_1}a_4)}\right)\Gamma\left(m_{D_{2i}}, \frac{m_{D_{2i}}\gamma_{th_1}}{\Omega_{D_{2i}}\rho_{D_{2i}}(a_3 - \gamma_{th_1}a_4)}\right)}{\Gamma(m_{D_{1i}})\Gamma(m_{D_{2i}})} e^{-\frac{m_{S_{1i}}\gamma_{th_1}}{a_1\rho_{S_{1i}}\Omega_{S_{1i}}}} \\ & \sum_{p_1=0}^{m_{S_{1i}}-1}\sum_{p_2=0}^{p_1}\sum_{p_3=0}^{p_2}\Bigg[\Bigg\{\left(\frac{m_{S_{1i}}\gamma_{th_1}}{a_1\Omega_{S_{1i}}}\right)^{p_1}\left(\frac{a_2\Omega_{S_{2i}}}{m_{S_{2i}}}\right)^{p_3}\binom{p_1}{p_2}\binom{p_2}{p_3}\Gamma(p_3 + m_{S_{2i}}) \\ & \Gamma(p_2 - p_3 + m_{R_i})\left(\frac{\varpi_i\rho_{R_i}\Omega_{R_iR_i}}{m_{R_i}}\right)^{p_2-p_3}\Bigg\}\Bigg/\Bigg\{\Gamma(m_{S_{2i}})\Gamma(m_{R_i})\Gamma(p_1+1) \\ & \left(1 + \frac{m_{S_{1i}}\gamma_{th_1}a_2\Omega_{S_{2i}}}{m_{S_{2i}}a_1m_{S_{1i}}}\right)^{m_{S_{2i}}+p_3}\left(1 + \frac{m_{S_{1i}}\gamma_{th_1}\varpi_i\rho_{R_i}\Omega_{R_iR_i}}{m_{R_i}a_1\rho_{S_i}\Omega_{S_{1i}}}\right)^{m_{R_i}+p_2-p_3}(\rho_{S_i})^{p_1-p_3}\Bigg\}\Bigg] \end{aligned} \tag{7.13}$$

At high SNRs, i.e, at high $\rho_{D_{1i}}$, $\rho_{D_{2i}}$, and ρ_{S_i}, asymptotic OP expression can be derived from (7.13) by considering the following facts:

- As $x \to 0$, $e^{-x} \to 1$ and $\gamma(m,x) \to x^m$. Small x values correspond to the high SNRs cases.
- At high SNRs, $(1/\rho_{S_i})^{p_1-p_3} \to 0$. Therefore, the only terms survive in the summations of (7.13) are the ones where $p_1 = p_3$, in turn, this equality means $p_1 = p_2 = p_3$.
- To observe effect of SI on OP at high SNRs, the term $\left(1+\frac{m_{S_{1i}}\gamma_{th_1}\varpi_i\rho_{R_i}\Omega_{R_iR_i}}{m_{R_i}a_1\rho_{S_i}\Omega_{S_{1i}}}\right)^{m_{R_i}}$ is not canceled out, which approaches to zero since SI variance is assumed to be not only linearly but also exponentially dependent on the transmitted power of the relay.

Then, the asymptotic OP expression is obtained as

$$P_{SSRS}^{\infty}(\gamma_{th_1}) = \prod_{i=1}^{L}\Bigg[1-\frac{\left(\frac{m_{D_{1i}}\gamma_{th_1}}{\Omega_{D_{1i}}\rho_{D_{1i}}(a_3-\gamma_{th_1}a_4)}\right)^{m_{D_{1i}}}}{\Gamma(m_{D_{1i}})}\Bigg)\Bigg(1-\frac{\left(\frac{m_{D_{2i}}\gamma_{th_1}}{\Omega_{D_{2i}}\rho_{D_{2i}}(a_3-\gamma_{th_1}a_4)}\right)^{m_{D_{2i}}}}{\Gamma(m_{D_{2i}})}\Bigg) \sum_{p_1=0}^{m_{S_{1i}}-1}\Bigg[\Bigg\{\binom{p_1+m_{S_{1i}}-1}{p_1}\Bigg(\frac{m_{S_{1i}}\gamma_{th_1}a_2\Omega_{S_{2i}}}{m_{S_{2i}}a_1\Omega_{S_{1i}}+m_{S_{1i}}\gamma_{th_1}a_2\Omega_{S_{2i}}}\Bigg)^{p_1}\Bigg\}\Bigg/ \Bigg\{\Bigg(1+\frac{m_{S_{1i}}\gamma_{th_1}a_2\Omega_{S_{2i}}}{m_{S_{2i}}a_1\Omega_{S_{1i}}}\Bigg)^{m_{S_{2i}}}\Bigg(1+\frac{m_{S_{1i}}\gamma_{th_1}\varpi_i\rho_{R_i}\Omega_{R_iR_i}}{m_{R_i}a_1\rho_{S_i}\Omega_{S_{1i}}}\Bigg)^{m_{R_i}}\Bigg\}\Bigg]\Bigg] \tag{7.14}$$

Asymptotic expression reveals that at high SNRs, the parameters dominating OP are SI channel parameters (shape and scale (variance) parameters), PA factors at the sources, and fading channel parameters between the sources and the relays. On the other hand, PA factors at the relays and the channel parameters between the relays and destinations are only effective at the low SNRs.

7.4.2. Outage Probability of Two Stage Relay Selection

For TSRS, outage occurs in two cases, namely, when K_R is an empty set or not, i.e., there is at least one relay satisfying condition given in (7.10) but mathematically no need to treat these states separately. For any data rate of the second user, R_{D_2}, the OP of TSRS is calculated as

$$
\begin{aligned}
P_{TSRS}(\gamma_{th_1},\gamma_{th_2}) &= \sum_{l=0}^{L} Pr(\min(\gamma_{D_{2i_T}}^{D_2},\gamma_{D_2}^{R_{i_T}}) < \gamma_{th_2}, |K_R| = l) \\
&= \sum_{l=0}^{L} \prod_{\substack{j=1 \\ R_i \in K_R}}^{l} \Big(1 - P_{\phi}(\gamma_{th_1},\gamma_{th_2})\Big) \binom{L}{l} \prod_{\substack{j=1 \\ R_i \notin K_R}}^{L-l} \Big(1 - Pr(R_i \in K_R)\Big). \\
&\quad \prod_{\substack{j=1 \\ R_i \in K_R}}^{l} \Big(Pr(R_i \in K_R)\Big)
\end{aligned}
\tag{7.15}
$$

The SINR threshold, γ_{th_2}, for HD and FD transmissions are $\gamma_{th_2} = 2^{2R_{D_2}} - 1$ and $\gamma_{th_2} = 2^{R_{D_2}} - 1$, respectively. The $|K_R|$ is the cardinality of K_R. $P_{\phi}(\gamma_{th_1},\gamma_{th_2}) = Pr(\min(\gamma_{D_{2i}}^{D_2},\gamma_{D_2}^{R_i}) > \gamma_{th_2} / \min\{\gamma_{D_1}^{R_i},\gamma_{D_{1i}}^{D_1},\gamma_{D_{1i}}^{D_2}\} > \gamma_{th_1})$ and it can be reformulated by considering the Bayes theorem as

$$
P_{\phi}(\gamma_{th_1},\gamma_{th_2}) = \frac{P_{\phi_1}(\gamma_{th_1},\gamma_{th_2}) P_{\phi_2}(\gamma_{th_1},\gamma_{th_2}) P_{\phi_3}(\gamma_{th_1},\gamma_{th_2})}{P_{R_i \in K_R}(\gamma_{th_1})} \ , \tag{7.16}
$$

where $P_{\phi_1}(\gamma_{th_1},\gamma_{th_2})$, $P_{\phi_2}(\gamma_{th_1},\gamma_{th_2})$, and $P_{\phi_3}(\gamma_{th_1},\gamma_{th_2})$ are defined as in (7.36) and their closed form expressions are given in (7.17), (7.18), and (7.19), respectively (Please refer to Appendix B).

$$
\begin{aligned}
P_{\phi_1}(\gamma_{th_1},\gamma_{th_2}) = 1 &- \frac{\gamma\Big(m_{D2i}, \frac{m_{D2i} U_{max}}{\Omega_{D_{2i}}}\Big)}{\Gamma(m_{D_{2i}})} - \frac{\Big(\frac{m_{D_{2i}} \gamma_{th_2} a_3 \epsilon_{D_{2i}}}{a_4 \tilde{m}_{D_{2i}} \Omega_{D_{2i}}}\Big)^{m_{D_{2i}}} e^{\frac{\tilde{m}_{D_{2i}}}{a_3 \epsilon_{D_{2i}} \rho_{D_{2i}}}}}{\Gamma(m_{D_{2i}}) \Big(1 + \frac{m_{D_{2i}} \gamma_{th_2} a_3 \epsilon_{D_{2i}}}{a_4 \tilde{m}_{D_{2i}} \Omega_{D_{2i}}}\Big)^{m_{D_{2i}}}} \\
&, \\
&\sum_{p_1=0}^{\tilde{m}_{D_{2i}}-1} \sum_{p_2=0}^{p_1} \Bigg[\frac{\binom{p_1}{p_2} \Gamma\Big(p_2 + m_{D_{2i}}, \big(\frac{m_{D_{2i}}}{\Omega_{D_{2i}}} + \frac{a_4 \tilde{m}_{D_{2i}}}{\gamma_{th_2} a_3 \epsilon_{D_{2i}}}\big) U_{max}\Big)}{\Gamma(p_1+1)(-\rho_{D_{2i}})^{p_1-p_2} \big(\frac{a_3 \epsilon_{D_{2i}}}{\tilde{m}_{D_{2i}}}\big)^{p_1-p_2} \Big(1 + \frac{m_{D_{2i}} \gamma_{th_2} a_3 \epsilon_{D_{2i}}}{a_4 \tilde{m}_{D_{2i}} \Omega_{D_{2i}}}\Big)^{p_2}} \Bigg]
\end{aligned}
\tag{7.17}
$$

where $U_{max} = \max\Big(\frac{\gamma_{th_2}}{\rho_{D_{2i}} a_4}, \frac{\gamma_{th_1}}{\rho_{D_{2i}}(a_3 - \gamma_{th_1} a_4)}\Big)$.

$$
P_{\phi_2}(\gamma_{th_1},\gamma_{th_2}) = 1 - \frac{\gamma\Big(m_{D_{1i}}, \frac{m_{D_{1i}} \gamma_{th_1}}{\rho_{D_{1i}} \Omega_{D_{1i}}(a_3 - \gamma_{th_1} a_4)}\Big)}{\Gamma(m_{D_{1i}})}, \tag{7.18}
$$

where $\gamma_{th_1} \leq \frac{a_3}{a_4}$, otherwise $P_{\phi_2}(\gamma_{th_1},\gamma_{th_2}) = 0$.

$$P_{\phi_3}(\gamma_{th_1},\gamma_{th_2}) = \sum_{(q_1,q_2,q_3)=\overrightarrow{0}}^{(m_{S_{1i}}-1,q_1,q_2)} \sum_{(k_1,k_2,k_3)=\overrightarrow{0}}^{(q_3+m_{S_{2i}}-1,k_1,k_2)} \left[\Phi_I \Phi_{II} \Phi_{III} \frac{\left(\frac{\varpi_i \rho_{R_i} \Omega_{R_i R_i}}{m_{R_i}}\right)^{k_2+q_2-k_3-q_3}}{\left(\rho_{S_i}\right)^{k_1+q_1-k_3-q_3}} \right] e^{-\frac{\gamma_{th_2} m_{S_{2i}} a_1 \Omega_{S_{1i}} + (\gamma_{th_2}+1) m_{S_{1i}} \gamma_{th_1} a_2 \Omega_{S_{2i}}}{a_1 a_2 \rho_{S_i} \Omega_{S_{1i}} \Omega_{S_{2i}}}}, \tag{7.19}$$

where $\sum_{(q_1,q_2,q_3)=\overrightarrow{0}}^{(m_{S_{1i}}-1,q_1,q_2)} \sum_{(k_1,k_2,k_3)=\overrightarrow{0}}^{(q_3+m_{S_{2i}}-1,k_1,k_2)} = \sum_{q_1=0}^{m_{S_{1i}}-1} \sum_{q_2=0}^{q_1} \sum_{q_3=0}^{q_2} \sum_{k_1=0}^{q_3+m_{S_{2i}}-1} \sum_{k_2=0}^{k_1} \sum_{k_3=0}^{k_2}$. $\overrightarrow{0}$ is a three dimensional zero vector and Φ_I, Φ_{II}, and Φ_{III} in expression of $P_{\phi_3}(\gamma_{th_1},\gamma_{th_2})$ are

$$\begin{aligned}
\Phi_I =& \frac{\binom{k_1}{k_2}\binom{k_2}{k_3}\binom{q_1}{q_2}\binom{q_2}{q_3}\Gamma(k_3+\tilde{m}_{R_i})\Gamma(k_2+q_2+m_{R_i}-k_3-q_3)\Gamma(q_3+m_{S_{2i}})}{\Gamma(m_{S_{2i}})\Gamma(m_{R_i})\Gamma(\tilde{m}_{R_i})\Gamma(k_1+1)\Gamma(q_1+1)} \\
& \left(\frac{m_{S_{1i}}\gamma_{th_1}}{a_1\Omega_{S_{1i}}}\right)^{q_1} \left(\frac{a_2\Omega_{S_{2i}}}{m_{S_{2i}}}\right)^{q_3-k_1} \left(\frac{a_1\epsilon_{R_i}}{\tilde{m}_{R_i}}\right)^{k_3} (\gamma_{th_2})^{k_1} \\
\Phi_{II} =& \frac{1}{\left(1+\frac{m_{S_{1i}}\gamma_{th_1}a_2\Omega_{S_{2i}}}{m_{S_{2i}}a_1\Omega_{S_{1i}}}\right)^{q_3+m_{S_{2i}}-k_1} \left(1+\frac{\gamma_{th_2}(m_{S_{2i}}a_1\Omega_{S_{1i}}+m_{S_{1i}}\gamma_{th_1}a_2\Omega_{S_{2i}})}{\tilde{m}_{R_i}a_2\Omega_{S_{1i}}\Omega_{S_{2i}}}\epsilon_{R_i}\right)^{k_3+\tilde{m}_{R_i}}} \\
\Phi_{III} =& \frac{1}{\left(1+\left(\frac{m_{S_{2i}}a_1\Omega_{S_{1i}}\gamma_{th_2}+(\gamma_{th_2}+1)m_{S_{1i}}\gamma_{th_1}a_2\Omega_{S_{2i}}}{m_{R_i}a_1a_2\Omega_{S_{1i}}\Omega_{S_{2i}}}\right)\frac{\varpi_i\rho_{R_i}\Omega_{R_iR_i}}{\rho_{S_i}}\right)^{k_2+q_2+m_{R_i}-k_3-q_3}}
\end{aligned} \tag{7.20}$$

The closed form of $Pr(R_i \in K_R)$ is obtained in the derivation of $P_{SSRS}(\gamma_{th_1})$, as given in (7.13).

Using the same approach as in derivation of $P^{\infty}_{SSRS}(\gamma_{th_1})$, asymptotic expressions for $P_{\phi_1}(\gamma_{th_1},\gamma_{th_2})$, $P_{\phi_2}(\gamma_{th_1},\gamma_{th_2})$, $P_{\phi_3}(\gamma_{th_1},\gamma_{th_2})$, and $P^{\infty}_{R_i\in K_R}(\gamma_{th_1})$ are derived as follows

$$P^{\infty}_{\phi_1}(\gamma_{th_1},\gamma_{th_2}) = 1 - \sum_{p_1=0}^{\tilde{m}_{D_{2i}}-1} \left[\frac{\Gamma\left(p_1+m_{D_{2i}}\right)\left(\frac{m_{D_{2i}}\gamma_{th_2}a_3\epsilon_{D_{2i}}}{a_4\tilde{m}_{D_{2i}}\Omega_{D_{2i}}}\right)^{m_{D_{2i}}}}{\Gamma(p_1+1)\Gamma(m_{D_{2i}})\left(1+\frac{m_{D_{2i}}\gamma_{th_2}a_3\epsilon_{D_{2i}}}{a_4\tilde{m}_{D_{2i}}\Omega_{D_{2i}}}\right)^{m_{D_{2i}}+p_2}} \right], \tag{7.21}$$

$$P^{\infty}_{\phi_2}(\gamma_{th_1},\gamma_{th_2}) = 1 - \frac{1}{\Gamma(m_{D_{1i}}+1)}\left(\frac{m_{D_{1i}}\gamma_{th_1}}{\rho_{D_{1i}}\Omega_{D_{1i}}(a_3-\gamma_{th_1}a_4)}\right)^{m_{D_{1i}}}, \tag{7.22}$$

$$P_{\phi_3}^{\infty}(\gamma_{th_1},\gamma_{th_2}) = \sum_{q_1=0}^{m_{S_{1i}}-1}\sum_{k_1=0}^{q_1+m_{S_{1i}}-1}\Bigg[\Bigg\{\Gamma(\tilde{m}_{R_i}+k_1)\Gamma(m_{S_{2i}}+q_1)\left(\frac{m_{S_{2i}}}{a_2\Omega_{S_{2i}}}\right)^{k_1-q_1}$$
$$\left(\frac{m_{S_{1i}}\gamma_{th_1}}{a_1\Omega_{S_{1i}}}\right)^{q_1}\left(\frac{\gamma_{th_2}a_1\epsilon_{R_i}}{\tilde{m}_{R_i}}\right)^{k_1}\Bigg\}\Bigg/\Bigg\{\Gamma(m_{S_{2i}})\Gamma(\tilde{m}_{R_i})\Gamma(k_1+1)\Gamma(q_1+1)$$
$$\left(1+\left(\frac{m_{S_{2i}}a_1\Omega_{S_{1i}}\gamma_{th_2}+(\gamma_{th_2}+1)m_{S_{1i}}\gamma_{th_1}a_2\Omega_{S_{2i}}}{m_{R_i}a_1a_2\Omega_{S_{1i}}\Omega_{S_{2i}}}\right)\frac{\varpi_i\rho_{R_i}\Omega_{R_iR_i}}{\rho_{S_i}}\right)^{m_{R_i}} \tag{7.23}$$
$$\left(1+\frac{\gamma_{th_2}(m_{S_{2i}}a_1\Omega_{S_{1i}}+m_{S_{1i}}\gamma_{th_1}a_2\Omega_{S_{2i}})}{\tilde{m}_{R_i}a_2\Omega_{S_{1i}}\Omega_{S_{2i}}}\epsilon_{R_i}\right)^{\tilde{m}_{R_i}+k_1}$$
$$\left(1+\frac{m_{S_{1i}}\gamma_{th_1}a_2\Omega_{S_{2i}}}{m_{S_{2i}}a_1\Omega_{S_{1i}}}\right)^{m_{S_{2i}}+q_1-k_1}\Bigg\}\Bigg],$$

and

$$P_{R_i\in K_R}^{\infty}(\gamma_{th_1}) = \left(1-\frac{\left(\frac{m_{D_{1i}}\gamma_{th_1}}{\Omega_{D_{1i}}\rho_{D_{1i}}(a_3-\gamma_{th_1}a_4)}\right)^{m_{D_{1i}}}}{\Gamma(m_{D_{1i}})}\right)\left(1-\frac{\left(\frac{m_{D_{2i}}\gamma_{th_1}}{\Omega_{D_{2i}}\rho_{D_{2i}}(a_3-\gamma_{th_1}a_4)}\right)^{m_{D_{2i}}}}{\Gamma(m_{D_{2i}})}\right)$$
$$\sum_{p_1=0}^{m_{S_{1i}}-1}\Bigg[\Bigg\{\binom{p_1+m_{S_{1i}}-1}{p_1}\left(\frac{m_{S_{1i}}\gamma_{th_1}a_2\Omega_{S_{2i}}}{m_{S_{2i}}a_1\Omega_{S_{1i}}+m_{S_{1i}}\gamma_{th_1}a_2\Omega_{S_{2i}}}\right)^{p_1}\Bigg\}\Bigg/$$
$$\Bigg\{\left(1+\frac{m_{S_{1i}}\gamma_{th_1}a_2\Omega_{S_{2i}}}{m_{S_{2i}}a_1\Omega_{S_{1i}}}\right)^{m_{S_{2i}}}\left(1+\frac{m_{S_{1i}}\gamma_{th_1}\varpi_i\rho_{R_i}\Omega_{R_iR_i}}{m_{R_i}a_1\rho_{S_i}\Omega_{S_{1i}}}\right)^{m_{R_i}}\Bigg\}\Bigg]. \tag{7.24}$$

Consequently, the asymptotic expression of $P_{TSRS}(\gamma_{th_1},\gamma_{th_2})$ is

$$P_{TSRS}^{\infty}(\gamma_{th_1},\gamma_{th_2}) = \sum_{l=0}^{L}\prod_{\substack{j=1\\R_i\in K_R}}^{l}\left(1-P_{\phi}^{\infty}(\gamma_{th_1},\gamma_{th_2})\right)\binom{L}{l}\prod_{\substack{j=1\\R_i\notin K_R}}^{L-l}\left(1-P_{R_i\in K_R}^{\infty}(\gamma_{th_1})\right)$$
$$\prod_{\substack{j=1\\R_i\in K_R}}^{l}\left(P_{R_i\in K_R}^{\infty}(\gamma_{th_1})\right), \tag{7.25}$$

where $P_{\phi}^{\infty}(\gamma_{th_1},\gamma_{th_2}) = P_{\phi_1}^{\infty}(\gamma_{th_1},\gamma_{th_2})P_{\phi_2}^{\infty}(\gamma_{th_1},\gamma_{th_2})P_{\phi_3}^{\infty}(\gamma_{th_1},\gamma_{th_2})/P_{R_i\in K_R}^{\infty}(\gamma_{th_1})$.

For pSIC and HD schemes, numerical results can be obtained from the above equations. Although $1/0$ takes place in (7.17) can be eliminated by using limit functions in software programs such as MATHEMATICA and MAPLE, we provide its pSIC counterpart as in (7.26). Simplification of other equations for pSIC and HD cases are straightforward and actually they can be reached by cancellation of the terms including ϵ_{R_i}, $\epsilon_{D_{2i}}$, and ϖ_i.

$$P_{\phi_1}^{pSIC}(\gamma_{th_1},\gamma_{th_2}) = Pr\left(|h_{R_{i2}}|^2 > \frac{\gamma_{th_1}}{a_3\rho_{D_{2i}} - a_4\rho_{D_{2i}}\gamma_{th_1}}\right) = 1 - \frac{\gamma\left(m_{D2i}, \frac{m_{D2i}U_{max}}{\Omega_{D_{2i}}}\right)}{\Gamma(m_{D_{2i}})} \tag{7.26}$$

7.5. Numerical Results

In this section, numerical results for OP are provided to validate the derived expressions. It is assumed that $P_T = 2P_S = 2P_{R_i}$ and $\sigma^2 = \sigma_{R_i}^2 = \sigma_{D_1}^2 = \sigma_{D_2}^2 = 1$. The path loss exponent, representing urban environment, is taken to be 3. The curves are plotted versus P_T/σ^2.

Fig. 7.2 verifies correctness of exact and asymptotic expressions of OP for SSRS strategy over Rayleigh fading environment, namely, (7.12) and (7.14). PAs are chosen as $a_1 = a_3 = 0.75$ ve $a_2 = a_4 = 0.25$. In meanwhile variances of channel gains are set to 1, and data rates are $R_{D_1} = 0.1$ bit per channel use (BPCU) and $R_{D_2} = 1$ BPCU. SI cancellation factors are chosen as $(\kappa_l, \vartheta_l) \in \{(1, 0.2), (1, 0.5)\}$. Simulation and analytical results coincide in excellent way for both FD and HD transmissions and FD transmission provides better performance in case of sufficient SI cancellation. Effect of SI is also illustrated, however, as SNR (P_T/σ^2) increases the same error floor is reached due to SIC

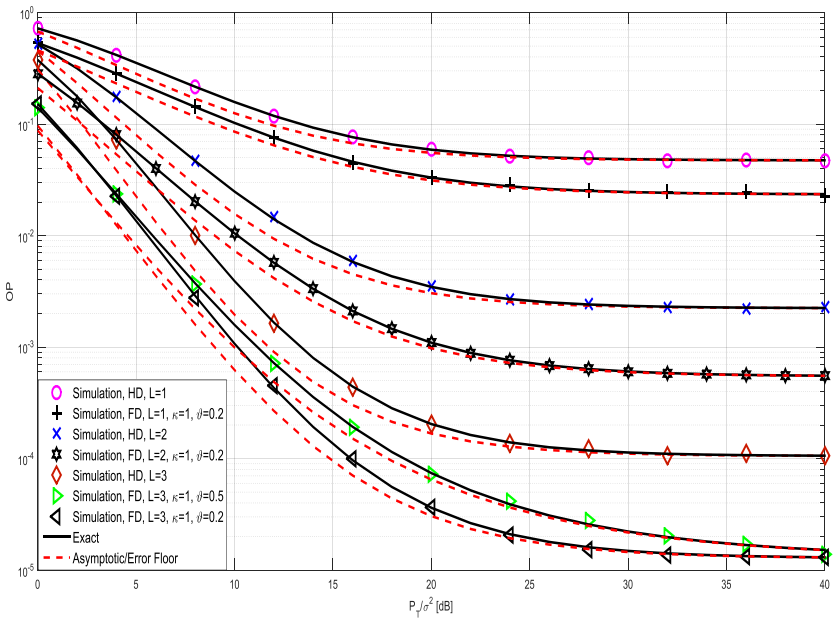

Figure 7.2: Exact, asymptotic, and simulation OPs of SSRS over Rayleigh fading channels.

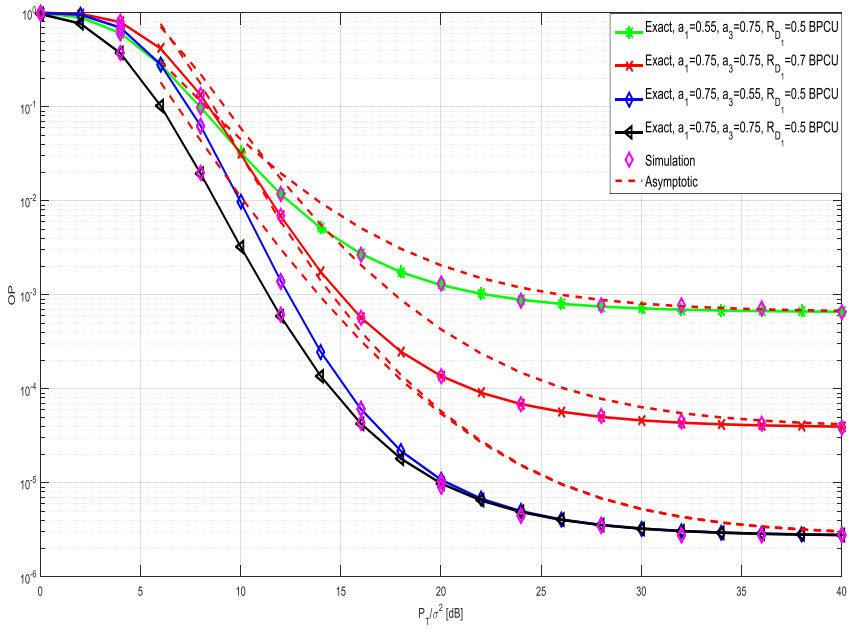

Figure 7.3: Exact, asymptotic, and simulation OPs of SSRS over Nakagami-m fading channels.

effect which dominates performance even if there are different SI powers. Furthermore, as number of relays increases OP decreases, i.e., substantial gain is attained. As P_T/σ^2 goes to infinity SINRs approach constant values, therefore, error floors occur. But error floor reduces as total number of relays increases, i.e., diversity order demonstrates its effect on the OP. In error floor region diversity order is not zero but due to the constant SINR values even if P_T/σ^2 increases, they attain fixed value and this results in error floor. Unlike HD systems where OP or SERs are proportional to the transmitted power, in turn SNR, as it goes to infinity, in the systems where FD or NOMA transmission is assumed, error probabilities are proportional to a constant value. For example, in FD transmission, error floor takes place if SI power is only linearly dependent on the transmitted power, which causes a fixed SINR value as P_T/σ^2 reaches infinity. However, no error floor is observed if SI power also exponentially depends on transmitted power as illustrated in this work. Actually, linearly or exponentially dependence of SI power is not the reason for zero or non-zero diversity order. Misinterpretation of diversity order as slope of log-log plot causes this undesired situation although diversity order is the number of independent paths from the source to the destination.

In Fig. 7.3, validity of exact and asymptotic expressions given in (7.12) and (7.14) for Nakagami-m fading channels for FD transmission is investigated, where all shaping parameters are set to 2 and scaling parameters (variances) are set to 1, thereby, distances are also equal to 1. Results are demonstrated for different PAs ($a_1 \in \{0.55, 0.75\}$ &

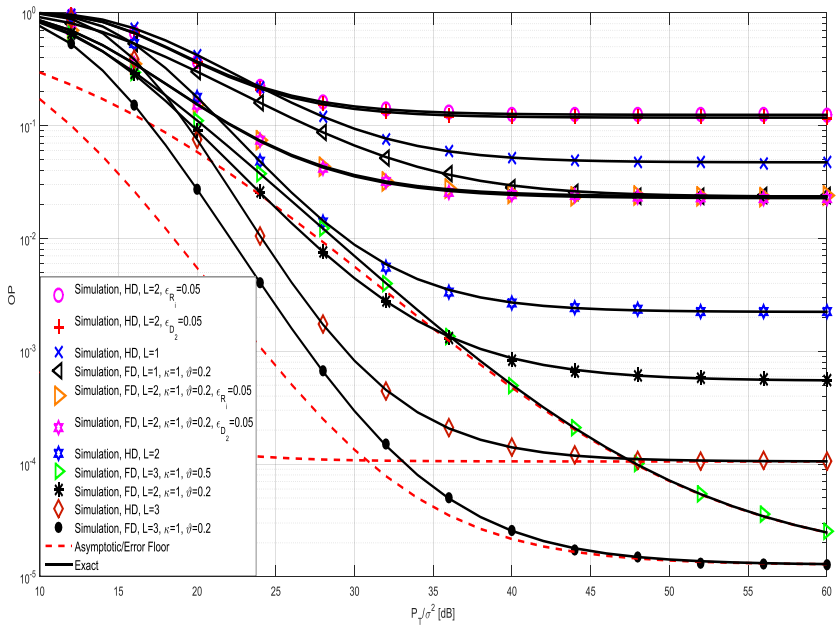

Figure 7.4: Exact, asymptotic, and simulation OPs of TSRS over Rayleigh fading channels.

$a_3 \in \{0.55, 0.75\}$) and data rates of user 1, $R_{D_1} \in \{0.5, 0.7\}$. The data rate of user 2 is set to $R_{D_2} = 1$, total number of relays is $L = 4$, and SI cancellation factors are chosen as $(\kappa_l, \vartheta_l) = (1, 0.2)$. The overlap of the simulation and exact results is excellent and asymptotic ones follow them. Error floor of two lower curves is the same even different powers are assigned to the user 1 at the relays. This result is not surprising since power allocation at the sources but not at the relays is effective on error floor, which is obvious as can be observed from (7.14).

Fig. 7.4 demonstrates results of OP for TSRS over Rayleigh fading environment for both HD and FD transmissions, where all parameter settings are the same as in Fig. 7.2. Additionally, to illustrate effect of ipSIC on performance, two schemes for both HD and FD protocols are considered where $\epsilon_{R_i} = \epsilon_{D_{2i}} = 0.05$ for $L = 2$. For the sake of figure clarity, asymptotic curves are only provided for $L = 3$. Exact and asymptotic curves are derived from (7.15) and (7.25), respectively. Exact and simulation results perfectly coincide with each other. Asymptotic curves excellently overlap with exact and simulation curves in error floors. All deductions in Fig. 7.2 for SSRS are also valid for TSRS. Unlike SSRS, SI is more effective where worse performance can be attained in case of insufficient SI cancellation. Imperfect SIC at the relay and destination has nearly the same effect and it reduces performance strictly.

Fig. 7.5 verifies correctness of the OP expression of TSRS for different shape/scale factors and also for imperfect SIC cases. Error floor happens due to SIC, imperfect SIC,

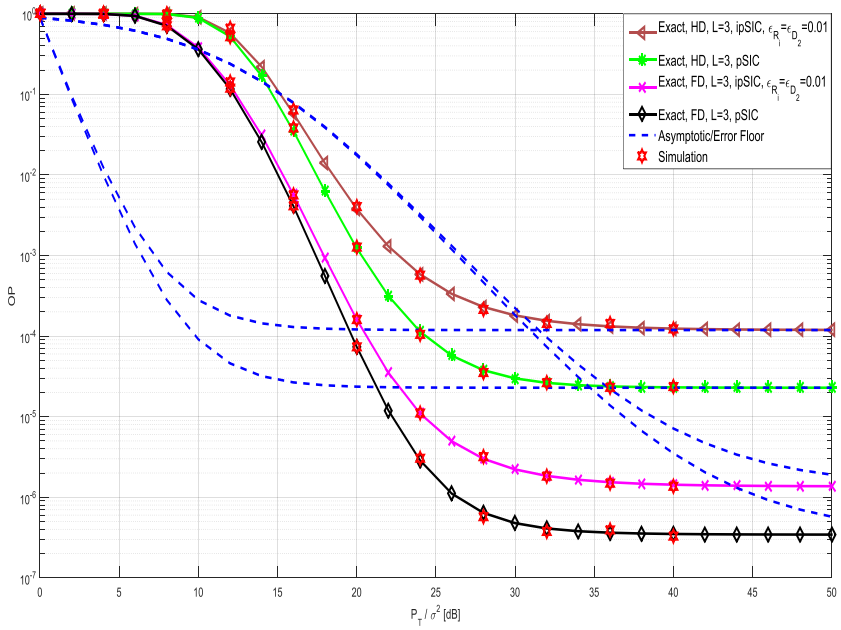

Figure 7.5: Exact, asymptotic, and simulation OPs of TSRS over Nakagami-m fading channels.

and insufficient SI cancellation. The shape and scale parameters are chosen as $(m_{S_{1i}} = 2, \Omega_{S_{1i}} = 1.55)$, $(m_{S_{2i}} = 3, \Omega_{S_{2i}} = 1.7)$, $(m_{D_{1i}} = 1.75, \Omega_{D_{1i}} = 1.3)$, $(m_{D_{2i}} = 1.5, \Omega_{D_{2i}} = 1.6)$, $(\tilde{m}_{R_i} = 2, 1)$, $(\tilde{m}_{D_{2i}} = 2, 1)$, and $(m_{R_iR_i} = 1.25, \Omega_{R_iR_i} = P_{R_i}^{0.2})$. Data rates are $R_{D_1} = 0.2$ BPCU and $R_{D_2} = 1$ BPCU. Total number of relays is $L = 3$ and ipSIC parameters are $\epsilon_{D_{2i}} = \epsilon_{R_i} = 0.01$. PA parameters are $a_1 = a_3 = 0.75$. Overlapping of exact and simulation results reveals validity of OP expressions for non-integer shaping parameters, namely, $m_{D_{1i}}$, $m_{D_{2i}}$, $\tilde{m}_{R_i}$, and $m_{R_iR_i}$, whereas other three ones are assumed to be integers. Although ipSIC parameters are set to a small value, %1, their effect on performance is enormous. The OP becomes about 9 times of the former value for both HD and FD transmission, at a P_T/σ^2 value of 40 dB.

Tables 7.1, 7.2, 7.3, 7.4 together with Fig. 7.6 and 7.7 illustrate different schemes of TSRS over Nakagami-m fading channels for optimum relay locations. All shape factors are set to 2 and scaling factors (variances) are assumed only characterized by relay location and path loss exponent, α. The nodes S_1, S_2, D_1, and D_2 are assumed to be located at the points $(x_{S_1}, y_{S_1}) = (-6, 6)$, $(x_{S_2}, y_{S_2}) = (-6, -6)$, $(x_{D_1}, y_{D_1}) = (6, -6)$, and $(x_{D_2}, y_{D_2}) = (6, 6)$, respectively, which corresponds to the case of equal distances among the relays and nodes. As assumed, the relays are clustered and located at the origin, thereafter, different schemes are assigned and related optimum relay locations are obtained. The relay's location is set to $\left(x_{R_l}, y_{R_l}\right) = \left(r\cos(\theta), r\sin(\theta)\right)$ where $r = n\times 6/64, n := 0:1:63$ and $\theta = p\times 6.28/64, p := 0:1:63$. All coordinates are in meters

Table 7.1: Optimum relay location of FD transmission for TSRS.

P_T/σ^2 (dB)	a_1	a_3	(κ_l, ϑ_l)	$(\epsilon_{R_l}, \epsilon_{D_{2l}})$	(R_{D_l}, R_{D_2})	(x_{R_l}, y_{R_l})	OP_{min}
50	0.55	0.75	(1, 0.31)	(0, 0)	(0.1, 1)	(0.000, 000)	3.69×10^{-2}
50	0.75	0.55	(1, 0.31)	(0, 0)	(0.1, 1)	(0.000, 000)	1.74×10^{-1}
50	0.75	0.75	(1, 0.31)	(0, 0)	(0.1, 1)	(0.000, 000)	1.75×10^{-1}
50	0.55	0.75	(1, 0.31)	(0, 0)	(0.1, 1)	(-4.415, -0.870)	6.27×10^{-4}
50	0.75	0.55	(1, 0.31)	(0, 0)	(0.1, 1)	(-5.386, -1.623)	3.70×10^{-4}
50	0.75	0.75	(1, 0.31)	(0, 0)	(0.1, 1)	(-4.421, -1.822)	9.10×10^{-4}
50	0.75	0.75	(1, 0.31)	(0, 0)	(0.3, 1)	(-4.875, -0.961)	6.58×10^{-3}
50	0.75	0.75	(1, 0.31)	(0, 0)	(0.1, 2)	(-4.421, -2.246)	8.52×10^{-2}
50	0.75	0.75	(1, 0.51)	(0, 0)	(0.1, 1)	(-5.048, -2.687)	2.19×10^{-2}
60	0.75	0.75	(1, 0.31)	(0, 0)	(0.1, 1)	(-5.879, -0.569)	1.70×10^{-7}
50	0.75	0.75	(1, 0.31)	$(10^{-4}, 10^{-4})$	(0.1, 1)	(-2.732, -1.818)	5.38×10^{-2}

and first three rows are not optimum relay locations but provided for comparison. Table

Table 7.2: Optimum distances of FD transmission for TSRS.

$d_{S_1R_l}$	$d_{S_2R_l}$	$d_{D_1R_l}$	$d_{D_2R_l}$	OP_{min}
8.485	8.485	8.485	8.485	3.69×10^{-2}
8.485	8.485	8.485	8.485	1.74×10^{-1}
8.485	8.485	8.485	8.485	1.75×10^{-1}
7.050	5.369	11.610	12.477	6.27×10^{-4}
7.648	4.420	12.198	13.702	3.70×10^{-4}
7.980	4.466	11.227	13.030	9.10×10^{-4}
7.051	5.163	11.986	12.912	6.58×10^{-3}
8.396	4.073	11.077	13.289	8.52×10^{-2}
8.739	3.447	11.534	14.054	2.19×10^{-2}
6.570	5.432	13.062	13.574	1.70×10^{-7}
8.474	5.307	9.682	11.720	5.38×10^{-2}

Table 7.3: Optimum relay location of HD transmission for TSRS.

P_T/σ^2 (dB)	a_1	a_3	$(\epsilon_{R_l}, \epsilon_{D_{2l}})$	(R_{D_l}, R_{D_2})	(x_{R_l}, y_{R_l})	OP_{min}
50	0.55	0.75	(0, 0)	(0.1, 1)	(0.000, 000)	4.02×10^{-5}
50	0.75	0.55	(0, 0)	(0.1, 1)	(0.000, 000)	8.37×10^{-6}
50	0.75	0.75	(0, 0)	(0.1, 1)	(0.000, 000)	3.39×10^{-5}
50	0.55	0.75	(0, 0)	(0.1, 1)	(-0.191, 1.959)	5.89×10^{-6}
50	0.75	0.55	(0, 0)	(0.1, 1)	(-1.379, 0.276)	4.91×10^{-6}
50	0.75	0.75	(0, 0)	(0.1, 1)	(-0.312, 0.468)	3.13×10^{-5}
50	0.75	0.75	(0, 0)	(0.3, 1)	(-1.247, 1.523)	7.48×10^{-5}
50	0.75	0.75	(0, 0)	(0.1, 2)	(-0.052, 0.078)	2.13×10^{-1}
55	0.75	0.75	(0, 0)	(0.1, 1)	(-1.188, 1.451)	1.24×10^{-8}
50	0.75	0.75	$(10^{-4}, 10^{-4})$	(0.1, 1)	(-0.036, 0.087)	1.45×10^{-1}

7.2 includes distances among each node and relays for the schemes provided in Table 7.1 for FD transmission. Similarly, Table 7.4 includes distances corresponding to the schemes provided in Table 7.3 for HD transmission. For FD transmission, all optimum locations fall in the third quarter of the cartesian system, i.e. relays move towards the second source, on the other hand, those of HD transmission are located in the second quarter and their changes with respect to origin are not as hard as that of FD. This interesting finding is due

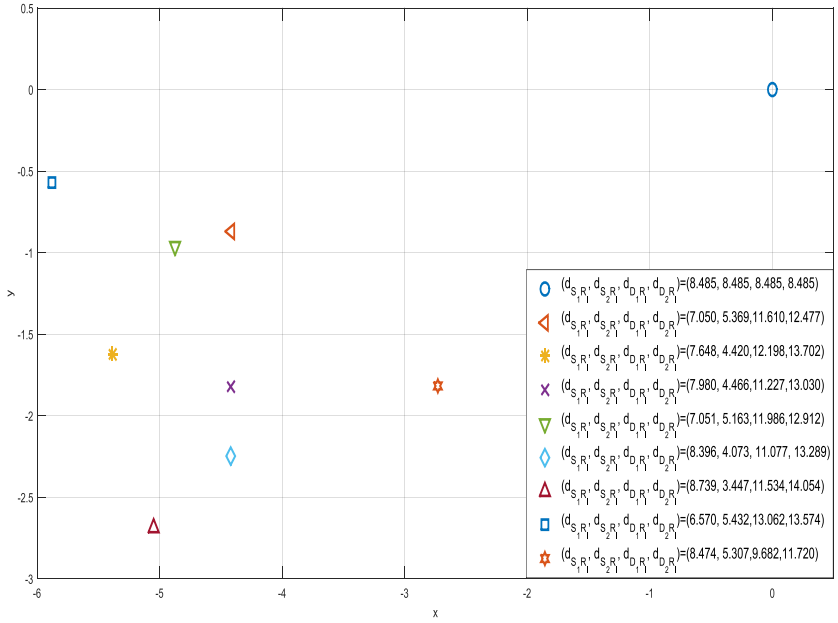

Figure 7.6: Optimum relay locations of FD transmission.

to SI effect which governs the best relay location of the FD transmission. Unequal power allocations at the sources and the relays result in better performance than equal allocations for both FD and HD protocols. Increasing total transmitted power in FD transmission moves the best relay location towards the middle of the sources. The best relay location of FD transmission is more sensitive to PA factors, users' data rates, ipSICs at the relay and user 2, and total power, whereas data rate of the second user and ipSICs are not more effective in HD transmission.

Table 7.4: Optimum distances of HD transmission for TSRS.

$d_{S_1R_l}$	$d_{S_2R_l}$	$d_{D_1R_l}$	$d_{D_2R_l}$	$OP_{\min}$
8.485	8.485	8.485	8.485	4.02×10^{-5}
8.485	8.485	8.485	8.485	8.37×10^{-6}
8.485	8.485	8.485	8.485	3.39×10^{-5}
7.076	9.853	10.083	7.393	5.89×10^{-6}
7.356	7.794	9.687	9.339	4.91×10^{-6}
7.935	8.613	9.037	8.393	3.13×10^{-5}
6.530	8.899	10.446	8.518	7.48×10^{-5}
8.393	8.504	8.577	8.467	2.13×10^{-1}
6.622	8.870	10.353	8.507	1.24×10^{-8}
8.398	8.522	8.572	8.450	1.45×10^{-1}

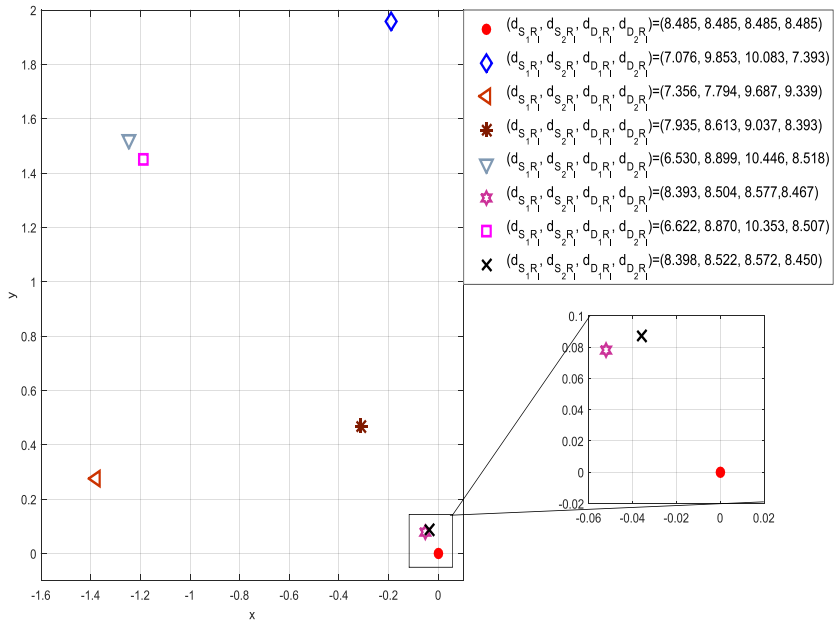

Figure 7.7: Optimum relay locations of HD transmission.

7.6. Conclusion

A system consisting of two sources and users with FD/HD multi relays, applying NOMA in both sources and relays with up and down link transmissions, is investigated over i.n.i.d. Nakagami-m fading environment for both perfect and imperfect SIC cases, where DF protocol is used. Two different relay selection methods are investigated in accordance with service quality priority, where priority is assumed for user 1. Exact and asymptotic OP expressions of both strategies for i.n.i.d. Nakagami-m fade are derived and validated via Monte-Carlo simulation technique. At the high SNRs, it is observed that SSRS throughput is almost not affected by PA factors at the selected relay and characteristics (shaping and scaling factors) of the channels among the selected relay and the two end users. However, it is dominated by PA factors at the sources and characteristics of the channels among the sources and selected relay and that of SI channel for FD transmission. For TSRS scheme, deductions of SSRS scheme are also valid for pSIC case but characteristics of the channel between the selected relay and user 2 and ipSIC at user 2 become effective on throughput when ipSIC takes place. Additionally, characteristics of ipSIC at the selected relay are also other substantial factors dominating throughput at the high SNR. Best relay locations of different schemes including combination of power allocations, data rates, ipSICs, and total powers are illustrated. The results demonstrate that optimum relay location changes toward to the second source for FD transmission to

eliminate SI effect and toward to the first source for HD transmission to eliminate SIC effect. Finally, non-zero diversity order is asserted and explained in details.

7.7. Appendix: Outage Probability Derivations

7.7.1. Outage Probability Derivation of Single Stage Relay Selection

The OP of SSRS selection scheme can be expressed and formulated in terms of integrals as

$$\begin{aligned} P_{SSRS}(\gamma_{th_1}) &= Pr(\min\{\gamma_{D_1}^{R_{i_S}}, \gamma_{D_{1i_S}}^{D_1}, \gamma_{D_{1i_S}}^{D_2}\} < \gamma_{th_1}) \\ &= \prod_{i=1}^{L} Pr(\min\{\gamma_{D_1}^{R_i}, \gamma_{D_{1i}}^{D_1}, \gamma_{D_{1i}}^{D_2}\} < \gamma_{th_1}) \\ &= \prod_{i=1}^{L} \big(1 - Pr(\min\{\gamma_{D_1}^{R_i}, \gamma_{D_{1i}}^{D_1}, \gamma_{D_{1i}}^{D_2}\} > \gamma_{th_1})\big) \\ &= \prod_{i=1}^{L} \big(1 - Pr(R_i \in K_R)\big), \end{aligned} \tag{7.27}$$

Due to the independence of channel gains, in turn the independence of $\gamma_{D_1}^{R_i}$, $\gamma_{D_{1i}}^{D_1}$, and $\gamma_{D_{1i}}^{D_2}$, $Pr(R_i \in K_R) = Pr(\gamma_{D_1}^{R_i} > \gamma_{th_1}) Pr(\gamma_{D_{1i}}^{D_1} > \gamma_{th_1}) Pr(\gamma_{D_{1i}}^{D_2} > \gamma_{th_1})$. Therefore, in order to obtain a closed form of $P_{SSRS}(\gamma_{th_1})$, it is sufficient to derive CDFs of $\gamma_{D_1}^{R_i}$, $\gamma_{D_{1i}}^{D_1}$, and $\gamma_{D_{1i}}^{D_2}$. The CDF of $\gamma_{D_1}^{R_i}$, $F_{\gamma_{D_1}^{R_i}}(\gamma_{th_1})$ is derived as follows.

$$\begin{aligned} F_{\gamma_{D_1}^{R_i}}(\gamma_{th_1}) &= Pr(\gamma_{D_1}^{R_i} < \gamma_{th_1}) \\ &= Pr\Big(\frac{a_1 \rho_{S_{1i}} |g_{S_i}|^2}{a_2 \rho_{S_{1i}} |h_{S_i}|^2 + \varpi_i \rho_{R_i} |h_{R_i R_i}|^2 + 1} < \gamma_{th_1}\Big) \\ &= Pr\left(|g_{S_i}|^2 < \frac{\gamma_{th_1}}{a_1 \rho_{S_{1i}}} \left(a_2 \rho_{S_{1i}} |h_{S_i}|^2 + \varpi_i \rho_{R_i} |h_{R_i R_i}|^2 + 1\right)\right) \\ &= \int_0^\infty \int_0^\infty F_{|g_{S_i}|^2}\left(\frac{\gamma_{th_1}}{a_1 \rho_{S_{1i}}} \big(a_2 \rho_{S_{1i}} x + \varpi_i \rho_{R_i} y + 1\big)\right) f_{|h_{S_i}|^2}(x) \\ &\quad f_{|h_{R_i R_i}|^2}(y) dx dy, \end{aligned} \tag{7.28}$$

where the CDFs and PDFs of the square of all channel gains are given in (7.29).

$$
\begin{aligned}
F_{|g_{S_i}|^2}(x) &= \frac{\gamma\left(m_{S_{1i}}, m_{S_{1i}}x/\Omega_{S_{1i}}\right)}{\Gamma(m_{S_{1i}})} \\
f_{|g_{S_i}|^2}(x) &= \frac{m_{S_{1i}}^{m_{S_{1i}}} x^{m_{S_{1i}}-1} e^{-m_{S_{1i}}x/\Omega_{S_{1i}}}}{\Omega_{S_{1i}}^{m_{S_{1i}}}\Gamma(m_{S_{1i}})} \\
F_{|h_{S_i}|^2}(x) &= \frac{\gamma\left(m_{S_{2i}}, m_{S_{2i}}x/\Omega_{S_{2i}}\right)}{\Gamma(m_{S_{2i}})} \\
f_{|h_{S_i}|^2}(x) &= \frac{m_{S_{2i}}^{m_{S_{2i}}} x^{m_{S_{2i}}-1} e^{-m_{S_{2i}}x/\Omega_{S_{2i}}}}{\Omega_{S_{2i}}^{m_{S_{2i}}}\Gamma(m_{S_{2i}})} \\
F_{|g_{R_{i1}}|^2}(x) &= \frac{\gamma\left(m_{D_{1i}}, m_{D_{1i}}x/\Omega_{D_{1i}}\right)}{\Gamma(m_{D_{1i}})} \\
f_{|g_{R_{i1}}|^2}(x) &= \frac{m_{D_{1i}}^{m_{D_{1i}}} x^{m_{D_{1i}}-1} e^{-m_{D_{1i}}x/\Omega_{D_{1i}}}}{\Omega_{D_{1i}}^{m_{D_{1i}}}\Gamma(m_{D_{1i}})} \\
F_{|h_{R_{i2}}|^2}(x) &= \frac{\gamma\left(m_{D_{2i}}, m_{D_{2i}}x/\Omega_{D_{2i}}\right)}{\Gamma(m_{D_{2i}})} \\
f_{|h_{R_{i2}}|^2}(x) &= \frac{m_{D_{2i}}^{m_{D_{2i}}} x^{m_{D_{2i}}-1} e^{-m_{D_{2i}}x/\Omega_{D_{2i}}}}{\Omega_{D_{2i}}^{m_{D_{2i}}}\Gamma(m_{D_{2i}})}
\end{aligned}
\tag{7.29}
$$

Similarly, CDFs and PDFs of ipSIC and SI are given in (7.30)

$$
\begin{aligned}
F_{|\tilde{g}_{S_i}|^2}(x) &= \frac{\gamma\left(\tilde{m}_{R_i}, \tilde{m}_{R_i}x\right)}{\Gamma(\tilde{m}_{R_i})} \\
f_{|\tilde{g}_{S_i}|^2}(x) &= \frac{\tilde{m}_{R_i}^{\tilde{m}_{R_i}} x^{\tilde{m}_{R_i}-1} e^{-\tilde{m}_{R_i}x}}{\Gamma(\tilde{m}_{S_{1i}})} \\
F_{|\tilde{h}_{R_{i2}}|^2}(x) &= \frac{\gamma\left(\tilde{m}_{D_{2i}}, \tilde{m}_{D_{2i}}x\right)}{\Gamma(\tilde{m}_{D_{2i}})} \\
f_{|\tilde{h}_{R_{i2}}|^2}(x) &= \frac{\tilde{m}_{D_{2i}}^{\tilde{m}_{D_{2i}}} x^{\tilde{m}_{D_{2i}}-1} e^{-\tilde{m}_{D_{2i}}x}}{\Gamma(\tilde{m}_{D_{2i}})} \\
F_{|h_{R_iR_i}|^2}(x) &= \frac{\gamma\left(m_{R_iR_i}, m_{R_iR_i}x/\Omega_{R_iR_i}\right)}{\Gamma(m_{R_iR_i})} \\
f_{|h_{R_iR_i}|^2}(x) &= \frac{m_{R_iR_i}^{m_{R_iR_i}} x^{m_{R_iR_i}-1} e^{-m_{R_iR_i}x/\Omega_{R_iR_i}}}{\Omega_{R_iR_i}^{m_{R_iR_i}}\Gamma(m_{R_iR_i})}
\end{aligned}
\tag{7.30}
$$

After substitution of $F_{|g_{S_i}|^2}(x)$, $f_{|h_{S_i}|^2}(x)$, and $f_{|h_{R_iR_i}|^2}(x)$ in (7.28) and carrying out the following steps, the closed form of $F_{\gamma_{D_1}^{R_i}}(\gamma_{th_1})$ is derived as in (7.31):

- Firstly, use the equality for upper incomplete gamma function given in [65, eq. (8.352)]: $\gamma\big(m_{S_{1i}}, z\big) = (m_{S_{1i}}-1)!\Big[1 - e^{-z}\sum_{p_1=0}^{m_{S_{1i}}-1}\frac{z^{p_1}}{p1!}\Big]$.
- Secondly, apply Binomial theorem to the term $\big(a_2\rho_{S_{1i}}x + \varpi_i\rho_{R_i}y + 1\big)^{p_1}$ twice to obtain $\big(a_2\rho_{S_{1i}}x + \varpi_i\rho_{R_i}y + 1\big)^{p_1} = \sum_{p_2=0}^{p_1}\sum_{p_3=0}^{p_2}\binom{p_1}{p_2}\binom{p_2}{p_3}\big(a_2\rho_{S_{1i}}x\big)^{p_3}\big(\varpi_i\rho_{R_i}y\big)^{p_2-p_3}$.
- Finally, after proper rearrangement, obtain two integrals which are in the form of Gamma function given in [65, eq. (8.310)], namely, $\Gamma(z) = \int_0^\infty e^{-t}t^{z-1}dt$.

$$
\begin{aligned}
F_{\gamma_{D_1}^{R_i}}(\gamma_{th_1}) =& 1 - e^{-\frac{m_{S_{1i}}\gamma_{th_1}}{a_1\rho_{S_{1i}}\Omega_{S_{1i}}}}\sum_{p_1=0}^{m_{S_{1i}}-1}\sum_{p_2=0}^{p_1}\sum_{p_3=0}^{p_2}\Bigg[\Bigg\{\left(\frac{m_{S_{1i}}\gamma_{th_1}}{a_1\Omega_{S_{1i}}}\right)^{p_1}\left(\frac{a_2\Omega_{S_{2i}}}{m_{S_{2i}}}\right)^{p_3}\binom{p_1}{p_2}\\
&\binom{p_2}{p_3}\Gamma(p_3+m_{S_{2i}})\Gamma(p_2-p_3+m_{R_i})\left(\frac{\varpi_i\rho_{R_i}\Omega_{R_iR_i}}{m_{R_i}}\right)^{p_2-p_3}\Bigg\}\Bigg/\\
&\Bigg\{\Gamma(m_{S_{2i}})\Gamma(m_{R_i})\Gamma(p_1+1)\left(1+\frac{m_{S_{1i}}\gamma_{th_1}a_2\Omega_{S_{2i}}}{m_{S_{2i}}a_1m_{S_{1i}}}\right)^{m_{S_{2i}}+p_3}\\
&\left(1+\frac{m_{S_{1i}}\gamma_{th_1}\varpi_i\rho_{R_i}\Omega_{R_iR_i}}{m_{R_i}a_1\rho_{S_i}\Omega_{S_{1i}}}\right)^{m_{R_i}+p_2-p_3}(\rho_{S_i})^{p_1-p_3}\Bigg\}\Bigg].
\end{aligned}
\tag{7.31}
$$

The closed form of $F_{\gamma_{D_{1i}}^{D_1}}(\gamma_{th_1})$ is

$$
\begin{aligned}
F_{\gamma_{D_{1i}}^{D_1}}(\gamma_{th_1}) &= Pr(\gamma_{D_{1i}}^{D_1} < \gamma_{th_1})\\
&= Pr\Big(\frac{a_3\rho_{D_{1i}}|g_{R_{i1}}|^2}{a_4\rho_{D_{1i}}|g_{R_{i1}}|^2+1} < \gamma_{th_1}\Big)\\
&= \begin{cases} 1 & \gamma_{th_1} \geq \frac{a_3}{a_4} \\ Pr\big(|g_{R_{i1}}|^2 < \frac{\gamma_{th_1}}{a_3\rho_{D_{1i}}-a_4\rho_{D_{1i}}\gamma_{th_1}}\big) & \gamma_{th_1} < \frac{a_3}{a_4}\end{cases}.\\
&= \begin{cases} 1 & \gamma_{th_1} \geq \frac{a_3}{a_4} \\ \frac{\gamma\left(m_{D_{1i}}, \frac{m_{D_{1i}}\gamma_{th_1}}{\rho_{D_{1i}}\Omega_{D_{1i}}(a_3-a_4\gamma_{th_1})}\right)}{\Gamma(m_{D_{1i}})} & \gamma_{th_1} < \frac{a_3}{a_4}\end{cases}
\end{aligned}
\tag{7.32}
$$

In the same manner, $F_{\gamma_{D_{1i}}^{D_2}}(\gamma_{th_1})$ is

$$
\begin{aligned}
F_{\gamma_{D_{1i}}^{D_2}}(\gamma_{th_1}) &= Pr(\gamma_{D_{1i}}^{D_2} < \gamma_{th_1})\\
&= \begin{cases} 1 & \gamma_{th_1} \geq \frac{a_3}{a_4} \\ \frac{\gamma\left(m_{D_{2i}}, \frac{m_{D_{2i}}\gamma_{th_1}}{\rho_{D_{2i}}\Omega_{D_{2i}}(a_3-a_4\gamma_{th_1})}\right)}{\Gamma(m_{D_{2i}})} & \gamma_{th_1} < \frac{a_3}{a_4}\end{cases}.
\end{aligned}
\tag{7.33}
$$

Inserting complementaries of (7.31), (7.32), and (7.33) into (7.27) together with the fact that $\Gamma(m) = \gamma(m,x) + \Gamma(m,x)$, the closed form of $P_{SSRS}(\gamma_{th_1})$ reduces to (7.12).

7.7.2. Outage Probability Derivation of Two Stage Relay Selection

$P_{TSRS}(\gamma_{th_1}, \gamma_{th_2})$ is rearranged as

$$
\begin{aligned}
P_{TSRS}(\gamma_{th_1},\gamma_{th_2}) &= \sum_{l=0}^{L} Pr(\min(\gamma_{D_{2i_T}}^{D_2}, \gamma_{D_2}^{R_{i_T}}) < \gamma_{th_2}, |K_R| = l) \\
&= \sum_{l=0}^{L} Pr(\min(\gamma_{D_{2i_T}}^{D_2}, \gamma_{D_2}^{R_{i_T}}) < \gamma_{th_2} \big/ |K_R| = l) Pr(|K_R| = l) \\
&= \sum_{l=0}^{L} \prod_{\substack{j=1 \\ R_i \in K_R}}^{l} \big(1 - Pr\big(\min(\gamma_{D_{2i}}^{D_2}, \gamma_{D_2}^{R_i}) > \gamma_{th_2} \big/ R_i \in K_R\big)\big) Pr(|K_R| = l) \\
&= \sum_{l=0}^{L} \binom{L}{l} \prod_{\substack{j=1 \\ R_i \in K_R}}^{l} \big(1 - P_\phi(\gamma_{th_1},\gamma_{th_2})\big) \prod_{\substack{j=1 \\ R_i \notin K_R}}^{L-l} \big(1 - Pr(R_i \in K_R)\big) \\
&\quad \times \prod_{\substack{j=1 \\ R_i \in K_R}}^{l} Pr(R_i \in K_R)
\end{aligned}
\tag{7.34}
$$

The closed form expression of $Pr(R_i \in K_R)$ in (7.34) is obtained in the derivation of $P_{SSRS}(\gamma_{th_1})$ in (7.13) and $P_\phi(\gamma_{th_1},\gamma_{th_2}) = Pr(\min(\gamma_{D_{2i}}^{D_2}, \gamma_{D_2}^{R_i}) > \gamma_{th_2} / \min\{\gamma_{D_1}^{R_i}, \gamma_{D_{1i}}^{D_1}, \gamma_{D_{1i}}^{D_2}\} > \gamma_{th_1})$, by the aid of Bayes theorem, we get

$$
\begin{aligned}
P_\phi(\gamma_{th_1},\gamma_{th_2}) &= \frac{Pr(\min(\gamma_{D_{2i}}^{D_2}, \gamma_{D_2}^{R_i}) > \gamma_{th_2}, \min(\gamma_{D_1}^{R_i}, \gamma_{D_{1i}}^{D_1}, \gamma_{D_{1i}}^{D_2}) > \gamma_{th_1})}{P_{R_i \in K_R}(\gamma_{th_1})} \\
&= \frac{P_{\phi_1}(\gamma_{th_1},\gamma_{th_2}) P_{\phi_2}(\gamma_{th_1},\gamma_{th_2}) P_{\phi_3}(\gamma_{th_1},\gamma_{th_2})}{P_{R_i \in K_R}(\gamma_{th_1})}
\end{aligned}
\quad , \tag{7.35}
$$

where $Pr(\min(\gamma_{D_{2i}}^{D_2}, \gamma_{D_2}^{R_i}) > \gamma_{th_2}, \min(\gamma_{D_1}^{R_i}, \gamma_{D_{1i}}^{D_1}, \gamma_{D_{1i}}^{D_2}) > \gamma_{th_1}) = Pr\big(\gamma_{D_{2i}}^{D_2} > \gamma_{th_2}, \gamma_{D_2}^{R_i} > \gamma_{th_2}, \gamma_{D_1}^{R_i} > \gamma_{th_1}, \gamma_{D_{1i}}^{D_1} > \gamma_{th_1}, \gamma_{D_{1i}}^{D_2} > \gamma_{th_1}\big)$. Using the independence of the channels, it can be rephrased into three independent components as in the numerator of the second line of (7.35). These components, namely, $P_{\phi_1}(\gamma_{th_1},\gamma_{th_2})$, $P_{\phi_2}(\gamma_{th_1},\gamma_{th_2})$ and $P_{\phi_3}(\gamma_{th_1},\gamma_{th_2})$, are defined as follows:

$$
\begin{aligned}
P_{\phi_1}(\gamma_{th_1},\gamma_{th_2}) &= Pr\left(|\tilde{h}_{R_{i2}}|^2 > \frac{a_4\rho_{D_{2i}}|h_{R_{i2}}|^2-\gamma_{th_2}}{\gamma_{th_2}a_3\epsilon_{D_{2i}}\rho_{D_{2i}}}, |h_{R_{i2}}|^2 > \frac{\gamma_{th_1}}{a_3\rho_{D_{2i}}-a_4\rho_{D_{2i}}\gamma_{th_1}}\right)\\
&= Pr\left(|\tilde{h}_{R_{i2}}|^2 < \frac{a_4\rho_{D_{2i}}|h_{R_{i2}}|^2-\gamma_{th_2}}{\gamma_{th_2}a_3\epsilon_{D_{2i}}\rho_{D_{2i}}}, |h_{R_{i2}}|^2 > U_{max}\right)\\
P_{\phi_2}(\gamma_{th_1},\gamma_{th_2}) &= Pr\left(|g_{R_{i1}}|^2 > \frac{\gamma_{th_1}}{a_3\rho_{D_{1i}}-a_4\rho_{D_{1i}}\gamma_{th_1}}\right)\\
P_{\phi_3}(\gamma_{th_1},\gamma_{th_2}) &= Pr\Bigg(|h_{S_i}|^2 > \frac{\gamma_{th_2}\left(\varpi_i\rho_{R_i}|h_{R_iR_i}|^2+1\right)}{a_2\rho_{S_i}},\\
&\qquad |g_{S_i}|^2 > \frac{\gamma_{th_1}\left(a_2\rho_{S_i}|h_{S_i}|^2+\varpi_i\rho_{R_i}|h_{R_iR_i}|^2+1\right)}{a_1\rho_{S_i}}\Bigg).
\end{aligned}
\tag{7.36}
$$

where $U_{max} = \max\left(\frac{\gamma_{th_2}}{a_4\rho_{D_{2i}}}, \frac{\gamma_{th_1}}{\rho_{D_{2i}}(a_3-a_4\gamma_{th_1})}\right)$. To find closed form of $P_{\phi_1}(\gamma_{th_1},\gamma_{th_2})$, we need to take the integral given in (7.37):

$$
\begin{aligned}
P_{\phi_1}(\gamma_{th_1},\gamma_{th_2}) &= Pr\left(|\tilde{h}_{R_{i2}}|^2 < \frac{a_4\rho_{D_{2i}}|h_{R_{i2}}|^2-\gamma_{th_2}}{\gamma_{th_2}a_3\epsilon_{D_{2i}}\rho_{D_{2i}}}, |h_{R_{i2}}|^2 > U_{max}\right)\\
&= \int_{U_max}^{\infty} F_{|\tilde{h}_{R_{i2}}|^2}\left(\frac{a_4\rho_{D_{2i}}x-\gamma_{th_2}}{\gamma_{th_2}a_3\epsilon_{D_{2i}}\rho_{D_{2i}}}\right) f_{|h_{R_{i2}}|^2}(x)dx.
\end{aligned}
\tag{7.37}
$$

and it is attained as in (7.17) after implementation of the following steps:

- Firstly, insert equivalences of $F_{|\tilde{h}_{R_{i2}}|^2}(x)$ and $f_{|h_{R_{i2}}|^2}(x)$ from (7.30) and (7.29) into (7.37).
- Secondly, insert the identity [65, eq. (8.352.1)] for lower incomplete Gamma function into (7.37) to obtain $\gamma\left(\tilde{m}_{D_{2i}},z\right) = (\tilde{m}_{D_{2i}}-1)!\left[1-e^{-z}\sum_{p_1=0}^{\tilde{m}_{D_{2i}}-1}\frac{z^{p_1}}{p1!}\right]$.
- Thirdly, use Binomial theorem to get $\left(\frac{a_4\rho_{D_{2i}}}{\gamma_{th_2}}x-1\right)^{p_1} = \sum_{p_2=0}^{p_1}\binom{p_1}{p_2}(-1)^{p_1-p_2}\left(\frac{a_4\rho_{D_{2i}}}{\gamma_{th_2}}x\right)^{p_2}$.
- Finally, after proper rearrangements, use the identity [65, eq. (8.350.2)] for upper incomplete Gamma function, namely, $\Gamma(z,x) = \int_x^{\infty} e^{-t}t^{z-1}dt$ to get closed form of the integral in (7.37), thereafter, closed form of $P_{\phi_1}(\gamma_{th_1},\gamma_{th_2})$ is reached as given in (7.17).

The second probability, $P_{\phi_2}(\gamma_{th_1},\gamma_{th_2})$, is

$$
P_{\phi_2}(\gamma_{th_1},\gamma_{th_2}) = \begin{cases} 0 & \gamma_{th_1} \geq \frac{a_3}{a_4} \\ 1-\dfrac{\gamma\left(m_{D_{1i}}, \frac{m_{D_{1i}}\gamma_{th_1}}{\rho_{D_{1i}}\Omega_{D_{1i}}(a_3-\gamma_{th_1}a_4)}\right)}{\Gamma(m_{D_{1i}})} & \gamma_{th_1} < \frac{a_3}{a_4} \end{cases}
\tag{7.38}
$$

and the third part of $P_{\phi}(\gamma_{th_1},\gamma_{th_2})$ can be derived as

$$P_{\phi_3}(\gamma_{th_1},\gamma_{th_2}) = \int_0^\infty \int_0^\infty \int_{\frac{\gamma_{th_2}\left(a_1\epsilon_{R_i}\rho_{S_i}\psi+\varpi_i\rho_{R_i}z+1\right)}{a_2\rho_{S_i}}}^\infty \int_{\frac{\gamma_{th_1}\left(a_2\rho_{S_i}y+\varpi_i\rho_{R_i}z+1\right)}{a_1\rho_{S_i}}}^\infty f_{|g_{S_i}|^2}(x)$$
$$f_{|h_{S_i}|^2}(y) f_{|h_{R_iR_i}|^2}(z) f_{|\tilde{g}_{S_i}|^2}(\psi) dx dy dz d\psi. \tag{7.39}$$

The closed form of $P_{\phi_3}(\gamma_{th_1},\gamma_{th_2})$ can be derived after carrying out the steps provided below:

- The order of integration is respectively with respect to x, y, z, and ψ.
- Substitute equivalences of $f_{|g_{S_i}|^2}(x)$, $f_{|h_{S_i}|^2}(y)$, $f_{|h_{R_iR_i}|^2}(z)$, and $f_{|\tilde{g}_{S_i}|^2}(\psi)$ into (7.39) from (7.29) and (7.30). Then make change of variable for x to convert the integral into the form of upper incomplete Gamma function [65, eq. (8.350.2)].
- Use the identity given in [65, eq. (8.350.2)] for upper incomplete Gamma function to obtain $\Gamma(m_{S_{1i}},x) = \Gamma(m_{S_{1i}})e^{-x}\sum_{q_1=0}^{m_{S_{1i}}-1}\frac{x^{q_1}}{\Gamma(q_1+1)}$.
- Apply Binomial theorem twice to derive $(a_2\rho_{S_i}y+\varpi_i\rho_{R_i}z+1)^{q_1} = \sum_{q_2=0}^{q_1}\sum_{q_3=0}^{q_2}\binom{q_1}{q_2}\binom{q_2}{q_3}(a_2\rho_{S_i}y)^{q_2}(\varpi_i\rho_{R_i}z)^{q_2-q_3}$ and represent the triple summations as $\sum_{q_1=0}^{m_{S_{1i}}-1}\sum_{q_2=0}^{q_1}\sum_{q_3=0}^{q_2} = \sum_{(q_1,q_2,q_3)=\overrightarrow{0}}^{(m_{S_{1i}}-1,q_1,q_2)}$, where $\overrightarrow{0}$ is a three dimensional zero vector.
- Integration over y is similar to integration over x. Therefore, track the same steps: Use expansion of upper incomplete Gamma function for integer numbers to get $\Gamma(q_3+m_{S_{2i}},x) = \Gamma(q_3+m_{S_{2i}})e^{-x}\sum_{k_1=0}^{q_3+m_{S_{2i}}-1}\frac{x^{k_1}}{\Gamma(k_1+1)}$. Then, apply Binomial theorem twice to derive $(a_1\epsilon_{R_i}\rho_{S_i}\psi+\varpi_i\rho_{R_i}z+1)^{k_1} = \sum_{k_2=0}^{k_1}\sum_{k_3=0}^{k_2}\binom{k_1}{k_2}\binom{k_2}{k_3}(a_1\epsilon_{R_i}\rho_{S_i}\psi)^{k_2}(\varpi_i\rho_{R_i}z)^{k_2-k_3}$ and represent the triple summations as $\sum_{k_1=0}^{q_3+m_{S_{2i}}-1}\sum_{k_2=0}^{k_1}\sum_{k_3=0}^{k_2} = \sum_{(k_1,k_2,k_3)=\overrightarrow{0}}^{(q_3+m_{S_{2i}}-1,k_1,k_2)}$.
- After proper simplifications, remaining two integrals are independent of each other and in the form of Gamma function given in [65, eq. (8.310)] which completes closed form derivation of $P_{\phi_3}(\gamma_{th_1},\gamma_{th_2})$ provided in (7.19).

8. RELAY SELECTION FOR NOMA BASED COOPERATIVE NETWORKS OVER SHADOWED FADING CHANNELS

8.1. Introduction

Spectral efficiency, services with high data rates, and massive connectivity are the main factors to be satisfied in the next generation wireless communication systems. Especially, to overcome exponentially growing mobile data volume, simultaneously transmission of different data types is the key factor in the fifth generation (5G) communication systems and beyond [2]. The volume of worldwide mobile data has been predicted to be about 136 exabytes or 5 zettabytes per month [3, 4]. This enormously growing demand means more spectrum should be used. But more spectrum is only possible in millimeter-wave (mmWave) bands, however, transmission in mmWave bands comes with many challenges such as high path losses, blockages, and poor signal diffraction properties [5].

Multi-input multi-output (MIMO) technique increases data rate [91], and likely, orthogonal frequency division multiplexing. Unfortunately, these methods also remain insufficient to fulfill ever-increasing mobile data demand. Hence, full-duplex (FD) transmission protocol, which always transmits and receives in the entire bandwidth, has been offered to double the data rate [10]. Although, efficient self-interference (SI) cancellation methods are available [11], this theoretical limit is unreachable since there is no possibility to entirely cancel out SI due to the large power difference between the power imposed by own transmissions and the low-power received signals arriving from remote transmit antennas. Another issue that cannot be addressed by the stated techniques is the sharing of block sources like time slots and frequency bands. Wasting of such sources disturbs researchers and, to cope with this un-solicited status, eventually non-orthogonal multiple access (NOMA) technique has been offered for high spectral efficiency, low-latency, reliable, and fairness wireless connectivity [12–15]. NOMA is applied in code or power domain. The superimposed signals are decomposed at multiple receivers by application of successive interference cancellation (SIC) technology to extract their own messages. In practical implementations, perfect SIC (pSIC) cancellation is infeasible, therefore, imperfect SIC (ipSIC) is a bottleneck of NOMA to be taken into consideration.

MIMO NOMA is introduced in [166] and demonstrated that it outperforms traditional orthogonal multiple access (OMA) technique. In addition to extending coverage area, consuming less power, improving reliability and security, cooperative relaying virtually forms a MIMO system. Therefore, it has been combined with NOMA technique to improve performance further [143]. Additionally, multi-relay systems with relay selection (RS) have inclusively been offered and investigated for both amplify/decode-and-forward (AF/DF) protocols to overcome deep fading over Rayleigh and Nakagami-m fades [41–49, 149, 150, 167]. Outage probability (OP) is commonly used as a performance evaluation parameter but sum rate is also considered. Unlike traditional OMA networks, it is impossible to select an optimum relay to simultaneously serve multiple users in NOMA networks. Hence, some preconditions such as service priority [41, 42], decoding of coded/joint modulated signals at relays (but in that case NOMA is only implemented at the relays/second hop) [45, 150], and buffer-aided transmission where access protocol is also considered/selected together with the link between the relay and source providing total target data rate (selection of this link named as partial RS [47]) [149] are assigned. After satisfaction of preconditions, a relay is selected in two stages. Moreover, RS is considered not only with fixed total number of relays but also with governing by a Poisson point process [43, 48], where nearly the same analyses are provided. Some analyses provide max-min criterion, which is a sub-optimum method, for comparison purpose together with the offered two-stage RS schemes [41]. Briefly, implementation of RS is attractive and essential to provide diversity.

Transmission in mmWave bands gives rise to high path loss, blockages, and poor diffraction properties, where attenuations in the range 28 dB–40 dB are reported [5]. Similar results have been previously provided; a person blocking line-of-sight (LOS) can lead to an attenuation up to 20 dB [168]. Therefore, modeling the wireless medium even as Nakagami-m fade remains inadequate, in sequence, analyses depending on such distribution models avoid comprehensive understanding of transmission techniques. Thereby, the systems under consideration should be investigated for both small-scale and large-scale faded transmission medium. To model such environments, composite distributions such as Rayleigh/Log-normal, Rician/Log-normal, and Nakagami/Log-normal are proposed, however, it is mathematically intractable to analyze the systems for such composite distributions. As an approximation, generalized-K distribution (GKD) is offered.

RS implementing NOMA technique is almost focused and studied over Rayleigh fading [41–48, 149, 150] except [49, 167] over Nakagami-m fading channels, where RS

for HD transmission protocol with pSIC and imperfect channel estimations is investigated in [49] and partial RS for HD with ipSIC and imperfect channel estimations in [167]. However, RS for FD transmission with ipSIC has not been given in any work ([43] is devoted to only pSIC in Rayleigh fading channel). FD transmission with ipSIC over Nakagami-m fade is carried out for a system consisting of a base station and two users, base station directly communicates with the near user, while it requires the help of a dedicated FD relay to communicate with the far user [169]. Apparently, even for Nakagami-m fading channels, RS for FD transmission has not been addressed yet and practical implementation of SIC, i.e., imperfect SIC has not been studied for RS, either.

In whole, by the motivation stated above, for a comprehensive analysis, RS in this work is investigated over independent-identically distributed (i.i.d.) generalized-K fading channels for a system consisting of a source, multiple HD/FD relays using DF protocol, and two far users without LOS between the source and them. Downlink NOMA with fixed power allocations (PAs) is used at both hops, namely, at the source and the relays. A two-stage RS scheme offered in [41], where decomposition of the messages belonging to user 1 is provided and then data rate of user 2 is maximized, i.e., priority is given to user 1, is implemented. SI and ipSIC are assumed to have Nakagami-m distribution. OP is focused, where SI variance is supposed to be exponentially and linearly dependent on transmitted power of the relay, therefore, both fading and non-fading SI cases are easily investigated by a single OP expression in addition to ipSIC at the relays and user 2.

The main contributions of this chapter can be summarized as follows:

- A slightly different but less complex cumulative distribution function (CDF) expression for square of a GKD random variable (RV), in turn for GKD RV, is obtained. Thereafter, approximated probability density function (PDF) and CDF expressions are offered based on generalized Gauss–Laguerre quadrature which are more robust and efficient than the approximation offered based on Gauss–Laguerre quadrature. Later approximation works from an analytical perspective, but it is not always numerically stable. Furthermore, approximation based on generalized Gauss–Laguerre quadrature approach is numerically stable, whereas CDFs based on generalized Hypergeometric function, Meijer's-G function, and Gauss–Laguerre quadrature are not stable at high values. Additionally, CDF expressed in terms of generalized Hypergeometric function can not be used for the case when the difference between the fading and shadowing factors is an integer but the proposed solution works.
- Approximated and asymptotic OP expressions are derived over i.i.d. slow

generalized-K fading channels for both HD and FD transmission with not only pSIC but also ipSIC, and their validity is verified via Monte Carlo simulation technique. Additionally, to demonstrate correctness of the proposed approximated PDF and CDF, OP expression for HD transmission based on pSIC assumption is also provided.

- For HD transmission, error floor of OP is dependent on the channel characteristics including that of ipSIC and PA factors but not on the transmitted power. Similarly, in addition to deductions for HD transmission, for FD transmission error floor is also dependent on the channel characteristics of SI. Insufficient SI cancellation leads to error floor like ipSIC. Moreover, effect of ipSIC at the selected relay and second user can be individually observed from the derived OP expression, likely, effect of SI. It is shown that ipSIC at the selected relay is more effective than the one at the second user.
- Contrary to common acceptance, nonzero diversity order assertion is provided and its dependence on channel characteristics is also omitted. Unlike channel characteristics, number of uncorrelated/independent multipaths is effective. If there are L relays/antennas at both transmitter and receiver or uncorrelated/independent paths at the receiver where multipath/Rake diversity is considered, diversity order is L even if error probability is saturated, i.e., it reaches to an error floor no matter what the type of channel is.

The remainder of this chapter is organized as follows. In Section 8.2, details of system model are provided. RS criterion is given in Section 8.3. The details of proposed approximated PDF and CDF are provided in Section 8.4. Section 8.5 includes derivations of approximated OP and asymptotic expression is given in Section 8.6. Numerical results are elaborated in Section 8.7. Finally, we conclude our work in Section 8.8.

8.2. System Model

We consider a multiple relay system with a source, S, and two users (D_1 and D_2) as depicted in Fig. 8.1. Due to deep fading and shadowing, there is no LOS between the source and users, and the communication is conducted via L FD/HD multiple relays with DF protocol. The information signals are assumed to have unit energy. A relay is selected to maximize the data rate of the second user but also providing service quality priority for user 1, D_1. The transmission is done via downlink NOMA. Without loss

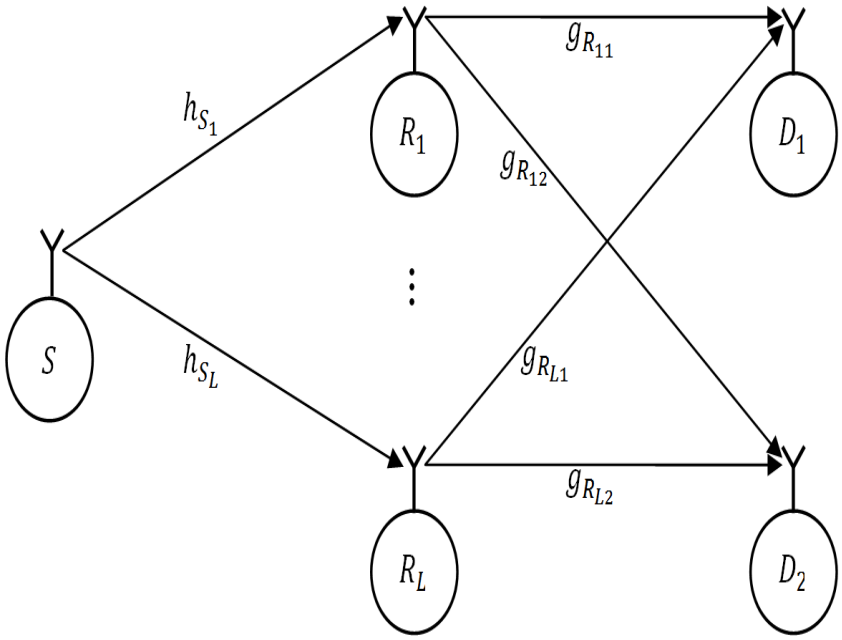

Figure 8.1: Multi-relay system.

of generality, relays are assumed to be clustered such that they are at the origin of the system. The PA coefficients at the S are represented as a_1 and a_2, where $a_1 + a_2 = 1$ and $a_1 > a_2$. Similarly, after DF process at the selected relay, detected signals are weighted in accordance with the service quality priority by PA coefficients a_3 and a_4, where $a_3 + a_4 = 1$ and $a_3 > a_4$. The relays are equipped with one transmit and one receive antennas. All channel gains are assumed to have generalized-K distribution, whereas SI and ipSIC are Nakagami-m distributed. The channel gains of the links S—i^{th} relay, i^{th} relay—D_1, i^{th} relay—D_2, ipSIC at the i^{th} relay, ipSIC at the D_2, and SI are h_{S_i}, $g_{R_{i1}}$, $g_{R_{i2}}$, $\tilde{g}_{R_i}$, $\tilde{g}_{D2}$ and $h_{R_iR_i}$, respectively. The characteristics of a GKD RV are represented by a quadruple $(m_f, m_s, \Omega_f, \Omega_s)$, where m_f, m_s, Ω_f, and Ω_s represent fading shape factor, shadowing shape factor, fading scale factor, and shadowing scale factor, respectively. We also use this quadruple representation for characteristics of the channel gains between the S and relays. However, the characteristics of the channel gains between the relays and D_1, and relays and D_2 are denoted by $(m_{D_1f}, m_{D_1s}, \Omega_{D_1f}, \Omega_{D_1s})$ and $(m_{D_2f}, m_{D_2s}, \Omega_{D_2f}, \Omega_{D_2s})$, respectively. The fading shape and scale parameters of the channel gains $\tilde{g}_R$, $\tilde{g}_{D2}$ and $h_{R_iR_i}$ are $(\tilde{m}_R, 1)$, $(\tilde{m}_{D2}, 1)$, and $(m_{RR}, \Omega_{R_iR_i} = \kappa_i P_{R_i}^{\vartheta_i - 1})$, respectively, where κ_i and ϑ_i are linear and exponential cancellation/attenuation factors depicting dependence of SI on the transmitted power, P_{R_i}, from each relay and both vary between 0 and 1, allows to individually investigate effect of SI and ipSIC on error floors. Finally, $\min(m_f, m_s)$, $\min(m_{D_2f}, m_{D_2s})$, and $\tilde{m}_R$ are assumed to take integer values.

The received signal at the i^{th} relay, where time indexing is omitted, is

$$Y_{R_i} = h_{S_i}(\sqrt{a_1 P_S}x_1 + \sqrt{a_2 P_S}x_2) + \varpi_i h_{R_i R_i} x_{R_i} + n_{R_i}, \tag{8.1}$$

where P_S is the source power, and x_1 and x_2 are the symbols transmitted to the first and second users, respectively, $x_{R_i} = \sqrt{a_3 P_{R_i}}\hat{x}_1 + \sqrt{a_4 P_{R_i}}\hat{x}_2$, $\hat{x}_1$ and $\hat{x}_2$ are previously decoded signals by SIC process. ϖ_i is 0 for HD and 1 for FD transmission. n_{R_i} is the additive Gaussian noise at relay i. Decoded signals are weighted in accordance with the service quality priority and retransmitted. Signal-to-interference-plus-noise ratio (SINR) related to the signal of the first user at the i^{th} relay is

$$\gamma_{D_1}^{R_i} = \frac{a_1 \rho_{S_i} |h_{S_i}|^2}{a_2 \rho_{S_i} |h_{S_i}|^2 + \varpi_i \rho_{R_i} |h_{R_i R_i}|^2 + 1}, \tag{8.2}$$

where $\rho_{S_i} = \frac{P_S}{\sigma_{R_i}^2}$, $\rho_{R_i} = \frac{P_{R_i}}{\sigma_{R_i}^2}$, and $\sigma_{R_i}^2$ is the variance of the additive Gaussian noise at relay i. Absolute value operator is represented by $|\cdot|$. SINR related to the signal of the second user at the i^{th} relay is

$$\gamma_{D_2}^{R_i} = \frac{a_2 \rho_{S_i} |h_{S_i}|^2}{a_1 \epsilon_{R_i} \rho_{S_i} |\tilde{g}_{R_i}|^2 + \varpi \rho_{R_i} |h_{R_i R_i}|^2 + 1}, \tag{8.3}$$

where ϵ_{R_i} models the amount of the ipSIC at the i^{th} relay and $0 \leq \epsilon_{R_i} \leq 1$.

The received signals at the destinations are

$$Y_{D_1} = \sqrt{a_3 P_{R_i}} g_{R_{i1}} x_1 + \sqrt{a_4 P_{R_i}} g_{R_{i1}} x_2 + n_{D_1} \tag{8.4}$$

and

$$Y_{D_2} = \sqrt{a_3 P_{R_i}} g_{R_{i2}} x_1 + \sqrt{a_4 P_{R_i}} g_{R_{i2}} x_2 + n_{D_2}. \tag{8.5}$$

n_{D_1} and n_{D_2} are the additive Gaussian noise at the destinations. The SINR related to the signal of the first user at itself is

$$\gamma_{D_{1i}}^{D_1} = \frac{a_3 \rho_{D_{1i}} |g_{R_{i1}}|^2}{a_4 \rho_{D_{1i}} |g_{R_{i1}}|^2 + 1}, \tag{8.6}$$

where $\rho_{D_{1i}} = \frac{P_{R_i}}{\sigma_{D_1}^2}$ and $\sigma_{D_1}^2$ is the noise variance at user 1. Similarly, SINR related to the signal of the first user at user 2 is

$$\gamma_{D_{1i}}^{D_2} = \frac{a_3 \rho_{D_{2i}} |g_{R_{i2}}|^2}{a_4 \rho_{D_{2i}} |g_{R_{i2}}|^2 + 1} \tag{8.7}$$

and SINR related to the signal of the second user at itself is

$$\gamma_{D_{2i}}^{D_2} = \frac{a_4 \rho_{D_{2i}} |g_{R_{i2}}|^2}{a_3 \epsilon_{D_2} \rho_{D_{2i}} |\tilde{g}_{D2}|^2 + 1}. \tag{8.8}$$

$\rho_{D_{2i}} = \frac{P_{R_i}}{\sigma_{D_2}^2}$, $\sigma_{D_2}^2$ is the variance of the noise at user 2, ϵ_{D_2} models the amount of the ipSIC at user 2 and $0 \leq \epsilon_{D_2} \leq 1$. Note that ρ_{S_i} and ρ_{R_i} in (8.2), $\rho_{D_{1i}}$ in (8.6), and $\rho_{D_{2i}}$ in (8.7) and (8.8) are signal-to-noise ratios (SNRs)

8.3. Relay Selection

The selection criterion used in this work has been offered in [41], where two stage RS firstly determines a set of relays ensuring service quality for user 1 (ensure messages of user 1 are decomposed at three nodes, namely, at the relay and both users) and then selecting a relay maximizing data rate of user 2. So the set of relays providing service quality priority condition is determined as follows:

$$\begin{aligned} K_R = \{\log(1+\gamma_{D_1}^{R_i}) \geq R_{D_1}, \log(1+\gamma_{D_1 i}^{D_1}) \geq R_{D_1}, \log(1+\gamma_{D_1 i}^{D_2}) \geq R_{D_1}\}, \\ i \in \{1, \cdots, L\}\}. \end{aligned} \tag{8.9}$$

R_{D_1} is the data rate of the D_1. This condition focuses on the decomposition of the signal of the first user at all three nodes, namely, at the relay, user 1, and user 2. Then, the relay maximizing data rate of D_2 is found as

$$i_T = \arg\max_i \{\min\{\log(1+\gamma_{D_2}^{R_i}), \log(1+\gamma_{D_{2i}}^{D_2})\}, i \in K_R\}. \tag{8.10}$$

Since a decision is made on the selected relay in (8.9) and (8.10) the prefactor $1/2$, which does not have any impact on the selected relay, is omitted for HD transmission.

8.4. Exact and Approximated PDF and CDF of Square of Generalized-*K* Distribution

In this section, PDF and CDF of square of a GKD RV are provided.

Let Y be a GKD RV and $X = |Y|^2$. In this case PDF of X for RV Y with characteristics $(m_f, m_s, \Omega_f, \Omega_s)$ is [66]

$$f_X(x) = \frac{2}{\Gamma(m_f)\Gamma(m_s)} b^{m_f+m_s} x^{\frac{m_f+m_s}{2}-1} K_{m_s-m_f}(2b\sqrt{x}). \tag{8.11}$$

where $b = \sqrt{\frac{m_f m_s}{\Omega_f \Omega_s}}$, $\Gamma(x)$ represents the gamma function [65, eq. (8.310.1)], and $K_\nu(x)$ is the ν^{th} order modified Bessel function of the second kind [65, eq. (8.432.6)].

Although, CDF for RV X is available in the literature [170, eq. (3)], we use the identity [67, eq. 1.12.1.2] and obtain a slightly different formula as

$$\begin{aligned} F_X(x) =& \frac{\Gamma(m_s - m_f)(b^2x)^{m_f}}{\Gamma(m_s)\Gamma(m_f+1)} {}_1F_2(m_f; m_f - m_s + 1, m_f + 1; b^2x) \\ &+ \frac{\Gamma(m_f - m_s)(b^2x)^{m_s}}{\Gamma(m_f)\Gamma(m_s+1)} {}_1F_2(m_s; m_s - m_f + 1, m_s + 1; b^2x), \end{aligned} \tag{8.12}$$

where ${}_1F_2(m; \nu, n; x)$ is the generalized hypergeometric function [65, eq. (9.14.1)]. Note that, there is no cosecant function in this formula and minus in front of the second term is canceled out while compared to the formula given in the literature. A critical point is that due to the generalized hypergeometric function, $F_X(x)$ does not preserve to be a CDF function at high x values. In this work, high x values take place in the cases of sufficient SI cancellation (combination of small κ_i and ϑ_i) and nearly perfect SIC (small ϵ_{D_2} and ϵ_{R_i}). The same deduction is also valid for Meijer's-G function formulation of this CDF. Furthermore, gamma function, $\Gamma(x)$, cannot be evaluated for negative integers, which means cases with integer value of $m_s - m_f$ or $m_f - m_s$ cannot be evaluated from the above form. Therefore, another representation of $F_X(x)$ becomes essential for our system analysis. As a solution the approximation of the PDF based on Gauss–Laguerre quadrature can be used, however, this approximation which named as mixture gamma distribution is not stable, either to analyze the system under consideration [171]. Hence, we offer the following approximation for the PDF, $f_X(x)$, based on generalized Gauss–Laguerre quadrature by using the identity [65, eq. (8.432.6)] for negative values, i.e., we use the fact $K_{m_s-m_f}(2b\sqrt{x}) = K_{-|m_s-m_f|}(2b\sqrt{x})$:

$$\tilde{f}_X(x) = \sum_{p=1}^{N} \left(\frac{W_p b^{2G_{ds}} x^{G_{ds}-1}}{\Gamma(m_f)\Gamma(m_s)} e^{-\frac{b^2}{T_p}x} \right) \tag{8.13}$$

where $G_{ds} = \min(m_f, m_s)$ and normalized Laguerre polynomial for generalized Gauss–Laguerre quadrature is chosen as $L(x, N, \beta) = \sum_{p=0}^{N} \binom{n+\beta}{n-p} \frac{(-x)^p}{\Gamma(p+1)}$. $\binom{n+\beta}{n-p}$

represents the Binomial coefficients and $\beta = |m_s - m_f|$ in the above approximation. T_p is the p^{th} zero of Laguerre polynomial $L(x, N, \beta)$. Therefore, the corresponding weight coefficients are calculated as $W_p = \frac{\Gamma(N+\beta+1)T_p}{\Gamma(N+1)[(N+1)L(x,N+1,\beta)]^2}$ [172]. In sequence, the approximated CDF, $F_X(x)$, is

$$\tilde{F}_X(x) = \sum_{p=1}^{N} \left(\frac{W_p T_p^{G_{ds}}}{\Gamma(m_f)\Gamma(m_s)} \gamma \left(G_{ds}, \frac{b^2}{T_p} x \right) \right), \tag{8.14}$$

where $\gamma(m, x)$ is the lower incomplete gamma function [65, eq. (8.350.1)].

On the other hand, it is possible that the above approximated CDF produces values slightly larger than 1 which violates CDF properties. Hence, a normalization is unavoidable. As x goes to infinity, $\tilde{F}_X(x)$ approaches to $W_{norm} = \sum_{p=1}^{N} \left(\frac{W_p T_p^{G_{ds}} \Gamma(G_{ds}+1)}{\Gamma(m_f)\Gamma(m_s)} \right)$. So using this normalization coefficient, W_p in (8.13) and (8.14) can be updated as $W_p := \frac{W_p}{W_{norm}}$.

As previously mentioned, the above representation is also used for the channels between the source and relays. The parameters in the approximation for the channels between the relays and user 1, $g_{R_{i1}}$, are denoted by G_{d1}, $W_{p,1}$, and $T_{p,1}$. For $g_{R_{i2}}$, the representations are G_{d2}, $W_{p,2}$, and $T_{p,2}$. Additionally, the total number of terms in the approximation, N, is taken to be 20 in all numerical calculations.

8.5. Exact Outage Probability

To find the OP, outage of the second user is divided into two parts, namely, the first component corresponds to K_R being an empty set and the second one is the situation even the K_R is not an empty set, the second user is in outage. However, it is not necessary to separate the outage condition into two components. Additionally, we introduce another pretty expression which is simpler than the methodology used in [41] for i.i.d. channel assumptions and, thereafter, in many other works. The reason for keeping the stated approach is that it can be used for future works on independent non-identically distributed (i.n.i.d.) channel assumptions where provided OP expression cannot be simplified by Binomial expansion equality. Moreover, the derived probability components related to a relay being in K_R can be used as a reference in future works. Having data rates of user 1 and 2 denoted by R_{D_1} and R_{D_2}, respectively, tracking the methodology of [41], OP can be expressed as follows.

$$
\begin{aligned}
P(\gamma_{th_1},\gamma_{th_2}) &= \sum_{l=0}^{L} Pr(\min(\gamma_{D_{2i_T^*}}^{D_2}, \gamma_{D_2}^{R_{i_T^*}}) < \gamma_{th_2}, |K_R| = l) \\
&= \sum_{l=0}^{L} Pr(\min(\gamma_{D_{2i_T^*}}^{D_2}, \gamma_{D_2}^{R_{i_T^*}}) < \gamma_{th_2} \big/ |K_R| = l) Pr(|K_R| = l) \\
&= \sum_{l=0}^{L} \big[1 - Pr\big(\min(\gamma_{D_{2i}}^{D_2}, \gamma_{D_2}^{R_i}) > \gamma_{th_2} \big/ R_i \in K_R\big)\big]^l Pr(|K_R| = l) \\
&= \sum_{l=0}^{L} \binom{L}{l} \big[1 - P_\phi(\gamma_{th_1},\gamma_{th_2})\big]^l \big[Pr(R_i \in K_R)\big]^l \\
&\qquad \big[1 - Pr(R_i \in K_R)\big]^{L-l}
\end{aligned}
\tag{8.15}
$$

where this probability is valid for $\gamma_{th_1} < \min\left(\frac{a_1}{a_2}, \frac{a_3}{a_4}\right)$, otherwise it is zero. The SINR threshold, γ_{th_i} where $i \in \{1,2\}$, for HD and FD transmissions are $\gamma_{th_i} = 2^{2R_{D_i}} - 1$ and $\gamma_{th_i} = 2^{R_{D_i}} - 1$, respectively. The $|K_R|$ is the cardinality of K_R. $Pr(R_i \in K_R) = Pr(\gamma_{D_1}^{R_i} > \gamma_{th_1}) Pr(\gamma_{D_{1i}}^{D_1} > \gamma_{th_1}) Pr(\gamma_{D_{1i}}^{D_2} > \gamma_{th_1})$ and derived as in (8.16) (Please see Appendix A for the derivation).

$$
\begin{aligned}
P_{R_i \in K_R}(\gamma_{th_1}) = \sum_{p=1}^{N} \sum_{k=0}^{G_{ds}-1} \sum_{k_1=0}^{k} \Bigg[& \frac{W_p T_p^{G_{ds}} \binom{k}{k_1} m_{R_iR_i}^{m_{R_iR_i}} (\varpi_i \rho_{R_i})^{k_1} \Gamma(G_{ds}) \Gamma(k_1 + m_{R_iR_i})}{\Gamma(m_f)\Gamma(m_s)\Gamma(k+1)\Gamma(m_{R_iR_i}) \Omega_{R_iR_i}^{m_{R_iR_i}}} \\
& \times \frac{\left(\frac{b^2 \gamma_{th_1}}{T_p \rho_{S_i}(a_1 - a_2\gamma_{th_1})}\right)^k}{\left(\frac{m_{R_iR_i}}{\Omega_{R_iR_i}} + \frac{b^2 \gamma_{th_1} \varpi_i \rho_{R_i}}{T_p \rho_{S_i}(a_1 - a_2\gamma_{th_1})}\right)^{k_1 + m_{R_iR_i}}} e^{-\frac{b^2 \gamma_{th_1}}{T_p \rho_{S_i}(a_1 - a_2\gamma_{th_1})}} \Bigg] \\
& \times \left[1 - F_{|g_{R_{i1}}|^2}\left(\frac{\gamma_{th_1}}{\rho_{D_{1i}}(a_3 - a_4\gamma_{th_1})}\right)\right] \left[1 - F_{|g_{R_{i2}}|^2}\left(\frac{\gamma_{th_1}}{\rho_{D_{2i}}(a_3 - a_4\gamma_{th_1})}\right)\right].
\end{aligned}
\tag{8.16}
$$

The conditional probability is $P_\phi(\gamma_{th_1},\gamma_{th_2}) = Pr(\min(\gamma_{D_{2i}}^{D_2}, \gamma_{D_2}^{R_i}) > \gamma_{th_2} / \min\{\gamma_{D_1}^{R_i}, \gamma_{D_{1i}}^{D_1}, \gamma_{D_{1i}}^{D_2}\} > \gamma_{th_1})$ and it can be reformulated by considering the Bayes theorem as in (8.17) (Please refer to Appendix B for the derivations of closed forms).

$$
P_\phi(\gamma_{th_1},\gamma_{th_2}) = \frac{P_{\phi_1}(\gamma_{th_1},\gamma_{th_2}) P_{\phi_2}(\gamma_{th_1},\gamma_{th_2}) P_{\gamma_{D_{1i}}^{D_1}}(\gamma_{th_1})}{P_{R_i \in K_R}(\gamma_{th_1})},
\tag{8.17}
$$

where the components of the numerator are defined in (8.36) and (8.39). Independence of channels, in turn, SINRs without a common channel gain, allows decomposition of the numerator into three components. Note that $P_{\gamma_{D_{1i}}^{D_1}}(\gamma_{th_1}) = Pr\left(\gamma_{D_{1i}}^{D_1} > \gamma_{th_1}\right)$ is the common term in the numerator and denominator ($P_{R_i \in K_R}(\gamma_{th_1})$ also includes this term) of $P_\phi(\gamma_{th_1},\gamma_{th_2})$, which cancels out and means conditional probability is independent

of the condition $\gamma_{D_{1i}}^{D_1} > \gamma_{th_1}$. However, we keep this term for the sake of the clarity, simplicity, and legibility. Now, let us again focus on the last line of (8.15) with the fact that $P_\phi(\gamma_{th_1}, \gamma_{th_2})$ can be expressed as in (8.17): Substituting this expression in the last line of (8.15), making proper cancellations, and considering the expansion of Binomial theorem, (8.15) reduces to

$$\begin{aligned} P(\gamma_{th_1}, \gamma_{th_2}) &= \sum_{l=0}^{L} \left(\binom{L}{l} \big[Pr(R_i \in K_R) - P_{\phi_1}(\gamma_{th_1}, \gamma_{th_2}) P_{\phi_2}(\gamma_{th_1}, \gamma_{th_2}) \right. \\ &\qquad \left. \times P_{\gamma_{D_{1i}}^{D_1}}(\gamma_{th_1}) \big]^l \big[1 - Pr(R_i \in K_R) \big]^{L-l} \right) \\ &= \left(1 - P_{\phi_1}(\gamma_{th_1}, \gamma_{th_2}) P_{\phi_2}(\gamma_{th_1}, \gamma_{th_2}) P_{\gamma_{D_{1i}}^{D_1}}(\gamma_{th_1}) \right)^L \end{aligned} \quad . \tag{8.18}$$

Alternatively, this result for i.i.d. assumption of all channel gains can also be reached by considering the OP of the investigated system with a single relay providing the same condition, i.e. accomplishing decomposition of the signals transmitted for user 1. For the second user, the coverage probability which is complementary of OP can be found as $Pr\big(\min(\gamma_{D_{2i}}^{D_2}, \gamma_{D_2}^{R_i}) > \gamma_{th_2}, \min\{\gamma_{D_1}^{R_i}, \gamma_{D_{1i}}^{D_1}, \gamma_{D_{1i}}^{D_2}\} > \gamma_{th_1} \big)$ which is the probability given in the numerator of $P_\phi\big(\gamma_{th_1}$, $\gamma_{th_2}\big)$. Therefore, OP of user 2 for multi-relay case becomes straightforward as in the last line of (8.18).

The three probability components in the numerator of the $P_\phi(\gamma_{th_1}, \gamma_{th_2})$, namely $P_{\phi_1}(\gamma_{th_2}, \gamma_{th_2})$, $P_{\gamma_{D_{1i}}^{D_1}}(\gamma_{th_1})$, and $P_{\phi_2}(\gamma_{th_1}, \gamma_{th_2})$ are given in (8.19), (8.20), and (8.21), respectively (Please refer to Appendix B for the derivations of closed forms)

$$P_{\phi_1}(\gamma_{th_1},\gamma_{th_2}) = \sum_{p=1}^{N}\sum_{k=0}^{G_{ds}-1}\sum_{k_1=0}^{k}\sum_{k_2=0}^{k_1}\sum_{k_3=0}^{k_2+\tilde{m}_R-1}\sum_{k_4=0}^{k_3}\Bigg[\frac{W_p T_p^{G_{ds}}\frac{\gamma_{th_2}b^2}{T_p a_2\rho_{S_i}}\binom{k}{k_1}\binom{k_1}{k_2}\binom{k_3}{k_4}m_{R_iR_i}^{m_{R_iR_i}}}{\Gamma(m_f)\Gamma(m_s)\Gamma(k+1)\Gamma(k_3+1)}$$
$$\times\frac{\tilde{m}_R^{\tilde{m}_R}\Gamma(k_2+\tilde{m})\Gamma(k_1-k_2+k_4+m_{R_iR_i})\Gamma(G_{ds})(a_1\epsilon_{R_i}\rho_{S_i})^{k_2}}{\Gamma(\tilde{m}_R)\Gamma(m_{R_iR_i})\Omega_{R_iR_i}^{m_{R_iR_i}}(\tilde{m}_R+\frac{\gamma_{th_2}b^2a_1\epsilon_{R_i}}{T_pa_2})^{k_2+\tilde{m}}}$$
$$\times\frac{(\varpi_i\rho_{R_i})^{k_1-k_2+k_4}\left(\frac{\left(\tilde{m}_RT_pa_2+\gamma_{th_2}b^2a_1\epsilon_{R_i}\right)\Lambda_m}{T_p\gamma_{th_2}a_1\epsilon_{R_i}\rho_{S_i}}\right)^{k_3}e^{-\left(\frac{\left(\tilde{m}_RT_pa_2+\gamma_{th_2}b^2a_1\epsilon_{R_i}\right)\Lambda_m}{T_p\gamma_{th_2}a_1\epsilon_{R_i}\rho_{S_i}}+\frac{\gamma_{th_2}b^2}{T_pa_2\rho_{S_i}}\right)}}{\left(\frac{m_{R_iR_i}}{\Omega_{R_iR_i}}+\frac{\gamma_{th_1}b^2\varpi_i\rho_{R_i}}{T_pa_2\rho_{S_i}}+\frac{\left(\tilde{m}_RT_pa_2+\gamma_{th_2}b^2a_1\epsilon_{R_i}\right)\Lambda_m\varpi_i\rho_{R_i}}{T_p\gamma_{th_2}a_1\epsilon_{R_i}\rho_{S_i}}\right)^{k_1-k_2+k_4+m_{R_iR_i}}}\Bigg],$$
$$+\sum_{p=1}^{N}\sum_{k=0}^{G_{ds}-1}\sum_{k_1=0}^{k}\Bigg[\frac{W_pT_p^{G_{ds}}\Gamma(G_{ds})\binom{k}{k_1}(\varpi_i\rho_{R_i})^{k_1}m_{R_iR_i}^{m_{R_iR_i}}\Gamma(k_1+m_{R_iR_i})(\frac{b^2\Lambda}{T_p})^k}{\Gamma(m_f)\Gamma(m_s)\Gamma(m_{R_iR_i})\Omega_{R_iR_i}^{m_{R_iR_i}}\left(\frac{m_{R_iR_i}}{\Omega_{R_iR_i}}+\frac{b^2\Lambda\varpi_i\rho_{R_i}}{T_p}\right)^{k_1+m_{R_iR_i}}}$$
$$\times\frac{e^{-\frac{b^2\Lambda}{T_p}}}{\Gamma(k+1)}\Bigg]-\sum_{p=1}^{N}\sum_{k=0}^{G_{ds}-1}\sum_{k_1=0}^{k}\sum_{q=0}^{\tilde{m}_R-1}\sum_{q_1=0}^{q}\Bigg[\frac{W_pT_p^{G_{ds}}\Gamma(G_{ds})\Gamma(k_1+q_1+m_{R_iR_i})}{\Gamma(m_f)\Gamma(m_s)\Gamma(k+1)\Gamma(q+1)\Gamma(m_{R_iR_i})}$$
$$\times\frac{\binom{k}{k_1}\binom{q}{q_1}m_{R_iR_i}^{m_{R_iR_i}}(\varpi_i\rho_{R_i})^{k_1+q_1}\left(\frac{b^2\Lambda}{T_p}\right)^k\left(\frac{\tilde{m}_Ra_2\Lambda_m}{\gamma_{th_2}a_1\epsilon_{R_i}\rho_{S_i}}\right)^{q_1}e^{-\left(\frac{b^2\Lambda}{T_p}+\frac{\tilde{m}_Ra_2\Lambda_m}{\gamma_{th_2}a_1\epsilon_{R_i}\rho_{S_i}}\right)}}{\Omega_{R_iR_i}^{m_{R_iR_i}}\left(\frac{m_{R_iR_i}}{\Omega_{R_iR_i}}+\frac{b^2\Lambda\varpi_i\rho_{R_i}}{T_p}+\frac{\tilde{m}_Ra_2\Lambda_m\varpi_i\rho_{R_i}}{\gamma_{th_2}a_1\epsilon_{R_i}\rho_{S_i}}\right)^{k_1+q_1+m_{R_iR_i}}}\Bigg] \tag{8.19}$$

where $\Lambda=\max\left(\frac{\gamma_{th_2}}{a_2\rho_{S_i}},\frac{\gamma_{th_1}}{a_1\rho_{S_i}-a_2\rho_{S_i}\gamma_{th_1}}\right)$ and $\Lambda_m=\max\left(0,\frac{\gamma_{th_1}}{a_1-a_2\gamma_{th_1}}-\frac{\gamma_{th_2}}{a_2}\right)$,

$$P_{\gamma_{D_{1i}}^{D_1}}(\gamma_{th_1}) = 1-F_{|g_{R_{i1}}|^2}\left(\frac{\gamma_{th_1}}{\rho_{D_{1i}}(a_3-a_4\gamma_{th_1})}\right), \tag{8.20}$$

and

$$P_{\phi_2}(\gamma_{th_1},\gamma_{th_2}) = \sum_{p=0}^{N}\sum_{k=0}^{G_{d2}-1}\sum_{k_1=0}^{k}\Bigg[\frac{W_{p,2}T_{p,2}^{G_{d2}}\Gamma\left(G_{d2}\right)\binom{k}{k_1}\left(a_3\epsilon_{D_2}\rho_{D_{2i}}\right)^{k_1}\left(\frac{\gamma_{th_2}b_{D2}^2}{T_{p,2}a_4\rho_{D_{2i}}}\right)^k}{\Gamma(m_{D_2f})\Gamma(m_{D_2s})\left(\tilde{m}_{D_2}+\frac{\gamma_{th_2}b_{D2}^2a_3\epsilon_{D_2}}{T_{p,2}a_4}\right)^{k_1+\tilde{m}_{D_2}}}$$
$$\times\frac{\tilde{m}_{D_2}^{\tilde{m}_{D_2}}e^{-\frac{\gamma_{th_2}b_{D2}^2}{T_{p,2}a_4\rho_{D_{2i}}}}}{\Gamma(k+1)\Gamma(\tilde{m}_{D_2})}\Gamma\left(k_1+\tilde{m}_{D_2},\frac{a_4\Lambda_2}{\gamma_{th_2}a_3\epsilon_{D_2}\rho_{D_{2i}}}\left(\tilde{m}_{D_2}+\frac{\gamma_{th_2}b_{D2}^2a_3\epsilon_{D_2}}{T_{p,2}a_4}\right)\right)$$
$$+F_{|\tilde{g}_{D_2}|^2}\left(\frac{a_4\Lambda_2}{\gamma_{th_2}a_3\epsilon_{D_2}\rho_{D_{2i}}}\right)\left(1-F_{|g_{R_{i2}}|^2}(\frac{\gamma_{th_1}}{\rho_{D_{2i}}\left(a_3-a_4\gamma_{th_1}\right)})\right)\Bigg], \tag{8.21}$$

where $\Lambda_2=\max\left(0,\frac{\gamma_{th_1}}{a_3-a_4\gamma_{th_1}}-\frac{\gamma_{th_2}}{a_4}\right)$.

For HD transmission with perfect SIC, $P_{\phi_1}(\gamma_{th_1},\gamma_{th_2})$ and $P_{\phi_2}(\gamma_{th_1},\gamma_{th_2})$ reduce to (8.22) and (8.23), respectively (Their derivations become straightforward while setting $\epsilon_{R_i}=\varpi_i=0$ in (8.40) and $\epsilon_{D_2}=0$ in (8.46)).

$$P_{\phi_1}^{HD,pSIC}(\gamma_{th_1},\gamma_{th_2}) = 1 - F_{|h_{S_i}|^2}\left(\max\left(\frac{\gamma_{th_2}}{a_2\rho_{S_i}}, \frac{\gamma_{th_1}}{a_1\rho_{S_i} - a_2\rho_{S_i}\gamma_{th_1}}\right)\right) \tag{8.22}$$

and

$$P_{\phi_2}^{HD,pSIC}(\gamma_{th_1},\gamma_{th_2}) = 1 - F_{|g_{R_{i2}}|^2}\left(\max\left(\frac{\gamma_{th_2}}{a_4\rho_{D_{2i}}}, \frac{\gamma_{th_1}}{a_3\rho_{D_{2i}} - a_4\rho_{D_{2i}}\gamma_{th_1}}\right)\right) \tag{8.23}$$

8.6. Asymptotic Outage Probability

To investigate, which parameters such as channel characteristics, HD and FD transmission, SI, and ipSIC are dominant at high SNR values (ρ_{S_i}, ρ_{R_i}, $\rho_{D_{1i}}$, and $\rho_{D_{2i}}$), the asymptotic expressions for each probability components are provided in this section.

At high SNRs, i.e., at low x values, the exact CDF given (8.12) becomes

$$F_X^{\infty}(x) = \begin{cases} \dfrac{\Gamma(G_{dm}-G_{ds})}{\Gamma(G_{dm})\Gamma(G_{ds}+1)} b^{2G_{ds}} x^{G_{ds}} & m_f \neq m_s \\ \dfrac{2}{\Gamma(G_{dm})\Gamma(G_{ds}+1)} b^{2G_{ds}} x^{G_{ds}} & m_s = m_f \end{cases}, \tag{8.24}$$

since as $x \to 0$, ${}_1F_2(m;\nu,n;x) \to 1$. The minimum and maximum shape factors are $G_{ds} = \min(m_f, m_s)$, $G_{dm} = \max(m_f, m_s)$, respectively. Similarly, asymptotic approximated CDF turns to

$$\tilde{F}_X^{\infty}(x) = \frac{b^{2G_{ds}} x^{G_{ds}}}{\Gamma(G_{dm})\Gamma(G_{ds}+1)} \sum_{p=1}^{N} \big(W_p\big). \tag{8.25}$$

Note that approximation does not work for equal shape factors, $m_s = m_f$, therefore, asymptotic expression does not include this case.

Herein after, to get asymptotic expressions of remaining probability components, all 1s in the denominators of SINRs are omitted and, without of loss of generality, equality of all SNRs is assumed ($\rho_{S_i} = \rho_{R_i} = \rho_{D_{1i}} = \rho_{D_{2i}}$).

Firstly, the derivation of asymptotic expression of $P_{R_i \in K_R}(\gamma_{th_1})$ is focused. Since $P_{R_i \in K_R}(\gamma_{th_1})$ consists of three components, its asymptotic expression is straightforward if the asymptotic expression for $Pr\big(\min\{\gamma_{D_1}^{R_i}, \gamma_{D_{1i}}^{D_1}, \gamma_{D_{1i}}^{D_2}\} > \gamma_{th_1}\big)$ is provided. Therefore, we write this component and derive its closed form by the aid of identity [65, 9.455.2] as

$$
\begin{aligned}
Pr^{\infty}(\gamma_{D_1}^{R_i} > \gamma_{th_1}) &= Pr\left(|h_{R_iR_i}|^2 < \frac{\rho_{S_i}\left(a_1 - a_2\gamma_{th_1}\right)}{\gamma_{th_1}\varpi_i\rho_{R_i}}|h_{S_i}|^2\right) \\
&= \int_0^{\infty} F_{|h_{R_iR_i}|^2}\left(\frac{a_1 - a_2\gamma_{th_1}}{\gamma_{th_1}\varpi_i}x\right) f_{|h_{S_i}|^2}(x)\,dx \\
&= \sum_{p=1}^{N}\Bigg[\frac{b^{2G_{ds}}W_p\Gamma\left(m_{R_iR_i}+G_{ds}\right)\left(m_{R_iR_i}\left(a_1 - a_2\gamma_{th_1}\right)\right)^{m_{R_iR_i}}}{\left(m_{R_iR_i}\left(a_1 - a_2\gamma_{th_1}\right) + \frac{b^2\gamma_{th_1}\varpi_i\Omega_{R_iR_i}}{T_p}\right)^{m_{R_iR_i}+G_{ds}}} \\
&\times \frac{\left(\gamma_{th_1}\varpi_i\Omega_{R_iR_i}\right)^{G_{ds}}}{\Gamma(m_f)\Gamma(m_s)\Gamma(m_{R_iR_i})}{}_2F_1\Bigg(1, m_{R_iR_i}+G_{ds}; m_{R_iR_i}+1; \\
&\frac{m_{R_iR_i}\left(a_1 - a_2\gamma_{th_1}\right)T_p}{m_{R_iR_i}\left(a_1 - a_2\gamma_{th_1}\right)T_p + b^2\gamma_{th_1}\varpi_i\Omega_{R_iR_i}}\Bigg)\Bigg]
\end{aligned}
\tag{8.26}
$$

An interesting result deduced from (8.26) is that this probability is independent of SNR. It depends on PA factors and channel characteristics. Moreover, its value can be reduced in case of successful SI cancellation since variance of SI dominates this probability.

Asymptotic $P_{\phi_1}(\gamma_{th}, \gamma_{th_2})$ can be derived by following the same methodology as in its exact derivation. Unlike its exact counterpart, this component simplifies to a single term where only a non-zero lower bound integral is remained and instead of two Binomial expansions, single expansion is applied. Closed form of $P_{\phi_1}^{\infty}(\gamma_{th}, \gamma_{th_2})$ is given as

$$
\begin{aligned}
P_{\phi_1}^{\infty}(\gamma_{th_1}, \gamma_{th_2}) &= Pr\left(|h_{S_i}|^2 > \frac{\gamma_{th_2}\left(a_1\epsilon_{R_i}\rho_{S_i}|\tilde{g}_{R_i}|^2 + \varpi_i\rho_{R_i}|h_{R_iR_i}|^2\right)}{a_2\rho_{S_i}}\right) \\
&= \int_0^{\infty}\int_0^{\infty}\int_{\frac{\gamma_{th_2}\left(a_1\epsilon_{R_i}\rho_{S_i}y + \varpi_i\rho_{R_i}z\right)}{a_2\rho_{S_i}}}^{\infty} f_{|h_{S_i}|^2}(x)\, f_{|\tilde{g}_{R_i}|^2}(y)\, f_{|h_{R_iR_i}|^2}(z)dxdydz \\
&= \sum_{p=0}^{N}\sum_{k=0}^{G_{ds}-1}\sum_{k_1=0}^{k}\Bigg[\frac{W_pT_p^{G_{ds}}\tilde{m}_R^{\tilde{m}_R}\Gamma\left(G_{ds}\right)\Gamma\left(k - k_1 + m_{R_iR_i}\right)}{\Gamma(m_f)\Gamma(m_s)\Gamma(k+1)\Gamma(\tilde{m}_R)\Gamma\left(m_{R_iR_i}\right)\Omega_{R_iR_i}^{m_{R_iR_i}}} \\
&\times \frac{\Gamma\left(k_1 + \tilde{m}_R\right)m_{R_iR_i}^{m_{R_iR_i}}\binom{k}{k_1}(a_1\epsilon_{R_i})^{k_1}(\varpi_i)^{k_1-k}\left(\frac{\gamma_{th_2}b^2}{T_pa_2}\right)^k}{\left(\frac{m_{R_iR_i}}{\Omega_{R_iR_i}} + \frac{\gamma_{th_2}b^2a_1\varpi_i}{T_pa_2}\right)^{k-k_1+m_{R_iR_i}}\left(\tilde{m}_R + \frac{\gamma_{th_2}b^2a_1\epsilon_{R_i}}{T_pa_2}\right)^{k_1+\tilde{m}_R}}\Bigg].
\end{aligned}
\tag{8.27}
$$

In case of pSIC, i.e., $\epsilon_{R_i} = 0$, the above equation can be simplified further, where only the terms with $k_1 = 0$ survive and all the components including related terms (components including ϵ_{R_i} and $\tilde{m}_R$) are canceled out. This cancellation lets one to focus only on the FD transmission with pSIC.

Finally by the aid of the identity [65, 9.455.2], asymptotic expression of the $P_{\phi_2}(\gamma_{th_1}, \gamma_{th_2})$ can be formulated and derived as

$$
\begin{aligned}
P_{\phi_2}^{\infty}(\gamma_{th_1},\gamma_{th_2}) &= Pr\left(|\tilde{g}_{D_2}|^2 < \frac{a_4 g_{R_{i2}}|^2}{\gamma_{th_2} a_3 \epsilon_{D_2}}\right) \\
&= \int_0^{\infty} F_{|\tilde{g}_{D_2}|^2}\left(\frac{a_4 x}{\gamma_{th_2} a_3 \epsilon_{D_2}}\right) f_{|g_{R_{i2}}|^2}(x)dx \\
&= \sum_{p=1}^{N}\Bigg[\frac{b_{D2}^{2G_{d2}} W_{p,2}\Gamma\left(G_{d2}+\tilde{m}_{D2}\right)\left(a_4\tilde{m}_{D2}\right)^{\tilde{m}_{D2}}\left(\gamma_{th_2}a_3\epsilon_{D_2}\right)^{G_{d2}}}{\Gamma(m_{D_2f})\Gamma(m_{D_2s})\left(a_4\tilde{m}_{D_2}+\frac{\gamma_{th_2}b_{D2}^2 a_3\epsilon_{D_2}}{T_{p,2}}\right)^{G_{d2}+\tilde{m}_{D_2}}} \\
&\quad\times\frac{{}_2F_1\left(1, G_{d2}+\tilde{m}_{D_2};\tilde{m}_{D_2}+1;\frac{\tilde{m}_{D_2}a_4T_{p,2}}{\tilde{m}_{D_2}a_4T_{p,2}+b_{D2}^{2G_{d2}}\gamma_{th_2}a_3\epsilon_{D_2}}\right)}{\Gamma(\tilde{m}_{D2}+1)}\Bigg].
\end{aligned}
\tag{8.28}
$$

Note that $P_{\phi_2}^{\infty}(\gamma_{th_1},\gamma_{th_2})$ is independent of SNR, which means it is a constant dependent on PA factors and channel characteristics. This is the reason why OP approaches to an error floor.

To shade light on diversity order (DO), firstly let's focus on asymptotic OP for HD with pSIC. Substituting the related asymptotic components into (8.18), $P^{HD,pSIC,\infty}(\gamma_{th_1},\gamma_{th_2})$ can be rephrased as

$$
\begin{aligned}
P^{HD,pSIC,\infty}(\gamma_{th_1},\gamma_{th_2}) &= \Bigg[1-\left(1-F_{|h_{S_i}|^2}^{\infty}\left(\frac{U_1}{\rho_{S_i}}\right)\right)\left(1-F_{|g_{R_{i1}}|^2}^{\infty}\left(\frac{U_2}{\rho_{D_{1i}}}\right)\right) \\
&\quad\times\left(1-F_{|g_{R_{i2}}|^2}^{\infty}\left(\frac{U_3}{\rho_{D_{2i}}}\right)\right)\Bigg]^L \\
&< \left[F_{|h_{S_i}|^2}^{\infty}\left(\frac{U_1}{\rho_{S_i}}\right)+F_{|g_{R_{i1}}|^2}^{\infty}\left(\frac{U_2}{\rho_{D_{1i}}}\right)+F_{|g_{R_{i2}}|^2}^{\infty}\left(\frac{U_3}{\rho_{D_{2i}}}\right)\right]^L,
\end{aligned}
\tag{8.29}
$$

where $U_1 = \max\left(\frac{\gamma_{th_2}}{a_2}, \frac{\gamma_{th_1}}{a_1-a_2\gamma_{th_1}}\right)$ $U_2 = \frac{\gamma_{th_1}}{a_3-a_4\gamma_{th_1}}$, and $U_3 = \max\left(\frac{\gamma_{th_2}}{a_4}, \frac{\gamma_{th_1}}{a_3-a_4\gamma_{th_1}}\right)$. While obeying the traditional approach provided in [82], the DO of the system under consideration for HD with pSIC as SNR approaches to infinity is $L \times \min\left(m_f, m_s, m_{D_1f}, m_{D_1s}, m_{D_2f}, m_{D_2s}\right)$. Now, let's consider the special case, i.e., $L = 1$, which means no diversity technique is applied and DO is $\min\left(m_f, m_s, m_{D_1f}, m_{D_1s}, m_{D_2f}, m_{D_2s}\right)$. However, this result does not make sense, since it is well-known that distribution of mobile medium governs the error probabilities (OP, symbol error rate, and so on). To us, without implementing any diversity method and talking about DO is unreasonable. Actually, the way to find the DO has been offered in [163, eq. (1)], where it is reformulated for our system as

$$
DO = \lim_{SNR\to\infty}\frac{\log\left(P^L(\gamma_{th_1},\gamma_{th_2})\right)}{\log\left(P^{L=1}(\gamma_{th_1},\gamma_{th_2})\right)}.
\tag{8.30}
$$

Briefly, DO is the ratio between the logarithm of OP for the system with L relays and the logarithm of OP for single relay as SNR approaches to infinity, while all other parameters are kept to be the same. Hence, according to this approach, DO is independent of channel characteristics and becomes L. This suites to the aim of the diversity techniques; the signals are transmitted such that probability of all copies facing deep fading is reduced.

Providing the above description, DO of all other combinations like HD transmission with ipSIC, FD transmission with pSIC, and FD transmission with ipSIC becomes straightforward. To shade more light on details of our assertion, the derivation of DO for remaining parts is indicated below.

Asymptotic expressions derived for $P_{\phi_1}^{\infty}(\gamma_{th_1},\gamma_{th_2})$ and $P_{\phi_2}^{\infty}(\gamma_{th_1},\gamma_{th_2})$ in (8.27) and (8.28), respectively, are shown to be independent of transmitted power but dependent solely on channel characteristics. Thereby, they are constant terms and causes OP to saturate, i.e., OP reaches to an error floor. Without loss of generality, these two probability components can be rephrased as $P_{\phi_1}^{\infty}(\gamma_{th_1},\gamma_{th_2}) = 1 - P_{ef}^{\phi_1}$ and $P_{\phi_2}^{\infty}(\gamma_{th_1},\gamma_{th_2}) = 1 - P_{ef}^{\phi_2}$. Note that $P_{ef}^{\phi_1} = F_{|h_{S_i}|^2}^{\infty}\left(\frac{U_1}{\rho_{S_i}}\right)$ and $P_{ef}^{\phi_2} = F_{|g_{R_{i2}}|^2}^{\infty}\left(\frac{U_3}{\rho_{D_{2i}}}\right)$ in case of HD transmission with pSIC as seen in (8.29). Hence, for all conditions, asymptotic OP turns to

$$\begin{aligned} P^{\infty}(\gamma_{th_1},\gamma_{th_2}) &= \left[1-\left(1-P_{ef}^{\phi_1}\right)\left(1-P_{ef}^{\phi_2}\right)\left(1-F_{|g_{R_{i1}}|^2}^{\infty}\left(\frac{U_2}{\rho_{D_{1i}}}\right)\right)\right]^{L} \\ &< \left[P_{ef}^{\phi_1}+P_{ef}^{\phi_2}+F_{|g_{R_{i1}}|^2}^{\infty}\left(\frac{U_2}{\rho_{D_{1i}}}\right)\right]^{L} \end{aligned}. \tag{8.31}$$

Clearly, in case of FD transmission with pSIC or HD/FD transmission with ipSIC, $F_{|g_{R_{i1}}|^2}^{\infty}\left(\frac{U_2}{\rho_{D_{1i}}}\right)$ becomes negligible and OP is dominated by $P_{ef}^{\phi_1}$ or $P_{ef}^{\phi_2}$. Apparently, OP reaches to an error floor and there is no point of increasing transmitted power in error floor region to change the slope but OP is significantly reduced by means of diversity techniques. Because of this error floor, in turn, zero slope of log – log plot, DO has been accepted to be zero. However, reduction of OP from $\left(P_{ef}^{\phi_1}+P_{ef}^{\phi_2}+F_{|g_{R_{i1}}|^2}^{\infty}\left(\frac{U_2}{\rho_{D_{1i}}}\right)\right)$ to $\left(P_{ef}^{\phi_1}+P_{ef}^{\phi_2}+F_{|g_{R_{i1}}|^2}^{\infty}\left(\frac{U_2}{\rho_{D_{1i}}}\right)\right)^{L}$ means DO is L.

8.7. Numerical Results

In this section, numerical results for OP are provided to validate the derived expressions. It is assumed that $P_T = 2P_S = 2P_{R_i}$ and $\sigma^2 = \sigma_{R_i}^2 = \sigma_{D_1}^2 = \sigma_{D_2}^2 = 1$. The total number of terms in the approximations is $N = 20$. The curves are plotted versus total SNR, P_T/σ^2. All parameter settings are provided in the explanation of each figure. In all

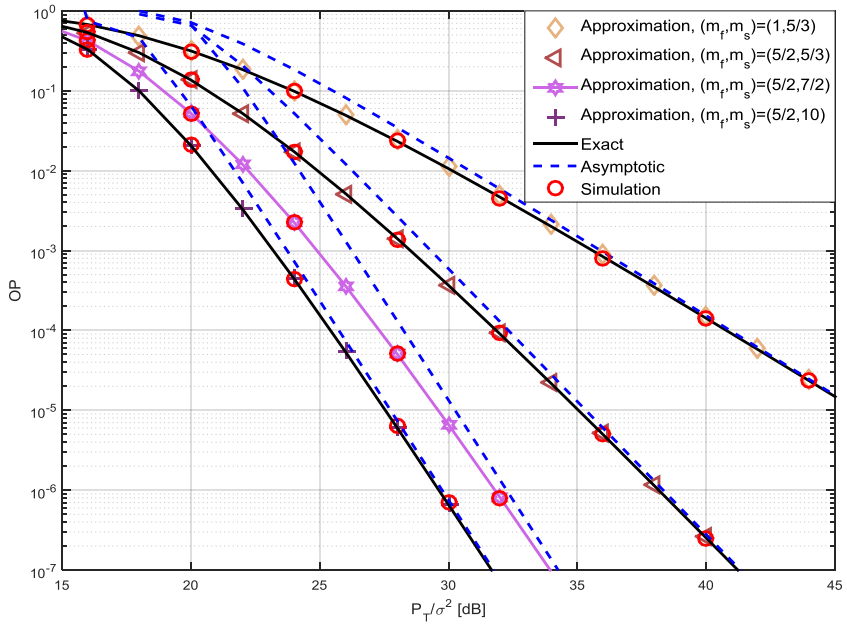

Figure 8.2: OP of HD transmission with perfect SIC.

figures approximated CDFs are used except Fig.8.2, where both exact and approximated expressions are used.

Fig.8.2 verifies correctness of OP expression given in (8.18) for HD transmission in case of perfect SIC, which also demonstrates robustness of the proposed approximated PDF and CDF. OP curves are calculated from (8.18) with using (8.20), (8.22) and (8.23). The exact and approximated CDFs in (8.12) and (8.14), respectively, are used. Their asymptotic counterparts are produced by (8.24) and (8.25), where both expressions have the same results. Channel characteristics for all three links are chosen to be the same with unit fading and shadowing scale factors. Multi-path fading and shadowing shape factors are assigned as $(m_f, m_s) \in \{(1, 5/3), (5/2, 5/3), (5/2, 7/2), (5/2, 10)\}$. PA factors are $a_1 = a_3 = 0.75$. Note that exact results cannot be calculated for $(m_f, m_s) = (5/2, 7/2)$, where the difference between fading and shadowing shape factors is an integer. Data rates are $R_{D_1} = 0.3$ bit per channel use (BPCU) and $R_{D_2} = 1$ BPCU. Total number of relays, L, is set to 2. Although, 3 approximated CDFs are used in (8.18), overlap of the exact and approximated OPs is almost excellent. Additionally, since $L = 2$, squaring operation increases the deviation further but it remains negligible. The deviation between exact and approximated results becomes larger as the difference between fading and shadowing scale factors, namely $|m_s - m_f|$, get smaller: The minor deviation (square of the error) in the most upper curve (It may not be detect from the curve but exists in numerical values) is an example of this situation. While the difference is set to $|m_s - m_f| = |2.1 - 2| = 0.1$ for the same settings, the deviation is negligible at lower total SNR (P_T/σ^2) and gradually

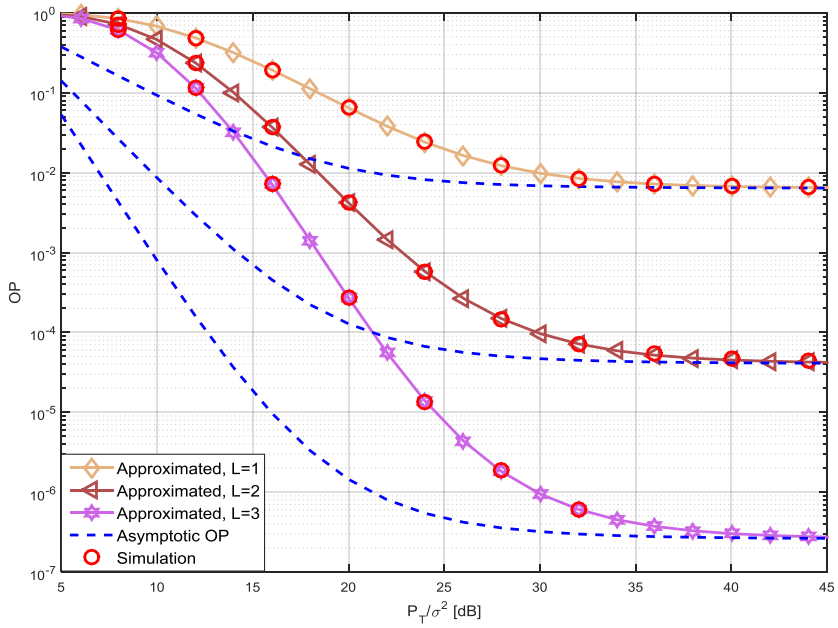

Figure 8.3: OP of FD transmission with imperfect SIC for different total number of relays.

increases to 20% at an OP value of 4.79912×10^{-7}. Even this result reveals robustness of the proposed approximation. As P_T/σ^2 increases, the deviation between asymptotic and exact curves decreases. Simulation results follow the exact ones which validates the correctness of the OP expression given (8.15). Comparison of two upper curves with the same shadowing shape factor demonstrates how performance is affected by fading and comparison of lower three curves shows dependence of performance on shadowing.

Fig.8.3 demonstrates effect of the total number of relays on OP and correctness of (8.15) for FD transmission in case of imperfect SIC. All fading and shadowing scale factors are set to 1. Shape factors are chosen as $(m_f, m_s) = (2, 5/2)$, $(m_{D_1 f}, m_{D_1 s}) = (3/2, 7/3)$, $(m_{D_2 f}, m_{D_2 s}) = (2, 8/3)$, $m_{R_i R_i} = 9/5$, $\tilde{m}_{R_i} = 2$, and $\tilde{m}_{D_2} = 8/5$. SI cancellation parameters, namely, linear and exponential attenuation parameters are set to $(\vartheta_i, \kappa_i) = (0.21, 0.1)$. The imperfect SIC parameters are taken to be $\epsilon_{R_i} = \epsilon_{D_2} = 0.01$. Total number of relays is $L \in \{1, 2, 3\}$. The data rates are set to $R_{D_1} = 0.2$ BPCU and $R_{D_2} = 1$ BPCU. PA factors are set to $a_1 = 0.55$ and $a_3 = 0.65$. Clearly, simulation and approximated results are nearly the same, furthermore, asymptotic ones also follow them. While considering the OP at the total SNR value of 30 dB, OP is nearly 10^{-2}, 10^{-4}, and 10^{-6} for $L = 1, 2, 3$, respectively. Evidently, $OP(L = 2) \simeq (OP(L = 1))^2$ and also $OP(L = 3) \simeq (OP(L = 1))^3$. This equality holds for every point in the error floor region, therefore, DO apparently equals to the total number of relays. Note that the reduction in OP is observed for the same channel characteristics which means it is not reasonable to

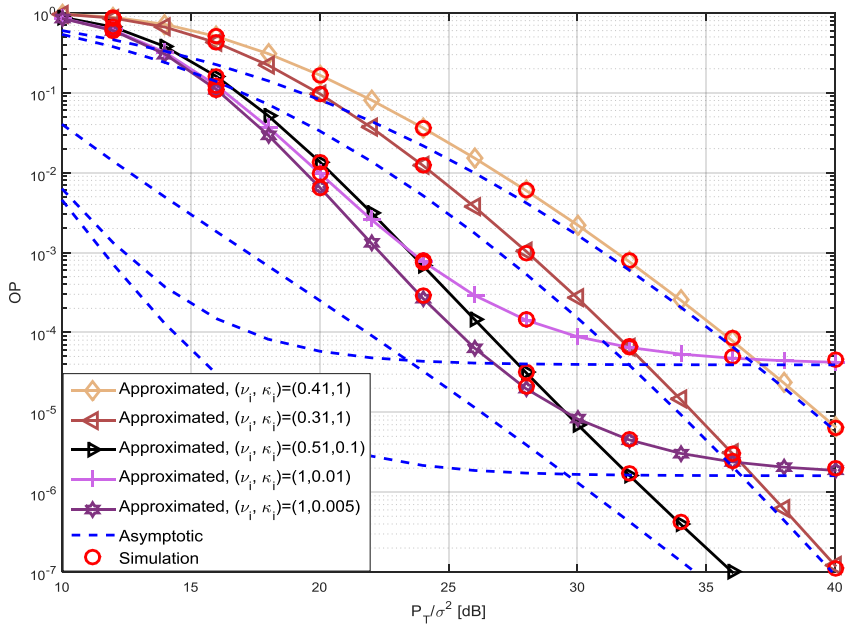

Figure 8.4: OP of FD transmission with different SI variances.

consider the effect of shaping factors as DO. Hence, at error floors unlike the common assumption of the zero DO, it can be evaluated as $\frac{\log(OP(L))}{\log(OP(L=1))}$ and without usage of any diversity technique, it does not make sense to talk about DO.

Fig. 8.4 shows the effect of SI on the performance for various combination of linear and exponential cancellation factors. The imperfect SIC factors, ϵ_{R_i} and ϵ_{D_2}, are set to 10^{-8} to solely observe the effect of SI on the performance, where $\tilde{m}_R = \tilde{m}_{D_2} = 1$. Other channel characteristics are the same as those of Fig. 8.3 except $m_{R_iR_i} = 2$. The data rates are set to $R_{D_1} = 0.3$ BPCU and $R_{D_2} = 2$ BPCU. PA factors are chosen as $a_1 = a_3 = 0.55$ and $(\vartheta_i, \kappa_i) \in \{(0.31, 1), (0.41, 1), (0.51, 0.1), (1, 0.01), (1, 0.005)\}$. Total number of relays, L is 3. Approximated curves coincide with simulation ones and asymptotic curves follow them. Apparently, as exponential factor increases performance degrades, consider the two upper curves with $(\vartheta_i, \kappa_i) = (0.41, 1)$ and $(\vartheta_i, \kappa_i) = (0.31, 1)$), since this corresponds to the increment of variance of SI. OP decreases as the linear cancellation factor becomes smaller (consider the curves with $(\vartheta_i, \kappa_i) = (1, 0.01)$ and $(\vartheta_i, \kappa_i) = (1, 0.005)$). Note that insufficient SI cancellation means variance of SI is only linearly proportional to the transmitted power, which eventually results in an error floor and it becomes meaningless to increase the transmitted power further. Therefore, to decrease error in case of insufficient SI cancellation, it is critical and essential to use diversity techniques.

Fig. 8.5 illustrates how performance changes in accordance with SI and imperfect SIC at the selected relay and the second user, D_2. Only approximated and simulation

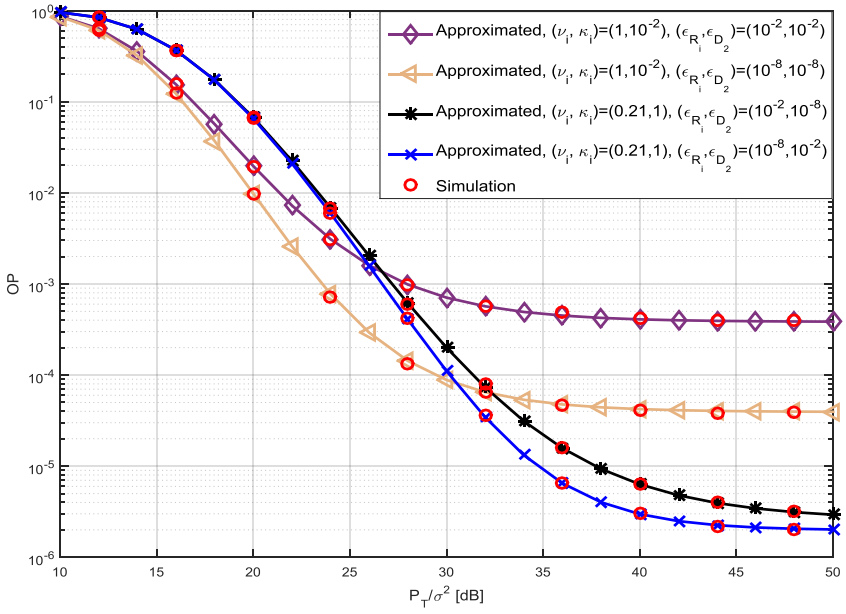

Figure 8.5: Effect of SI and ipSIC on OP at the selected relay and second user.

results are provided and for the sake of clarity, asymptotic ones are omitted. Shape factors are chosen as $(m_f, m_s) = (2, 5/2)$, $(m_{D_1 f}, m_{D_1 s}) = (3/2, 7/3)$, $(m_{D_2 f}, m_{D_2 s}) = (2, 8/3)$, $m_{R_i R_i} = 2$, $\tilde{m}_{R_i} = 2$, and $\tilde{m}_{D_2} = 2$. The data rates are set to $R_{D_1} = 0.3$ BPCU and $R_{D_2} = 2$ BPCU. PA factors are chosen as $a_1 = a_3 = 0.55$ and $(\vartheta_i, \kappa_i) \in \{(0.21, 1), (1, 0.01)\}$. The ipSIC factors at the selected relay and D_2 are chosen as $\epsilon_{R_i} \in \{10^{-8}, 10^{-2}\}$ and $\epsilon_{D_2} \in \{10^{-8}, 10^{-2}\}$. All the variances are set to 1 except that of SI. Total number of relays is 3. Case of ipSIC and pSIC at both nodes for FD transmission with constant SI variance, $(\vartheta_i, \kappa_i) = (1, 0.01)$, is demonstrated by $\epsilon_{R_i} = \epsilon_{D_2} = 10^{-2}$ and $\epsilon_{R_i} = \epsilon_{D_2} = 10^{-8}$, respectively. As seen from the two upper curves, ipSIC degrades the performance. To investigate the effect of ipSIC at the selected relay (second user (D_2)), SI at the selected relay and SIC at the second user (selected relay) are chosen to be $(\vartheta_i, \kappa_i) = (0.21, 1)$ and $\epsilon_{D_2} = 10^{-8}$ ($\epsilon_{R_i} = 10^{-8}$), respectively. From the two lower curves, it is observed that at low and high SNRs, the cases of ipSIC at the selected relay and second user have nearly the same performance but at the mid-range ipSIC at the selected relay degrades the performance more than that of the second user. Furthermore, even if sufficient SIC is conducted, error floor will take place in case of insufficient SI cancellation (See the second curve from the top). All the curves validate our approximated results.

8.8. Conclusion

In this paper, two stage relay selection over i.i.d. slow fading generalized-K distributed channels, namely, fading and shadowing channels, is investigated for HD/FD transmission with imperfect SIC, where DF protocol is used. A new closed form CDF for generalized-K distribution is derived. Thereafter, robust approximated PDF and CDF are offered based on generalized Gauss-Laguerre quadrature. Since stable OP expression cannot be derived based on exact PDF and CDF (even if it is derived and correct from analytical perspective, it produces unstable values at the low SNR values), approximated expression is obtained based on offered approximated PDF and CDF. Similarly, asymptotic OP is also provided. Approximated and asymptotic equations are validated via Monte Carlo simulation technique. Effects of SI, ipSIC, fading and shadowing on OP are demonstrated and it is also shown that RS can sufficiently reduce OP. Finally, nonzero diversity order is asserted and related details are provided.

8.9. Appendix: Derivations of Probabilities in OP Expression

The probability of a relay providing service quality and conditional probability takes place in OP expression are derived in this part.

8.9.1. Probability of a Relay Providing Service Quality

Due to the independence of channel gains, in turn the independence of $\gamma_{D_1}^{R_i}$, $\gamma_{D_{1i}}^{D_1}$, and $\gamma_{D_{1i}}^{D_2}$, probability of a relay being in the subset of relays providing priority criterion is

$$\begin{aligned} P_{R_i \in K_R}(\gamma_{th_1}) &= Pr\big(\min\{\gamma_{D_1}^{R_i}, \gamma_{D_{1i}}^{D_1}, \gamma_{D_{1i}}^{D_2}\} > \gamma_{th_1}\big) \\ &= Pr(\gamma_{D_1}^{R_i} > \gamma_{th_1}) Pr(\gamma_{D_{1i}}^{D_1} > \gamma_{th_1}) Pr(\gamma_{D_{1i}}^{D_2} > \gamma_{th_1}) \end{aligned} \tag{8.32}$$

Therefore, in order to obtain a closed form of $P_{R_i \in K_R}(\gamma_{th_1})$, it is sufficient to derive $Pr(\gamma_{D_1}^{R_i} > \gamma_{th_1})$, $Pr(\gamma_{D_{1i}}^{D_1} > \gamma_{th_1})$, and $Pr(\gamma_{D_{1i}}^{D_2} > \gamma_{th_1})$. The first one is expressed as:

$$
\begin{aligned}
Pr(\gamma_{D_1}^{R_i} > \gamma_{th_1}) &= Pr(\gamma_{D_1}^{R_i} > \gamma_{th_1}) \\
&= Pr(\frac{a_1\rho_{S_i}|h_{S_i}|^2}{a_2\rho_{S_i}|h_{S_i}|^2 + \chi} > \gamma_{th_1}) \\
&= Pr\left(|h_{S_i}|^2 > \frac{\gamma_{th_1}\chi}{\rho_{S_i}\left(a_1 - a_2\gamma_{th_1}\right)}\right) \\
&= \int_0^{\infty}\int_{\psi_1}^{\infty} f_{|h_{S_i}|^2}(x)\, f_{|h_{R_iR_i}|^2}(y)dxdy,
\end{aligned}
\tag{8.33}
$$

where $\chi = \varpi_i\rho_{R_i}|h_{R_iR_i}|^2 + 1$ and $\psi_1 = \frac{\gamma_{th_1}(\varpi_i\rho_{R_i}y+1)}{\rho_{S_i}(a_1-a_2\gamma_{th_1})}$. Since derivation of the $Pr(\gamma_{D_1}^{R_i} > \gamma_{th_1})$ based on the exact PDF or CDF of $|h_{S_i}|^2$ results in unstable results at low SNR values, we use approximated PDF given in (8.13) for the derivation of this probability. CDF and PDF of $|h_{R_iR_i}|^2$ are given respectively as follows

$$
\begin{aligned}
F_{|h_{R_iR_i}|^2}(x) &= \frac{\gamma\left(m_{R_iR_i}, m_{R_iR_i}x/\Omega_{R_iR_i}\right)}{\Gamma(m_{R_iR_i})} \\
f_{|h_{R_iR_i}|^2}(x) &= \frac{m_{R_iR_i}^{m_{R_iR_i}}x^{m_{R_iR_i}-1}e^{-m_{R_iR_i}x/\Omega_{R_iR_i}}}{\Omega_{R_iR_i}^{m_{R_iR_i}}\Gamma(m_{R_iR_i})}
\end{aligned}
\tag{8.34}
$$

After substitution of $\tilde{f}_{|h_{S_i}|^2}(x)$ and $f_{|h_{R_iR_i}|^2}(y)$ given in (8.13) and (8.34) into (8.33) and carrying out the following steps, the closed form of $Pr(\gamma_{D_1}^{R_i} > \gamma_{th_1})$ is derived as in (8.35):

- Firstly, invert the inner integral into lower incomplete gamma function and use the equality given in [65, eq. (8.352.1)] to obtain $\Gamma\big(G_{ds}, z\big) = \Gamma(G_{sd})e^{-z}\sum_{k=0}^{G_{sd}-1}\frac{z^k}{\Gamma(k+1)}$, where $z = \frac{b^2}{T_p}\frac{\gamma_{th_1}(\varpi_i\rho_{R_i}y+1)}{\rho_{S_i}(a_1-a_2\gamma_{th_1})}$
- Secondly, apply Binomial theorem to the term $\big(\varpi_i\rho_{R_i}y+1\big)^{p_1}$ to obtain $\big(\varpi_i\rho_{R_i}y+1\big)^{p_1} = \sum_{k_1=0}^{k}\binom{k}{k_1}\big(\varpi_i\rho_{R_i}y\big)^{k_1}$.
- Finally, after proper rearrangement, obtain the integrals which is in the form of Gamma function given in [65, eq. (8.310)], namely, $\Gamma(z) = \int_0^{\infty} e^{-t}t^{z-1}dt$.

$$
\begin{aligned}
Pr(\gamma_{D_1}^{R_i} > \gamma_{th_1}) = &\sum_{p=1}^{N}\sum_{k=0}^{G_{ds}-1}\sum_{k_1=0}^{k}\Bigg[\frac{W_pT_p^{G_{ds}}\binom{k}{k_1}m_{R_iR_i}^{m_{R_iR_i}}(\varpi_i\rho_{R_i})^{k_1}\Gamma(G_{ds})}{\Gamma(m_f)\Gamma(m_s)\Gamma(k+1)\Gamma(m_{R_iR_i})\Omega_{R_iR_i}^{m_{R_iR_i}}} \\
&\times\frac{\Gamma(k_1+m_{R_iR_i})\left(\frac{b^2\gamma_{th_1}}{T_p\rho_{S_i}(a_1-a_2\gamma_{th_1})}\right)^k}{\left(\frac{m_{R_iR_i}}{\Omega_{R_iR_i}}+\frac{b^2\gamma_{th_1}\varpi_i\rho_{R_i}}{T_p\rho_{S_i}(a_1-a_2\gamma_{th_1})}\right)^{k_1+m_{R_iR_i}}}e^{-\frac{b^2\gamma_{th_1}}{T_p\rho_{S_i}(a_1-a_2\gamma_{th_1})}}\Bigg].
\end{aligned}
\tag{8.35}
$$

The second probability is derived as below:

$$
\begin{aligned}
Pr(\gamma_{D_{1i}}^{D_1} > \gamma_{th_1}) &= 1 - Pr(\gamma_{D_{1i}}^{D_1} < \gamma_{th_1}) \\
&= 1 - Pr(\frac{a_3\rho_{D_{1i}}|g_{R_{i1}}|^2}{a_4\rho_{D_{1i}}|g_{R_{i1}}|^2 + 1} < \gamma_{th_1}) \\
&= 1 - Pr\left(|g_{R_{i1}}|^2 < \frac{\gamma_{th_1}}{\rho_{D_{1i}}(a_3 - a_4\gamma_{th_1})}\right), \\
&= 1 - F_{|g_{R_{i1}}|^2}\left(\frac{\gamma_{th_1}}{\rho_{D_{1i}}(a_3 - a_4\gamma_{th_1})}\right)
\end{aligned}
\tag{8.36}
$$

and following the same steps as above, the third term turns to

$$
Pr(\gamma_{D_{1i}}^{D_2} > \gamma_{th_1}) = 1 - F_{|g_{R_{i2}}|^2}\left(\frac{\gamma_{th_1}}{\rho_{D_{2i}}(a_3 - a_4\gamma_{th_1})}\right), \tag{8.37}
$$

which completes the derivation of $P_{R_i \in K_R}(\gamma_{th_1})$ as in (8.16).

8.9.2. Derivation of Conditional Probability

The conditional probability $P_\phi(\gamma_{th_1}, \gamma_{th_2})$ can be rephrased as follows:

$$
\begin{aligned}
P_\phi(\gamma_{th_1}, \gamma_{th_2}) &= \frac{Pr(\min(\gamma_{D_{2i}}^{D_2}, \gamma_{D_2}^{R_i}) > \gamma_{th_2}, \varkappa_i > \gamma_{th_1})}{P_{R_i \in K_R}(\gamma_{th_1})} \\
&= \frac{P_{\phi_1}(\gamma_{th_1}, \gamma_{th_2}) P_{\phi_2}(\gamma_{th_1}, \gamma_{th_2}) Pr\left(\gamma_{D_{1i}}^{D_1} > \gamma_{th_1}\right)}{P_{R_i \in K_R}(\gamma_{th_1})}
\end{aligned}
\tag{8.38}
$$

and $\varkappa_i = \min\{\gamma_{D_1}^{R_i}, \gamma_{D_{1i}}^{D_1}, \gamma_{D_{1i}}^{D_2}\}$. $Pr\left(\gamma_{D_{1i}}^{D_1} > \gamma_{th_1}\right)$ is given in (8.36). The transition from the first line of (8.38) to the second line is because of independence of channels, in turn, SINRs without a common channel gain, which allows decomposition of the numerator into three independent components. $P_{\phi_1}(\gamma_{th_1}, \gamma_{th_2})$ and $P_{\phi_2}(\gamma_{th_1}, \gamma_{th_2})$ are respectively defined as follows:

$$
\begin{aligned}
P_{\phi_1}(\gamma_{th_1}, \gamma_{th_2}) &= Pr\left(\gamma_{D_1}^{R_i} > \gamma_{th_1}, \gamma_{D_2}^{R_i} > \gamma_{th_2}\right) \\
P_{\phi_2}(\gamma_{th_1}, \gamma_{th_2}) &= Pr\left(\gamma_{D_{1i}}^{D_2} > \gamma_{th_1}, \gamma_{D_{2i}}^{D_2} > \gamma_{th_2}\right)
\end{aligned}
\quad . \tag{8.39}
$$

Firstly, define $\chi = \varpi_i\rho_{R_i}|h_{R_iR_i}|^2 + 1$, $\Lambda = \max\left(\frac{\gamma_{th_2}}{a_2\rho_{S_i}}, \frac{\gamma_{th_1}}{a_1\rho_{S_i} - a_2\rho_{S_i}\gamma_{th_1}}\right)$, $\eta = \varpi_i\rho_{R_i}z + 1$, $\Lambda_m = \max\left(0, \frac{\gamma_{th_1}}{a_1 - a_2\gamma_{th_1}} - \frac{\gamma_{th_2}}{a_2}\right)$, and $\eta_1 = \frac{\gamma_{th_2}\left(a_1\epsilon_{R_i}\rho_{S_i}y + \eta\right)}{a_2\rho_{S_i}}$ thereafter, the first probability, namely $P_{\phi_1}(\gamma_{th_1}, \gamma_{th_2})$, can be reformulated as

$$
\begin{aligned}
P_{\phi_1}(\gamma_{th_1},\gamma_{th_2}) &= Pr\left(\frac{a_2\rho_{S_i}|h_{S_i}|^2}{a_1\epsilon_{R_i}\rho_{S_i}|\tilde{g}_{R_i}|^2+\chi} > \gamma_{th_2}, \frac{a_1\rho_{S_i}|h_{S_i}|^2}{a_2\rho_{S_i}|h_{S_i}|^2+\chi} > \gamma_{th_1}\right) \\
&= Pr\left(|h_{S_i}|^2 > \frac{\gamma_{th_2}\left(a_1\epsilon_{R_i}\rho_{S_i}|\tilde{g}_{R_i}|^2+\chi\right)}{a_2\rho_{S_i}}, |h_{S_i}|^2 > \Lambda\chi\right) \\
&= Pr\left(|h_{S_i}|^2 > \frac{\gamma_{th_2}\left(a_1\epsilon_{R_i}\rho_{S_i}|\tilde{g}_{R_i}|^2+\chi\right)}{a_2\rho_{S_i}}, \frac{\gamma_{th_2}\left(a_1\epsilon_{R_i}\rho_{S_i}|\tilde{g}_{R_i}|^2+\chi\right)}{a_2\rho_{S_i}} > \Lambda\chi\right) \\
&\quad + Pr\left(|h_{S_i}|^2 > \Lambda\chi, \frac{\gamma_{th_2}\left(a_1\epsilon_{R_i}\rho_{S_i}|\tilde{g}_{R_i}|^2+\chi\right)}{a_2\rho_{S_i}} < \Lambda\chi\right) \\
&= Pr\left(|h_{S_i}|^2 > \frac{\gamma_{th_2}\left(a_1\epsilon_{R_i}\rho_{S_i}|\tilde{g}_{R_i}|^2+\chi\right)}{a_2\rho_{S_i}}, |\tilde{g}_{R_i}|^2 > \frac{a_2\Lambda_m\chi}{\gamma_{th_2}a_1\epsilon_{R_i}\rho_{S_i}}\right) \\
&\quad + Pr\left(|h_{S_i}|^2 > \Lambda\chi, |\tilde{g}_{R_i}|^2 < \frac{a_2\Lambda_m\chi}{\gamma_{th_2}a_1\epsilon_{R_i}\rho_{S_i}}\right).
\end{aligned}
\tag{8.40}
$$

Therefore, two probability components should be derived based on the last two lines in (8.40), which are defined as $P^1_{\phi_1}(\gamma_{th_1},\gamma_{th_2})$ and $P^2_{\phi_1}(\gamma_{th_1},\gamma_{th_2})$:

$$
\begin{aligned}
P^1_{\phi_1}(\gamma_{th_1},\gamma_{th_2}) &= Pr\left(|h_{S_i}|^2 > \frac{\gamma_{th_2}\left(a_1\epsilon_{R_i}\rho_{S_i}|\tilde{g}_{R_i}|^2+\chi\right)}{a_2\rho_{S_i}}, |\tilde{g}_{R_i}|^2 > \frac{a_2\Lambda_m\chi}{\gamma_{th_2}a_1\epsilon_{R_i}\rho_{S_i}}\right) \\
&= \int_0^\infty \int_{\frac{a_2\Lambda_m\eta}{\gamma_{th_2}a_1\epsilon_{R_i}\rho_{S_i}}}^\infty \int_{\eta_1}^\infty f_{|h_{S_i}|^2}(x)\, f_{|\tilde{g}_{R_i}|^2}(y)\, f_{|h_{R_iR_i}|^2}(z) dx dy dz.
\end{aligned}
\tag{8.41}
$$

To obtain closed form of this component, we use (8.13), (8.34), and the following PDF of $|\tilde{g}_{R_i}|^2$

$$
f_{|\tilde{g}_{R_i}|^2}(x) = \frac{\tilde{m}_R^{\tilde{m}_R} x^{\tilde{m}_R-1} e^{-\tilde{m}_R x}}{\Gamma(\tilde{m}_R)},
\tag{8.42}
$$

and it is attained as in (8.43) after implementation of the following steps:

- Firstly, insert equivalences of $\tilde{f}_{|h_{S_i}|^2}(x)$, $f_{|\tilde{g}_{R_i}|^2}(y)$ and $f_{|h_{R_iR_i}|^2}(z)$ into (8.41).
- Secondly, convert the most inner integral into the form of upper incomplete Gamma function and insert the identity [65, eq. (8.352.1)] for upper incomplete Gamma function to obtain $\Gamma\big(G_{ds},z\big) = \Gamma(G_{ds})e^{-z}\sum_{k=0}^{G_{ds}-1}\frac{z^k}{\Gamma(k+1)}$, where $z = \frac{b^2\gamma_{th_2}\left(a_1\epsilon_{R_i}\rho_{S_i}y+\varpi_i\rho_{R_i}z+1\right)}{T_p a_2\rho_{S_i}}$.
- Thirdly, use Binomial theorem twice to get $\left(a_1\epsilon_{R_i}\rho_{S_i}y+\varpi_i\rho_{R_i}z+1\right)^k = \sum_{k_1=0}^{k}\sum_{k_2=0}^{k_1}\binom{k}{k_1}\binom{k_1}{k_2}\left(a_1\epsilon_{R_i}\rho_{S_i}y\right)^{k_2}\left(\varpi_i\rho_{R_i}z\right)^{k_1-k_2}$.
- Fourthly, inserting $f_{|\tilde{g}_{R_i}|^2}(y)$ in (8.42) into the integration (Up to this step, no need to insert closed form of $f_{|\tilde{g}_{R_i}|^2}(y)$ into (8.41)) and transform the integral into upper incomplete Gamma function. Thereafter, use the identity [65, eq.

(8.352.1)] for upper incomplete Gamma function to get $\Gamma\big(k_2+\tilde{m}_R,z\big)=\Gamma(k_2+\tilde{m}_R)e^{-z}\sum_{k_3=0}^{k_2+\tilde{m}_R-1}\frac{z^{k_3}}{\Gamma(k_3+1)}$, where $z=\frac{\big(\tilde{m}T_pa_2+\gamma_{th_2}b^2a_1\epsilon_{R_i}\big)\Lambda_m}{T_p\gamma_{th_2}a_1\epsilon_{R_i}\rho_{S_i}}(\varpi_i\rho_{R_i}z+1)$. Then, apply Binomial theorem to get $(\varpi_i\rho_{R_i}z+1)^{k_3}=\sum_{k_4=0}^{k_3}\binom{k_3}{k_4}(\varpi_i\rho_{R_i}z)^{k_4}$.

- Finally, insert closed form of $f_{|h_{R_iR_i}|^2}(z)$ in (8.34) into (8.42) and after proper rearrangements, the integral is in the form of Gamma function, which completes the derivation of $P_{\phi_1}^1(\gamma_{th_1},\gamma_{th_2})$ as given in (8.43).

$$P_{\phi_1}^1(\gamma_{th_1},\gamma_{th_2})=\sum_{p=1}^{N}\sum_{k=0}^{G_{ds}-1}\sum_{k_1=0}^{k}\sum_{k_2=0}^{k_1}\sum_{k_3=0}^{k_2+\tilde{m}_R-1}\sum_{k_4=0}^{k_3}\Bigg[\frac{W_pT_p^{G_{ds}}\frac{\gamma_{th_2}b^2}{T_pa_2\rho_{S_i}}\binom{k}{k_1}\binom{k_1}{k_2}\binom{k_3}{k_4}m_{R_iR_i}^{m_{R_iR_i}}}{\Gamma(m_f)\Gamma(m_s)\Gamma(k+1)\Gamma(k_3+1)}$$
$$\times\frac{\tilde{m}_R^{\tilde{m}_R}\Gamma(k_2+\tilde{m})\Gamma(k_1-k_2+k_4+m_{R_iR_i})\Gamma(G_{ds})(a_1\epsilon_{R_i}\rho_{S_i})^{k_2}}{\Gamma(\tilde{m}_R)\Gamma(m_{R_iR_i})\Omega_{R_iR_i}^{m_{R_iR_i}}(\tilde{m}_R+\frac{\gamma_{th_2}b^2a_1\epsilon_{R_i}}{T_pa_2})^{k_2+\tilde{m}}}$$
$$\times\frac{(\varpi_i\rho_{R_i})^{k_1-k_2+k_4}\left(\frac{\big(\tilde{m}_RT_pa_2+\gamma_{th_2}b^2a_1\epsilon_{R_i}\big)\Lambda_m}{T_p\gamma_{th_2}a_1\epsilon_{R_i}\rho_{S_i}}\right)^{k_3}e^{-\left(\frac{\big(\tilde{m}_RT_pa_2+\gamma_{th_2}b^2a_1\epsilon_{R_i}\big)\Lambda_m}{T_p\gamma_{th_2}a_1\epsilon_{R_i}\rho_{S_i}}+\frac{\gamma_{th_2}b^2}{T_pa_2\rho_{S_i}}\right)}}{\left(\frac{m_{R_iR_i}}{\Omega_{R_iR_i}}+\frac{\gamma_{th_1}b^2\varpi_i\rho_{R_i}}{T_pa_2\rho_{S_i}}+\frac{\big(\tilde{m}_RT_pa_2+\gamma_{th_2}b^2a_1\epsilon_{R_i}\big)\Lambda_m\varpi_i\rho_{R_i}}{T_p\gamma_{th_2}a_1\epsilon_{R_i}\rho_{S_i}}\right)^{k_1-k_2+k_4+m_{R_iR_i}}}\Bigg] \tag{8.43}$$

The remaining probability component, $P_{\phi_1}^2(\gamma_{th_1},\gamma_{th_2})$, can be rephrased as

$$\begin{aligned}P_{\phi_1}^2(\gamma_{th_1},\gamma_{th_2})&=Pr\left(|h_{S_i}|^2>\Lambda\chi,|\tilde{g}_{R_i}|^2<\frac{a_2\Lambda_m\chi}{\gamma_{th_2}a_1\epsilon_{R_i}\rho_{S_i}}\right)\\&=\int_0^{\infty}\int_{\Lambda\eta}^{\infty}\int_0^{\frac{a_2\Lambda_m\eta}{\gamma_{th_2}a_1\epsilon_{R_i}\rho_{S_i}}}f_{|h_{S_i}|^2}(x)\,f_{|\tilde{g}_{R_i}|^2}(y)\,f_{|h_{R_iR_i}|^2}(z)dxdydz\\&=\int_0^{\infty}\int_{\Lambda\eta}^{\infty}f_{|h_{S_i}|^2}(x)\,f_{|h_{R_iR_i}|^2}(z)dxdz-\\&\quad\int_0^{\infty}\int_{\Lambda\eta}^{\infty}\int_{\frac{a_2\Lambda_m\eta}{\gamma_{th_2}a_1\epsilon_{R_i}\rho_{S_i}}}^{\infty}f_{|h_{S_i}|^2}(x)\,f_{|\tilde{g}_{R_i}|^2}(y)\,f_{|h_{R_iR_i}|^2}(z)dxdydz.\end{aligned} \tag{8.44}$$

For this formulation let's follow the same steps as in the derivation of (8.35) and (8.43) for the first and second components, respectively and get the closed form as follows

$$P^2_{\phi_1}(\gamma_{th_1},\gamma_{th_2}) = \sum_{p=1}^{N}\sum_{k=0}^{G_{ds}-1}\sum_{k_1=0}^{k}\Bigg[\frac{W_p T_p^{G_{ds}}\Gamma(G_{ds})\binom{k}{k_1}(\varpi_i\rho_{R_i})^{k_1} m_{R_iR_i}^{m_{R_iR_i}}(\frac{b^2\Lambda}{T_p})^k}{\Gamma(m_f)\Gamma(m_s)\Gamma(k+1)\Gamma(m_{R_iR_i})\Omega_{R_iR_i}^{m_{R_iR_i}}} \times \frac{\Gamma(k_1+m_{R_iR_i})e^{-\frac{b^2\Lambda}{T_p}}}{\left(\frac{m_{R_iR_i}}{\Omega_{R_iR_i}}+\frac{b^2\Lambda\varpi_i\rho_{R_i}}{T_p}\right)^{k_1+m_{R_iR_i}}}\Bigg] - \sum_{p=1}^{N}\sum_{k=0}^{G_{ds}-1}\sum_{k_1=0}^{k}\sum_{q=0}^{\tilde{m}_R-1}\sum_{q_1=0}^{q}\Bigg[\frac{W_p T_p^{G_{ds}}\Gamma(G_{ds})\Gamma(k_1+q_1+m_{R_iR_i})\binom{k}{k_1}\binom{q}{q_1}}{\Gamma(m_f)\Gamma(m_s)\Gamma(k+1)\Gamma(q+1)\Gamma(m_{R_iR_i})} \times \frac{m_{R_iR_i}^{m_{R_iR_i}}(\varpi_i\rho_{R_i})^{k_1+q_1}\left(\frac{b^2\Lambda}{T_p}\right)^k\left(\frac{\tilde{m}_R a_2\Lambda_m}{\gamma_{th_2}a_1\epsilon_{R_i}\rho_{S_i}}\right)^{q_1} e^{-\left(\frac{b^2\Lambda}{T_p}+\frac{\tilde{m}_R a_2\Lambda_m}{\gamma_{th_2}a_1\epsilon_{R_i}\rho_{S_i}}\right)}}{\Omega_{R_iR_i}^{m_{R_iR_i}}\left(\frac{m_{R_iR_i}}{\Omega_{R_iR_i}}+\frac{b^2\Lambda\varpi_i\rho_{R_i}}{T_p}+\frac{\tilde{m}_R a_2\Lambda_m\varpi_i\rho_{R_i}}{\gamma_{th_2}a_1\epsilon_{R_i}\rho_{S_i}}\right)^{k_1+q_1+m_{R_iR_i}}}\Bigg]. \tag{8.45}$$

This ends up the derivation of $P_{\phi_1}(\gamma_{th_1},\gamma_{th_2}) = P^1_{\phi_1}(\gamma_{th_1},\gamma_{th_2}) + P^2_{\phi_1}(\gamma_{th_1},\gamma_{th_2})$. The second component, $P_{\phi_2}(\gamma_{th_1},\gamma_{th_2})$, is reformulated as

$$\begin{aligned}
P_{\phi_2}(\gamma_{th_1},\gamma_{th_2}) &= Pr\left(\frac{a_3\rho_{D_{2i}}|g_{R_{i2}}|^2}{a_4\rho_{D_{2i}}|g_{R_{i2}}|^2+1} > \gamma_{th_1}, \frac{a_4\rho_{D_{2i}}|g_{R_{i2}}|^2}{a_3\epsilon_{D_2}\rho_{D_{2i}}|\tilde{g}_{D2}|^2+1} > \gamma_{th_2}\right)\\
&= Pr\left(|g_{R_{i2}}|^2 > \frac{\gamma_{th_2}\left(a_3\epsilon_{D_2}\rho_{D_{2i}}|\tilde{g}_{D_2}|^2+1\right)}{a_4\rho_{D_{2i}}}, |g_{R_{i2}}|^2 > \frac{\gamma_{th_1}}{\rho_{D_{2i}}\left(a_3-a_4\gamma_{th_1}\right)}\right)\\
&= Pr\left(|g_{R_{i2}}|^2 > \frac{\gamma_{th_2}\left(a_3\epsilon_{D_2}\rho_{D_{2i}}|\tilde{g}_{D_2}|^2+1\right)}{a_4\rho_{D_{2i}}}, \frac{\gamma_{th_2}\left(a_3\epsilon_{D_2}\rho_{D_{2i}}|\tilde{g}_{D_2}|^2+1\right)}{a_4\rho_{D_{2i}}}\right.\\
&\quad \left.> \frac{\gamma_{th_1}}{\rho_{D_{2i}}\left(a_3-a_4\gamma_{th_1}\right)}\right) + Pr\left(|g_{R_{i2}}|^2 > \frac{\gamma_{th_1}}{\rho_{D_{2i}}\left(a_3-a_4\gamma_{th_1}\right)},\right.\\
&\quad \left.\frac{\gamma_{th_2}\left(a_3\epsilon_{D_2}\rho_{D_{2i}}|\tilde{g}_{D_2}|^2+1\right)}{a_4\rho_{D_{2i}}} < \frac{\gamma_{th_1}}{\rho_{D_{2i}}\left(a_3-a_4\gamma_{th_1}\right)}\right)\\
&= Pr\left(|g_{R_{i2}}|^2 > \frac{\gamma_{th_2}\left(a_3\epsilon_{D_2}\rho_{D_{2i}}|\tilde{g}_{D_2}|^2+1\right)}{a_4\rho_{D_{2i}}}, |\tilde{g}_{D_2}|^2 > \frac{a_4\Lambda_2}{\gamma_{th_2}a_3\epsilon_{D_2}\rho_{D_{2i}}}\right)\\
&\quad + Pr\left(|g_{R_{i2}}|^2 > \frac{\gamma_{th_1}}{\rho_{D_{2i}}\left(a_3-a_4\gamma_{th_1}\right)}, |\tilde{g}_{D_2}|^2 < \frac{a_4\Lambda_2}{\gamma_{th_2}a_3\epsilon_{D_2}\rho_{D_{2i}}}\right)
\end{aligned} \tag{8.46}$$

where $\Lambda_2 = \max\left(0, \frac{\gamma_{th_1}}{a_3-a_4\gamma_{th_1}} - \frac{\gamma_{th_2}}{a_4}\right)$. So $P_{\phi_2}(\gamma_{th_1},\gamma_{th_2})$ can be rewritten as

$$\begin{aligned}
P_{\phi_2}(\gamma_{th_1},\gamma_{th_2}) &= \int_{\psi_2}^{\infty}\int_{\psi_3}^{\infty} f_{|g_{R_{i2}}|^2}(x) f_{|\tilde{g}_{D_2}|^2}(y)dxdy\\
&\quad + \int_{0}^{\psi_2}\int_{\frac{U_2}{\rho_{D_{2i}}}}^{\infty} f_{|g_{R_{i2}}|^2}(x) f_{|\tilde{g}_{D_2}|^2}(y)dxdy
\end{aligned} \tag{8.47}$$

where $\psi_2 = \frac{a_4\Lambda_2}{\gamma_{th_2}a_3\epsilon_{D_2}\rho_{D_{2i}}}$, $\psi_3 = \frac{\gamma_{th_2}\left(a_3\epsilon_{D_2}\rho_{D_{2i}}y+1\right)}{a_4\rho_{D_{2i}}}$, the last double integral turns to two independent integrals and can be expressed in terms of CDFs. Closed form of the

first double integral in (8.47) is obtained as in (8.49) by following the similar method to the derivation of (8.35) and (8.43), where the inner integral is transformed into upper incomplete Gamma function, thereafter Binomial expansion is used, and finally remaining integral is again converted to form of upper incomplete Gamma function. The approximated PDF of $|g_{R_{i2}}|^2$, to distinguish it from those of $|h_{S_i}|^2$ and $|g_{R_{i1}}|^2$, is denoted as

$$\tilde{f}_{|g_{R_{i2}}|^2}(x) = \sum_{p=1}^{N} \left(\frac{W_{p,2} b_{D2}^{2G_{d2}} x^{G_{d2}-1}}{\Gamma(m_{D_2 f})\Gamma(m_{D_2 s})} e^{-\frac{b_{D2}^2}{T_{p,2}} x} \right) \tag{8.48}$$

where $G_{d2} = \min(m_{D_2 f}, m_{D_2 s})$ and $b_{D2} = \sqrt{\frac{m_{D_2 f} m_{D_2 s}}{\Omega_{D_2 f} \Omega_{D_2 s}}}$. (8.48) is used in (8.47) to get (8.49).

$$\begin{aligned} P_{\phi_2}(\gamma_{th_1}, \gamma_{th_2}) = \sum_{p=0}^{N} \sum_{k=0}^{G_{d2}-1} \sum_{k_1=0}^{k} \Bigg[& \frac{W_{p,2} T_{p,2}^{G_{d2}} \Gamma\left(G_{d2}\right) \binom{k}{k_1} \left(a_3 \epsilon_{D_2} \rho_{D_{2i}}\right)^{k_1} \left(\frac{\gamma_{th_2} b_{D2}^2}{T_{p,2} a_4 \rho_{D_{2i}}}\right)^{k}}{\Gamma(m_{D_2 f})\Gamma(m_{D_2 s}) \left(\tilde{m}_{D_2} + \frac{\gamma_{th_2} b_{D2}^2 a_3 \epsilon_{D_2}}{T_{p,2} a_4}\right)^{k_1 + \tilde{m}_{D_2}}} \\ & \times \frac{\tilde{m}_{D_2}^{\tilde{m}_{D_2}} e^{-\frac{\gamma_{th_2} b_{D2}^2}{T_{p,2} a_4 \rho_{D_{2i}}}}}{\Gamma(k+1)\Gamma(\tilde{m}_{D_2})} \Gamma\left(k_1 + \tilde{m}_{D_2}, \frac{a_4 \Lambda_2}{\gamma_{th_2} a_3 \epsilon_{D_2} \rho_{D_{2i}}} \left(\tilde{m}_{D_2} + \frac{\gamma_{th_2} b_{D2}^2 a_3 \epsilon_{D_2}}{T_{p,2} a_4}\right)\right) \\ & + F_{|\tilde{g}_{D_2}|^2}\left(\frac{a_4 \Lambda_2}{\gamma_{th_2} a_3 \epsilon_{D_2} \rho_{D_{2i}}}\right) \left(1 - F_{|g_{R_{i2}}|^2}\left(\frac{\gamma_{th_1}}{\rho_{D_{2i}}\left(a_3 - a_4 \gamma_{th_1}\right)}\right)\right) \Bigg]. \end{aligned} \tag{8.49}$$

9. DF MULTI-HOP NETWORKS OVER NAKAGAMI-*m* FADING CHANNELS

9.1. Introduction

The multi-hop communication systems have been offered to extend coverage area and to make power more manageable [173]. In multi-hop communication systems, the main purpose is to realize the transmission through the relays in between. Therefore, coverage area extension is accomplished without the need for too much power in the transmitter part.

Multi-hop communication was first examined in [174]. In this work, OP expressions are provided for both DF and AF protocols, where the expression of DF case is in a closed form for i.i.d. Nakagami-m fading channels. On the other hand, an upper bound of OP for AF over i.n.i.d. Nakagami-m fading channels is given in terms of inverse Laplace Transform, hence, it can be calculated via numerical inversion of the Laplace transform. Lower and upper bounds of OP for the same work with co-channel interference and AF protocol over i.n.i.d. Nakagami-m fades are derived in [175]. In [176], closed forms of OP and SER expressions for the system studied in [175] are obtained for i.i.d. Nakagami-m fading channels. A multi-hop system with AF transmission is investigated over i.n.i.d. Generalized Gamma distribution channels in [177]. In this study, moment generating function (MGF) of end-to-end SNR is presented, hence, SER of M-ary coherent modulations can be calculated numerically.

Multi-hop networks with DF protocol over i.n.i.d. Nakagami-m fading channels have also been examined in detail [178–181]. In [178], FD transmission is investigated and OP expression is given in terms of the infinite Gamma series representation. In the work of [179], exact analytical expression for the e2e OP considering the effects of co-channel interference caused by inter-relay links and the echo interference at the FD relays is provided. Additionally, an OP expression for HD transmission protocol is also introduced. However, the complexity of the derived expression and its impractical implementation can easily be realised. The SER analysis for HD transmission is focused in [180], where a symbol transition matrix (STM) whose entries are the symbol transition probabilities of a relay in a DF relaying system is defined. Using the STM as a state transition matrix of a discrete-time Markov chain, the source-to-destination STM is shown to be the product of intermediate STMs in multihop DF relaying systems. The probability

of correct decision at the destination is shown to be the trace of the source-to-destination STM divided by the modulation order.

Without any doubt, next generation communication systems will operate in mmWave bands, therefore, effect of fading and shadowing unfortunately becomes more dominant than ever. Hence, multi-hop systems seem to be revised again. One of the most recent work over i.n.i.d Nakagami-m fading channels with DF protocol considering co-channel interference is illustrated in [181]. In this work, i.n.i.d. channel assumption is not stated directly but values of shaping factors are probabilisticaly determined based on line of sight. Thereafter, all performance criteria are calculated over all possible occurrences. In the stated work, while CDF is obtained, the terms resulting from the product of polynomials are given by ordering from the smallest to the largest degree. In our work, terms in the CDF are given without ordering since no need to waste effort to calculated coefficients of each term. Furthermore, unlike [181] where SER of each modulation type is separately evaluated based on conditional probabilities, closed form of SER for M-PSK and M-QAM is provided in a single term based on MGF method. Moreover, SER expression is not derived for M-PSK in [181]. Additionally, closed form of ergodic capacity is also derived which is simpler than that given in [181]. Consequently, simplicity of the derived expressions is essential for both future works and easy interpretations. Furthermore, in case of the smaller number of hops, direct path (DP) signal cannot be ignored and should also be taken into consideration. For this reason, analysis with DP case are additionally provided. The closed form expressions for MGF, OP, and SER considering DP are derived.

The remainder of this chapter is organized as follows. In Section 9.2, details of system model are provided. OP, SER, and ergodic capacity derivations are given in Section 9.3, 9.4, and 9.5, respectively. Analysis of the system considering availability of DP is detailed in 9.6. Numerical results are elaborated in Section 9.7. Finally, we conclude our work in Section 9.8.

9.2. System Model

In this work, a multi-hop communication network consisting of a source and $(N-1)$ HD DF relays given in Fig. 9.1 is revised over i.n.i.d. Nakagami-m fading channels. Ergodic capacity, OP, and SER expressions are provided in closed form which are simpler than the existing ones.

The signal at the source and decomposed signal at the each relay is represented with x_i which has unit energy. The channel gain of the i^{th} hop is represented as h_i with m_i

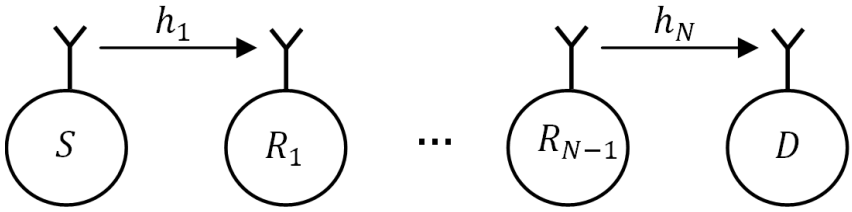

Figure 9.1: The multi-hop system under the consideration.

shaping and Ω_i scaling factors, $i \in \{1, 2, \dots N\}$. The received signal is decoded and retransmitted at each relay. The receipt signal at each hop is

$$Y_{R_i} = h_i \sqrt{P_i} x_i + n_{R_i}, \tag{9.1}$$

where n_{R_i} is the additive Gauss noise (AGN) at the i^{th} hop. The power at the each hop is given by P_i; in that case P_1 is the source power and P_N is the power of $(N-1)^{th}$ relay. Hence, SNR at each relay is $\gamma_i = P_i |h_i|^2 / \sigma_i^2$ and inverse of its expected value is $\lambda_i = \sigma_i^2 / (P_i \Omega_i)$, where $|\cdot|$ is absolute value operator and σ_i^2 denotes variance of the AGN at i^{th} hop.

9.3. Outage Probability

Usage of DF protocol means the overall system is in outage if any hop is in outage. Therefore, outage case is mathematically represented by $\min\{\gamma_1, \gamma_2, \cdots, \gamma_N\} < \gamma_{th}$, where γ_{th} is the SNR threshold corresponds to the data rate R, therefore, $\gamma_{th} = 2^{2R} - 1$. The equivalence instantaneous SNR of the overall system is shown by $\gamma_{eq} = \min\{\gamma_1, \gamma_2, \cdots, \gamma_N\}$. So OP expression, in turns CDF of γ_{eq}, is

$$\begin{aligned} F_{\gamma_{eq}}(\gamma_{th}) &= Pr(\min\{\gamma_1, \gamma_2, \cdots, \gamma_N\} < \gamma_{th}) \\ &= 1 - \prod_{i=1}^{N} Pr(\gamma_i > \gamma_{th}) \\ &= 1 - \prod_{i=1}^{N} \frac{\Gamma(m_i, m_i \lambda_i \gamma_{th})}{\Gamma(m_i)} \end{aligned}, \tag{9.2}$$

where, the gamma function is $\Gamma(m_i) = \int_0^\infty t^{m_i - 1} e^{-t} dt$ [65, eq. (8310.1)] and upper incomplete Gamma function is $\Gamma(m_i, x) = \int_x^\infty t^{m_i - 1} e^{-t} dt$ [65, eq. (8350.2)]. The last line of the equality is reached by using the fact that $\Gamma(m_i) = \Gamma(m_i, x) + \gamma(m_i, x)$, i.e.,

$\Gamma(m_i,x)/\Gamma(m_i) = 1-\gamma(m_i,x)/\Gamma(m_i,x)$ is considered. $\gamma(m_i,x) = \int_0^x t^{m_i-1}e^{-t}dt$ is the lower incomplete gamma function [65, eq. (8350.1)]. For integer m_i values, $\frac{\Gamma(m_i,x)}{\Gamma(m_i)} = e^{-x}\sum_{p_i=0}^{m_i-1}\frac{x^{p_i}}{\Gamma(p_i+1)}$, so $F_{\gamma_{eq}}(\gamma_{th})$ can be rephrased as follows:

$$F_{\gamma_{eq}}(\gamma_{th}) = 1-\sum_{p_1=0}^{m_1-1}\sum_{p_2=0}^{m_2-1}\cdots\sum_{p_N=0}^{m_N-1}\left[\prod_{i=1}^{N}\left(\frac{(m_i\lambda_i)^{p_i}}{\Gamma(p_i+1)}\right)x^p e^{-\omega x}\right], \tag{9.3}$$

where $p=\sum_{i=1}^{N}p_i$ and $\omega=\sum_{i=1}^{N}(m_i\lambda_i)$. This ends up the derivation of OP.

9.4. SER Analysis

Taking inverse Laplace transform of (9.3) and multiplying it by s results in MGF of γ_{eq} [65, eq. (17.11) and (17.12.2)] as follows:

$$M_{\gamma_{eq}}(-s) = 1-\sum_{p_1=0}^{m_1-1}\sum_{p_2=0}^{m_2-1}\cdots\sum_{p_N=0}^{m_N-1}\left[\psi_N\frac{s}{(s+\omega)^{p+1}}\right], \tag{9.4}$$

where $\psi_N = \prod_{i=1}^{N}\left(\frac{(m_i\lambda_i)^{p_i}}{\Gamma(p_i+1)}\right)\Gamma(p+1)$. Based on MGF method, SER expression is obtained by the equility $\sum_{q=1}^{Q}a_q\int_0^{\theta_q}M_{\gamma_{\text{eq}}}\left(-\frac{\lambda_{\text{mod}}}{\sin^2(\theta)}\right)d\theta$ [74, eq. (5.3)]. Closed form of the SER expression is derived as below

$$P_{SER} = \sum_{q=1}^{Q}a_q\left\{\theta_q-\sum_{p_1=0}^{m_1-1}\sum_{p_2=0}^{m_2-1}\cdots\sum_{p_N=0}^{m_N-1}\left[\psi_N I_p\left(\theta_q;\lambda_{\text{mod}};\omega\right)\right]\right\}. \tag{9.5}$$

The modulation dependent parameters are provided in Table 2.1. The integral $I_k\left(\theta_q;\lambda_{\text{mod}};b_i\right)$ in the P_{SER} is given in (9.6).

$$I_k\left(\theta_q;\lambda_{\text{mod}};b_i\right) = \int_0^{\theta_q}\frac{\lambda_{\text{mod}}(\sin^2(\theta))^k}{(b_i\sin^2(\theta)+\lambda_{\text{mod}})^{k+1}}d\theta. \tag{9.6}$$

The integral in (9.6) for $k=0$ is derived by aid of the identity [65, eq. (2.262.1)] as

$$I_0\left(\theta_q;\lambda_{\text{mod}};b_i\right) = \begin{cases}\Psi\arctan\left(\frac{\tan(\theta_q)}{\Psi}\right) & \theta_q<\frac{\pi}{2}\\ \frac{\Psi\pi}{2} & \theta_q=\frac{\pi}{2}\\ \Psi\left(\pi+\arctan\left(\frac{\tan(\theta_q)}{\Psi}\right)\right) & \theta_q>\frac{\pi}{2}\end{cases}, \tag{9.7}$$

where $\Psi = \sqrt{\frac{\lambda_{\text{mod}}}{\lambda_{\text{mod}}+b_i}}$. The $I_k\left(\theta_q;\lambda_{\text{mod}};b_i\right)$ under $k \geq 1$ and $0 \leq \theta_q \leq \pi$ conditions turns to

$$I_k\left(\theta_q;\lambda_{\text{mod}};b_i\right) = \frac{1}{\left(\lambda_{\text{mod}}\right)^{1/2}\left(\lambda_{\text{mod}}+b_i\right)^{k+1/2}}\left[\frac{T}{2^{2k}}\binom{2k}{k} + \frac{(-1)^k}{2^{2k-1}}\sum_{j=0}^{k-1}(-1)^j\binom{2k}{j}\frac{\sin[(2k-2j)T]}{2k-2j}\right], \tag{9.8}$$

where $T = \frac{1}{2}\tan^{-1}\frac{N_1}{D_1} + \frac{1}{\pi}\left(1 - \frac{(1+\text{sign}(D_1))}{2}\text{sign}(N_1)\right)$, $N_1 = 2\sqrt{\lambda_{\text{mod}}(\lambda_{\text{mod}}+b_i)}\sin(2\theta_q)$ and $D_1 = (2\lambda_{\text{mod}}+b_i)\cos(2\theta_q) - b_i$.

9.5. Ergodic Capacity

The ergodic capacity can be derived based on CDF method as [75, eq. (38)]

$$R_{Avg.} = \log_2(e)\int_0^\infty \frac{1-F_{\gamma_{eq}}(x)}{x+1}dx. \tag{9.9}$$

After inserting the (9.3) into (9.9), ergodic capacity becomes

$$R_{Avg.} = 1 - \sum_{p_1=0}^{m_1-1}\sum_{p_2=0}^{m_2-1}\cdots\sum_{p_N=0}^{m_N-1}\left[\prod_{i=1}^{N}\left(\frac{(m_i\lambda_i)^{p_i}}{\Gamma(p_i+1)}\right)\int_0^\infty \frac{x^p e^{-\omega x}}{x+1}dx\right]. \tag{9.10}$$

The integral in this equation is [56, eq. (39)]

$$\begin{aligned} I_p(\omega) &= \int_0^\infty \frac{x^p e^{-\omega x}}{x+1}dx \\ &= e^{\omega}\Gamma(p+1)\Gamma(-p,\omega) \end{aligned}. \tag{9.11}$$

9.6. Analysis of Multi-Hop with Direct Path

In case of the smaller number of hops, availability of a direct path (DP) between the source and destination is possible with a high probability, which provides diversity. Since it increases diversity order by 1. Hence, merging the signals of the DP and last hop with maximal ratio combining (MRC) decreases error rates (SERs) and OP significantly, similarly other combining techniques such as selection combining (SC). Let's assume

the DP channel gain distributes as Nakagami-m and represent it with h_{DP}, its shaping factor with m_{DP} and scaling factor as Ω_{DP}. So, the SNR related to the DP becomes $\gamma_{DP} = P_1|h_{DP}|^2/\sigma_N^2$ and inverse of its expected value is $\lambda_{DP} = \sigma_N^2/(P_1\Omega_{DP})$. After MRC processing at the destination, SNR is

$$\gamma_{MRC} = \gamma_{eq} + \gamma_{DP}. \tag{9.12}$$

Note that the exact SNR is $\gamma_{MRC} = \gamma_N + \gamma_{DP}$ but we focus on $\gamma_{MRC} = \gamma_{eq} + \gamma_{DP}$ to simplify the analysis. Actually, this is a tight bound and generally used in the literature without mentioning exact SNR. Therefore, MGF of γ_{MRC} turns to

$$M_{\gamma_{MRC}}(-s) = M_{\gamma_{eq}}(-s)M_{\gamma_{DP}}(-s). \tag{9.13}$$

The MGF related to DP is [74, eq. (5.15)]

$$M_{\gamma_{DP}}(-s) = \frac{(m_{DP}\lambda_{DP})^{m_{DP}}}{(s + m_{DP}\lambda_{DP})^{m_{DP}}}. \tag{9.14}$$

Inserting (9.4) and (9.14) into (9.13) results in

$$M_{\gamma_{MRC}}(-s) = \frac{(m_{DP}\lambda_{DP})^{m_{DP}}}{(s + m_{DP}\lambda_{DP})^{m_{DP}}} - \sum_{NHOP}\left[\frac{\psi_N\,(m_{DP}\lambda_{DP})^{m_{DP}}\,s}{(s+\omega)^{p+1}\,(s + m_{DP}\lambda_{DP})^{m_{DP}}}\right]. \tag{9.15}$$

For the sake of clarity, the shorthand abbreviation $\sum_{NHOP} = \sum_{p_1=0}^{m_1-1}\sum_{p_2=0}^{m_2-1}\cdots\sum_{p_N=0}^{m_N-1}$ is used. To get closed form of CDF and tractable integrals in SER calculations, we define $\phi(s) = \frac{1}{(s+\omega)^{p+1}(s+m_{DP}\lambda_{DP})^{m_{DP}}}$ and use partial decomposition to get

$$\phi(s) = \sum_{m=1}^{p+1}\left(\frac{C_m^{\omega}}{(s+\omega)^m}\right) + \sum_{m=1}^{m_{DP}}\left(\frac{C_m^{DP}}{(s + m_{DP}\lambda_{DP})^m}\right), \tag{9.16}$$

where C_m^{ω} and C_m^{DP} are

$$\begin{aligned} C_m^{\omega} &= \frac{(-1)^{p-m+1}\Gamma(p + m_{DP} - m + 1)}{\Gamma(m_{DP})\Gamma(p - m + 2)\,(m_{DP}\lambda_{DP} - \omega)^{p+m_{DP}-m+1}} \\ C_m^{DP} &= \frac{(-1)^{m_{DP}-m}\Gamma(p + m_{DP} - m + 1)}{\Gamma(p+1)\Gamma(m_{DP} - m + 1)\,(\omega - m_{DP}\lambda_{DP})^{p+m_{DP}-m+1}} \end{aligned}. \tag{9.17}$$

Substituting (9.16) into (9.15) gives

$$M_{\gamma_{MRC}}(-s) = \frac{(m_{DP}\lambda_{DP})^{m_{DP}}}{(s+m_{DP}\lambda_{DP})^{m_{DP}}} - \sum_{NHOP}\Bigg[\sum_{m=1}^{p+1}\Big(\frac{\psi_N\,(m_{DP}\lambda_{DP})^{m_{DP}}\,C_m^{\omega}s}{(s+\omega)^m}\Big) + \sum_{m=1}^{m_{DP}}\Big(\frac{\psi_N\,(m_{DP}\lambda_{DP})^{m_{DP}}\,C_m^{DP}s}{(s+m_{DP}\lambda_{DP})^m}\Big)\Bigg]. \tag{9.18}$$

Closed form expression for SER based on MGF method is straightforward as in (9.5) except the first term in (9.18) results in the integral $\int_0^{\theta_q}\left(\frac{\sin^2(\theta)}{\sin^2(\theta)+c}\right)^k$ with the closed form given in [74, eq. (5A.26)] and the integrals in the summations are as in (9.6).

The CDF, in turn OP, is the inverse Laplace transform of $M_{\gamma_{MRC}}(-s)/s$ and derived as

$$F_{\gamma_{MRC}}(x) = \frac{\Gamma(m_{DP}) - \Gamma(m_{DP} - m_{DP}\lambda_{DP}x)}{\Gamma(m_{DP})} - \sum_{NHOP}\Bigg[\sum_{m=1}^{p+1}\Big(\frac{\psi_N\,(m_{DP}\lambda_{DP})^{m_{DP}}\,C_m^{\omega}x^{m-1}e^{-\omega x}}{\Gamma(m)}\Big) + \sum_{m=1}^{m_{DP}}\Big(\frac{\psi_N\,(m_{DP}\lambda_{DP})^{m_{DP}}\,C_m^{DP}x^{m-1}e^{-\omega x}}{\Gamma(m)}\Big)\Bigg]. \tag{9.19}$$

This ends up the derivation of OP and SER expressions for the multi-hop system with DP.

9.7. Numerical Results

In this section, the validity of the derived OP and SER expressions is shown by numerical and simulation results. The variances at the hops are assumed to be equal, $\sigma^2 = \sigma_i^2 = 1$. The curves are plotted versus total SNR, $P_T/\sigma^2 = \sum_{i=1}^{N} P_i/\sigma^2$. The total power is $P_T = \sum_{i=1}^{N} P_i$. The data rate threshold is set to $R = 2$ bits/s/Hz, hence, SNR threshold becomes $10\log 10(15) = 11.76$ dB. Channel scale factors are $\Omega_i = 1$ for all hops. The total number of hops is at most 4. For the multi-hop system without DP, the shaping factors are $m_i = 2$ for OP curves, additionally, a case with all shaping factors being different, $(m_1, m_2, m_3, m_4) = (2, 3, 4, 1)$, is also provided. QPSK (4-PSK/QAM), 16-PSK, and 16-QAM SER curves are also illustrated for this distinct shape factors. OP and SER curves are calculated from (9.3) and (9.5), respectively. OP curves of multi-hop system with DP are produced from (9.19). The shaping factors are $m_i = 2$ for multi-hop channels, whereas $m_{DP} \in \{1, 2\}$ for DP. To accommodate the path loss effect, we set the normalized distance between the hops, d to 1 and, therefore, the normalized distance

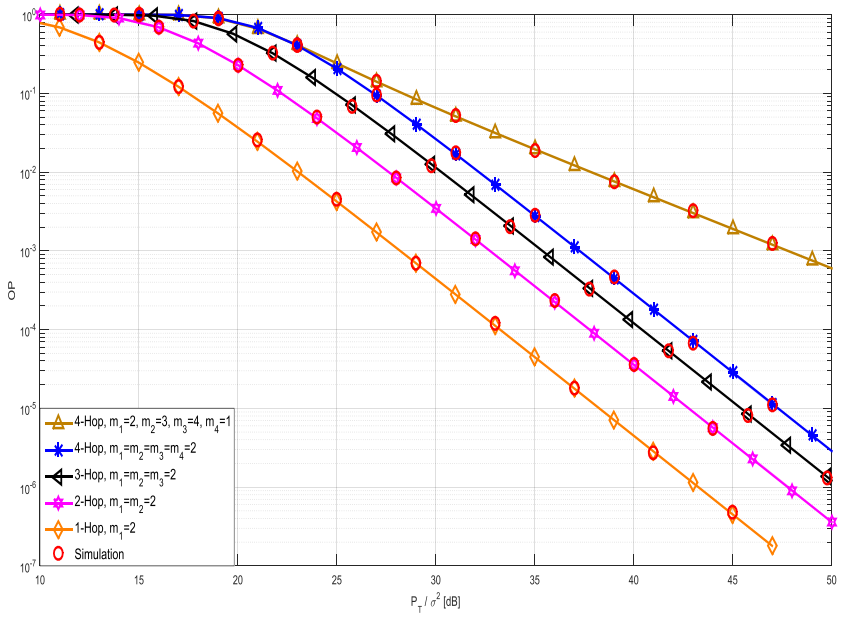

Figure 9.2: OP of the multi-hop transmission.

between the source and destination, d_{DP} roughly becomes total number of hops. Path lost exponent is set to 3 to represent urban transmission environment.

Fig. 9.2 demonstrates that as number of hops increases performance degrades. The loss in SNR for the same shaping factor, $m_i = 2$, is 5 dB, 7 dB, and 8.6 dB while number of hops changes from 1 to 4 at OP value of 10^{-4}. As a common mistake in the literature, curves are plotted versus the power of the source which means an unfair comparison. In that case the loss in SNR becomes 2 dB, 2.23 dB, and 2.58 dB. The hop that causes the performance of the top curve to be so bad is the fourth one. In this hop shape factor is $m_4 = 1$, which corresponds to Rayleigh fading channel and is the weakest hop. Keep in mind, considering a multi-hop transmission without any direct path from the source to the relays, from the relays to the relays, and from the relays to the destination causes an asymptotic analysis. Therefore, given curves are upper bounds.

Fig. 9.3 illustrates the SER performance of the system under consideration, namely the multi-hop system with FD relays, where curves are given for QPSK (4-PSK/QAM), 16-PSK, and 16-QAM. The almost excellent overlapping of the numerical and simulation results shows the validity of the derived expression.

Fig. 9.4 shows ergodic capacity performance of the multi-hop system. As in OP curves, channel variances are set to $\Omega_i = 1$. Total number of hops is at most 4 and $m_i \in \{1, 2\}$. As number of hops increases, capacity decreases. While the difference is high at low SNR values (P_T/σ^2), this difference decreases gradually at high values. The average capacity decreases as the fading shape factor decreases, that is, the effect of

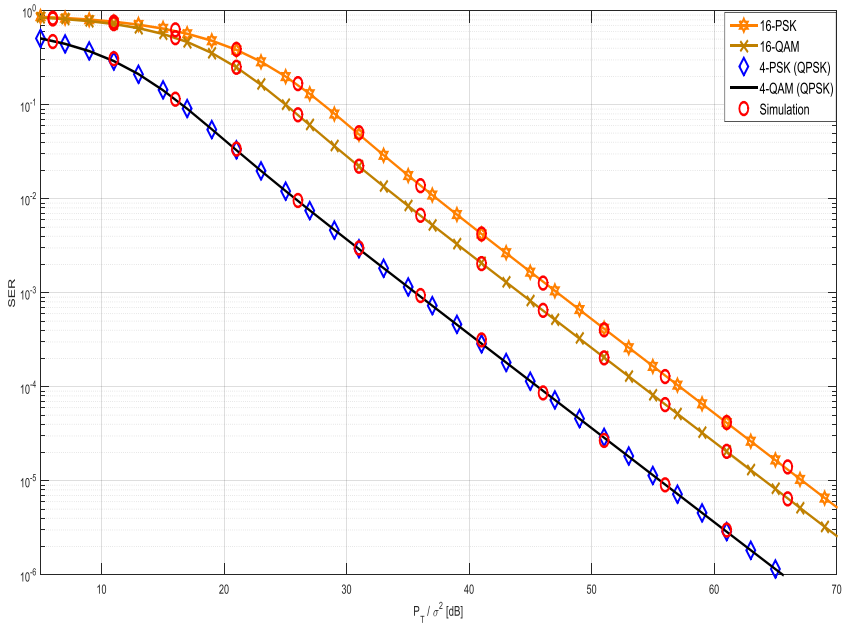

Figure 9.3: SER of multi-hop transmission.

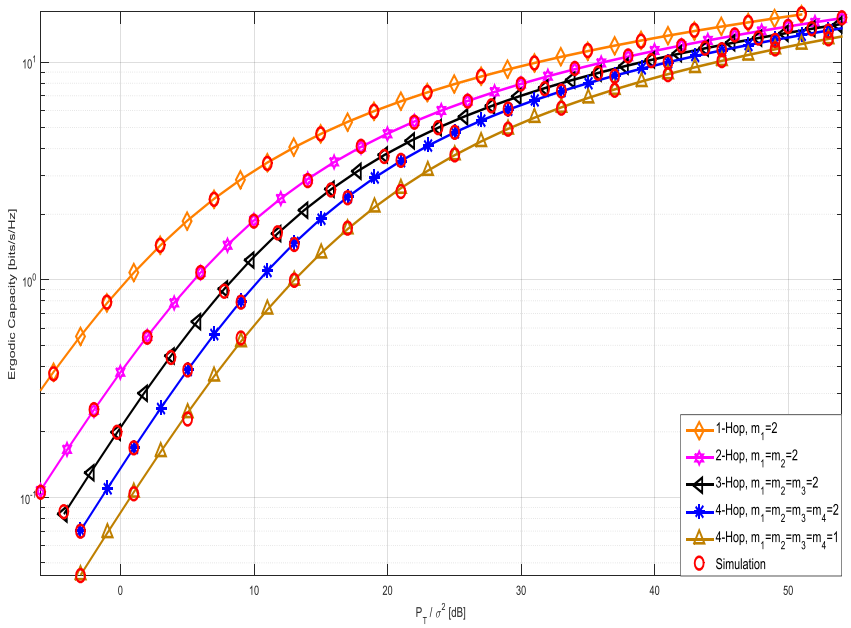

Figure 9.4: Ergodic capacity of the multi-hop networks.

fading increases. The overlap of the numerical and simulation results is excellent.

Fig. 9.5 validates the accuracy of OP expression for the multi-hop system with DP, in turn, this also proves the validity of SER expression since OP/CDF is derived from MGF. The gain in total SNR at an OP value of 10^{-6} for lower three curves (from left to right) with respect to the OP of the multi-hop system without considering DP signal (the most upper curve) is about 18 dB, 9.5 dB, and 7 dB, respectively. The effect of path loss is impressive which can be observed from the two lowest curves and the change in total SNR is about 8.5

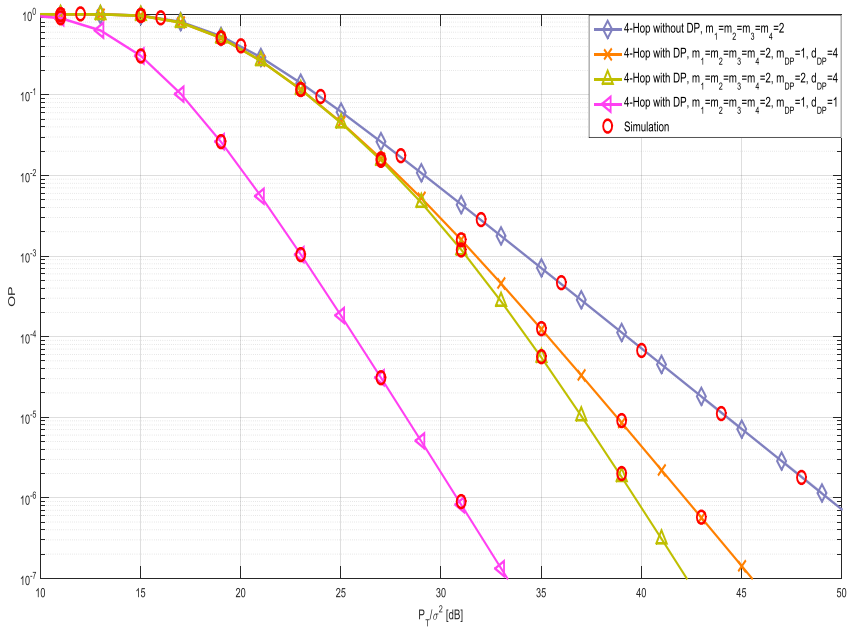

Figure 9.5: OP of MRC for multi-hop with DP.

dB at an OP value of 10^{-6}. At low total SNRs, DP signal is negligible due to the path loss effect. However, as SNR increases direct link becomes dominant. Therefore, especially in case of smaller number of hops, it does not make sense to ignore the signal of DP. Clearly, availability of DP provides diversity which improves the performance significantly.

9.8. Conclusion

The analysis of the DF multi-hop systems over i.n.i.d. Nakagami-m fading channels is revised. Firstly, simpler expressions for OP, SER, and ergodic capacity are derived and validated for the system without DP between the source and destination. Thereafter, the system with existence of DP link is considered and closed for expressions for MGF, OP, and SER are derived, where the closed form MGF of the system without DP is used. All analytical expressions are validated via Monte-Carlo simulation technique. Furthermore, it is shown that DP provides diversity. Hence, it improves performance and it should not be omitted in the case of smaller number of hops.

10. CONCLUSION

In this thesis, bidirectional and unidirectional relayed communication networks are investigated over independent (non-)identically distributed Rayleigh, Nakagami-m, and generalized-K wireless media for HD/FD transmission schemes, AF/DF relay protocols, and OMA/NOMA techniques. To mitigate degradation effects of fading/shadowing channels, mainly two different diversity techniques, namely, multi-antenna and multi-relay networks, are considered with generalized antenna and relay selections. Generalized selections include all cases, i.e., single antenna/relay selection and use of all antennas/relays (beamforming). Generalized antenna selection reduces hardware complexity but keeps offered performance gain of multi-input multi-output systems. Additionally, cooperative communication is investigated with relay selection to provide benefits of spatial diversity.

The first investigated system is a bidirectional system with two multi-antenna sources and an AF relay equipped with a single antenna. HD transmission with OMA technique is considered. Generalized antenna selection, i.e., GSC and GST, is carried out over i.i.d. slow Rayleigh fading environments for both transmission and reception. Exact and asymptotic expressions for CDF of e2e SNR, in turn, SOP of the system, and SSER based on MGF method for M-PSK and M-QAM are derived in closed form. Additionally, approximated SSER for M-PSK is also introduced based on CDF method. SER calculations for M-PSK and M-QAM are provided in a unique expression, which decreases the number of equations and simplifies analysis. Thereafter, the accuracy of the obtained expressions is validated by the aid of Monte Carlo simulation technique, where results demonstrate that hardware complexity, i.e., number of radio frequencies, can be reduced without significant loss in performance such as OP and SER.

The second analyzed system is a generalization of the first system, where relay has also multi-antenna with all other assumptions kept to be the same. Since it is not possible to select an antenna that simultaneously maximizes e2e SNRs of both sources in such systems, selection strategy is offered to help the source equipped with fewer antennas, thereby, diversity order of the link between the relay and the source having fewer antennas is increased. Single antenna selection at the relay means TAS/RAS. Therefore, generalized antenna selection at the source with fewer antennas and antenna selection at the relay is GST/RAS and TAS/GSC. Multi-antenna selection at the source having more antennas means GST and GSC. SOP and SSER expressions are derived and validated. Numerical

results illustrate that SOP and SSER can be significantly reduced by the offered antenna selection strategy.

The third system is similar to the first one except HD transmission and reciprocity assumption between the relay and the sources. Instead FD transmission is assumed and unlike reciprocal channel gains, forward and backward paths between the sources and relay are taken to be different which happens in practice but makes the mathematical analysis much harder. Additionally, FD transmission results in self-interference (SI), hence, fading SI also makes the problem to be further complicated. Despite all, a novel TRAS method selecting a pair of antennas for transmission and reception at terminal sources is proposed, where effective e2e SINR is maximized and all antenna space is used for either transmission or reception which results in a reduction in the total number of antennas at each terminal node. With four different AS scenarios, the exact SOP for fading SI and the exact, approximated, and asymptotic SOP expressions for non-fading SI are derived and validated. It is shown that performance can be significantly improved by the usage of offered TRAS strategy at terminal sources. In addition, it outperforms the selection strategy using maximum-paths from two divided antenna sets at each source, where one set is only used for transmission and the other one for reception. For different SI values, optimum power allocations are demonstrated and factors affecting optimum relay location are also elaborated. Each AS scenario produces the lowest SOP for different combinations of SI occurrences, power allocations, and relay locations.

In the remaining three works, RS is investigated for unidirectional relayed networks. In the first work, an FD variable gain AF multi-relay cooperative-diversity system with(out) DP/LOS between the source and destination is studied over i.i.d. (i.n.i.d.) slow Rayleigh fading channels. Generalized RS is investigated for two extreme cases; single RS and use of all relays, i.e., MRT/beamforming. By developing an equivalent link, the approximated PDF and CDF of a dual-hop link with FD relay are obtained, thereafter, the adopted approximated PDF and CDF are offered. Then, approximated and asymptotic expressions for OP, MGF, and SER of GST with(out) DP are derived. Additionally, approximated ergodic capacity expressions are also obtained and validated. For equal rates, a substantial reduction in SER can be obtained by FD transmission as compared to HD one. Furthermore, significant improvement in performance measures such as OP and SER is attained by the cooperative diversity (network with DP) as compared to the network without DP.

Two of remaining works are related to NOMA, first one consisting of two sources and two users with no line-of-sight among the sources and users but the second network

has only one source, are based on NOMA technique using HD and FD transmission protocols, where a DF relay is selected out of multi-relays in two stages to maximize data rate of the second user with providing quality service for the first user. The former network, which includes an extra selection method named as single stage RS given priority and maximizing data rate of the first user, is analyzed over i.n.i.d. Nakagami-m fade and later one over i.i.d. generalized-K fade. In both systems imperfect SIC is also considered. Unlike existing works, derived expressions are unique and valid for all cases such as FD and HD together with perfect and imperfect SIC, i.e. expressions are not given separately but in a single compact form. Exact OP expression is derived for Nakagami-m, whereas, analysis over generalized-K fade is done based on approximated PDF where generalized Gauss-Laguerre quadrature approach is used to obtain a robust approximation. Additionally, a slightly different CDF expression of generalized-K distribution is presented. Thereafter, the validity of approximation is verified by the aid of the exact CDFs, where results are almost excellent. For both systems, the effect of each component such as perfect SIC, imperfect SIC, and SI for FD transmission on error floor of OP is demonstrated.

Lastly, DF multi-hop systems with/out direct link are revised and simpler expressions are introduced for MGF, OP, and SER. The validity of derived expressions is shown via Monte-Carlo simulation technique. Moreover, especially for smaller number of hops, the importance of the signal of direct path is illustrated and it is shown that omitting this signal is unreasonable since it provides diversity, identified as cooperative diversity in the literature.

Finally, to summarize, generalized transmit/receive antenna selection is investigated for HD two-way relay networks and results demonstrate that hardware complexity can be reduced without significant reduction in performance such as OP and SER. Additionally, for the first time in the literature, transmit/receive antenna selection is presented for FD bidirectional networks without reciprocity assumption of forward and backward paths between the sources and relay which makes the analysis realistic as in practice (real implementation). Furthermore, analysis of generalized relay selection in unidirectional/one-way networks reveals that, unlike generalized antenna selection and contrary to common belief due to always plotting curves with respect to source power/SNR, diversity gain cannot be reached or is negligible or is in reverse direction (negative gain). In brief, maximum ratio transmission does not provide such performance as in antenna implementation and its practical application in conjunction with the availability of direct path is possible with rake receiver together maximal ratio combining

at the receiver side. Besides, relay selection is examined in two different NOMA based transmission networks with HD/FD and imperfect SIC schemes; unlike available works, OP expressions are provided in a single term involving all conditions. Finally, nonzero diversity order assertion is declared and supported by analytical derivations. Unlike common myth, error floor (Some common reasons of error floor are insufficient SI cancellation, imperfect SIC, restriction on relay location, and even design of the whole system can also be a reason as in the system analyzed in Chapter 7 over i.n.i.d. Nakagami-m fades) does not mean zero diversity order but it is intrinsic property of the system under consideration.

REFERENCES

[1] Laneman J.N., Tse D.N., Wornell G.W., (2004), "Cooperative diversity in wireless networks: Efficient protocols and outage behavior", IEEE Transactions on Information theory, 50(12), 3062–3080.

[2] Tsiropoulos G.I., Yadav A., Zeng M., Dobre O.A., (2017), "Cooperation in 5G hetnets: Advanced spectrum access and D2D assisted communications", IEEE Wireless Communications, 24(5), 110–117.

[3] Ericsson T., (2018), "Ericsson mobility report", November, 1–32.

[4] Union I., (2015), "IMT traffic estimates for the years 2020 to 2030", Report ITU-R M. 2370–0, ITU-R Radiocommunication Sector of ITU, 1–51.

[5] Rappaport T.S., MacCartney G.R., Samimi M.K., Sun S., (2015), "Wideband millimeter-wave propagation measurements and channel models for future wireless communication system design", IEEE Transactions on Communications, 63(9), 3029–3056.

[6] Telatar E., (1999), "Capacity of multi-antenna Gaussian channels", European transactions on telecommunications, 10(6), 585–595.

[7] Foschini G.J., Gans M.J., (1998), "On limits of wireless communications in a fading environment when using multiple antennas", Wireless personal communications, 6(3), 311–335.

[8] Rankov B., Wittneben A., (2007), "Spectral efficient protocols for half-duplex fading relay channels", IEEE Journal on selected Areas in Communications, 25(2), 379–389.

[9] Sun C., Yang C., (2011), "Is two-way relay more energy efficient?", IEEE Global Telecommunications Conference (GLOBECOM), 1–6, Houston, Texas, USA, 5–9 December.

[10] Zhang Z., Chai X., Long K., Vasilakos A.V., Hanzo L., (2015), "Full duplex techniques for 5G networks: self-interference cancellation, protocol design, and relay selection", IEEE Communications Magazine, 53(5), 128–137.

[11] Hong S., Brand J., Choi J.I., Jain M., Mehlman J., Katti S., Levis P., (2014), "Applications of self-interference cancellation in 5G and beyond", IEEE Communications Magazine, 52(2), 114–121.

[12] Ding Z., Lei X., Karagiannidis G.K., Schober R., Yuan J., Bhargava V.K., (2017), "A survey on non-orthogonal multiple access for 5G networks: Research challenges and future trends", IEEE Journal on Selected Areas in Communications, 35(10), 2181–2195.

[13] Aldababsa M., Toka M., Gokceli S., Kurt G., Kucur O., (2018), "A tutorial on nonorthogonal multiple access for 5G and beyond", Wireless Communications and Mobile Computing, 2018.

[14] Liu Y., Elkashlan M., Ding Z., Karagiannidis G.K., (2016), "Fairness of user clustering in MIMO non-orthogonal multiple access systems", IEEE Communications Letters, 20(7), 1465–1468.

[15] Shin W., Vaezi M., Lee B., Love D.J., Lee J., Poor H.V., (2017), "Non-orthogonal multiple access in multi-cell networks: Theory, performance, and practical challenges", IEEE Communications Magazine, 55(10), 176–183.

[16] Vaezi M., Ding Z., Poor H.V., (2019), "Multiple access techniques for 5G wireless networks and beyond", 1st Edition, Springer.

[17] Yadav S., Upadhyay P.K., Prakriya S., (2014), "Performance evaluation and optimization for two-way relaying with multi-antenna sources", IEEE transactions on vehicular technology, 63(6), 2982–2989.

[18] Wang R., Tao M., (2012), "Outage performance analysis of two-way relay system with multi-antenna relay node", IEEE International Conference on Communications (ICC), 3538–3542, Ottawa, ON, Canada, 10–15 June.

[19] Mo J., Tao M., Liu Y., Wang R., (2014), "Secure beamforming for MIMO two-way communications with an untrusted relay", IEEE Transactions on Signal Processing, 62(9), 2185–2199.

[20] Zhang M., Yi H., Yu H., Luo H., Chen W., (2013), "Joint optimization in bidirectional multi-user multi-relay MIMO systems: Non-robust and robust cases", IEEE transactions on vehicular technology, 62(7), 3228–3244.

[21] Chiong C.W., Rong Y., Xiang Y., (2013), "Channel training algorithms for two-way MIMO relay systems", IEEE Transactions on signal processing, 61(16), 3988–3998.

[22] Arti M., Mallik R.K., Schober R., (2013), "Beamforming and combining in two-way AF MIMO relay networks", IEEE Communications Letters, 17(7), 1400–1403.

[23] Zhang R., Liang Y.C., Chai C.C., Cui S., (2009), "Optimal beamforming for two-way multi-antenna relay channel with analogue network coding", IEEE Journal on Selected Areas in Communications, 27(5), 699–712.

[24] Guo H., Wang L., (2011), "Performance analysis of two-way amplify-and-forward relaying with beamforming over Nakagami-m fading channels", 7th International Conference on Wireless Communications, Networking and Mobile Computing, 1–4, Wuhan, China, 23–25, September.

[25] Molisch A.F., Win M.Z., (2004), "MIMO systems with antenna selection", IEEE microwave magazine, 5(1), 46–56.

[26] Amarasuriya G., Tellambura C., Ardakani M., (2012), "Two-way amplify-and-forward multiple-input multiple-output relay networks with antenna selection", IEEE Journal on Selected Areas in Communications, 30(8), 1513–1529.

[27] Yang N., Yeoh P.L., Elkashlan M., Collings I.B., Chen Z., (2012), "Two-way relaying with multi-antenna sources: Beamforming and antenna selection", IEEE Transactions on Vehicular Technology, 61(9), 3996–4008.

[28] Yang K., Yang N., Xing C., Wu J., (2013), "Relay antenna selection in MIMO two-way relay networks over Nakagami-m fading channels", IEEE Transactions on Vehicular Technology, 63(5), 2349–2362.

[29] Fang Z., Wang X., Yuan X., (2013), “Beamforming design for multiuser two-way relaying: A unified approach via max-min SINR”, IEEE transactions on signal processing, 61(23), 5841–5852.

[30] Tao M., Wang R., (2012), “Linear precoding for multi-pair two-way MIMO relay systems with max-min fairness”, IEEE Transactions on signal processing, 60(10), 5361–5370.

[31] Song K., Ji B., Huang Y., Yang L., (2013), “Performance of antenna selection for two-way relay networks with physical network coding”, International Conference on Wireless Communications and Signal Processing, 1–5, Hangzhou, China, 24–26 October.

[32] Li J., Cimini L.J., Ge J., Zhang C., Feng H., (2015), “Optimal and suboptimal joint relay and antenna selection for two-way amplify-and-forward relaying”, IEEE Transactions on Wireless Communications, 15(2), 980–993.

[33] Hu C.C., Kao Y.C., (2016), “Kalman-based relay/antenna selection for two-way MIMO-relay networks”, IEEE 5th Global Conference on Consumer Electronics, 1–4, Kyoto, Japan, 11–14 October.

[34] Hu C.C., Liu G.F., Chen B.H., (2015), “Joint relay/antenna selection and precoding design for two-way MIMO amplify-and-forward relaying systems”, IEEE Transactions on vehicular technology, 65(7), 4854–4864.

[35] Zhao Y., Adve R., Lim T.J., (2006), “Improving amplify-and-forward relay networks: Optimal power allocation versus selection”, IEEE International Symposium on Information Theory, 1234–1238, Seattle, WA, USA, 9–14 July.

[36] Zou Y., Champagne B., Zhu W.P., Hanzo L., (2014), “Relay-selection improves the security-reliability trade-off in cognitive radio systems”, IEEE Transactions on Communications, 63(1), 215–228.

[37] Zhu J., Zou Y., Champagne B., Zhu W.P., Hanzo L., (2015), “Security–reliability tradeoff analysis of multirelay-aided decode-and-forward cooperation systems”, IEEE Transactions on Vehicular Technology, 65(7), 5825–5831.

[38] Zou Y., Zhu J., Li X., Hanzo L., (2016), “Relay selection for wireless communications against eavesdropping: A security-reliability trade-off perspective”, IEEE Network, 30(5), 74–79.

[39] Guo Q., Feng W., (2019), “Joint relay and eavesdropper selection strategy against multiple eavesdroppers over Nakagami-m fading channels in cooperative decode-and-forward relay networks”, IEEE Access, 7, 37980–37988.

[40] Guo H., Yang Z., Zhang L., Zhu J., Zou Y., (2017), “Joint cooperative beamforming and jamming for physical-layer security of decode-and-forward relay networks”, IEEE Access, 5, 19620–19630.

[41] Ding Z., Dai H., Poor H.V., (2016), “Relay selection for cooperative NOMA”, IEEE Wireless Communications Letters, 5(4), 416–419.

[42] Yang Z., Ding Z., Wu Y., Fan P., (2017), “Novel relay selection strategies for cooperative NOMA”, IEEE Transactions on Vehicular Technology, 66(11), 10114–10123.

[43] Yue X., Liu Y., Kang S., Nallanathan A., Ding Z., (2018), “Spatially random relay selection for full/half-duplex cooperative NOMA networks”, IEEE Transactions on Communications, 66(8), 3294–3308.

[44] Zhao J., Ding Z., Fan P., Yang Z., Karagiannidis G.K., (2018), “Dual relay selection for cooperative NOMA with distributed space time coding”, IEEE Access, 6, 20440–20450.

[45] Xu P., Yang Z., Ding Z., Zhang Z., (2018), “Optimal relay selection schemes for cooperative NOMA”, IEEE Transactions on Vehicular Technology, 67(8), 7851–7855.

[46] Lee S., Da.Costa D.B., Vien Q.T., Duong T.Q., de Sousa.Jr R.T., (2016), “Non-orthogonal multiple access schemes with partial relay selection”, IET Communications, 11(6), 846–854.

[47] Ju J., Duan W., Sun Q., Gao S., Zhang G., (2019), “Performance analysis for cooperative NOMA with opportunistic relay selection”, IEEE Access, 7, 131488–131500.

[48] Chen J., Yang L., Alouini M.S., (2018), “Performance analysis of cooperative NOMA schemes in spatially random relaying networks”, IEEE Access, 6, 33159–33168.

[49] Zhang Y., Ge J., Serpedin E., Radaydeh R.M., Hu Y., (2018), “On cooperative NOMA relay selection under Nakagami-*m* fading and imperfect channel estimation”, Transactions on Emerging Telecommunications Technologies, 29(12), e3535.

[50] Fidan E., Kucur O., (2015), “Performance of multi–antenna two–way relay networks with generalized antenna selection over Rayleigh fading channels”, IEEE 23nd Signal Processing and Communications Applications Conference (SIU’15), 577–580, Malatya, Turkey, 16-19 May.

[51] Fidan E., Kucur O., (2016), “Performance of two-way AF MIMO relay networks with single and multiple antenna selection schemes”, IEEE 27th Annual International Symposium on Personal, Indoor, and Mobile Radio Communications (PIMRC), 1–6, Valencia, Spain, 4–8 September.

[52] Fidan E., Kucur O., (2017), “Performance of two-way relay networks with generalized transmit and receive antenna selection over Rayleigh fading channels”, Wireless Personal Communications, 95(4), 4789–4805.

[53] Fidan E., Kucur O., (2017), “SSER analysis of AF MIMO TWRNs with single and multiple antenna selection schemes”, IEEE 25th Signal Processing and Communications Applications Conference (SIU’17), 1–4, Antalya, Turkey, 15–18 May.

[54] Fidan E., Kucur O., (2017), “Outage performance of two way full-duplex relay networks with antenna selection”, IEEE Advances in Wireless and Optical Communications (RTUWO), 126–131, Riga, Latvia, 2–3 November.

[55] Fidan E., Kucur O., (2018), “Performance of transceiver antenna selection in two way full-duplex relay networks over Rayleigh fading channels”, IEEE Transactions on Vehicular Technology, 67(7), 5909–5921.

[56] Fidan E., Kucur O., (2020), "Performance of cooperative full-duplex AF relay networks with generalised relay selection", IET Communications, 14(5), 800–810.

[57] Fidan E., Kucur O., (2019), "On relay selection for NOMA based cooperative networks", IEEE 27th Signal Processing and Communications Applications Conference (SIU'19), 1–4, Sivas, Turkey, 24–26 April.

[58] Fidan E., Kucur O., (2020), "Relay selection with imperfect SIC for FD/HD NOMA cooperative networks over Nakagami-m fades", To be submitted to IEEE Transactions on Communications, 1–27.

[59] Fidan E., Kucur O., (2020), "Relay selection for cooperative NOMA networks over fading and shadowing channels", 28th Signal Processing and Communications Applications Conference (SIU'20), 1–4, Gaziantep, Turkey, 5–7 October.

[60] Fidan E., Kucur O., (2020), "On relay selection over shadowed fading channels for NOMA based cooperative networks", Submitted to IEEE Transactions on Vehicular Technology, 1–13.

[61] Fidan E., Kucur O., (2020), "Performance of decode–and–forward multihop networks over i.n.i.d. Nakagami-m fading channels", 28th Signal Processing and Communications Applications Conference (SIU'20), 1–4, Gaziantep, Turkey, 5–7 October.

[62] Shankar P.M., (2017), "Fading and shadowing in wireless systems", 2nd Edition, Springer.

[63] Papoulis A., Pillai S.U., (2002), "Probability, random variables, and stochastic processes", 4th Edition, Tata McGraw-Hill Education.

[64] Nakagami M., (1960), "The m-distribution—a general formula of intensity distribution of rapid fading", Statistical methods in radio wave propagation, 3–36.

[65] Jeffrey A., Zwillinger D., (2007), "Table of integrals, series, and products", 7th, Elsevier.

[66] Yilmaz F., Alouini M.S., (2010), "Extended generalized-K (EGK): A new simple and general model for composite fading channels", arXiv preprint arXiv:1012.2598.

[67] Prudnikov A.P., Brychkov Y.A., Marichev O.I., (1986), "Integrals and series: Special functions", 1st Edition, Gordon and Breach Science.

[68] Cover T., Gamal A.E., (1979), "Capacity theorems for the relay channel", IEEE Transactions on information theory, 25(5), 572–584.

[69] Tse D., Viswanath P., (2005), "Fundamentals of wireless communication", 1st Edition, Cambridge university press.

[70] Vaezi M., Schober R., Ding Z., Poor H.V., (2019), "Non-orthogonal multiple access: Common myths and critical questions", IEEE Wireless Communications, 26(5), 174–180.

[71] Molisch A.F., (2012), "Wireless communications", 2nd Edition, John Wiley & Sons.

[72] Brennan D.G., (1959), "Linear diversity combining techniques", Proceedings of the IRE, 47(6), 1075–1102.

[73] Shortall W.E., (1973), “A switched diversity receiving system for mobile radio”, IEEE Transactions on Vehicular Technology, 22(4), 185–191.

[74] Simon M.K., Alouini M.S., (2005), “Digital communication over fading channels”, 2nd Edition, John Wiley & Sons.

[75] Yang L., Qaraqe K., Serpedin E., Alouini M.S., (2013), “Performance analysis of amplify-and-forward two-way relaying with co-channel interference and channel estimation error”, IEEE Transactions on Communications, 61(6), 2221–2231.

[76] Nosratinia A., Hunter T.E., Hedayat A., (2004), “Cooperative communication in wireless networks”, IEEE communications Magazine, 42(10), 74–80.

[77] Coşkun A.F., Kucur O., (2013), “Performance analysis of hybrid transmit antenna selection/maximal-ratio transmission in Nakagami-m fading channels”, Wireless Communications and Mobile Computing, 13(13), 1234–1245.

[78] Alouini M.S., Simon M.K., (2000), “An MGF-based performance analysis of generalized selection combining over Rayleigh fading channels”, IEEE Transactions on Communications, 48(3), 401–415.

[79] Cai X., Giannakis G.B., (2004), “Performance analysis of combined transmit selection diversity and receive generalized selection combining in Rayleigh fading channels”, IEEE Transactions on Wireless Communications, 3(6), 1980–1983.

[80] Louie R.H., Li Y., Vucetic B., (2010), “Practical physical layer network coding for two-way relay channels: Performance analysis and comparison”, IEEE Transactions on Wireless Communications, 9(2), 764–777.

[81] McKay M.R., Grant A.J., Collings I.B., (2007), “Performance analysis of MIMO-MRC in double-correlated Rayleigh environments”, IEEE Transactions on Communications, 55(3), 497–507.

[82] Wang Z., Giannakis G.B., (2003), “A simple and general parameterization quantifying performance in fading channels”, IEEE Transactions on Communications, 51(8), 1389–1398.

[83] Wang T., Cano A., Giannakis G.B., Laneman J.N., (2007), “High-performance cooperative demodulation with decode-and-forward relays”, IEEE Transactions on communications, 55(7), 1427–1438.

[84] Popovski P., Yomo H., (2007), “Wireless network coding by amplify-and-forward for bi-directional traffic flows”, IEEE Communications Letters, 11(1), 16–18.

[85] Joung J., Sayed A.H., (2009), “Multiuser two-way amplify-and-forward relay processing and power control methods for beamforming systems”, IEEE Transactions on Signal Processing, 58(3), 1833–1846.

[86] Panah A.Y., Heath R.W., (2010), “MIMO two-way amplify-and-forward relaying with imperfect receiver CSI”, IEEE Transactions on vehicular technology, 59(9), 4377–4387.

[87] Upadhyay P.K., Prakriya S., (2011), “Performance of two-way opportunistic relaying with analog network coding over Nakagami-m fading”, IEEE Transactions on Vehicular Technology, 60(4), 1965–1971.

[88] Yang J., Fan P., Duong T.Q., Lei X., (2011), “Exact performance of two-way AF relaying in Nakagami-m fading environment”, IEEE Transactions on Wireless Communications, 10(3), 980–987.

[89] Guo H., Ge J., Ding H., (2011), “Symbol error probability of two-way amplify-and-forward relaying”, IEEE Communications Letters, 15(1), 22–24.

[90] Zhou X., Bai B., Chen W., (2015), “Greedy relay antenna selection for sum rate maximization in amplify-and-forward MIMO two-way relay channels under a holistic power model”, IEEE Communications Letters, 19(9), 1648–1651.

[91] Tse D.N.C., Viswanath P., Zheng L., (2004), “Diversity-multiplexing tradeoff in multiple-access channels”, IEEE Transactions on Information Theory, 50(9), 1859–1874.

[92] Choi D., Lee J.H., (2014), “Outage probability of two-way full-duplex relaying with imperfect channel state information”, IEEE Communications Letters, 18(6), 933–936.

[93] Zhang Z., Ma Z., Ding Z., Xiao M., Karagiannidis G.K., (2016), “Full-duplex two-way and one-way relaying: average rate, outage probability, and tradeoffs”, IEEE Transactions on Wireless Communications, 15(6), 3920–3933.

[94] Li Y., Li N., Peng M., Wang W., (2016), “Relay power control for two-way full-duplex amplify-and-forward relay networks”, IEEE Signal Processing Letters, 23(2), 292–296.

[95] Zheng G., (2014), “Joint beamforming optimization and power control for full-duplex MIMO two-way relay channel”, IEEE Transactions on Signal Processing, 63(3), 555–566.

[96] Shim Y., Choi W., Park H., (2016), “Beamforming design for full-duplex two-way amplify-and-forward MIMO relay”, IEEE Transactions on Wireless Communications, 15(10), 6705–6715.

[97] Zhang Z., Chen Z., Shen M., Xia B., (2016), “Spectral and energy efficiency of multipair two-way full-duplex relay systems with massive MIMO”, IEEE journal on selected areas in communications, 34(4), 848–863.

[98] Zhou M., Song L., Li Y., Li X., (2015), “Simultaneous bidirectional link selection in full duplex MIMO systems”, IEEE Transactions on Wireless Communications, 14(7), 4052–4062.

[99] Jang S., Ahn M., Lee H., Lee I., (2016), “Antenna selection schemes in bidirectional full-duplex MIMO systems”, IEEE Transactions on Vehicular Technology, 65(12), 10097–10100.

[100] Cui H., Ma M., Song L., Jiao B., (2014), “Relay selection for two-way full duplex relay networks with amplify-and-forward protocol”, IEEE Transactions on Wireless Communications, 13(7), 3768–3777.

[101] Zhang J., Li Q., Kim K.J., Wang Y., Ge X., Zhang J., (2016), “On the performance of full-duplex two-way relay channels with spatial modulation”, IEEE Transactions on Communications, 64(12), 4966–4982.

[102] Hu J., Liu F., Liu Y., (2017), “Achievable rate analysis of two-way full duplex relay with joint relay and antenna selection”, IEEE Wireless Communications and Networking Conference (WCNC), 1–5, San Francisco, CA, USA, 19–22 March.

[103] Duarte M., Dick C., Sabharwal A., (2012), “Experiment-driven characterization of full-duplex wireless systems”, IEEE Transactions on Wireless Communications, 11(12), 4296–4307.

[104] Li Q., Yu M., Pandharipande A., Ge X., Zhang J., Zhang J., (2016), “Performance of virtual full-duplex relaying on cooperative multi-path relay channels”, IEEE Transactions on Wireless Communications, 15(5), 3628–3642.

[105] Kwon T., Lim S., Choi S., Hong D., (2010), “Optimal duplex mode for DF relay in terms of the outage probability”, IEEE Transactions on Vehicular Technology, 59(7), 3628–3634.

[106] Rui X., Hou J., Zhou L., (2010), “On the performance of full-duplex relaying with relay selection”, Electronics letters, 46(25), 1674–1676.

[107] Suraweera H.A., Krikidis I., Yuen C., (2013), “Antenna selection in the full-duplex multi-antenna relay channel”, IEEE international conference on communications (ICC), 4823–4828, Budapest, Hungary, 9–13 June.

[108] Xia B., Li C., Jiang Q., (2016), “Outage performance analysis of multi-user selection for two-way full-duplex relay systems”, IEEE Communications Letters, 21(4), 933–936.

[109] Ji X., Zheng B., Cai Y., Zou L., (2012), “On the study of half-duplex asymmetric two-way relay transmission using an amplify-and-forward relay”, IEEE Transactions on Vehicular Technology, 61(4), 1649–1664.

[110] Li J.W., Lin C., (2017), “On the optimal power allocation for two-way full-duplex AF relay networks”, IEEE Transactions on Signal Processing, 65(21), 5702–5715.

[111] Ju M., Kim I.M., (2010), “Relay selection with ANC and TDBC protocols in bidirectional relay networks”, IEEE Transactions on Communications, 58(12), 3500–3511.

[112] Yang K., Cui H., Song L., Li Y., (2014), “Joint relay and antenna selection for full-duplex AF relay networks”, IEEE international conference on communications (ICC), 4454–4459, Sydney, NSW, Australia, 10–14 June.

[113] Bayrakdar M.E., (2020), “Cooperative communication based access technique for sensor networks”, International Journal of Electronics, 107(2), 212–225.

[114] Kim D., Park S., Ju H., Hong D., (2014), “Transmission capacity of full-duplex-based two-way ad hoc networks with ARQ protocol”, IEEE Transactions on Vehicular Technology, 63(7), 3167–3183.

[115] Li P., Guo S., Zhuang W., (2013), “Optimal transmission scheduling of cooperative communications with a full-duplex relay”, IEEE Transactions on Parallel and Distributed Systems, 25(9), 2353–2363.

[116] Lu W., Wang J., (2014), “Opportunistic spectrum sharing based on full-duplex cooperative OFDM relaying”, IEEE communications Letters, 18(2), 241–244.

[117] Sun L., Zhang T., Li Y., Niu H., (2012), “Performance study of two-hop amplify-and-forward systems with untrustworthy relay nodes”, IEEE Trans. Veh. Technol., 61(8), 3801–3807.

[118] Sun L., Ren P., Du Q., Wang Y., Gao Z., (2015), “Security-aware relaying scheme for cooperative networks with untrusted relay nodes”, IEEE Commun. Lett., 19(3), 463–466.

[119] Wang W., Teh K.C., Li K.H., (2016), “Relay selection for secure successive AF relaying networks with untrusted nodes”, IEEE Trans. Inf. Forensics Security, 11(11), 2466–2476.

[120] Kuhestani A., Mohammadi A., Mohammadi M., (2018), “Joint relay selection and power allocation in large-scale MIMO systems with untrusted relays and passive eavesdroppers”, IEEE Trans. Inf. Forensics Security, 13(2), 341–355.

[121] Kramer G., Gastpar M., Gupta P., (2005), “Cooperative strategies and capacity theorems for relay networks”, IEEE Transactions on Information Theory, 51(9), 3037–3063.

[122] Krikidis I., Suraweera H.A., Smith P.J., Yuen C., (2012), “Full-duplex relay selection for amplify-and-forward cooperative networks”, IEEE Transactions on Wireless Communications, 11(12), 4381–4393.

[123] de Lima C.H., Alves H., Nardelli P.H., Latva.aho M., (2017), “Effects of relay selection strategies on the spectral efficiency of wireless systems with half-and full-duplex nodes”, IEEE Transactions on Vehicular Technology, 66(8), 7578–7583.

[124] Sofotasios P.C., Fikadu M.K., Muhaidat S., Freear S., Karagiannidis G.K., Valkama M., (2017), “Relay selection based full-duplex cooperative systems under adaptive transmission”, IEEE Wireless Communications Letters, 6(5), 602–605.

[125] Wang D., Zhang R., Cheng X., Yang L., Chen C., (2017), “Relay selection in full-duplex energy-harvesting two-way relay networks”, IEEE Transactions on Green Communications and Networking, 1(2), 182–191.

[126] Zhong B., Zhang Z., (2017), “Secure full-duplex two-way relaying networks with optimal relay selection”, IEEE Communications Letters, 21(5), 1123–1126.

[127] Li Q., Feng S., Ge X., Mao G., Hanzo L., (2017), “On the performance of full-duplex multi-relay channels with DF relays”, IEEE transactions on Vehicular Technology, 66(10), 9550–9554.

[128] Wang Y., Xu Y., Li N., Xie W., Xu K., Xia X., (2016), “Relay selection of full-duplex decode-and-forward relaying over Nakagami-m fading channels”, IET Communications, 10(2), 170–179.

[129] Jing Y., Jafarkhani H., (2009), “Single and multiple relay selection schemes and their achievable diversity orders”, IEEE Transactions on Wireless Communications, 8(3), 1414–1423.

[130] Chu S.I., (2012), “Performance of amplify-and-forward cooperative diversity networks with generalized selection combining over Nakagami-m fading channels”, IEEE Commun. Lett., 16(5), 634–637.

[131] Wang L., Cai Y., Yang W., Yang W., (2013), “Performance analysis of transmit beamforming and relay selection with feedback delay and channel estimation errors”, International Conference on Wireless Communications and Signal Processing, 1–6, Hangzhou, China, 24–26 October.

[132] Nomikos N., Charalambous T., Vouyioukas D., Karagiannidis G.K., (2018), “Low-complexity buffer-aided link selection with outdated CSI and feedback errors”, IEEE Transactions on Communications, 66(8), 3694–3706.

[133] Eddaghel M.M., Mannai U.N., Chen G.J., Chambers J.A., (2013), “Outage probability analysis of an amplify-and-forward cooperative communication system with multi-path channels and max–min relay selection”, IET Communications, 7(5), 408–416.

[134] Sheng G., Dang S., Zhang Z., Kocan E., Pejanovic M., (2019), “OFDM with index modulation assisted by multiple amplify-and-forward relays”, IEEE Wirel. Commun. Lett., 8(3), 789–792.

[135] Nguyen B.V., Afolabi R.O., Kim K., (2013), “Dependence of outage probability of cooperative systems with single relay selection on channel correlation”, IEEE communications letters, 17(11), 2060–2063.

[136] Riihonen T., Werner S., Wichman R., (2011), “Hybrid full-duplex/half-duplex relaying with transmit power adaptation”, IEEE Transactions on Wireless Communications, 10(9), 3074–3085.

[137] Osorio D.P.M., Olivo E.E.B., Alves H., Santos.Filho J.C.S., Latva.aho M., (2016), “An adaptive transmission scheme for amplify-and-forward relaying networks”, IEEE Transactions on Communications, 65(1), 66–78.

[138] Airod F.E., Chafnaji H., Tamtaoui A., (Rabat, Morocco, November 2017), “Performance analysis for amplify and forward full-duplex relaying with direct link over Nakagami-m fading channel”, Proc. IEEE International Conference on Wireless Networks and Mobile Communications (WINCOM), 1–6, Rabat, Morocco, 1–4 November.

[139] Osorio D.M., Olivo E.B., Alves H., Santos.Filho J.C.S., Latva.aho M., (2015), “Exploiting the direct link in full-duplex amplify-and-forward relaying networks”, IEEE Signal Processing Letters, 22(10), 1766–1770.

[140] Wang Q., Dong Y., Xu X., Tao X., (2015), “Outage probability of full-duplex AF relaying with processing delay and residual self-interference”, IEEE Communications Letters, 19(5), 783–786.

[141] Ma Y., Pasupathy S., (2004), “Efficient performance evaluation for generalized selection combining on generalized fading channels”, IEEE Transactions on Wireless Communications, 3(1), 29–34.

[142] Seddik K.G., Sadek A.K., Su W., Liu K.R., (2006), “Outage analysis of multi-node amplify-and-forward relay networks”, IEEE Wireless Communications and Networking Conference (WCNC), 1184–1188, Las Vegas, NV, USA, 3–6 April.

[143] Ding Z., Peng M., Poor H.V., (2015), “Cooperative non-orthogonal multiple access in 5G systems”, IEEE Communications Letters, 19(8), 1462–1465.

[144] Lv L., Chen J., Ni Q., Ding Z., Jiang H., (2018), "Cognitive non-orthogonal multiple access with cooperative relaying: A new wireless frontier for 5G spectrum sharing", IEEE Communications Magazine, 56(4), 188–195.

[145] Dai L., Wang B., Yuan Y., Han S., Chih.Lin I., Wang Z., (2015), "Non-orthogonal multiple access for 5G: Solutions, challenges, opportunities, and future research trends", IEEE Communications Magazine, 53(9), 74–81.

[146] Kim J.B., Lee I.H., (2015), "Non-orthogonal multiple access in coordinated direct and relay transmission", IEEE Communications Letters, 19(11), 2037–2040.

[147] Men J., Ge J., Zhang C., (2016), "Performance analysis of nonorthogonal multiple access for relaying networks over Nakagami-m fading channels", IEEE Transactions on Vehicular Technology, 66(2), 1200–1208.

[148] Deng D., Fan L., Lei X., Tan W., Xie D., (2017), "Joint user and relay selection for cooperative NOMA networks", IEEE Access, 5, 20220–20227.

[149] Alkhawatrah M., Gong Y., Chen G., Lambotharan S., Chambers J.A., (2019), "Buffer-aided relay selection for cooperative NOMA in the internet of things", IEEE Internet of Things Journal, .

[150] Li H., Li J., Lv L., (2019), "Joint relay-and-antenna selection for cooperative non-orthogonal multiple access", IET Communications, 13(13), 2012–2019.

[151] Liu X., Yang L., Chen J., Zheng F., (2019), "On the performance of Nth best relay selection scheme for NOMA-based cooperative relaying networks with SWIPT", IEEE 89th Vehicular Technology Conference (VTC2019-Spring), 1–5, Kuala Lumpur, Malaysia, 28 April–1 May 2019.

[152] Tang X., An K., Guo K., Wang X., Li J., Zhou F., et al., (2019), "On the performance of two-way multiple relay non-orthogonal multiple access-based networks with hardware impairments", IEEE Access, 7, 128896–128909.

[153] Junior A.T., Olivo E.E.B., Osorio D.P.M., de Lima C.H.M., Alves H., (2019), "Performance analysis of full-duplex relay-aided NOMA systems using partial relay selection", IEEE Transactions on Vehicular Technology, 69, 1.

[154] Li Y., Li Y., Chu X., Ye Y., Zhang H., (2019), "Performance analysis of relay selection in cooperative NOMA networks", IEEE Communications Letters, 23(4), 760–763.

[155] Lei H., Yang Z., Park K.H., Ansari I.S., Guo Y., Pan G., Alouini M.S., (2019), "Secrecy outage analysis for cooperative NOMA systems with relay selection schemes", IEEE Transactions on Communications, 67(9).

[156] Yu C., Ko H.L., Peng X., Xie W., (2019), "Secrecy outage performance analysis for cooperative NOMA over Nakagami-m channel", IEEE Access, 7, 79866–79876.

[157] Wang Z., Peng Z., (2019), "Secrecy performance analysis of relay selection in cooperative NOMA systems", IEEE Access, 7, 86274–86287.

[158] Feng Y., Yan S., Liu C., Yang Z., Yang N., (2018), "Two-stage relay selection for enhancing physical layer security in non-orthogonal multiple access", IEEE Transactions on Information Forensics and Security, 14(6), 1670–1683.

[159] Lei H., Yang Z., Park K.H., Ansari I.S., Pan G., Alouini M.S., (2019), "On physical layer security of multiple-relay assisted NOMA systems", IEEE International Conference on Communications Workshops (ICC Workshops), 1–6, Shanghai, China, 20–24 May.

[160] Zou Y., Champagne B., Zhu W.P., Hanzo L., (2015), "Relay-selection improves the security-reliability trade-off in cognitive radio systems", IEEE Transactions on Communications, 63(1), 215–228.

[161] Zhu J., Zou Y., Champagne B., Zhu W.P., Hanzo L., (2016), "Security–reliability tradeoff analysis of multirelay-aided decode-and-forward cooperation systems", IEEE Transactions on Vehicular Technology, 65(7), 5825–5831.

[162] Yan C., Harada A., Benjebbour A., Lan Y., Li A., Jiang H., (2015), "Receiver design for downlink non-orthogonal multiple access (NOMA)", IEEE 81st Vehicular Technology Conference (VTC Spring), 1–6, Glasgow, UK, 11–14 May.

[163] Godavarti M., Hero A.O., (2002), "Diversity and degrees of freedom in wireless communications", IEEE International Conference on Acoustics, Speech, and Signal Processing (ICASSP), 2861–2864, Orlando, FL, USA, 13–17 May.

[164] Smith P.J., Dmochowski P.A., Chiani M., Giorgetti A., (2013), "On the number of independent channels in multi-antenna systems", IEEE Transactions on Wireless Communications, 13(1), 75–85.

[165] Kader M.F., Shahab M.B., Shin S.Y., (2017), "Exploiting non-orthogonal multiple access in cooperative relay sharing", IEEE Communications Letters, 21(5), 1159–1162.

[166] Ding Z., Adachi F., Poor H.V., (2015), "The application of MIMO to non-orthogonal multiple access", IEEE Transactions on Wireless Communications, 15(1), 537–552.

[167] Yan X., Ge J., Zhang Y., Gou L., (2018), "Noma-based multiple-antenna and multiple-relay networks over nakagami-m fading channels with imperfect CSI and SIC error", IET Communications, 12(17), 2087–2098.

[168] Collonge S., Zaharia G., Zein G.E., (2004), "Influence of the human activity on wide-band characteristics of the 60 GHz indoor radio channel", IEEE Transactions on Wireless Communications, 3(6), 2396–2406.

[169] Aswathi V., Babu A., (2019), "Full/half duplex cooperative NOMA under imperfect successive interference cancellation and channel state estimation errors", IEEE Access, 7, 179961–179984.

[170] Bithas P.S., Sagias N.C., Mathiopoulos P.T., Karagiannidis G.K., Rontogiannis A.A., (2006), "On the performance analysis of digital communications over generalized-*K* fading channels", IEEE Communications Letters, 10(5), 353–355.

[171] Atapattu S., Tellambura C., Jiang H., (2011), "A mixture gamma distribution to model the SNR of wireless channels", IEEE Transactions on Wireless Communications, 10(12), 4193–4203.

[172] Abramowitz M., Stegun I.A., (1965), "Handbook of mathematical functions with formulas, graphs, and mathematical table", 1st Edition, National Bureau of Standards Applied Mathematics series 55.

[173] Laneman J.N., Wornell G.W., (2000), "Energy-efficient antenna sharing and relaying for wireless networks", IEEE Wireless Communications and Networking Conference (WCNC), 7–12, Chicago, IL, USA, 23–28 September.

[174] Hasna M.O., Alouini M.S., (2003), "Outage probability of multihop transmission over Nakagami-m fading channels", IEEE Communications Letters, 7(5), 216–218.

[175] Xia M., Aissa S., (2013), "Impact of co-channel interference on the performance of multi-hop relaying over Nakagami-m fading channels", IEEE Communications Letters, 3(2), 133–136.

[176] Mesleh R., Ikki S.S., Amin O., (2014), "Multi-hop relaying systems in the presence of co-channel interference over Nakagami-m fading channels", IET Communications, 8(4), 483–491.

[177] Yilmaz F., Kucur O., (2008), "Exact performance of wireless multihop transmission for M-ary coherent modulations over generalized gamma fading channels", IEEE 19th International Symposium on Personal, Indoor and Mobile Radio Communications (PIMRC), 1–5, Cannes, France, 15-18 September.

[178] Han S., Chen L., Meng W., Li C., (2015), "Outage probability of multi-hop full-duplex DF relay system over Nakagami-m fading channels", IEEE/CIC International Conference on Communications in China (ICCC), 1–6, Shenzhen, China, 2–4 November.

[179] Katla R., Babu A., (2016), "Outage performance of multihop full duplex relaying system over Nakagami-m fading channels", IEEE Annual India Conference (INDICON), 1–6, Bangalore, India, 16–18 December.

[180] Kim Y.G., Beaulieu N.C., (2014), "Relay advantage criterion for multihop decode-and-forward relaying systems", IEEE Transactions on Wireless Communications, 13(4), 1988–1999.

[181] Belbase K., Tellambura C., Jiang H., (2019), "Coverage, capacity, and error rate analysis of multi-hop millimeter-wave decode and forward relaying", IEEE Access, 69638–69656.

BIOGRAPHY

Efendi Fidan has recieved his B.Sc. degree in Electrical and Electronics Engineering from Bosphorus University in 2003 and his M.Sc. degree in Electronics Engineering from Gebze Technical University in 2010. He has been doing Ph.D at Gebze Technical University since 2012. He has been working in the Scientific and Technological Research Council of Turkey (TÜBİTAK) since 2004. His research interests are multi-antenna and relay communications.

APPENDICES

Appendix A: Journal Articles (SCI/SCI-EXP) Based on the Thesis

The journal articles are as follows:

- Fidan E., Kucur O., (2017), "Performance of two-way relay networks with generalized transmit and receive antenna selection over Rayleigh fading channels", Wireless Personal Communications, 95(4), 4789–4805.
- Fidan E., Kucur O., (2018), "Performance of transceiver antenna selection in two way full-duplex relay networks over Rayleigh fading channels", IEEE Transactions on Vehicular Technology, 67(7), 5909–5921.
- Fidan E., Kucur O., (2018), "Performance of cooperative full-duplex AF relay networks with generalised relay selection", IET Communications, 14(5), 800–810.
- Fidan E., Kucur O., (2020), "On Relay Selection over Shadowed Fading Channels for NOMA based cooperative networks", Submitted to IEEE Transactions on Vehicular Technology, 1–27.
- Fidan E., Kucur O., (2020), "Relay selection with imperfect SIC for FD/HD NOMA cooperative networks over Nakagami-m Fades", To be submitted to IEEE Transactions on Communications, 1–27.

Appendix B: Conference Proceedings Based on the Thesis

The conference proceedings are as follows:

- Fidan E., Kucur O., (2016), "Performance of two-way AF MIMO relay networks with single and multiple antenna selection schemes", IEEE 27th Annual International Symposium on Personal, Indoor, and Mobile Radio Communications (PIMRC), 1–6, Valencia, Spain, 4–8 September.
- Fidan E., Kucur O., (2017), "Outage performance of two way full-duplex relay networks with antenna selection", IEEE Advances in Wireless and Optical Communications (RTUWO), 126–131, Riga, Latvia, 2–3 November.

Appendix C: National Proceedings Based on the Thesis

The national proceedings are as follows:

- Fidan E., Kucur O., (2015), "Performance of multi-antenna two-way relay networks with generalized antenna selection over Rayleigh Fading Channels", IEEE 23nd Signal Processing and Communications Applications Conference (SIU'15), 577–580, Malatya, Turkey, 16-19 May.
- Fidan E., Kucur O., (2017), "SSER analysis of AF MIMO TWRNs with single and multiple antenna selection schemes", IEEE 25th Signal Processing and Communications Applications Conference (SIU'17), 1–4, Antalya, Turkey, 15–18 May.
- Fidan E., Kucur O., (2019), "On Relay Selection for NOMA Based Cooperative Networks", IEEE 27th Signal Processing and Communications Applications Conference (SIU'19), 1–4, Sivas, Turkey, 24–26 April.
- Fidan E., Kucur O., (2020), "Relay Selection for Cooperative NOMA Networks over Fading and Shadowing Channels", 28th Signal Processing and Communications Applications Conference (SIU'20), 1–4, Gaziantep, Turkey, 5–7 October.
- Fidan E., Kucur O., (2020), "Performance of Decode-and-Forward Multihop Networks over i.n.i.d. Nakagami-m Fading Channels", 28th Signal Processing and Communications Applications Conference (SIU'20), 1–4, Gaziantep, Turkey, 5–7 October.